NBS TECHNICAL NOTE

404

Radiochemical Analysis:

Activation Analysis, Instrumentation, Radiation Techniques, and Radioisotope Techniques July 1965 through June 1966

Edited by James R. DeVoe

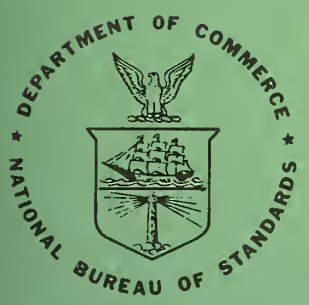

U.S. DEPARTMENT OF COMMERCE
National Bureau of Standards

THE NATIONAL BUREAU OF STANDARDS

The National Bureau of Standards[1] provides measurement and technical information services essential to the efficiency and effectiveness of the work of the Nation's scientists and engineers. The Bureau serves also as a focal point in the Federal Government for assuring maximum application of the physical and engineering sciences to the advancement of technology in industry and commerce. To accomplish this mission, the Bureau is organized into three institutes covering broad program areas of research and services:

THE INSTITUTE FOR BASIC STANDARDS . . . provides the central basis within the United States for a complete and consistent system of physical measurements, coordinates that system with the measurement systems of other nations, and furnishes essential services leading to accurate and uniform physical measurements throughout the Nation's scientific community, industry, and commerce. This Institute comprises a series of divisions, each serving a classical subject matter area:

—Applied Mathematics—Electricity—Metrology—Mechanics—Heat—Atomic Physics—Physical Chemistry—Radiation Physics—Laboratory Astrophysics[2]—Radio Standards Laboratory,[2] which includes Radio Standards Physics and Radio Standards Engineering—Office of Standard Reference Data.

THE INSTITUTE FOR MATERIALS RESEARCH . . . conducts materials research and provides associated materials services including mainly reference materials and data on the properties of materials. Beyond its direct interest to the Nation's scientists and engineers, this Institute yields services which are essential to the advancement of technology in industry and commerce. This Institute is organized primarily by technical fields:

—Analytical Chemistry—Metallurgy—Reactor Radiations—Polymers—Inorganic Materials—Cryogenics[2]—Materials Evaluation Laboratory—Office of Standard Reference Materials.

THE INSTITUTE FOR APPLIED TECHNOLOGY . . . provides technical services to promote the use of available technology and to facilitate technological innovation in industry and government. The principal elements of this Institute are:

—Building Research—Electronic Instrumentation—Textile and Apparel Technology Center—Technical Analysis—Center for Computer Sciences and Technology—Office of Weights and Measures—Office of Engineering Standards Services—Office of Invention and Innovation—Clearinghouse for Federal Scientific and Technical Information.[3]

---

[1] Headquarters and Laboratories at Gaithersburg, Maryland, unless otherwise noted; mailing address Washington, D. C., 20234.

[2] Located at Boulder, Colorado, 80302.

[3] Located at 5285 Port Royal Road, Springfield, Virginia, 22151.

UNITED STATES DEPARTMENT OF COMMERCE • John T. Connor, Secretary
NATIONAL BUREAU OF STANDARDS • A. V. Astin, Director

TECHNICAL NOTE 404
ISSUED SEPTEMBER 30, 1966

Radiochemical Analysis:

Activation Analysis, Instrumentation, Radiation Techniques, and Radioisotope Techniques July 1965 through June 1966

Edited by James R. DeVoe

Radiochemical Analysis Section
Analytical Chemistry Division
Institute for Materials Research

For sale by the Superintendent of Documents, U.S. Government Printing Office
Washington, D.C., 20402 - Price $1.25

FOREWORD

The Analytical Chemistry Division was established as a separate division at the National Bureau of Standards on September 1, 1963, and became part of the Institute for Materials Research in the February 1, 1964, reorganization. It consists at present of nine sections and about 100 technical personnel encompassing some 45 different analytical competences from activation analysis and atomic absorption to vacuum fusion and X-ray spectroscopy. These competences, and in turn the sections which they comprise, are charged with research at the forefront of analysis as well as awareness of the practical sample, be it standard reference material or service analysis. In addition it is their responsibility to inform others of their efforts.

Formal publication in scientific periodicals is highly important. In addition, however, it has been our experience that informal, annual summaries of progress describing efforts of the past year can be very valuable in disseminating information. At the National Bureau of Standards such publications fit logically into the category of a Technical Note. In 1966 we plan to issue these summaries for all of our sections The following is the third annual report on progress of the Radiochemical Analysis and Activation Analysis Sections.

W. Wayne Meinke, Chief
Analytical Chemistry Division

PREFACE

During the period for which this report is written, the Radiochemical Analysis Section was divided into two sections: The Radiochemical Analysis Section and the Activation Analysis Section. At the present time this split has only superficial implications in that the sections have the same section chief and this third progress report encompasses the activities of both sections. Next year a progress report will be written for each section.

It is the intent of these sections to develop measurement techniques for the qualitative, quantitative and structural analysis of materials through the use of radioisotopes. Since the Analytical Chemistry Division is interested specifically in the characterization of very pure materials, and since radiochemical methods are particularly suitable, a large portion of these sections' effort is directed towards the analysis of very small concentrations of the elements.

A basic requirement for the development of such measurement techniques using radioisotopes is the thorough understanding of the chemical, nuclear, and physical principles which form the foundation of a new analytical measurement technique. However, it is essential that the developed methods be practical in the sense that they can be used successfully on materials in which science and industry have an interest. Therefore, these developed techniques are applied to the analysis of NBS Standard Reference Materials where considerable cross checking of analytical techniques is required throughout the process of certification. Some misunderstanding has existed as to whether the Analytical Chemistry Division certifies a particular analytical method. Under no circumstances is this done. The material is certified for composition and therefore, it should be independent of the analytical technique that is used. These sections are attempting to make detailed error analyses of the methods used to assure as high an accuracy as possible.

The Activation Analysis Section is composed of the nuclear reactor and the Linac group while the Radiochemical Analysis Section retains the radiation techniques and radioisotope techniques groups. In addition, the Radiochemical Analysis Section retains groups in nuclear instrumentation and nuclear chemistry which consult with both sections.

A roster of the groups in these sections is listed in part 7. The National Bureau of Standards has several programs whereby a scientist from the United States or abroad may work in our laboratories for one or two years. It is hoped that by utilizing these programs the two sections will be able to perpetuate a stimulating environment.

In order to specify adequately the procedures, it has been necessary occasionally to identify commercial materials and equipment in this report. In no case does such identification imply recommendation or endorsement by the National Bureau of Standards, nor does it imply that the material or equipment identified is necessarily the best available for the purpose.

James R. DeVoe, Chief
Radiochemical Analysis Section
and Activation Analysis Section
Analytical Chemistry Division

TABLE OF CONTENTS

Table of Contents (Cont.)

LIST OF FIGURES

List of figures (cont.)

List of figures (cont.)

LIST OF TABLES

List of tables (cont.)

RADIOCHEMICAL ANALYSIS: ACTIVATION ANALYSIS, INSTRUMENTATION, RADIATION TECHNIQUES, AND RADIOISOTOPE TECHNIQUES

July 1965 to June 1966

Edited by James R. DeVoe

ABSTRACT

This is the third summary of progress of radiochemical analysis which encompasses the work of both the Radiochemical Analysis and Activation Analysis Sections of the Analytical Chemistry Division at the National Bureau of Standards.

Pertinent information on the irradiation facilities of the nuclear reactor, Linac, and Cockroft-Walton generator are described. A number of analyses of standard reference materials by activation analysis are described (e.g., Cu in cast iron, SRM 82b; Se in selenium steel, SRM 1170; Al in steel, SRM 14e; and V in stainless steel, SRM 73c). Various aspects of the technical problems in activation analysis such as its use for homogeneity testing, production of suitable flux monitors, and experimental design with respect to increasing selectivity (such as by using variable neutron energy) and reducing systematic and random errors, are presented. A realistic procedure for estimating sensitivity and for designing the analysis to optimize the detection limit is described. A computer program that resolves complex decay curves utilizes parameter changes convenient for the conversational aspect of "time sharing" digital computers. A highly specific radiochemical separation for copper using a type of amalgam exchange is described.

Description of specialized data handling equipment as well as information on a fast rise preamplifier, solid state detector system, and other special instruments such as a pneumatic transport system rabbit sensor, are presented.

A description of the laboratories used in Mössbauer spectroscopy is presented. Special problems in radiation detection

for use in a spectrometer are also described. The Standard Reference Material Program for chemical shift in Mössbauer spectroscopy is discussed with particular reference to the search for a tin standard. The computer program, "Parlors M," that is used for resolving complex Mössbauer spectra is presented in its entirety in Appendix II.

The use of thin layer chromatography in conjunction with radioactive reagent analysis for trace elements is described. Substoichiometric radioisotope dilution continues to be studied by evaluating systematic and random errors, as well as by developing the technique from physico-chemical principles such as controlled potential coulometry.

James R. DeVoe, Chief
Radiochemical Analysis Section
and Activation Analysis Section
Analytical Chemistry Division

Key words:

NBS reactor, NBS Linac, Cockroft-Walton generator, digital computers, activation analysis, standard reference materials, photo-neutron reactions, flux monitors, Cu, Se, Al, V in irons and steels; homogeneity testing, pneumatic rabbit sensor, Mössbauer spectroscopy, tin standard for chemical shift, PARLORS program for Mössbauer spectra, Mössbauer instrumentation, Mössbauer laboratories, radiometric trace chromatography, radioisotope dilution, substoichiometry by controlled potential coulometry, radiochemical separations, theoretical detection limits for activation analysis, CLSQ program for multicomponent decay, solid state detectors, electronic data handling.

1. INTRODUCTION

A. Liaison Activities

1. Scope of Liaison

It has been found to be extremely valuable to have one person (called the Radiochemistry Coordinator) at the NBS nuclear reactor facility who can coordinate the activities of the radiochemists with the reactor personnel. The following areas of coordination are encompassed in the liaison activity:

a. Inform and obtain approval from the reactor utilization committee for all changes to existing radiochemical facilities in the reactor building. This includes modification of hoods in the radiochemical laboratories, installation of additional facilities such as the clean room, Cockroft-Walton neutron generator, counting rooms, pneumatic tube facilities and special cooling water installations, for example. The project leaders ascertain the extent of facilities, modifications or installations and submit this information to the coordinator who in turn secures the necessary approval.

b. Coordinate the use of existing facilities by radiochemists with respect to reactor utilization (such as requests for irradiations), laboratory utilization, and health physics. This activity performs the function of informing the radiochemists about the proper procedure for utilizing the reactor facilities and of working with the reactor personnel on the formulation of proper operating procedures.

c. Perform the functions stated in a and b above, with all radiochemists using the facilities in the reactor building. This includes radiochemists from other laboratories as well as those from the National Bureau of Standards.

2. Present Liaison with Other Government Agencies

It is the expressed intent of the Director of the Nuclear Reactor to make the wide range of facilities that have been discussed in other reports [1, pp 9-12; 2; 3] available to representatives other than those at the National Bureau of Standards when such facilities are not already being used to full capacity and when the proposed work fulfills a mission of NBS.

An information meeting was held in July 1965 for the purpose of explaining the available irradiation facilities and radiochemical laboratories in the reactor facility. This meeting was attended by representatives of the Atomic Energy Commission, Federal Bureau of Investigation, Food and Drug Administration, Internal Revenue Service, Post Office Department, U. S. Coast Guard Oceanographic Unit, U. S. Geological Survey and the University of Maryland.

The U. S. Geological Survey has negotiated an agreement to use radiochemical laboratory space and the reactor irradiation facility. Negotiations are in progress with the Internal Revenue Service, Food and Drug Administration and the Post Office Department.

It is of particular importance for the efficient operation of the radiochemistry laboratory in the reactor building to have the Radiochemistry Coordinator be the central focal point for assisting these scientists from other laboratories.

B. Scope of Facilities

Since a variety of facilities is becoming available to both the Activation Analysis and Radiochemical Analysis Sections, it is expedient to describe these facilities in each of the research categories presented in this report. Considerable progress has been made in reaching an operable state in each of the projects since we have occupied the reactor building and the general purpose laboratories in Gaithersburg. The nuclear reactor being operated by Division 314 is expected to go critical

in the fall of 1966 with full power operation expected in early 1967.

In spite of the difficulties resulting from the fact that the reactor is not yet in operation, the work by the Activation Analysis Section on certification of standard reference materials has been progressing very well. We are continuing to use the Naval Research Laboratory's reactor, but since we are now occupying our own laboratories in the NBS reactor many samples are transported to our laboratories after irradiation.

The linear electron accelerator, being operated by Division 231, has become operational in a limited sense, and our group was the first to assemble a target in the beam. We expect to gain much information in the next few months on the potential of the NBS machine for our research projects.

A 14-MeV neutron generator in the Activation Analysis Section is close to operation and will be used initially to support the Standard Reference Material Program in the area of oxygen analysis.

The basic equipment for performing a variety of radiation spectroscopies is now available as is the necessary equipment (produced by the nuclear instrumentation group in the Radiochemical Analysis Section) for handling large amounts of data.

Studies are continuing on radiochemical separations, and a careful investigation of the detection sensitivity, accuracy and precision in activation analysis is being made.

The group in radiation techniques has completed work on the standard reference material for chemical shift of iron compounds in Mössbauer spectroscopy. In conjunction with this work was the modification of the NBS spectrometer to allow the simultaneous analysis of two absorbers on the same electromechanical drive. This dual spectrum approach results in a significant increase in precision of the spectral parameters. Considerable advance has been made in the interpretation of these parameters with respect to structural chemical determinations.

Efforts have been successfully made to improve upon the sensitivity of the radioisotopic tracer techniques. The development of radiochromatographic separations of many elements suggests that it is feasible to consider that complementary radiometric methods present a satisfactory multi-element trace analysis. The use of radioisotope dilution in electrochemical separations indicates that better sensitivity may be obtained than the usual methods which measure current.

Now that our move to Gaithersburg is completed, greater effort will be placed on research in areas that will improve measurement techniques and in areas that have not been carefully studied with respect to their application to analytical chemistry.

2. ACTIVATION ANALYSIS

A. Facilities

1. Nuclear Reactor

Work has progressed toward completion of modifications of laboratories and existing pneumatic tube facilities at the NBS reactor. The completed laboratories in the cold and warm areas are now being occupied by personnel from the Activation Analysis and Radiochemical Analysis Sections. Future plans will include completion of the radiological laboratories with their counting room, the neutron generator facility, a clean room, changes in hood exhaust systems and an extended pneumatic tube system.

Seven laboratories have been remodeled in the warm (B-wing) area by replacing fume-type hoods with stainless steel radioactivity hoods, which doubles the hood space available. Also modified were the sink units, to give stainless steel sinks and drainboards. A typical radiochemistry laboratory, used for moderate levels (tens of mCi) of radioactivity, is shown in figure 1. Other modifications made in this area include two laboratories in which benches and cabinets were installed for use as counting rooms.

Our higher level radiochemical separations and activation analyses will be carried out in the radiological laboratories in the C-wing area below the reactor in the Reactor Building. Modifications [1] in this area are in progress and include an island of four hoods in room C-001, with the pneumatic tube receivers in a single eight-foot hood. In the adjoining radiological laboratory (C-002) the pneumatic tube receivers are being recessed into each of four radiochemical hoods around the periphery of the room in order to minimize contamination in transfer for radiochemical separations. Samples will be transferred for counting by a pneumatic shuttle system to the adjoining counting room C-003.

A clean room is being constructed in the hot cell area (B-wing) to give a dust-free, controlled environment for activation

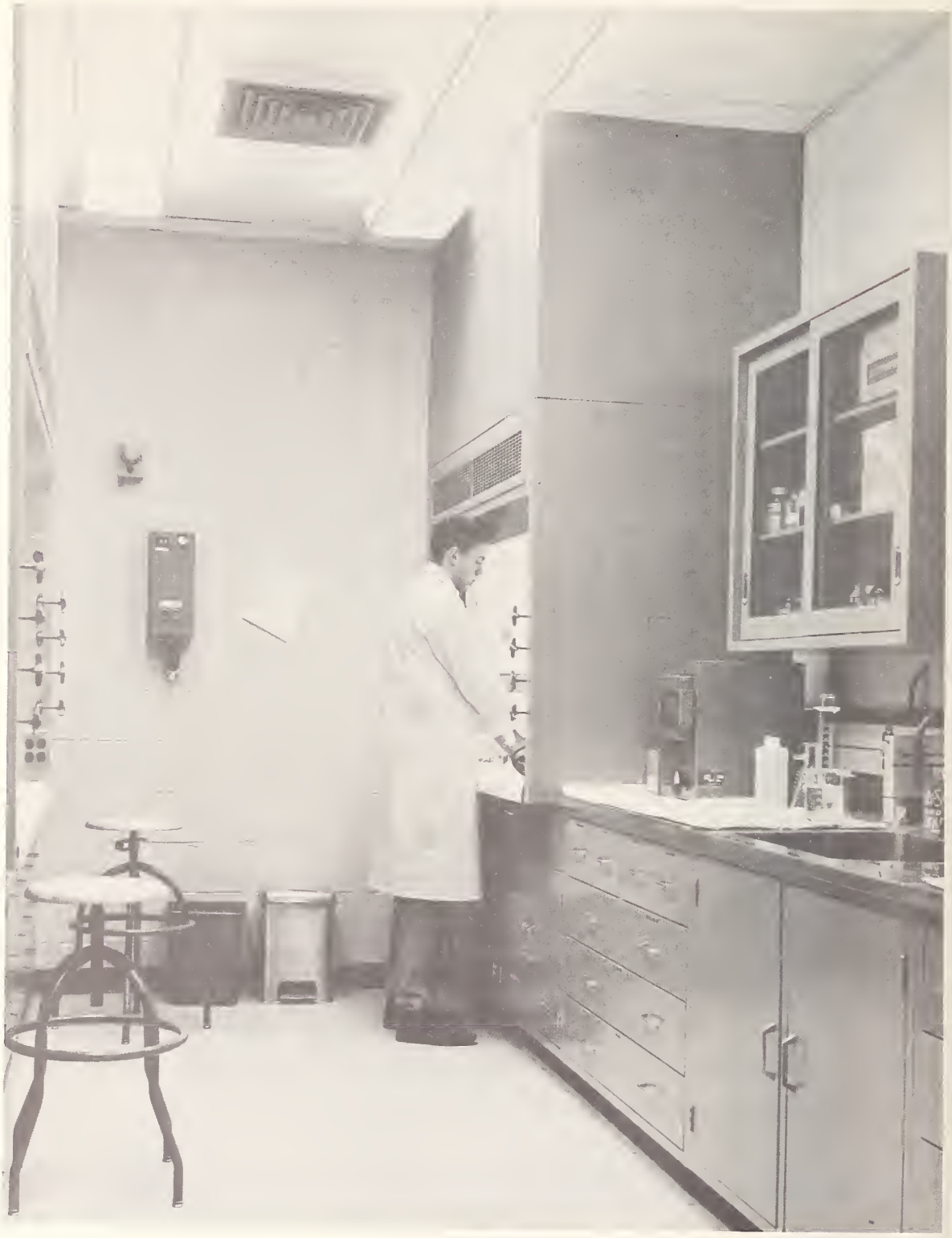

Figure 1. Typical radiochemistry laboratory
B-Wing, Building 235

analysis sample preparation. This room, constructed of modular demountable steel panels, has working dimensions of approximately 15 by 22 feet, and an anteroom for change to particulate-free clothing. The room uses the horizontal laminar air-flow principle, with all air filtered through "absolute" filters to reduce impurity dust to a minimum. A hood, benches, and glove boxes are located in the room for chemical and physical operations. It is anticipated that the use of this clean room will assist in the attainment of a new dimension in the sensitivities for activation analysis for trace constituents in many materials.

As discussed in the previous annual progress report [1, pp 2 and 3], we plan to extend the pneumatic tube system to include five new terminals in the NBSR. These will include two in the top of the core, one in the fast flux converter thimble, one in the thermal column and one in a liquid nitrogen cooled terminal. At least one receiver and sending device from the reactor terminals will be installed at a later date in a hood in each of the modified B-wing laboratories.

(G. W. Smith)

2. Fast Neutron Activation Facility

This facility, located in the hot cell bay (room B125) in building 235, essentially consists of a 14-MeV neutron generator housed in a biological shield. It also includes provisions for incorporation of pneumatic transfer systems, associated counting equipment and essential services.

a. Neutron Generator. The Activatron 210* (Technical Measurement Corporation) neutron generator (figure 2) is capable of a maximum deuteron beam current of 500 μA producing a maximum output of 2×10^{10} $n \cdot s^{-1}$ at the tritium target. The maximum usable flux is of the order of 3×10^{9} $n \cdot cm^{-2} s^{-1}$. Neutrons are produced by bombarding a tritium loaded target with 150 keV deuterons producing the $^{3}H(d,n)^{4}He$ reaction. The neutron output is essentially monoenergetic and isotropic.

* For disclaimer of equipment and materials see last paragraph of preface.

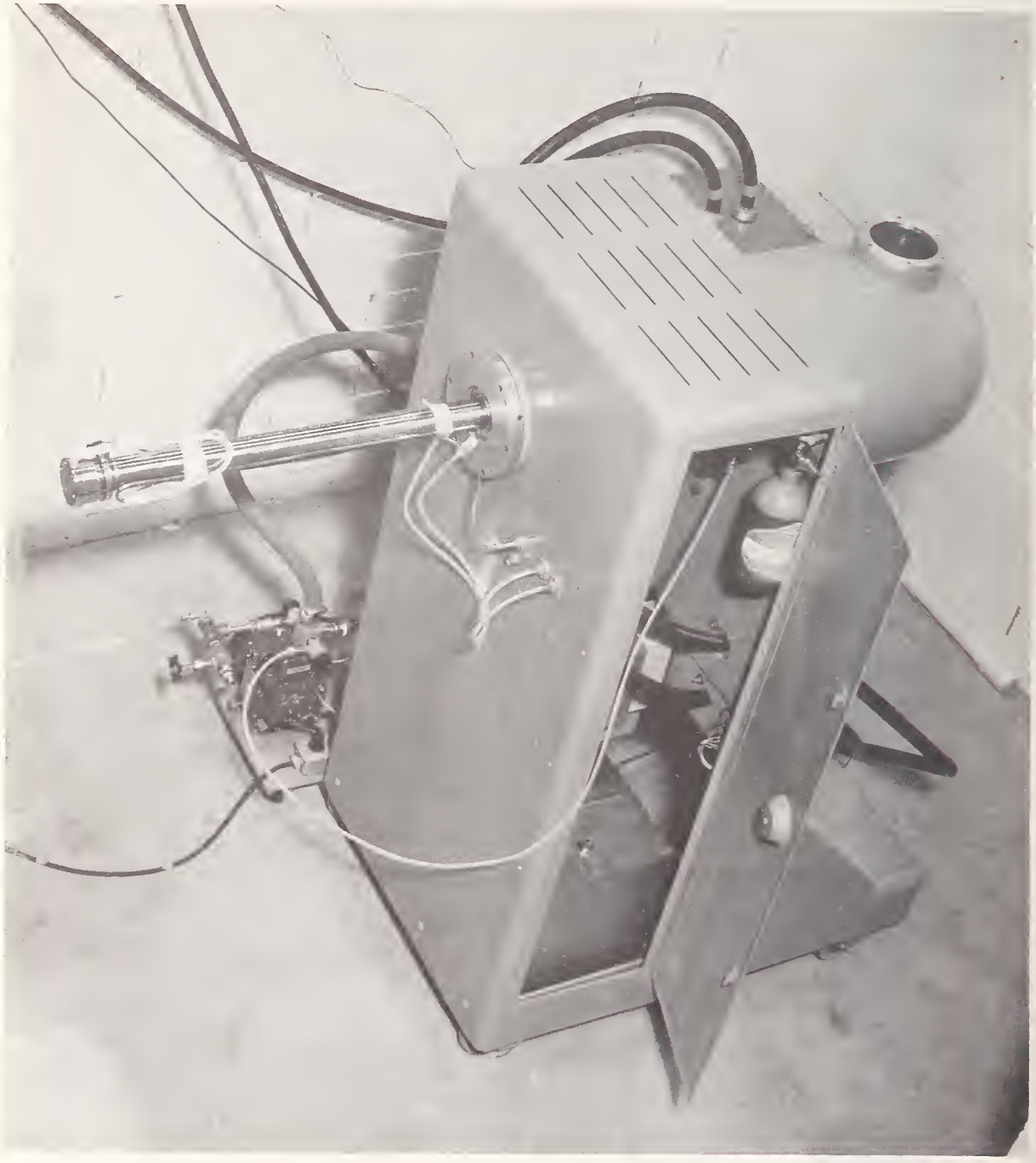

Figure 2. Neutron Generator

The accelerator is assembled and operating. Preliminary evaluation of the machine using a beam of hydrogen gas shows it to be capable of its rated beam output. Over a period of about two hours, the beam is found to be stable within ±5% at peak beam intensity and ±3% at 50% beam intensity.

b. Biological Shield. The protective shield (figures 3 and 4) occupies an area approximating 450 square feet. It consists of a 7 ft high and 32 in thick outer wall within which is enclosed an inner shield which is approximately 6 ft 4 in high and 24 in thick. The inner shield encloses a 2 ft x 4 ft x 5 ft deep experimental well over which slides a 16 in thick overlapping lid.

Figure 3. Outside view of biological shield and console

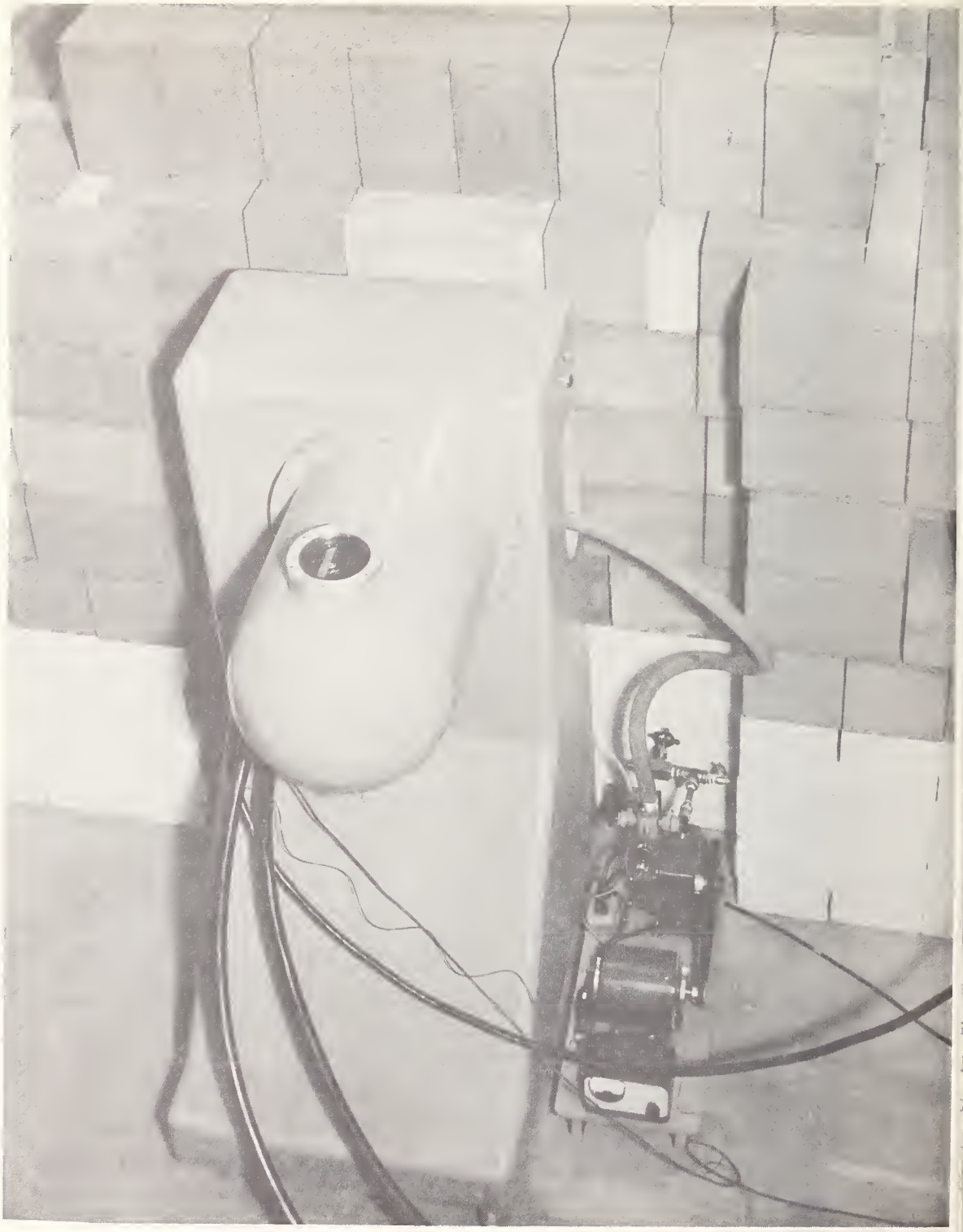

Figure 4. Inside view of biological shield showing neutron generator in position

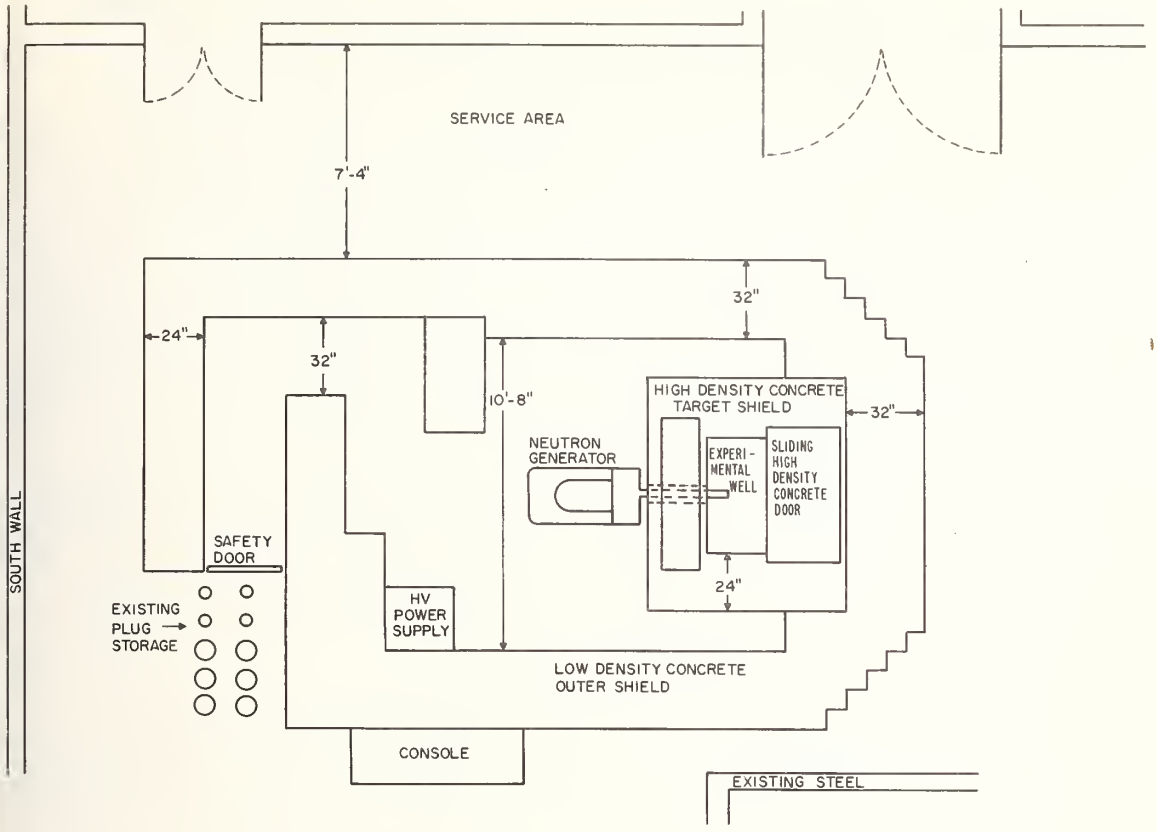

Figure 5. Floor plan of biological shield

The outer structure is constructed from 4 in x 8 in x 16 in standard concrete blocks ($\simeq$130 lb/ft^3) stacked in an interlocking pattern. The bulk of the inner shield is identically stacked using 8 in x 8 in x 12 in iron aggregate high density blocks ($\simeq$180 lb/ft^3). Entry to the facility is made through an interlocked safety door. Allowance has been made in the inner shield for exit and entry of the pneumatic tubes. A view of the plan for the biological shield is shown in figure 5. Except for the high density blocks, the entire shield structure is painted with water-sealing paint.

Except for the lid over the inner shield and the safety door, the entire structure is essentially complete and ready to house the neutron generator. Design and construction of the lid and safety door are in progress.

c. Pneumatic Transfer System. The primary system design includes a special dual-birotational sample target assembly. The system controller design allows for simultaneous irradiation and sequential counting of the standard and unknown between two 4 in x 3 in NaI(Tl) scintillation detectors connected to a 400-channel pulse height analyzer system. Other significant details include irradiations in a nitrogen atmosphere, manual and semiautomatic operation modes, and a sample spinning device. A general block diagram (figure 6) illustrates the design layout of this system.

The rotating target assembly is essentially complete and awaiting motor driving mechanisms. The controller is partially designed. The operating sequence of the entire system has been worked out and is ready to be incorporated in the controller design.

Provisions have been made for the proper handling of tritium targets in a glove box during installation and disposal. The exhaust from the roughing pump will be vented via the glove box exhaust.

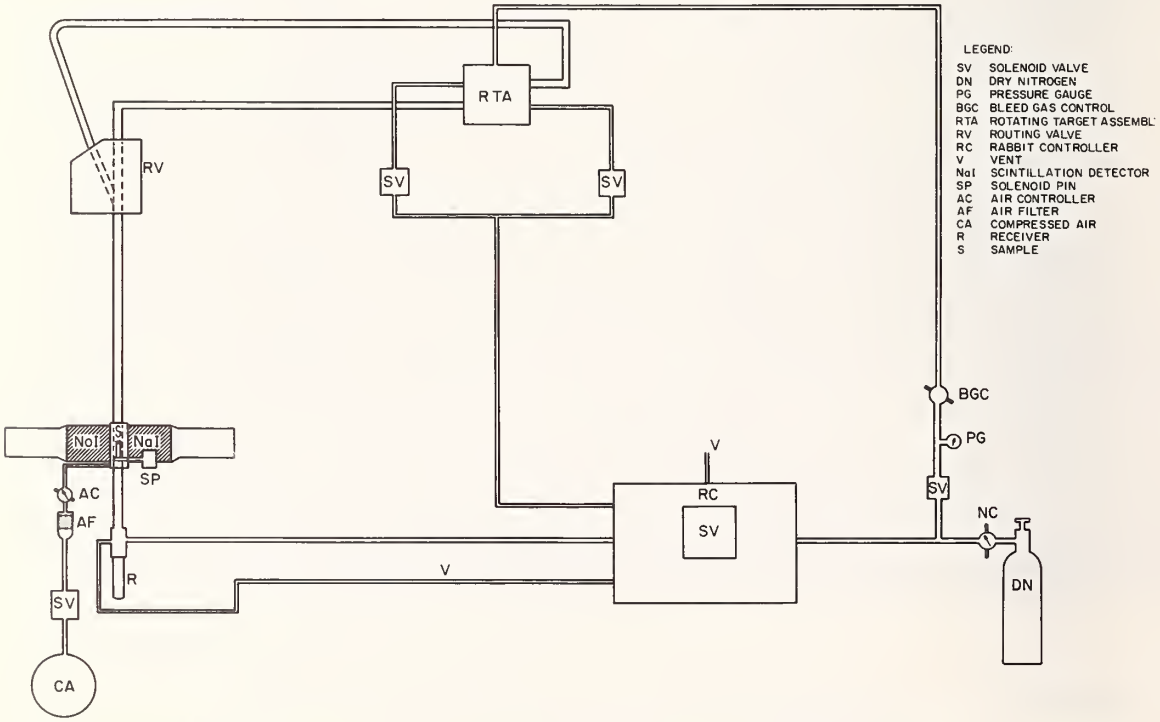

Figure 6. Schematic design of pneumatic transfer system

A compressed air line (70 lb/in^2) and essential electrical services have been provided.

(S. Nargolwalla and G. W. Smith)

3. The NBS Linac

A forty-kilowatt microwave linear electron accelerator has been installed in building 245 at the NBS Gaithersburg facility. By utilizing suitable radiators to intercept the electron beam, large quantities of high energy bremsstrahlung can be generated. These high energy photons can induce photonuclear reactions in many elements, giving rise to radioactive products. We have designed and constructed a bremsstrahlung target and associated pneumatic transfer equipment and are currently testing it.

a. Target. The electrons from the accelerator enter the target assembly through a three-inch diameter titanium window of 0.003 inches in thickness. The photon producing targets consist of six tungsten discs, 2 inches in diameter and 0.008 inches in thickness. Since pure tungsten has a tendency to flake, 100 microinches of gold has been plated on the discs to prevent contaminating the cooling water.

The tungsten discs are held in position by stainless steel plates which maintain a separation of 0.125 inches between the target elements. This is for circulation of cooling water. Three inches of water behind the last target plate absorb most of the electron beam not converted in the tungsten.

Since the total mass of the target assembly is susceptible to heating by scattered radiation, a stainless steel water jacket surrounds it. Iron-constantan thermocouples monitor the temperature of the target assembly as well as the rest of the apparatus.

The flow rate of cooling water through the target can be adjusted remotely by means of a motor driven assembly coupled to gate valves in the inlet line.

b. Pneumatic Transfer System. A pneumatic system with several receiving locations is being installed for transfer of the sample to and from the target area.

The terminal section at the target end is located directly behind the target assembly. The sample, upon arriving at the irradiation position strikes a microswitch actuating arm providing a positive signal of its arrival.

Air is injected into the terminal tube at a tangent to the tube about one inch below the tube. This spins the rabbit, cooling it and allowing a more homogeneous irradiation. At the end of a preset irradiation, the spinning air is automatically turned off and return air turned on, bringing the sample back to the desired receiving location.

c. Beam Absorbers. It is necessary to absorb the intense photon and associated neutron flux produced in the target to prevent activation and thermal damage to the environment of the assembly. The target and sample terminal are surrounded by an annulus of high purity, water-cooled lead in a stainless steel jacket. Three inches of lead surround the target assembly and sample terminal on the side and nine inches absorb the direct photon beam.

Details on the design of this system will be published at a later date.

(F. A. Lundgren and G. J. Lutz)

4. Naval Research Laboratory (NRL) Nuclear Reactor

In anticipation of the extensive program in neutron activation analysis to be carried on at the NBS reactor when it becomes operational, a small program was started in 1964 utilizing the facilities of the Naval Research Laboratory nuclear reactor, located in southeast Washington, D. C. The primary objective of this program was to gain experience in the experimental aspects of neutron activation analysis. A secondary objective was to carry on as much of a program in research and actual analysis as possible, the samples primarily originating either with the NBS Standard Reference Material Program or as service analyses.

The NRL Reactor is a 1-megawatt swimming pool type, with a rectangular core grid currently using 30 grid positions. Three in-core irradiation positions are available (Glory tubes Nos. 1, 1A, and 2) at a thermal neutron flux of approximately 8×10^{12} $n \cdot cm^{-2} s^{-1}$ and a gold-cadmium ratio of 2 to 3. In addition, two pneumatic tube terminals are located on graphite ledges above and to each side of the core. These pneumatic tube terminals have a thermal neutron flux of about 0.8×10^{12} $n \cdot cm^{-2} s^{-1}$ and a gold-cadmium ratio of 11.0. It has previously been reported that these pneumatic tube irradiation positions have a significant neutron flux gradient in both the vertical and horizontal directions [1, p 41]. The Analytical Chemistry Division of NBS leased a radiochemical hood and associated space in the radiochemistry laboratory located in the NRL reactor building. This has enabled the use of our own detector system and multi-channel analyzer for the analysis of very short-lived radioisotopes (e.g., 17.5 s ^{77m}Se, and 19 s ^{197m}Hf) and allowed radiochemical separations when necessary with a minimum of delay (figures 7 and 8). A pneumatic tube delivery terminal located just outside the radiochemistry laboratory, with an opening through the wall for rapid handling of irradiated samples, has been indispensable in the analysis of short half-life radioisotopes (figure 8). The 3 in x 3 in NaI(Tl) detector used for routine counting is enclosed in a 2-in lead brick shield. A second 3 in x 3 in NaI(Tl) detector shown immediately above the lead shield in figure 8 may be used together with the first detector for gamma-gamma coincidence counting upon removal of the roof of the shield. For further details see the experimental section below.

(D. A. Becker and G. W. Smith)

Figure 7. Radiochemical hood and counting equipment in the NRL radiochemistry laboratory

OFFICIAL UNITED STATES NAVY PHOTOGRAPH

Figure 8. Pneumatic tube terminal and detector shield in the NRL radiochemistry laboratory Official United States Navy Photograph

5. Digital Computer Facilities

The common facility that has an extreme impact on the function of all of our projects is the digital computer facility. We are continuing to emphasize the use of the multistation approach and find that this system is the most practical for our purposes. We are using the system described in last year's report [1] with the exception that the computer center is now located at the site of a computer service center in the Washington, D. C. area. One problem which occurs with the multistation teletype console use is the data transmission time. At ten characters per second the transmission time for large numbers of gamma-ray spectra can amount to hours per day. The use of a leased-line Tel-pak installation can remove this problem since transmission in the ten-kilohertz range can be realized. Costs for a central data transmission system of this type are not excessive. From the user's point of view, the computer is thus brought into the laboratory and is immediately available. Not only is this extremely valuable in getting the computing work done, but it tends to stimulate ideas on how experiments can be better accomplished to make use of this rapid calculating ability.

a. Least Squares Calculations. We have programmed the computer to do a variety of calculations of interest in activation analysis. Among the most useful of these computations are those of least-square solutions. Program GAUFIT utilizes the procedure described by Robinson [5] for fitting a gamma-ray photopeak to a Gaussian distribution by an iterative least-squares approach. Another program has been written to analyze complex decay curves. We are currently inserting the procedure described by Cumming [6] for iterative determination of the decay constants. We have programmed the computer to fit complex gamma-ray spectra with up to 50 subgroups using up to nine standards.

b. Other Computations. The computer has been programmed to do spectrum stripping. This stepwise analysis is

particularly suitable for the time-shared computer system, as the almost conversational communication between user and computer allows for detailed examination of the analysis as it proceeds.

We have programmed the computer to do a variety of other calculations such as plotting data, selecting optimum time for irradiation and decay in an activation analysis, maintaining inventories of radionuclides, gamma-ray photopeak integration with correction for decay and normalization to flux monitors, and correcting for flux perturbation during an irradiation.

(G. J. Lutz and J. R. DeVoe)

B. Analyses with Nuclear Reactor

1. Determination of Copper in Standard Reference Material 82b Nickel-Chromium Cast Iron by Gamma-Gamma Sum Coincidence Spectrometry

a. Introduction. The element copper is often easily determined as a minor constituent in an iron matrix by the neutron activation analysis technique. However, it was found that this particular sample presented a number of problems. Nickel-chromium cast iron Standard Reference Material SRM 82b contains a total of eleven elements, with 1.2% nickel and 0.75% manganese along with the 0.03% copper (table 1).

Conventional nondestructive neutron activation analysis for copper in this matrix is beset with difficulties. Two copper radioisotopes are available for use, copper-66 and copper-64. The copper-66 radioisotope (5.1 min $T_{1/2}$) cannot be used because of low sensitivity and interference of the 1.11-MeV gamma ray from nickel-65, as well as the large amount of Compton continuum background due to the 1.81-MeV gamma ray from manganese-56. The copper-64 radioisotope (12.9-h $T_{1/2}$) by itself also would give extremely poor results, since the 1.34-MeV gamma ray is of very low abundance and the 0.51-MeV gamma ray from positron annihilation coincides with the Compton edge from 0.85 MeV gamma ray of manganese-56. In addition, the manganese-56 radioactivity produced by a short irradiation (10 minutes)

is more than 840 times that due to copper-64. In fact, the total radioactivity of the sample compared to the copper is such that the copper is almost completely obscured in the gamma-ray spectrum (figure 11). These conditions indicate the need for a radiochemical separation of the radioactive copper from the balance of the interfering radioactivity. However, such a separation is difficult and time consuming. Also these iron samples contain a relatively large proportion of carbon and silicon (table 1) which are almost impossible to bring completely into solution.

The best possible answer to this predicament would be the use of a rapid, simple instrumental method of discriminating against all other interfering radioactivities and to count only the copper-64 radioactivity. The technique of gamma-gamma sum coincidence spectrometry is such an instrumental technique. The detection of positron annihilation is well suited for sum coincidence spectrometry, since the 180° angular correlation of the annihilation radiation virtually assures that two 3 in x 3 in NaI(Tl) scintillation detectors in close geometry

Table 1. Approximate composition of SRM 82b, nickel-chromium cast iron

Element	Concentration (% by weight)
Iron	92.7
Carbon	2.8
Manganese	0.75
Phosphorus	0.022
Sulfur	0.007
Silicon	2.10
Nickel	1.2
Chromium	0.33
Vanadium	0.023
Titanium	0.024
Copper	0.03

will detect both 0.51-MeV gamma rays from a high percentage of the positrons emitted. Such a coincidence arrangement discriminates against all other radioactivity except radioisotopes emitting positrons or gamma rays in cascade. In addition, by setting the threshold level at 0.3 MeV, all radioactivity except gamma rays between 0.3 and 0.9 MeV is discriminated against for the gamma-ray region of interest (0.8 to 1.2 MeV). As a result of the above instrumental discrimination in favor of the positron annihilation radiation, it was expected that the 1.02-MeV sum coincidence peak could be isolated with minimal interference from other matrix radioactivity. Possible interferences by long-lived positron emitters formed by the highly probable (n,γ) nuclear reaction include zinc-65, cadmium-107, antimony-122, and europium-152m. These elements were known to be below detection in the sample under analysis.

b. Instrumentation. A schematic diagram of the sum coincidence spectrometer is shown in figure 9. Two opposed 3 in x 3 in NaI(Tl) scintillation detectors with associated sample holder were used to position the sample precisely between the centers of the two detectors, and as close to the detectors as possible (for high efficiency). The anode output from the photomultiplier tube on the detector goes directly into the summing preamplifier. The preamplified last dynode output leads into the B and C inputs of the coincidence resolver and routing unit. Then, when properly connected as shown in figure 9, the sum coincidence pulses are emitted from the blocking output of the resolver and channeled into the 0-99 subgroup of the multichannel analyzer. The noncoincident pulses enter the 100-199 (B detector) and 200-299 (C detector) subgroups of the analyzer [1].

The prompt coincidence electronic circuitry used had a slow (2 μs) resolving time. Faster resolving times were not necessary since discrimination of nuclear transition times was not of interest in this application. The prompt coincidence analyzer drives the delayed coincidence input of the

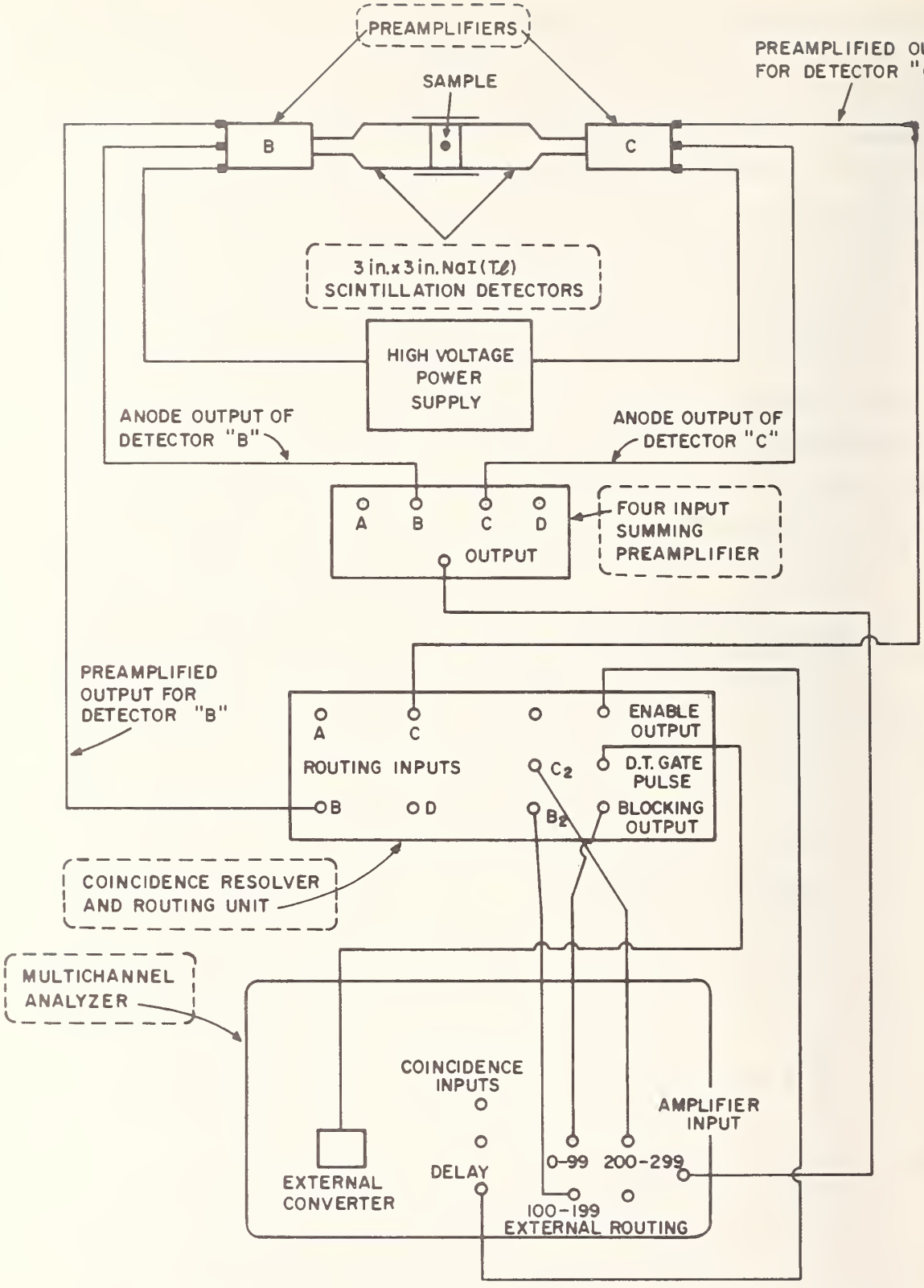

Figure 9. Gamma-gamma sum coincidence spectrometer

multichannel analyzer due to the two microsecond resolving time logic of the coincidence analyzer. This coincidence logic is appropriate for the time constants associated with sodium iodide detectors and the counting rates encountered in this work.

c. Experimental. The samples of nickel-chromium cast iron granules were held in the base of a polyethylene snap-cap vial (3/8 in diameter) by means of cellulose paper (figure 10). This vial was forced into a Lusteroid test tube for counting. The tube fit snugly into a polyethylene and bakelite sample holder, which reproducibly positioned the sample in the geometrical center of the two opposed detectors.

Several preliminary irradiations were made to compare the standard nondestructive activation analysis techniques with the proposed sum coincidence technique. After concluding that the analysis could be done nondestructively using the coincidence technique, a series of irradiations were made on samples of 100 mg to 500 mg in size to determine the effects of neutron shielding.

The actual analysis was accomplished with both samples and standards individually packed in polyethylene snap-cap vials. The samples consisted of accurately weighed quantities of the nickel-chromium cast iron (approximately 500 mg) tightly forced into the bottom of a vial with cellulose tissue. The configuration of the sample was essentially a disk with a diameter of 9 mm (the inside diameter of the polyethylene vial) and a height of about 3 mm. The standards consisted of 25 to 50 microliters of a copper solution (analyzed reagent grade copper, 99.9+%) placed on several layers of heavy filter paper in the bottom of a snap-cap vial and allowed to dry. This produced a standard with very close to the same geometrical configuration as the samples. The standards were then packed with cellulose tissue to prevent movement in the vial. Blank snap-cap vials with tissue and filter paper were made to determine the copper content of these materials. Copper foil flux monitors were

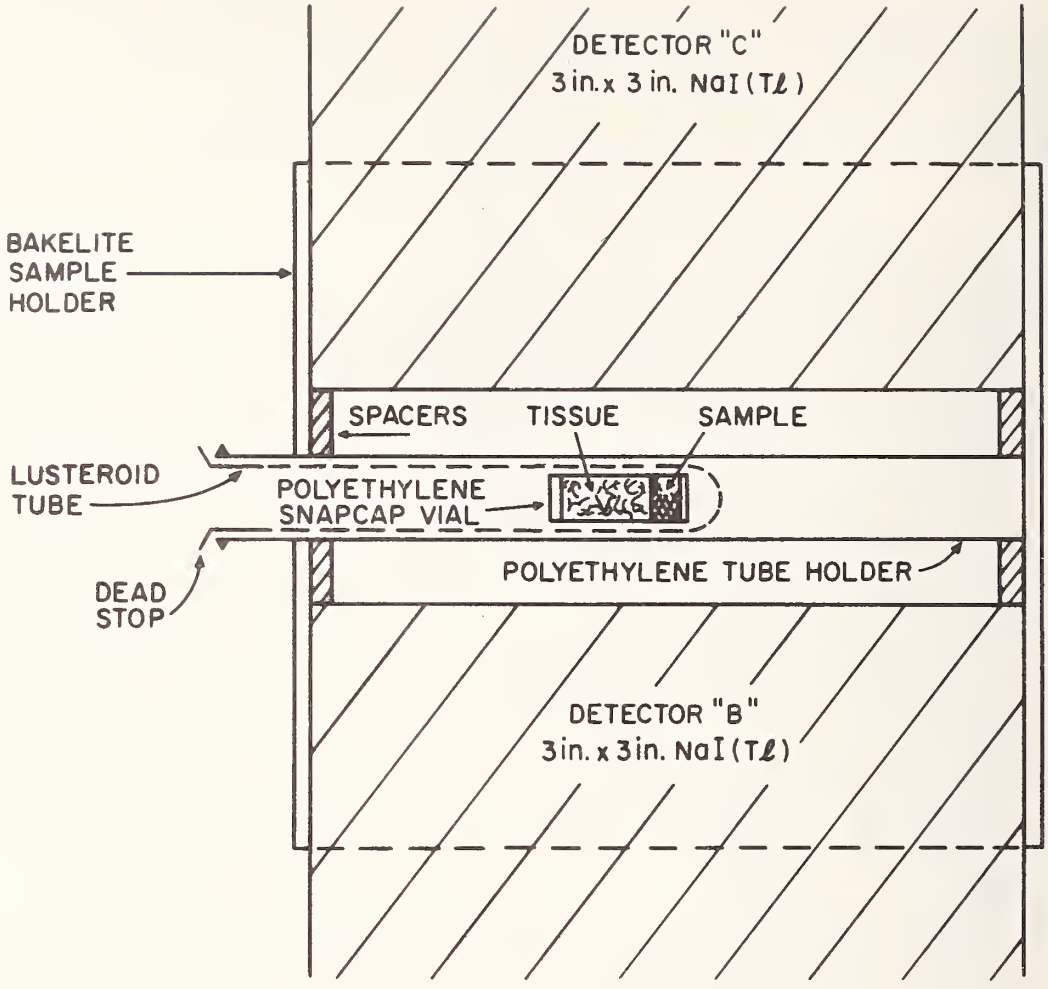

Figure 10. Sample positioning with respect to the detectors

attached to the base of the samples, standards, and blanks to normalize for neutron flux. They were then each irradiated for 15 minutes at a thermal neutron flux of 8×10^{11} $n \cdot cm^{-2} s^{-1}$ in the north pneumatic tube terminal of the NRL nuclear reactor, allowed to decay for one day, and then counted for 12 minutes in the sum coincidence spectrometer as described above. The flux monitors were counted after two days decay for 1.2 minutes, using standard gamma-ray spectrometry. The gamma-ray peaks due to copper-64 from the spectra of the samples, standards, and flux monitors were integrated and corrected to zero time.

d. Results and Discussions. The results of preliminary irradiations may be found in figures 11 and 12. Figure 11 depicts the normal gamma-ray spectrum of the nickel-chromium cast iron after 20 hours decay with the discriminator set at 0.3 MeV. The overriding radioactivity present is manganese-56, with the 0.51 MeV gamma ray from copper-64 almost completely obscured by the manganese Compton edge. Figure 12 shows the gamma-gamma sum coincidence spectrum of the same sample at approximately the same time. In this figure the 1.02 MeV sum peak from copper-64 is the primary radioactivity present and may be easily determined nondestructively with simple integration of the gamma-ray peak. The results of preliminary irradiations to determine the effect of sample size on any potential neutron self-shielding showed no significant difference in the relative copper concentration between the 100 mg and 500 mg samples. In addition, computer calculations on the neutron attenuation expected with the nickel-chromium cast iron predicted about 2% for a 100 mg sample and 3% for a 500 mg sample.

The results of the determination of copper in nickel-chromium cast iron are given in table 2. Nine analyses were made on different 500 mg samples. The average determined was 0.0317 ±0.0002% copper (± value is the S_D of the average). The values determined by the NBS wet chemical method [7] averaged 0.0376 ±0.0007% copper; the values obtained by the NBS industrial cooperators were 0.036% and 0.035% copper. These other values averaged 14% above the results for activation analysis, which suggests a negative bias in the activation analysis results. Subsequent investigation revealed the presence of such a negative bias due to gamma-ray attenuation in the sample. The preliminary irradiations of samples of different sizes was intended to reveal just such a bias. However, due to the peculiar configuration of the counting technique, the gamma-ray attenuation was not affected by sample size, but was relatively

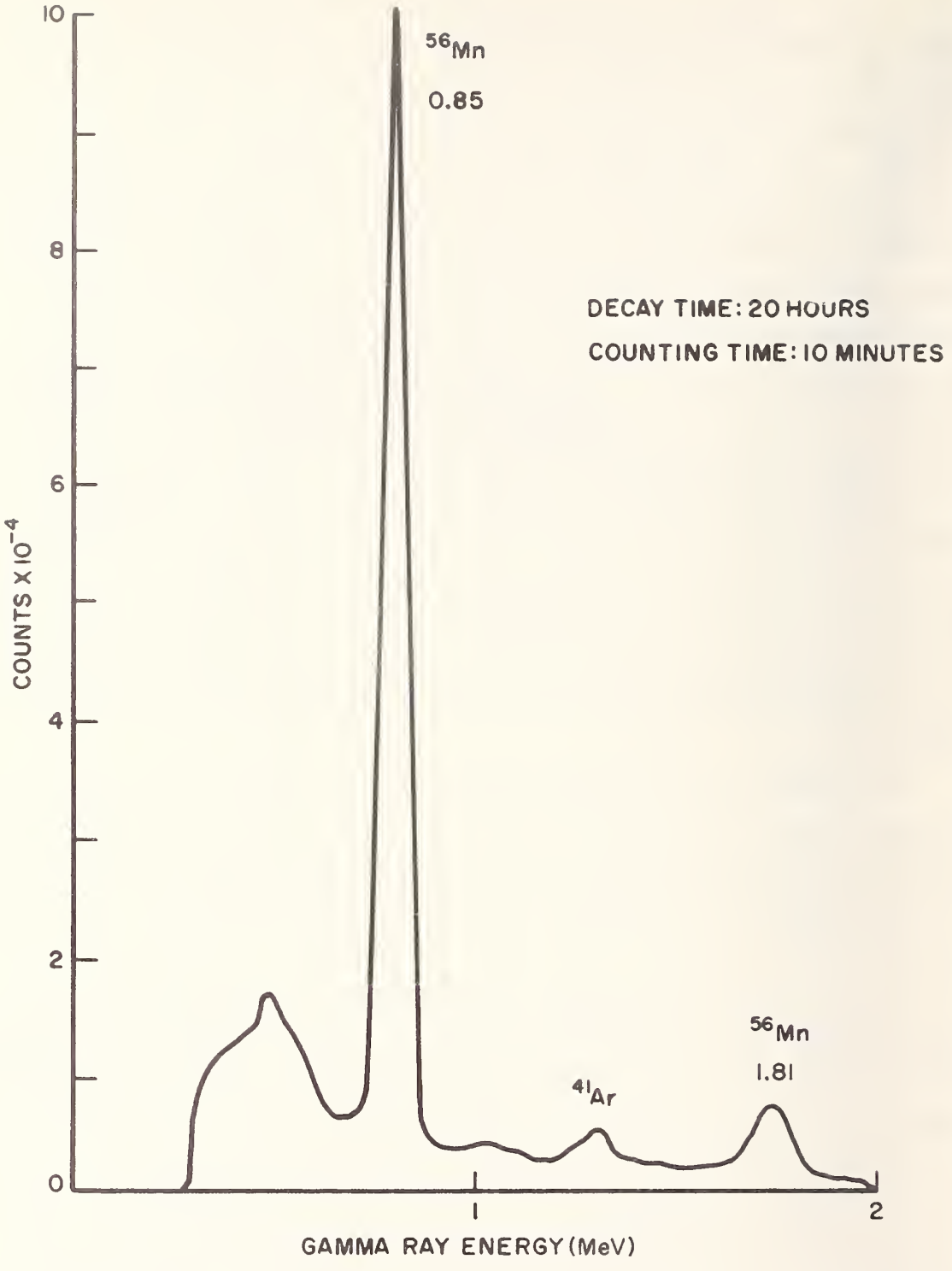

Figure 11. Normal gamma ray spectrum of SRM Cast Iron 82b

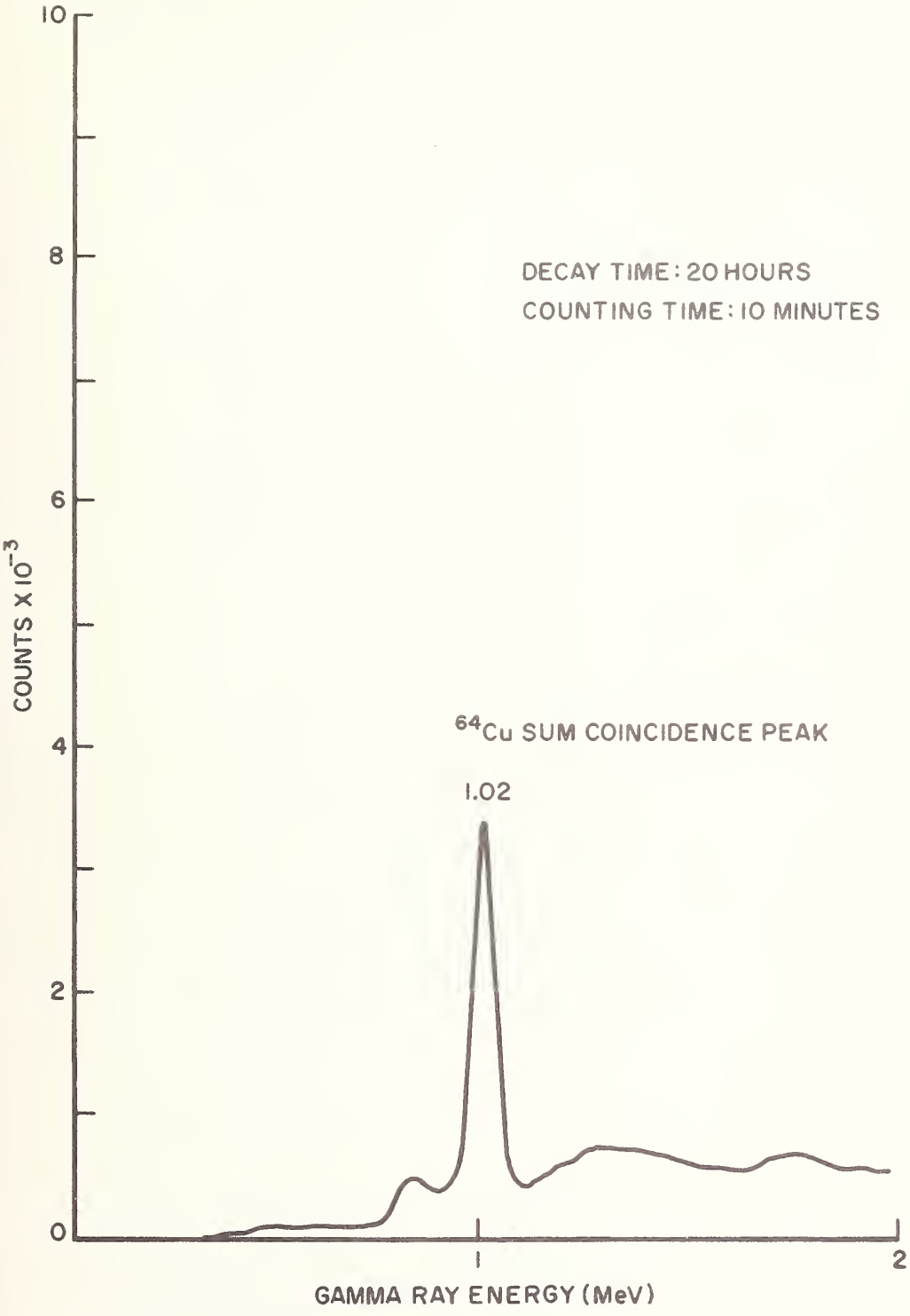

Figure 12. Sum coincidence spectrum of SRM Cast Iron 82b

Table 2. Results of Activation Analysis for copper in SRM 82b

Sample No.	Copper concentration (%) [a]	Sample weight (mg)
0093	0.0319	507.3
0094	0.0321	514.1
0095	0.0327	510.1
0096	0.0324	500.8
0097	0.0324	510.7
0098	0.0314	502.7
0101	0.0310	511.9
0102	0.0309	508.8
0104	0.0316	509.6
Average =	0.0317 ±0.00022% copper [b]	

[a] Note discussion on negative bias in text.

[b] ± value is the S_D of the average.

constant for all samples. This anomaly results from the effective sample shape of a disk, with the plane of the disk parallel to the axis of the detectors. Thus, the effective thickness of the sample is the diameter of the snap-cap vial, which is nine millimeters. This effective thickness remains the same whether the sample weight is 100 mg or 500 mg. Very rough preliminary experiments on the gamma-ray attenuation expected in such a configuration gave a value of about 10%, which is of the same order as the negative bias found in the results when the neutron self-shielding is included. This problem of gamma-ray attenuation, which has also been experienced in several other analyses, is being examined much more thoroughly. A change in the sample orientation and/or the determination of an accurate correction term should allow this gamma-gamma sum coincidence technique to be used for simple interference-free nondestructive activation analysis of copper in most matrices.

(D. A. Becker and G. W. Smith)

2. Homogeneity Testing by Neutron Activation Analysis: Determination of Homogeneity of Dissolved Metal Chelates in Military Metal-in-Lubricating Oil Standards

Testing for sample homogeneity usually requires a survey analytical technique. This is because most homogeneity testing requires rapid multiple element high precision analyses. Neutron activation analysis is not normally used as a survey instrument, since many matrices and/or components produce interferences which require tedious and time consuming radiochemical separations. However, nondestructive neutron activation analysis does permit rapid multiple element analyses in some samples. The requirements are that the element(s) of interest be determined nondestructively and that the induced radioactivity from the matrix or other components does not significantly interfere with the determination. This noninterference may result either from a low induced radioactivity level or a significantly different half-life.

The above conditions were met recently when the NBS Standard Reference Material Program required homogeneity testing of some metal-in-oil standards. These standards consist of ten metal chelates dissolved in a viscous lubricating oil (50 SAE) at nine different concentration levels. The metals were aluminum, copper, nickel, iron, chromium, silver, tin, magnesium, lead and silicon at the concentration levels of 1, 3, 5, 10, 30, 50, 100, 300, and 500 parts per million, respectively. These standards were to be used by the Defense Department in calibrating analytical instruments for the determination of engine wear in military aircraft by the analysis of their lubricating oils.

Since the organometallic chelates required a relatively high temperature for dissolution in the oil, due to their low solubility at room temperature, several questions arose concerning the homogeneity of the metals in the oil at room temperature both immediately after cooling and at the end of their estimated shelf life of six months. These questions involved deviations

from homogeneity caused by possible precipitation or colloid formation, by incomplete dissolution or mixing, or by subsequent formation of concentration gradients in the oil solution due to density variations.

The Activation Analysis Section was requested to make a survey of the relative concentrations of several elements in these metal-in-oil standards. Difficulties would be experienced in the use of most survey analytical methods in the analysis of a viscous hydrocarbon oil, especially at the lower concentration levels, but this matrix is ideal for neutron activation analysis due to the extremely low radioactivity induced by the matrix. The elements chosen for the analysis were the two most sensitive for a short irradiation and decay time, aluminum and copper. These two elements are chemically very different and should adequately represent the metals added to the lubricating oil. In addition, their decay schemes indicate that they can be determined in the presence of each other. The aluminum has a short half-life (2.3 minutes) with high energy gamma ray (1.78 MeV) and may be counted immediately after irradiation with no interference, using a gamma-ray scintillation spectrometer. The copper-64 has a relatively long half-life (12.9 hours) and the 0.51 MeV gamma ray produced by its positron annihilation may also be determined (after decay of the aluminum) with minimal interference using a gamma-ray scintillation spectrometer. Metal in oil concentration levels of 1, 50, and 500 parts per million were analyzed.

a. Experimental. The samples were prepared for irradiation by completely filling a small precleaned polyethylene snap-cap vial (2/5 fluidram size; capacity about 1.5 cm^3 [1, p26] with the lubricating oil, attaching a copper foil flux monitor in reproducible geometry, and sealing in a NRL polyethylene rabbit. The samples were then individually irradiated in the north pneumatic tube irradiation position in the NRL Reactor at a thermal neutron flux of 8×10^{11} $n \cdot cm^{-2} s^{-1}$ [1, p45].

The irradiation times were 1 minute for the 50 and 500 ppm levels, and 10 minutes for the 1 ppm level. By use of the pneumatic tube delivery terminal just outside the radiochemistry laboratory, the total decay time between the end of the irradiation and the start of the aluminum count was limited to 1.5 minutes. This interval included removal of the copper foil flux monitor (with storage of the monitor behind four inches of lead) and transfer of the lubricating oil to a clean tared polyethylene snap-cap vial. The vial with oil was then reweighed after counting in order to determine the exact amount of oil present when the sample was counted.

The counting equipment utilized was a 3 in x 3 in NaI(Tl) scintillation detector and 400-channel pulse height analyzer. The counting conditions were kept constant for each element and each concentration level, but varied among groups. The distance from the sample to the detector varied from 0.5 to 10.5 cm., which gave some control over the count rate seen by the detector. Total peak counts accumulated averaged 100,000 for the higher concentration levels and 15,000 for the 1 ppm level.

b. Results and Discussion. Preliminary irradiations showed no significant radioactivity in the pure lubricating oil (before addition of the metal chelates). Also, irradiation of the oil containing the chelates showed no significant interference in the aluminum and copper gamma ray spectroscopy.

The results of the first homogeneity test are given in table 3. These samples had been prepared less than one month before analysis. After three additional months of standing, a second test was made (table 4). Values given in both tables are "normalized Percentages" defined as:

$$\frac{\text{Relative Concentration at a Sampling Level}}{\text{Avg. Relative Concentration for 3 Sampling Levels}} \times 100$$

Tests for rejection of outlying observations were applied to the values 96.7 and 97.3% in table 3 and 91.7 and 109.7% in table 4 using the Dixon statistical criterion [8, pp. 17-3 to

Table 3. Normalized percentages of aluminum and copper in military metal-in-lubricating oil standards - first sampling

Sample No.	Concentration (ppm)	Sampling Level	Normalized Percentages Aluminum	Copper
0106	500	Upper		
0107	"	"	101.0	100.2
0108	"	"		
0110	"	Middle	100.3	100.8
0111	"	"		
0112	"	Lower		
0113	"	"	98.6	99.1
0114	"	"		
0115	50	Upper		
0116	"	"	100.0	101.9
0121	"	"		
0117	"	Middle		
0118	"	"	100.3	99.3
0122	"	"		
0119	"	Lower		
0120	"	"	99.7	98.9
0123	"	"		
0125	1	Upper	101.2	101.6[a]
0126	"	"		
0128	1	Middle	100.5	96.7[b]
0129	"	"		
0130	"	Lower		
0131	"	"	99.0	97.3[c]
0132	"	"		

[a] Cu sample 0125 only.
[b] Cu sample 0129 only.
[c] Cu samples 0130 and 0131 only.

Table 4. Normalized percentages of aluminum and copper in military metal-in-lubricating oil standards - second sampling

Sample No.	Concentration (ppm)	Sampling Level	Normalized Percentages Aluminum	Copper
0241	500	Upper		
0242	"	"	100.4	100.0
0243	"	"		
0244	"	Middle		
0245	"	"	101.2	100.9
0246	"	"		
0247	"	Lower		
0248	"	"	98.3	99.0
0249	"	"		
0253	50	Upper	100.2	100.0
0255	"	"		
0256	"	Middle		
0257	"	"	101.7	102.5
0258	"	"		
0259	50	Lower		
0260	"	"	98.2	97.6
0261	"	"		
0265	1	Upper		
0266	"	"	109.7	100.2
0267	"	"		
0268	"	Middle		
0269	"	"	91.7[a]	97.1
0270	"	"		
0271	"	Lower		
0272	"	"	98.6	102.7
0273	"	"		

[a] Rejected value - See Text, p. 31.

17-5]. The population mean and standard deviation (σ) were considered to be unknown. Using the method in the reference cited, only the value 91.7% was rejected at a level (α) of 0.05 probability. This is the probability that we would be rejecting an observation that really belongs in the group of data.

The "F" test for variability [8, pp. 4-8 to 4-9] was then applied, comparing upper to middle, upper to lower, and middle to lower in both samplings. At the 0.05 level of significance (α), no difference in variability was found between sampling levels in either table 3 or table 4. This is a 95% confidence interval estimate of the ratios of the true variances $\frac{\sigma A^2}{\sigma B^2}$, etc. between levels (e.g. A and B) of each sampling.

Mean values were calculated from the different sampling levels in tables 3 and 4 and plotted in figure 13. It is apparent that the upper points differ from the lower points by 2.2% in the first sampling and by 2.7% in the second. In order to

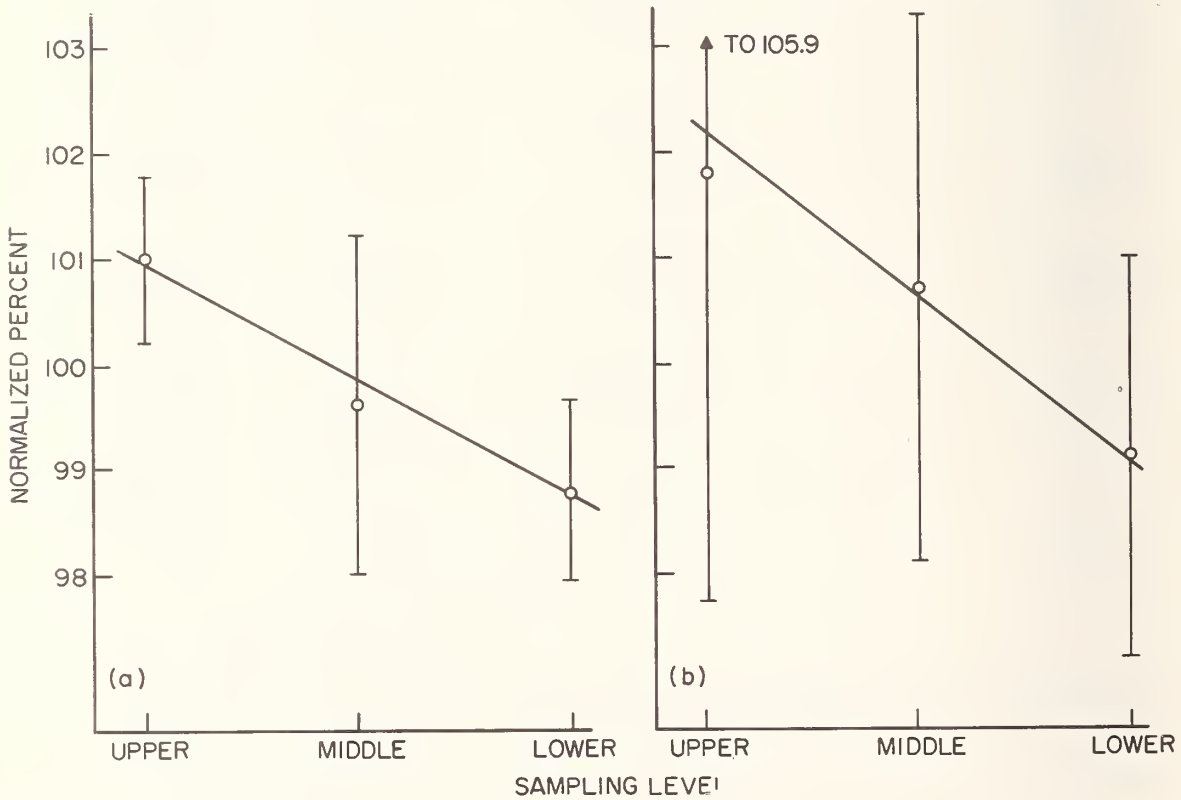

Figure 13. Plot of averaged data from first (a) and second (b) samplings with 95% confidence limits

determine if these differences were statistically significant, a short test [8,p 15-5] was applied. In the first sampling, at the 0.05 level of significance, the upper value was shown to exceed the lower. In the second sampling, the upper level did not exceed the lower at the same level of significance. Because this short test might result in "an error of the second kind," that is, not show a difference where one exists, more discriminating tests were applied. The first [8,pp 3-34 to 3-36], which assumes that the variability between levels is unknown but equal, and a second, "the method of pairs" [8, pp 3-38 to 3-40], both showed that the upper value did not exceed the lower, at the same 0.05 significance level.

The plot of the data (figure 13) shows the 95% confidence limits for each point representing a mean, and the lines drawn are estimated by eye. For no known reason, the confidence ranges of the points in the second sampling are wider.

The second set of samples also included a composite sample at each concentration level, composed of one third of each level mixed together. The results from the composite samples are compared with averages of each level in table 5. They show relative concentrations which vary from the average of the individual samples. This may be due to incomplete mixing or sampling problems.

c. Conclusion. The results indicate a slight inhomogeneity in the metal in lubricating oil standards. That the tendency should be to rise instead of settle is not surprising since the density of the metal chelates is less than the density of the pure oil.

Upon consultation with T. W. Mears and C. L. Stanley, who prepared the oils, it was found that the difference in homogeneity is within the limits of precision of the analytical technique used (emission spectrographic analysis). Data from two Armed Services laboratories showed that "within laboratory" precision (based on successive triplicate determinations on the

Table 5. Comparison of aluminum and copper composite samples with averages for same elements at 1, 50, and 500 ppm. (Data in Normalized percent)

Concentration (ppm)	Aluminum		Copper	
	Composite	Avg of Levels	Composite	Avg of Levels
500	102.3	100.0	102.1	100.0
50	98.2	100.0	97.7	100.0
1	114.9	100.0[a]	92.8	100.0

[a] Assumed to be 100.0. Value of 91.7 rejected by Dixon statistical criterion.

same sample) varied from ±5 to 10% standard deviation in 5 out of 6 cases,* for the levels 3, 50, and 500 ppm. It is therefore believed that the homogeneity as determined is sufficient for the purpose outlined.

(D. A. Becker and G. W. Smith)

3. Fast Neutron Activation Analysis

a. Introduction. Activation analysis with 14 MeV neutrons offers certain attractive features absent in thermal neutron activation work; for example, bulk matrix interference from (n,γ) products, and the possibility of second order reactions are almost completely eliminated. In this respect, analysis with reactor spectrum neutrons generally suffers seriously since many samples contain large amounts of sodium and chlorine.

Depending upon the particular element under consideration, 14 MeV neutron activation offers a choice of nuclear reactions, any one or all of which could be used in the optimization of the analytical procedure. In general, three predominant reactions can be induced, i.e., (n,p), (n,α), and $(n,2n)$. In the light elements, the appropriate selection of a reaction considerably simplifies their determination. The elements, O, F, N,

* One set of aluminum determinations at the 500 ppm level had a precision of ±2% standard deviation.

Al, and Si, are in this category. Recent developments in the field of 14-MeV neutron activation analysis indicate that this approach lends itself extremely well to the interference-free determination of oxygen at concentration levels below 100 ppm. The analysis is both rapid and nondestructive. The $^{16}O(n,p)^{16}N$ reaction is utilized, and only those gamma pulses exceeding 4.5 MeV are recorded. The entire analysis is instrumental and is completed within two minutes.

Considerable interest in the oxygen content of metals has been indicated by industry. Therefore, a number of standard reference materials have been analyzed for oxygen by analytical techniques other than neutron activation analysis. These are carbon steels (SRM 1041, 1042, 1044, 1045), ingot iron and low alloy steels (SRM 400 and 1100 series) and other nonferrous samples of interest which include some of the titanium-based alloys. These standard reference materials have oxygen content varying from 0.003 -0.1%.

The metal standards described above impose strict criteria which suitable analytical techniques must satisfy. For instance, it is desirable to express oxygen at the 30 ppm level to within ±5% standard deviation of a single determination. Accuracy should be within the precision limits.

A survey of literature on the subject reveals the great interest that has recently been generated in the search and development of precise and accurate analytical methods for oxygen. A number of nonnuclear methods, e.g. vacuum fusion, inert gas fusion, etc., although capable of high sensitivities (<5 ppm O) suffer from inaccuracies due to incomplete oxygen recovery from the sample matrix. Analytical techniques utilizing 14 MeV neutrons are found to be good to approximately 20 ppm oxygen in dense samples. However, there is a definite deficiency in the evaluation of certain nuclear measurement characteristics like flux depression parameters and gamma attenuation factors which directly affect the accuracy of the technique. In addition, nonhomogeneity of samples introduces further errors. Our

approach to these problems is being directed toward a detailed study of the effect of flux depression and gamma attenuation in thick samples in an effort to perfect a technique fully satisfying the accuracy requirements of the Standard Reference Materials Program. At the peak flux capacity of the neutron generator it is hoped that oxygen determinations will be feasible at the 100 ppm level and possibly lower with high precision and accuracy.

b. Planned Experimental Approach for Oxygen Analysis. The inherent nonhomogeneous and nonuniform nature of fast neutron fluxes as obtained from neutron generators has been the prime factor governing the design and construction of a suitable target assembly. Previous research has indicated that considerable improvement in reproducibility of analysis can be made if samples could be rotated. A target assembly which allows irradiation of both standard and unknown while rotating around two different and perpendicular oriented axes is being considered. Certain features associated with this target design will allow direct determination of correction factors resulting from flux depression and gamma attenuation with a high degree of precision. These correction factors can then be applied to noramlize the oxygen activity generated in an unknown sample to that in a basic laboratory standard. Benzoic acid (SRM 350) is one of several primary standards being considered.

In the past, the nonavailability of sample containers of low oxygen content has been a limiting factor insofar as the sensitivity of the analysis is concerned. In an effort to improve upon this situation, we have recently acquired a limited number of polyethylene snap-cap vials moulded under a nitrogen atmosphere. Hopefully, the oxygen content of such vials will be at least two orders of magnitude less than those in current use. The new vials will be evaluated carefully for both absolute magnitude and variability of oxygen content. Due precautions will be taken to exclude oxygen during sample preparation and

irradiation. The pneumatic transfer system has the capability of operating in a nitrogen atmosphere.

Special sample preparation techniques will be explored. The variation in oxygen content resulting from surface treatment will be studied. Efforts will be directed toward standardized encapsulation and treatment of samples prior to analyses.

c. Summary. The main emphasis in this program will be placed on the development of a precise and accurate technique for oxygen analysis in metal samples. Standard reference materials certified for oxygen (particularly steel) are of vital concern for use in calibration of the available methods. Umpire calibration of such methods is a key factor in obtaining high quality steels. It is hoped that the fast activation facility will contribute in this area of interest, and provide answers to questions of great importance not only to industry but also to the analyst interested in oxygen analysis of high precision and accuracy. Experience gained during this program will broaden the scope of this facility so as to incorporate analysis of other light elements such as F, N, Si, Al, etc., and at the same time allow certain fundamental nuclear studies associated with cross section measurements and fission to be pursued.

(S. Nargolwalla and G. W. Smith)

4. Production and Use of Copper Foil Flux Monitors for High Precision Neutron Activation Analysis Utilizing Short-Lived Radioisotopes

a. Introduction. In the NBS neutron activation analysis program utilizing the NRL Nuclear Reactor, several problems were encountered which preclude the simultaneous irradiation of sample and standard. First, there is a large flux gradient in the pneumatic tube terminal irradiation position (vertically 0.68%/mm; horizontally, 0.37%/mm) [1, p 46]. Thus, even if irradiated together, the sample and standard would not be in

the same neutron flux. Second, once in the pneumatic tube, no control can be exercised over the rabbit as to orientation to the high flux side. It is then not known *a priori* in which direction the horizontal flux gradient occurs and as a result a correction could not be applied. Third, many of the analyses for the Standard Reference Material Program either require or are most easily accomplished by the use of short half-life radioisotopes (e.g., 2.3 min ^{28}Al, 3.7 min ^{52}V, 18 s ^{77m}Se, 19 s ^{179m}Hf) which decay too rapidly for the standard to be counted with the sample. To overcome these problems, a system of flux monitoring was developed which would normalize the fluxes encountered under the above conditions.

The element decided upon for the flux monitor was copper. The copper-64 radioisotope of this element has a 12.9-h half-life with a high abundance 0.51 MeV gamma-ray from its positron annihilation [9]. It can thus be counted at any time up to 2 days after a 20-second irradiation at 8×10^{11} $n \cdot cm^{-2} s^{-1}$. This allows the immediate concern to be focused on the sample counting. However, the half-life is short enough so that prepared monitors may be reused after several weeks decay. In addition, copper is exceptional in that its neutron activation cross section is practically linear with energy with no large resonance peaks [10]. The relative copper activation for any neutron flux will then closely approximate the activation of the majority of the elements to be analyzed. Elements which have a high resonance integral (activation or absorption) should either use a flux monitor of the same element (standard) or careful control must be exercised over the neutron energy distribution during the irradiations. Many of the most commonly used flux monitors actually have very high resonance integrals or absorption peaks, and therefore should only be used with caution when the element of interest does not have a corresponding neutron absorption cross section (table 6).

Table 6. Useful information on commonly used flux monitors

Element	Useful radioactivity produced $T_{1/2}$	Isotope	γ-energy (MeV)	Thermal cross sec. (barns)	Resonance integral (barns)	Highest Resonance Peak[a] Cross sec. (barns)	Neut. ener. (keV)
Copper	5.1m	^{66}Cu	0.83 1.04	2.3	4.4[b]	42	2.1
	12.9h	^{64}Cu	0.51	4.5			
Cobalt	10.5m	^{60m}Co	1.33	18			
	5.2y	^{60}Co	1.17 1.33	37	75 [b]	6,400	0.135
Gold	64.8h	^{198}Au	0.41	98.8	1558 [c]	30,000	0.0047
Indium	54.2m	^{116}In	1.29	154	2640 [b]	40,000	0.0013
Iron	45d	^{59}Fe	1.10	1.1	2.1[c]	88	28
Manganese	2.58h	^{56}Mn	0.845 1.81	13.3	14.2[b]	2,000	0.350
Silver	260d	^{110m}Ag	0.66	3	1160 [b]	12,500	0.0052

[a] Neutron Cross Sections (2nd Ed.) BNL 325 (1958).
[b] Lyon, W. S., ed., Guide to Activation Analysis, Van Nostrand Co., (1964), p 28.
[c] Westinghouse Nuclear Chart, Westinghouse Atomic Power Department.

All other data taken from G. E. Chart of the Nuclides, Eighth Edition, (March, 1965).

The physical and chemical properties of copper are also excellent for this application. Copper is readily available in pure form (99.9%, reagent grade) as a foil and is quite inexpensive. It is relatively ductile, does not corrode in the usual laboratory atmosphere and will dissolve easily in concentrated nitric acid if an aliquot is desired. In addition, copper may be easily alloyed with pure lead, to form a dilute alloy for monitoring a high neutron flux. The alloy concentrations of 1% Cu-in-Pb and 0.1% Cu-in-Pb have been successfully produced and rolled into approximately 5 mil foils using a simple hand rolling mill.

b. Production and Use of Copper and Copper-Lead Flux Monitors. The copper foil used was reagent grade foil from a laboratory supply house, obtained in 5 mil thickness. A 3/16-in diameter paper punch was used to obtain disks which weighed approximately 20.5 mg each. These pure copper foil disks were then mounted on a suitable base material (cardboard, cellulose tape, or plastic) with cellulose tape (figure 14a). Tests showed no significant 0.51 MeV radioactivity from these base materials for an irradiation period of up to 30 minutes at a neutron flux 8×10^{11} $n \cdot cm^{-2} s^{-1}$.

The copper-lead alloys were prepared by placing the proper weight of copper foil and reagent grade lead into a covered vycor crucible, and by strongly heating with a gas-oxygen torch for several hours. Occasional mechanical mixing was also done with a vycor stirring rod. After thoroughly alloying the metals, the alloy was poured into an appropriate mold to produce a small ingot. Each ingot after annealing was rolled into a foil approximately 5 mils thick using a small hand rolling mill. The foil was then cut or punched into a suitable sample size using a scissors or paper punch. These foil disks may then be fixed on a suitable base material or left as prepared for affixing to the sample container. The cardboard as used for the pure copper foils was not a suitable base material for the copper-

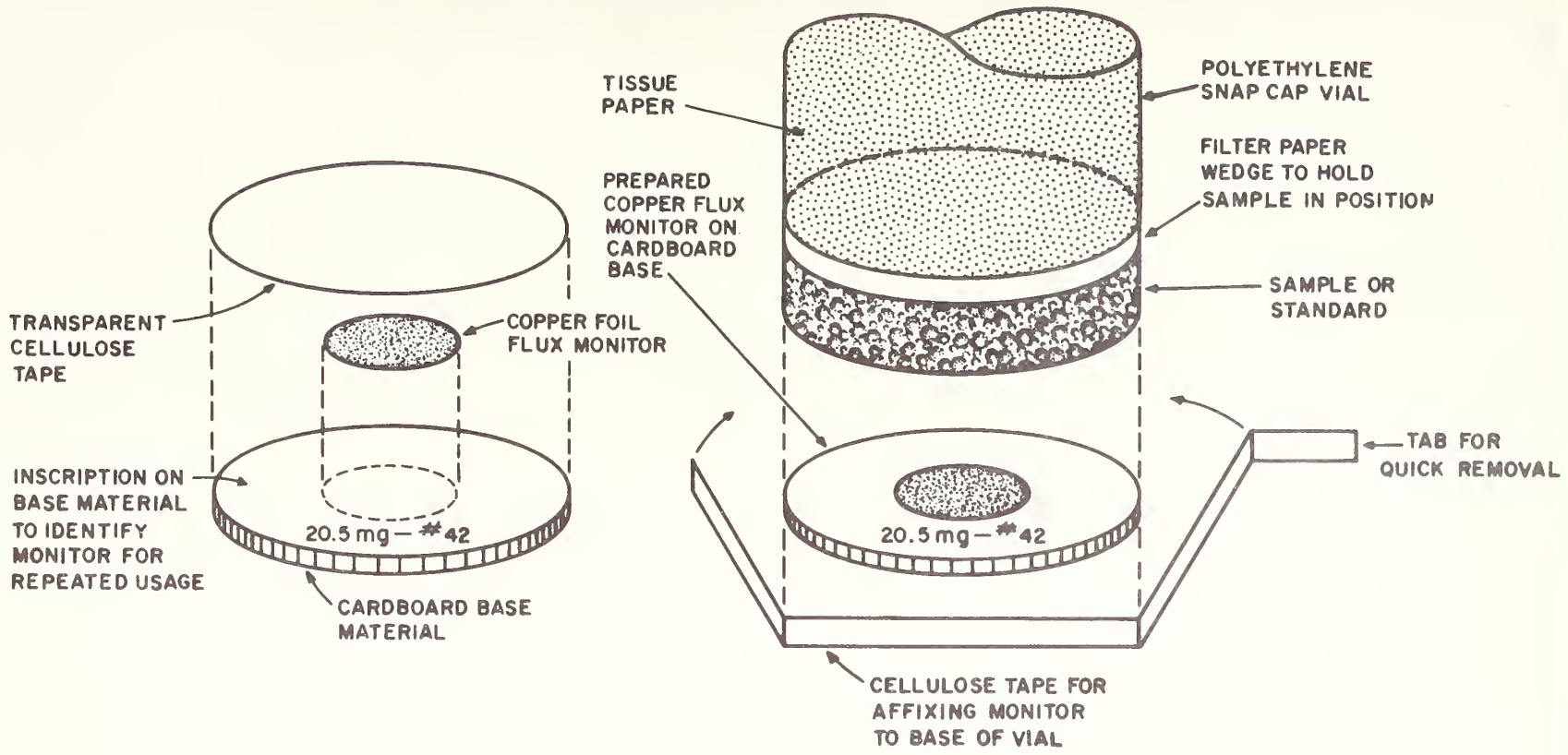

Figure 14a. Exploded view of copper foil flux monitor mounted on cardboard base

Figure 14b. Exploded view of a copper foil flux monitor attachment to a sample container

lead alloy monitors, since upon irradiation in the higher neutron flux it contributed a significant fraction of the total radioactivity formed. Several thicknesses of cellulose "magic mending" tape seem to contribute no radioactivity in the gamma-ray region of interest, however. The use of a base material (or tape encapsulation) does permit easy reuse of the flux monitor, and does permit easy marking of the monitor as to identification and monitor weight.

The absolute copper content of the alloy need never be determined if the comparator technique is used for the actual analysis. Once it has been established that a good alloy has been produced, the weight of the alloy gives the relative amount of copper present in the flux monitor. In this case the same alloy should be used for a given series of determinations.

Use of the flux monitors, once they are prepared, entails affixing them to the sample (standard) container as desired. In this work, the samples and standards were encapsulated in polyethylene snap-cap vials (figure 14b)[1, p 26] which have a flat, circular bottom of 3/8-in diameter. Cardboard base material was used for the copper foils, with the 3/16-in foil disk exactly centered in the middle of the 3/8-in diameter cardboard disk and kept there by cellulose tape. Then, by fixing the cardboard monitor to the base of the vial, as shown in figure 14, the foil flux monitor is held securely in position exactly in the center of the vial base and up against the base. The monitor may be held in place with a narrow strip of cellulose tape, leaving a tab on one end so that the tape, monitor, and base may be quickly removed from the sample. Using this technique it was possible to begin counting a sample only 30 seconds after the end of the irradiation.

c. Results and Discussion. The results of the use of these foil flux monitors are found in table 7. Sample A gives the reproducibility of the counting technique exclusive

Table 7. Flux monitor reproducibility

Sample	No. of counts (samples)	Experimental S_D (%)	Counting[a] statistics S_D (%)
A) ^{137}Cs std.- repeated counts of stationary standard	6	0.22	0.14
B) Flux monitor - repeated counts of same sample (reproducibility of positioning)	6	0.40	0.20
C) Copper foils - six foils irradiated together	6	0.65	0.14
	6	0.51	0.14
	6	0.60	0.14
Average		0.59	
D) 0.1% Copper-Pb alloy - 10 foils irradiated together	10	1.43	0.32
" " " " 10 " " "	10	0.81	0.32
" " " " 6 " " "	6	1.00	0.17
Average		1.08	
E) Variation of neutron flux observed[b]			
	12	0.58	0.25
Irradiation time of 0.50 minutes	6	1.46	0.23
	9	1.52	0.62
	12	0.71	0.23
Irradiation time of 1.25 minutes	12	1.74	0.22
Irradiation time of 2.0 minutes	13	2.05	0.10
Irradiation time of 10.0 minutes	15	3.87	0.12
	15	1.34	0.12
Average		1.66	

[a] Counting statistics are: $\frac{\sqrt{\text{total peak counts}}}{\text{total peak counts}} \times 100 = \%\ S_D$ of counting.

[b] These values are taken from actual analysis samples - flux monitor counts.

of sample, which seems to be about 1.6 times the counting statistics. In Sample B, the reproducibility decreases slightly due to monitor repositioning. However, this increases the relative standard deviation (S_D) to only two times that due to counting statistics. In Sample C, the reproducibility decreases by a factor 4.2 times the counting statistics - probably due in large extent to an inherent error of about 0.5% in the weighing procedure used, since a micro- or semimicro-balance was not available and an analytical balance was used. The alloy foils (Sample D) show greater variation and give an average S_D of 1.08%. Thus, the above data show that by using pure copper foil flux monitors a precision of up to 0.59% S_D may be obtained in experimental neutron activation analysis with short irradiations. If the copper-lead alloy foils are used, this precision decreases to about 1.08% S_D. The poorer precision in the alloy foils is attributed to inhomogeneity in the alloy composition.

Sample E gives experimental results of a series of pure copper foil flux monitors irradiated for identical periods of time under analysis conditions. It may be seen from the average S_D of 1.66% that the NRL reactor neutron flux is fairly constant over short periods of time. However, the S_D range is from 0.58% (very close to the 0.59% of groups of six foils irradiated at the same time) to 3.87%. These data indicate that without some form of flux monitoring, it is left up to chance to determine the precision of the neutron activation analysis results. Thus, the final decision as to whether or not the extra work of producing and using a flux monitor is necessary depends on the type of analytical work that is to be done with the activation analysis technique. If high precision quantitative neutron activation analysis is desired, then a flux monitor of some sort is definitely required with each sample; and if the element itself cannot be used as a suitable flux monitor, copper in one form or another seems to be an excellent compromise.

(D. A. Becker)

5. Resonance Neutron Activation Analysis

a. Introduction. In contrast to the usual radiative capture (n,γ) method of neutron activation analysis with thermal neutrons, it is possible to induce the same reactions in the so-called resonance energy region. In the neutron energy range between 0.1 and 10^3 eV, certain isotopes, usually above Z = 30, show sharp, high intensity cross section peaks. In principle then, by the use of substantially monochromatic beams from a neutron spectrometer, a high degree of activation analysis selectivity should be possible. Such a technique is calculated to have an upper limit of about 20 eV, since the neutron intensity falls off as $1/E^2$, limiting the sensitivity. Because in most cases the resonance peaks do not overlap, interfering gamma-ray peaks from induced radioactivities will be minimized, benefiting selectivity with certain elements as will be shown below.

Using resonance data available [10,11] and a simplified Breit-Wigner relationship [12], total resonance peak integrals were calculated which revealed 20 stable isotopes with integral cross sections of 300 to 3×10^4 barns. (Elements above atomic number 83 were not considered, because of their radioactive or fissionable properties). The relationship used in the calculation was:

Total resonance peak integral (barns) =

$$I_p = \frac{2\pi^2 \lambda\!\!\!^{-2} g \Gamma_n \Gamma_\gamma}{\Gamma E_o \times 10^{-24}}$$

where: g = statistical weight factor = 1/2, except when I = 0, then g = 1.

Γ_n = neutron scattering width (eV)

Γ_γ = neutron absorption width (eV)

Γ = neutron total width (eV)

E_o = resonance energy (eV)

$$2\pi^2 \lambda\!\!\!^{-2} = \frac{\lambda\!\!\!^{-2}}{2} = \frac{4.12 \times 10^{-18}}{E_o}$$

λ = neutron wavelength (cm)

From these total peak resonance integrals and the neutron flux as a function of energy, amounts of induced radioactivity were calculated. Table 8 gives these values for induced nuclide disintegration rates and major gamma-ray peak cpm per microgram for 15 elements. Though the specific activities produced are well below those induced in conventional thermal neutron activation [13], the peak counting rates exceed the usual minimum of 10 cpm necessary for radioactivities over 1 hour in half-life [13].

More significantly, calculated signal-to-noise (gamma-ray peak to gamma-ray background, for example) values were enhanced. Enhancement is defined as the ratio:

$$\frac{\text{S/N Resonance neutron activation}}{\text{S/N Thermal neutron activation}}$$

Calculations were made comparing induced radioactivities (dps) obtained for a minor constituent in a matrix, by conventional thermal neutron activation and by resonance neutron activation. It was assumed that background gamma-ray activity was subtracted, and that in the enhancement calculation, all factors such as detector efficiency, gamma-ray abundance and peak-to-total ratio cancel out. For 1 ppm hafnium in oxygen (1 μg in 1.125 g H_2O), to form 19 s ^{179m}Hf and 29 s ^{19}O, the enhancement at saturation was 2.4×10^3. In the case of 1% of europium in lanthanum, to give 9.3 h ^{152m}Eu and 40.2 h ^{140}La after 24 hours of irradiation, the enhancement was 23. These cases are typical of the range of enhancement expected for the elements in table 8, depending upon the matrix element.

On the basis of the above considerations it was decided to carry out at the Naval Research Laboratory preliminary experiments to verify, by the use of indium and iridium foils, the calculated induced radioactivity levels. This was to be a prelude to a later more detailed investigation at the National Bureau of Standards Reactor.

Table 8. Resonance neutron activation, resonance integrals and induced radioactivity

Target Isotope	Resonance peak energy (eV)	Calc. peak res. integral (barns)	Induced radio-isotope	Half life	Radioactivity produced[a] per microgram (dpm)	Prin. γ-ray peak (cpm)[b]
^{176}Lu	0.143	9.2×10^{3}	^{177}Lu	6.8d	6.8×10^{5}	2.5×10^{5}
^{151}Eu	0.461	7.3×10^{3}	^{152m}Eu	9.3h	7.0×10^{5}	5.3×10^{4}
^{168}Yb	0.597	3.6×10^{4}	^{169}Yb	32d	9.6×10^{3}	64
^{191}Ir	0.654	2.4×10^{3}	^{192}Ir	74d	6.8×10^{4}	2.3×10^{3}
^{151}Eu	1.055	3.7×10^{3}	^{152m}Eu	9.3h	4.4×10^{4}	2.3×10^{4}
^{177}Hf	1.100	3.5×10^{3}	^{178m}Hf	4.3s	1.3×10^{4}	6.0×10^{3}
^{103}Rh	1.257	1×10^{3}	^{104}Rh	42s	2.8×10^{3}	1.1×10^{2}
^{193}Ir	1.303	1.1×10^{3}	^{194}Ir	19h	7.6×10^{3}	5.1×10^{3}
^{115}In	1.457	2.8×10^{3}	^{116m}In	54m	2.2×10^{3}	2.0×10^{3}
^{185}Re	2.156	2.6×10^{3}	^{186}Re	91h	5.6×10^{3}	4.1×10^{2}
^{165}Ho	3.92	3.3×10^{2}	^{166}Ho	27.2h	4.6×10^{2}	84
^{169}Tm	3.92	1.37×10^{3}	^{170}Tm	129d	1.92×10^{3}	35
^{181}Ta	4.28	3.8×10^{2}	^{182}Ta	115d	274	18
^{197}Au	4.906	1.2×10^{3}	^{198}Au	2.7d	576	440
^{147}Pm	5.43	6.9×10^{2}	^{148}Pm	5.4d	5×10^{2}	2.5×10^{2}
^{99}Tc	5.64	1.4×10^{2}	^{100}Tc	16s	116	87
^{178}Hf	7.80	1.83×10^{3}	^{179m}Hf	19s	6.8×10^{3}	2×10^{3}
^{152}Sm	8.01	2.12×10^{3}	^{153}Sm	47h	80	20

[a] Irradiation at 10^{14} n·cm^{-2}s^{-1} flux to saturation, or 24 hours, whichever is shorter. Also optimized by a factor of 5 to probable improved NBS reactor conditions.

[b] Calculated for parameters of principal gamma-ray (factors such as peak-to-total ratio, branching ratio, fraction unconverted transmission in 164 mg Cm^{-2} absorber) using a 5 in x 4 in NaI(Tl) well-type detector.

b. Experimental. A neutron spectrometer is in operation at the Naval Research Laboratory under the direction of R. Vogt in which beryllium, germanium, or other single crystals are used to produce neutron beams of narrow energy ranges in the 0.1 to 10 eV region and above. A generalized schematic of the neutron spectrometer used is shown in figure 15.

Foils were irradiated in the neutron beam by holding in a simple wooden jig with tape. Counting by gamma spectrometry was done using a 400-channel pulse height analyzer by means of a 3 in x 3 in sodium iodide crystal. Irradiations were made on foils of indium and iridium for periods approximating one half-life of the respective radioisotopes $^{116m'}$In (54 min $T_{1/2}$) and ^{194}Ir (19 h $T_{1/2}$). In the case of indium, the count rate of its major gamma-ray peak (1.27 MeV) agreed closely with the value as shown in table 8, when normalized to probable NBS reactor conditions, with corrections for neutron absorption. The iridium value, based on counting of the 0.328 MeV gamma-ray, was low by a factor of 10, probably caused in part by uncorrected gamma-ray absorption in the 2-mil iridium foil.

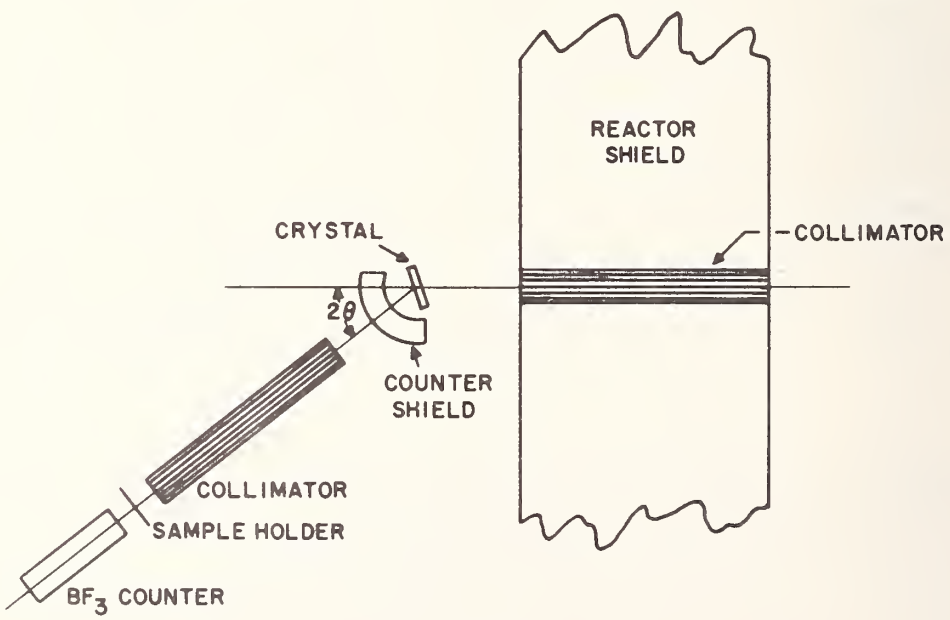

Figure 15. Schematic of neutron spectrometer

c. Conclusions. The preliminary results show promise for a unique approach to a selective method of neutron activation analysis for 15 elements, in which the matrix interference may be reduced to a minimum. It may be necessary, unless extremely thin large area foils are available, to predissolve samples and use a thin layer of solution in 2 in x 2 in square cells for the irradiation. Such an irradiation configuration will avoid excessive neutron absorption at the sacrifice of necessitating probable blank corrections. It might also be necessary to develop a method of simultaneous standard (perhaps internal) irradiation for flux normalization. In addition, use of a pneumatic terminal at such an irradiation site can be considered.

(G. W. Smith)

6. Special Analyses

a. Selenium in Standard Reference Material 1170 Selenium Steel. The analysis of a selenium steel chip was undertaken by neutron activation analysis. The selenium concentration was about 0.3%, with about 0.78% manganese and five additional elements present. The 17.5 s half life selenium-77m radioisotope was chosen, since it would give a sensitive and rapid analysis with little or no interference from the long-lived radioisotopes formed from a very short irradiation. Preliminary results showed a serious problem of gamma-ray attenuation for the 160 keV gamma-ray energy, even with the smallest practical sample size. To compensate for this, the sample and standard were put into almost identical matrices. For the sample, this consisted of dissolution and evaporation to perchlorate salts with dilution to a known volume. For the standard, a synthetic mixture of ferric nitrate and manganese dioxide was dissolved, evaporated to perchlorate salts, a known amount of pure selenium added, and diluted to volume. This resulted in a selenium standard which contained almost identical amounts of iron, manganese and selenium per unit

volume as the sample. The samples and standards were then encapsulated in polyethylene snap-cap vials. Copper foil flux monitors were attached in reproducible geometry to the samples and standards, and irradiated for 20 seconds in the pneumatic tube facility of the NRL reactor. Immediate counting, which was normalized for flux differences, gave a selenium concentration of 0.293 ± 0.003% (± value is S_D of individual value). Although preirradiation chemical treatment can result in the generation of a blank, no significant blank level was produced by this procedure. NBS wet chemical results were 0.298% selenium (by SO_2 reduction, subsequent iodimetric titration) while the NBS cooperators obtained 0.288% and 0.290% (iodimetric titration) and 0.294% (gravimetric). The average of these other analyses is 0.292_5% selenium, which compares very closely to the activation analysis result of 0.293% selenium. (This analysis will be combined with several others and published in a more complete form in the periodical literature.)

(D. A. Becker, G. W. Smith, and E. D. Anderson)

b. Aluminum in Standard Reference Material 14e Basic Open Hearth Steel. The analysis for aluminum in almost any matrix is difficult by most convenitonal analytical techniques. It is especially difficult when the aluminum is present as a minor constituent among eighteen other elements, and is partially present as refractory aluminum trioxide and aluminum nitride. The analysis was requested to be done by rapid, nondestructive neutron activation analysis since the use of this technique should overcome the above problems. The main difficulty in carrying out the activation analysis technique is caused by the presence of 0.40% manganese in the steel. The manganese-56 produced by neutron irradiation has a 1.81-MeV gamma ray which coincides almost exactly with the 1.78-MeV gamma ray from the aluminum-28. This requires decay curve analysis which may be either instrumental or manual. The instrumental technique consists of complement subtraction (using the pulse height analyzer) of all of the manganese activity

from the original spectrum taken immediately after irradiation. The manual technique consists of taking two spectra, the second after all of the aluminum radioactivity has decayed, and manually subtracting the integrated peak counts (corrected for decay) to obtain the pure aluminum activity at the time of the first count. Appropriate standards were made from pure aluminum with enough manganese added to precisely duplicate the sample radioactivity. Copper foil flux monitors were used with both samples and standards. The results gave values of 0.059_0 ± 0.0024% aluminum by the manual technique and 0.061_2 ± 0.0008% aluminum by the instrumental technique (± values are S_D of the average, number of determinations are 6 and 5, respectively). These results agree rather closely with the NBS wet chemical results of 0.061% aluminum and the NBS cooperators' results of 0.0595% aluminum. (This analysis will be combined with several others and published in a more complete form in the periodical literature.)

(D. A. Becker and G. W. Smith)

c. Vanadium in Standard Reference Material 73c Stainless Steel. A stainless steel in the form of turnings was received for analysis of vanadium by neutron activation. The aim composition of the steel was 0.032% vanadium, 12.8% chromium, 0.36% manganese, 0.12% copper and ten other elements each with a concentration of less than 0.45%. The vanadium-52 radioisotope ($T_{1/2}$ = 3.7 minutes) must be used for analysis, and this radioisotope is also formed from the nuclear reactions ^{52}Cr (n,p) ^{52}V and ^{55}Mn (n,α) ^{52}V. Preliminary experiments with pure chromium and manganese established that these elements in the concentrations present in this sample would contribute only negligible amounts of vanadium-52 radioactivity to the amount formed by the (n,γ) reaction on vanadium-51. Approximately 100 mg samples were encapsulated in polyethylene snap-cap vials with flux monitors attached. Standards were made from commercial spectrographically pure vanadium metal

(99.7% pure) and encapsulated identically to the samples. Analysis by the comparator technique yielded a value of 0.0330% vanadium, which is significantly higher than the value of 0.028% vanadium found by NBS wet chemical techniques. Extensive examination eliminated all but one probable source of error, the standard. To check this, a large piece of polycrystalline vacuum refined vanadium metal was obtained from the NRL Metallurgy Division (stated 99.95+% purity) and some purified V_2O_5 was obtained from Dr. John Taylor, of the National Bureau of Standards Analysis and Purification Section. Standards were made of each of these three vanadium sources and analyzed by neutron activation analysis for relative vanadium content. The vanadium from NRL was found to have the highest theoretical vanadium content and was assumed to be 100% vanadium. Later, NBS spectrographic analysis confirmed a metal impurity level of <0.05%. Compared to this, the "spec-pure" vanadium (stated 99.7% purity) actually had a relative vanadium content of 98.6%, and the V_2O_5 (supposedly stoichiometric) had only 98.4% V_2O_5. However, this correction was not enough to resolve the entire conflict with the wet chemical technique, so a second analysis was made with the NRL vanadium standard using the method of standard addition [14, 15, 16, 17]. In this technique, known amounts of vanadium standard solution are added to the stainless steel chip samples and the solution allowed to evaporate. This produces a standard which contains an amount of vanadium equal to that added plus the amount contained in the steel sample present. This added vanadium upon evaporation is deposited upon the entire outer surface of the steel. Since equal portions of the added vanadium should be located on opposite sides of each piece of steel, the neutron and gamma-ray attenuation seen by the added vanadium should approximate that seen by the vanadium in the interior of the steel particles. Then, when the varying amounts of added vanadium are plotted versus the count rate, a straight line extrapolation to zero count rate will give the vanadium content of steel

present in the sample. In actuality, the least squares analysis of twelve data points taken at five different total vanadium concentrations gave the value of 0.0326 ± 0.0008% vanadium (± value is S_D of least squares plot of data), which compares very favorably to the results from the comparator technique of 0.0330 ± 0.0003% vanadium (corrected for the standard vanadium content; ± value is S_D of the average). Later results for this steel by NBS cooperating laboratories gave values of 0.031 and 0.0284 ± 0.0003% vanadium, all by wet chemical oxidation-reduction titrimetry. Thus, a discrepancy still exists between the wet chemical and activation results, which cannot be explained at present. (This analysis will be combined with several others and published in a more complete form in the periodical literature.)

(D. A. Becker, G. W. Smith, E. D. Anderson)

d. Survey of Pure Titanium Metal. Neutron activation analysis utilizing short half-life radioisotopes at times requires the use of a flux monitor with a corresponding short half-life. A sample of very pure titanium (advertised purity 99.999%) was obtained from a commercial source for testing as a flux monitor. Titanium should be especially suitable in this respect since the only radioisotope produced via the (n,γ) nuclear reaction is the 5.8 minute titanium-51. In addition, the neutron spectrum has a resonance absorption integral of 3.8 barns with no total cross section peak greater than 100 barns, which should preclude strong distortion of the total titanium radioactivity by small changes in the neutron energy spectrum. To check the titanium for impurities, two samples (1.4 and 39.8 mg in weight) were cut off with a jeweler's saw, etched in ultrapure nitric acid (triple distilled from quartz) and irradiated for separate 12-minute periods at a neutron flux of about 8×10^{11} $n \cdot cm^{-2} s^{-1}$. The samples were counted on a 3 in x 3 in NaI(Tl) scintillation detector with associated 400-channel pulse height analyzer and the decay followed for

several days. The results showed a manganese impurity of about 0.5 ppm, and a very small gamma-ray peak at an energy of 0.44 MeV, probably due to gold-198. Neither of these impurities should interfere with the primary gamma ray of 0.32 MeV from the titanium-51 under the normal conditions of short irradiation and short decay time before counting.

(D. A. Becker and G. W. Smith)

e. Determination of Impurities in Pyrolytic Graphite. Recently several publications have proposed the use of pyrolytic graphite as an electrodeposition matrix for preconcentration in neutron activation analysis [18, 19, 20, 21], which is a technique that shows promise. Since its usefulness is limited by the purity of the graphite matrix, it was decided to look at the impurity levels of contaminants in a pyrolytic graphite available to us. A sample (1/4 in diameter by 1/2 in long) was obtained from Dr. R. G. Bates, of the Electrochemical Analysis Section at NBS. The vendor of this graphite was Beryllium Corp. of America, while the pyrolytic graphite used in the above referenced papers was obtained from the General Electric Corp. [21].

Two freshly cleaved samples were taken from the center portion of the graphite rod. The sample weights were 126.1 mg (sample No. 1) and 151.0 mg (sample No. 2). Sample 1 was not cleaned beyond fresh cleaving; however, sample 2 was etched in ultrapure nitric acid (triple distilled in quartz) and rinsed several times in distilled deionized water. Each were encapsulated in nitrogen-filled polyethylene snap-cap vials. The nitrogen atmosphere was necessary to reduce the adsorption of argon from the air onto the surface of the graphite before and during irradiation. Both samples were irradiated for 30 minutes at a thermal neutron flux of 8×10^{11} $n \cdot cm^{-2} s^{-1}$ in the pneumatic tube facility of the NRL nuclear reactor, and counted with a 3 in x 3 in NaI(Tl) scintillation detector and 400-channel pulse height analyzer. Subsequently, the second sample was again cleaned in ultrapure nitric acid and deionized water and reirradiated for 3.0 hours at a thermal neutron flux of 8×10^{12} $n \cdot cm^{-2} s^{-1}$ in

glory tube No. 1 of the NRL reactor. Sample handling and counting was identical to that of the previous irradiations.

The results of the determinations of impurity levels for the uncleaned and cleaned pyrolytic graphite samples are found in table 9. The uncleaned graphite (sample 1) contained sodium, chlorine, manganese and an unidentified positron emitter in significant quantities (figure 16). The irradiation of the second (cleaned) sample at a similar neutron flux and irradiation time showed a reduced sodium and chlorine content of the graphite. However, even with a cleaned graphite base, unless the gamma-ray energy of the electrodeposited element(s) was in an area of the gamma-ray spectrum free of background peaks, a background subtraction as blank correction would be required for the determination of small amounts of an element. The re-cleaned graphite sample (sample 2) when subjected to a longer irradiation at higher neutron flux (3.0 hours at 3×10^{12} n·cm^{-2} s^{-1}) produced significant amounts of radioactivity covering the gamma-ray energy range of 0 to 2.8 MeV (figure 17). In addition to the sodium, chlorine, and manganese radioactivity present in figure 16, the increased sensitivity reveals a relatively high impurity level of tungsten in the graphite. The radioactive

Table 9. Impurity levels in pyrolytic graphite[a]

	Concentrations found (ppm)	
Element	Sample 1 (uncleaned)	Sample 2 (cleaned)
Sodium	13.	0.0016[b]
Chlorine	4.2	--n.d.
Manganese	0.023	0.0091
Tungsten	--n.d.[c]	9.1[d]

[a] Graphite obtained from Beryllium Corp. of America.
[b] Identification verified by $T_{1/2}$ determination of 14.0 h ^{24}Na.
[c] Limit of detection estimated to be ~90 ppm tungsten.
[d] Identification verified by $T_{1/2}$ determinations of 21 h and 23 h for the gamma rays of 0.48 MeV and 0.69 MeV from ^{187}W.

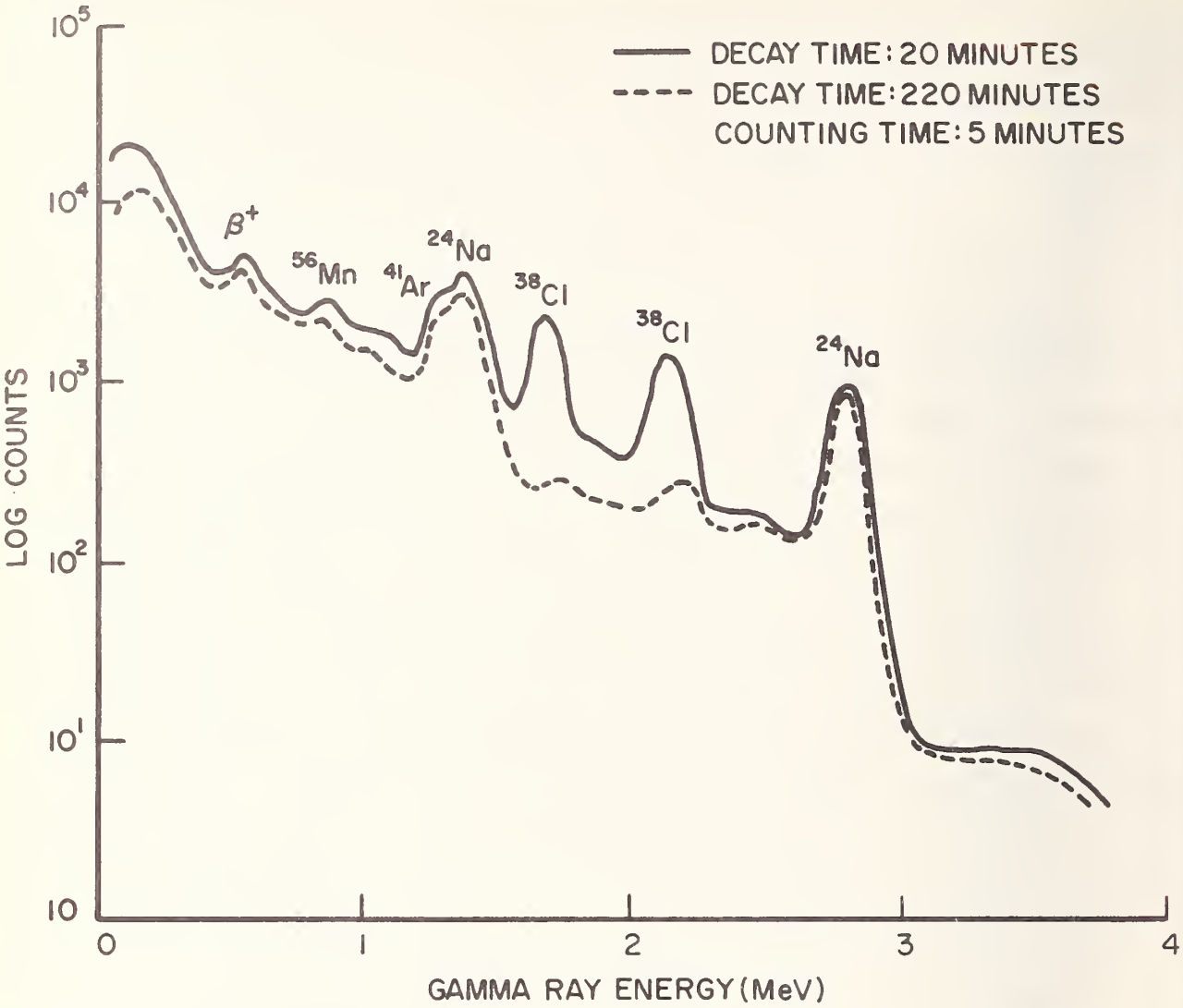

Figure 16. Impurity radioactivity in pyrolytic graphite, sample 1.

tungsten-187 produced upon neutron irradiation has a half life of 24.0 hours and abundant gamma rays from 0.07 MeV to 0.69 MeV [22]. The presence of tungsten in the graphite is probably due to containers of apparatus used in the manufacturing process.

Comparison of these values to the impurity levels to be found in the pyrolytic graphite used by Bassos, et al., is difficult, since they quoted no impurity levels and included only one spectrum of the graphite [21]. However, from this spectrum it is estimated that their impurity levels are about the same

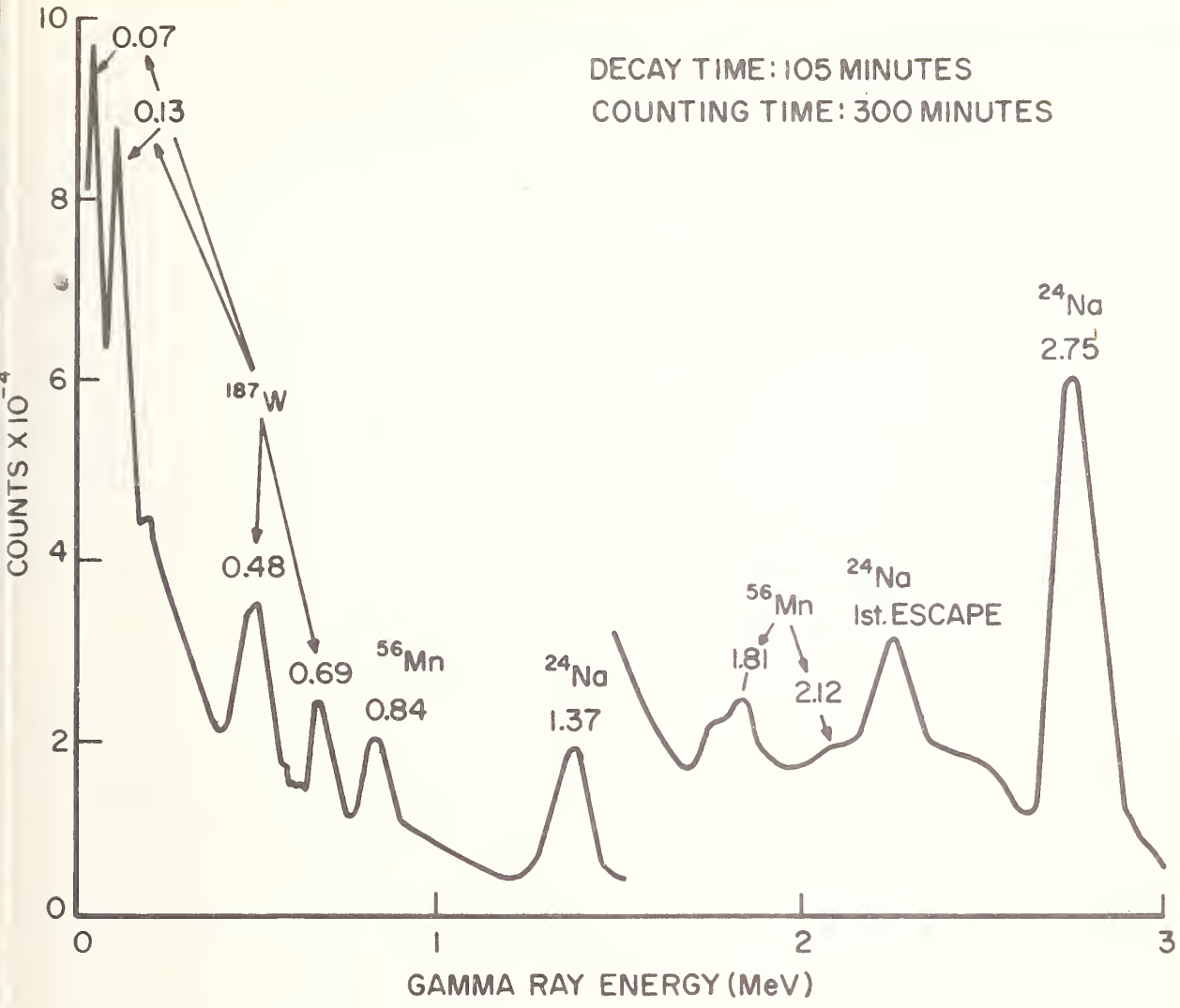

Figure 17. Impurity radioactivity in pyrolytic graphite, sample 2, second irradiation

as those found in the uncleaned graphite examined in this study. In addition, unless their spectrum is mislabeled, the presence of an aluminum-28 gamma-ray peak ($T_{1/2}$ = 2.3 min) after twenty minutes decay time would indicate an enormous impurity of aluminum, which would be very detrimental to short-lived activation analysis.

(D. A. Becker and G. W. Smith)

C. Photon Activation Analysis Using the NBS LINAC

1. Introduction

The NBS LINAC is approaching completion. A rather extensive program in photon activation analysis utilizing the accelerator is planned. We will concentrate on those analyses for which photon activation is extremely well suited. Analyses which can be done rapidly, nondestructively by this method and inconveniently by other methods will be investigated.

2. Meta-stable Isomers

A number of stable isotopes have meta-stable states with half life adequate to be usable in activation analysis. These states can be produced by inelastic scattering of neutrons, photons and charged particles. If samples containing these isotopes are irradiated with photons of energy below the threshold for particle emission, the only radioactivity produced will be that due to the meta-stable isomers. Thus, one has a potentially specific method for those elements which exhibit this phenomenon. About twenty elements can probably be determined this way. There is very little cross section data available on these reactions, but experiments by other workers indicate that one can analyze well below a microgram for many of the elements of interest. Since these isomers are induced by relatively low energy gamma rays, corrections will be necessary for the photon flux attenuation in different matrices. This will be a function of the composition of the matrix and the energy level of the isomer.

3. The Light Elements

The elements carbon, oxygen, nitrogen and fluorine are not analyzed well with thermal neutrons. This is due to very low cross sections and because in all cases except fluorine, the n,γ product of the most abundant isotope is stable. In the case of carbon and oxygen, sensitivity and reliability of other analytical methods often suffer because of the blank problem.

The most serious problem in photon activation of these elements is that their γ,n products are positron emitters. Since most elements yield positron emitters upon high-energy photon irradiation, high precision analysis of the light elements without separation would not be very reliable in many cases. In the case of carbon, nitrogen and fluorine, we would expect to design a chemical separation after irradiation. These separations would follow classical chemical methods used in the determination of these elements. In the case of oxygen, we will try to utilize either ^{16}O $(\gamma,2n)$ ^{14}O or ^{18}O (γ,p) ^{17}N reactions. ^{14}O emits a 2.2 MeV gamma radiation and decays with a 71 second half life. ^{17}N emits delayed neutrons with a 4.4 second half life.

4. Other Analyses

There are many other analyses for which photon activation should be very well suited. Among these would be the determination of magnesium by the reaction ^{25}Mg (γ,p) ^{24}Na.

Although the sensitivity of this reaction is perhaps not as high as the ^{26}Mg (n,γ) ^{27}Mg reaction, ^{24}Na is a very convenient radioisotope to count and it would appear that this reaction will be attractive for many magnesium analyses.

Iron is usually determined using the reaction ^{58}Fe (n,γ) ^{59}Fe. Because of the low abundance of ^{58}Fe and the long half life of ^{59}Fe, this is not a very sensitive analysis. We hope to improve the sensitivity of analysis for iron by utilizing the reaction ^{54}Fe (γ,n) ^{53}Fe. ^{53}Fe has an 8.5 minute half life. Chemical separation will normally be required.

The thermal neutron activation product of niobium is short-lived and has a low energy gamma ray. The (γ,n) product, ^{92}Nb, has a 10.1 day half life and an 890 keV gamma ray. A suitable delay for the decay of shorter lived activities should allow for the nondestructive determination of niobium in many samples.

Many other potentially nondestructive analyses exist via activation with a high energy bremsstrahlung beam. Judicious

selection of irradiation energy and time and utilization of solid state detectors should allow the realization of these analyses.

(G. J. Lutz)

D. Experimental Design in Activation Analysis

1. Introduction

One of the general aims of the program in activation analysis is the planning of experiments in such a manner that sources of systematic error may be recognized and eliminated insofar as is practicable. The necessity for such a study becomes apparent when one considers the increased sensitivity and improved counting precision in activation analysis, due to the availability of more intense sources of bombarding particles or radiation; accuracy has not improved correspondingly, for it is often limited by factors other than counting precision. One may attack the systematic error problem in a number of different ways. For example, the experiment may be so designed that certain types of systematic error do not arise. On the other hand, statistical parameters which originate in the treatment of the data may be used as guides to indicate the presence and nature of possible trouble. Also, by means of appropriate pre-experimental mathematical analyses, one may plan an activation experiment so that it is best designed to determine the component of interest.

In what follows we shall consider, first, methods for improving the accuracy of activation analysis in two important respects: (1) the elimination of sources of systematic error in chemical yield and detection efficiency by applying the principle of "over-all" isotope dilution, (2) the correction of external and self-absorption of gamma rays by means of a semi-empirical treatment. Next, the use and interpretation of an on-line computer program for analyzing multicomponent decay curves will be considered. Finally, radionuclide and detector characteristics, together with the statistical aspects of radioactive decay, will be considered in order to specify

"limits of detection" for given radionuclides in the presence and absence of interfering radionuclides.

2. Elimination of Certain Sources of Systematic Error

a. "Over-all" Isotope Dilution. Systematic errors may arise during chemical processing of a sample, if the recovery is less than 100%; errors may also arise in the subsequent detection process if the (relative) counting efficiency is not known accurately. Both sources of error may be minimized by an isotope dilution process whereby the "diluting" isotope is added to the sample as early as possible - perhaps even before irradiation - and is then detected along with the radioactive activation product after chemical separation and mounting have taken place. In this way the diluting isotope may give an over-all measure of chemical yield and detection efficiency, and thus serve to indicate quantitatively the amount of the activation product originally present. The usual precautions of isotope mixing and nonfractionation, of course, apply. A major reason for the feasibility of the "over-all" approach is that for most elements there are available isotopes which are not likely to be produced in the type of irradiation planned, and that there are many powerful means for instrumentally discriminating between isotopes.

The principle of over-all isotope dilution is given in equations (1).

$$R = AYE \qquad (1a)$$

$$R_d = A_d Y E_d \qquad (1b)$$

$$A = (R/R_d)(E_d/E)A_d \qquad (1c)$$

where R, A, Y, E represent counting rate, initial disintegration rate (activity), chemical yield, and detection efficiency, respectively. "d" refers to the diluting radioisotope. Note that A_d need not be known absolutely; it may simply be referred to an initial (pre-irradiation, prechemistry) counting rate where the detection efficiency is fixed. Thus, as usual, the chemical yield has no influence upon the results (unless it is

disasterously low). In addition, however, the necessity for determining absolute detection efficiencies, and therefore one possible source of systematic error, has vanished. In the simplest cases the relative detection efficiency, (E_d/E), may be constant; then equation (1c) will take the almost trivial form,*

$$A = \text{Const.} \cdot (R/R_d)$$

For example, with a number of types of radiation detector the detection efficiency is proportional (or approximately proportional) to the solid angle. In such cases, the relative detection efficiency would be independent of changes in geometry, except possibly for small corrections which could be determined with far greater accuracy than corrections in absolute detection efficiencies. Other situations where the relative detection efficiency changes (for example, due to absorption effects) are presently under consideration. Systematic errors in correction factors for relative efficiency are certainly smaller than those in correction factors for absolute efficiencies.

The approach may be illustrated by the activation analysis of ^{23}Na with thermal neutrons, using ^{22}Na as the diluting isotope. Even a nanogram of ^{23}Na will yield sufficient ^{24}Na under reasonable irradiation and counting conditions to yield a relative standard deviation due to counting of only 0.03%. It is highly unlikely that chemical processing and counting will, in general, lead to an accuracy commensurate with such an index of precision. The utilization of ^{22}Na, as outlined above, may allow one to obviate systematic errors in recovery and detection efficiency which would otherwise be limiting. ^{22}Na may be added before irradiation, if desired, since it will not be produced by thermal neutrons, and the two radionuclides may be resolved by differences in half life or gamma ray energy.

* The logical extreme of constant relative detection efficiency occurs in the use of an "internal spike", where the same radioisotope is added in order to determine the detection efficiency. The diluting isotope may nearly serve this purpose as well as correct for lack of quantitative recovery. Isotopes having similar energies but different half lives may be the most desirable.

b. Accurate (γ) Self-Absorption Corrections; A Semi-Empirical Approach. Systematic errors in the determination of relative gamma emission rates may arise unless radioactive samples and standards are counted under identical circumstances or unless great care is taken to correct for differences in geometry, external absorption and self-absorption. The corrections become more vital with increased solid angle, decreased gamma energy, and increased sample and absorber density. One approach to the problem would include a rigorous mathematical treatment which considers, for each differential volume element of the sample, the gamma peak efficiency resulting from an integration over all angles, and including the combined effects of inherent peak efficiency and self- and external-absorption for each differential solid angle. Such a calculation would then be followed by integration over the total volume of the sample. A similar calculation would have to be carried out for each sample-type and location and gamma energy, and would be far from trivial; a Monte Carlo approach probably would be in order. At the other extreme, one might determine peak efficiencies entirely by experiment. Such an approach, in principle, would yield the highest accuracy, but it might be limited by feasibility of preparing representative standards for all configurations, energies, and sample-matrices of interest. As a reasonable alternative, an approximate treatment has been pursued, in which the principle factors affecting the peak efficiency are separated into "average" values, and in which one or two semi-empirical parameters are introduced to allow an accurate correlation with experiment.

Calculations have been made in which detailed consideration has been given to the effects of geometrical configuration upon external- and self-absorption of gamma radiation. The effects of geometry on absorption and peak detection efficiency have been related, in turn, to a "mean" sample thickness, and all three factors (peak efficiency, external absorption, and self-absorption) have been combined to give

a more accurate estimate of detection efficiency. The resulting formalism is quite simple: external absorption is given by the factor, $e^{-\bar{\nu}\ell'}$; self-absorption, by $(\frac{1-e^{-\bar{\nu}\ell}}{\bar{\nu}\ell})$. ℓ and ℓ' are dimensionless and represent the sample and absorber thicknesses, respectively; and $\bar{\nu}$ represents a geometrical correction factor which depends upon ℓ and ℓ' and upon the sample-detector configuration. $\bar{\nu}$ has been evaluated for a range of configurations and thicknesses, using the GE-235 time-sharing computer.

In order to illustrate the above approach, absorption corrections have been estimated for aluminum and lead samples, each 4 mm thick, and located 2.5 cm and 11.5 cm (h) above a 7.6 cm x 7.6 cm-diam NaI detector having a 4 mm thick aluminum absorber. For each location and each element two gamma energies were considered, 0.20 MeV and 1.00 MeV. Calculated values for the external and self-absorption factors are given in tables 10 and 11, respectively.

Table 10. External absorption factor (f_a) for aluminum absorber

	h = 11.5 cm	h = 2.5 cm
0.20 MeV	0.874	0.844
1.00 MeV	0.934	0.918

Table 11. Self-absorption factor (f_s)

	Aluminum		Lead	
	11.5 cm	2.5 cm	11.5 cm	2.5 cm
0.20 MeV	0.933	0.920	0.225	0.184
1.00 MeV	0.970	0.958	0.852	0.820

To make the illustration more concrete one may estimate the resulting detection efficiencies by including published values for total and peak/total efficiencies [23]. For example,

Al(1.00 MeV,2.5cm): $\text{Eff} \approx \varepsilon_{pk} \cdot f_a \cdot f_s = (0.0403)(0.918)(0.958) = 0.0354$

Pb(0.20 MeV,11.5cm): $\text{Eff} \approx \varepsilon_{pk} \cdot f_a \cdot f_s = (0.0230)(0.874)(0.225) = 0.00452$

For highest accuracy, as stated above, the best approach is to fix the conditions for calibration (counting of the standard) so that they are identical to those for counting the sample. Generally, this may best be accomplished by dissolving the sample and counting the solution in a container which is as similar as possible in size and location as that used for the standard. If, however, varying configurations and sample matrices are to be used - as, for example, in nondestructive activation analysis - it may be difficult to achieve exact replication of sample and standard counting conditions. For this reason a semiempirical approach, using the above formalism, seems desirable. Connection between experiment and theory will be made by introducing an experimental normalization factor α_0. Normalization will take place using a convenient sample-type and reference energy. Probably the most reasonable choice for the sample will be a dilute aqueous solution of specified volume and configuration. Small deviations from the theoretical formalism with variations in ℓ (sample size and nature) or E (energy) may then be determined empirically for variations about the reference point. One may find that relatively few observations away from the reference point will be required, and that rather wide interpolation (vs. ℓ and E) will still yield sufficiently accurate values for the absorption corrections.

3. Decay Curve Analysis: Interpretation of Statistical Parameters

A computer program for the analysis of multicomponent decay curves has been prepared in BASIC for use with the time-sharing computer (See Section 2.A.5). A detailed discussion of the program, its use, interpretation, and examples are given in Appendix I. The principal point to be made here is that by careful examination of the statistical parameters which are included in the output, one may frequently locate sources of error either in the experimental data or in the model assumed.

The "on-line" aspect of the mathematical analysis leads to an enormous advantage with respect to rapid changes in model or data (where permissible) in response to such statistical indicators. Such changes, of course, must have valid physical and statistical bases.

The principal indicators of possible systematic error include: results which are negative by more than a few times the corresponding standard errors; χ^2/ν, as a measure of goodness of fit; and the magnitudes and trends of the ratios of the observed deviations of individual observations to their assumed standard deviations. (Reasonable limits for these indicators are tabulated in Appendix I.) Among the errors which may be detected are: "wrong" observations (outliers), wrong "models" (for example, missing components or incorrect half lives) and extra sources of random error. This last aspect may be of particular importance with respect to the standard error estimates for the components. The on-line "trouble-shooting" use of the program is illustrated in Appendix I, taking data from radionuclide mixtures produced in photonuclear and fission reactions.

4. Detection Limits and the Planning of Experiments

An examination of the statistical aspects of radiation detection has been carried out for two purposes: (1) to specify statistically-meaningful "limits of detection" for radioactive species resulting from nuclear reactions, (2) to plan experiments in such a manner that an optimum or satisfactory detection limit is achieved. Limit of detection is here taken to be that level at which the relative standard error for the radioactivity in question is equal to 0.50. This somewhat arbitrary criterion results from a compromise between errors of the first and second kinds. Specifically, it is equivalent to accepting about a 36% probability of failing to detect a "real" sample where the test is carried out at the 5% level of significance. It should be recognized that the detection limit, which refers to a "true"

limiting activity level, is not the same as the critical level, above which an observed result is considered significant.

In the absence of interfering radionuclides, the detection limit, A_m, may be expressed as

$$A_m = \frac{2}{\varepsilon T}\left(1 + [1 + N_b]^{1/2}\right) \qquad (2)$$

where ε represents the detection efficiency; T, the "mean" counting interval; and N_b, the number of background counts. Equation (2) assumes that the background is well known, and it applies equally well to long-lived species and to those which decay significantly during measurement. Calculations based upon the above equation have allowed the selection of "best" counting systems for long- and short-lived radionuclides depending upon the relative efficiencies and backgrounds of the various possible detectors. The form of equation (2) also allows one to specify useful lower limits for the background and its standard deviation.

For many detection systems there are continuously variable parameters, such as upper and lower discriminators which alter both the background, b, and detection efficiency, ε. As a result, in order to design the method of detection to give the minimum value for A_m, it is necessary to express b and ε in terms of the continuous variables, and to analyze the system by means of equation (2). Such an approach to a "triangular" efficiency curve accompanied by a "rectangular" background curve, for example, led to the conclusion that the minimum detection limit obtains when the discriminator includes about 2/3 of the energy interval centered about the peak. The best setting, however, does depend upon the value of N_b, and the above result applies only when $N_b \gg 1$.

When there are several radionuclides which must be observed simultaneously and resolved by means of decay analysis or spectrometry, the effects of interference upon the respective detection limits must be considered. The particular problem of decay curve analysis has been dealt with using a

suitable modification of the previously discussed computer program. The calculation cannot be carried out directly but requires an iterative procedure which is based on the general form of equation (1) and the requirement that the relative standard error of A_m be 0.50. In this way, one may determine, *a priori*, the limit of detection for a given radionuclide in a mixture having specified levels of other radionuclides.

On the basis of such a calculation, one may introduce changes into the experimental plan (different irradiation and delay times, counting intervals, detection systems, chemical separations, etc.) so as to attain a more satisfactory detection limit, if desirable. In order to serve as an illustration, a calculation has been carried out for a hypothetical experiment involving two nuclides: one considered the contaminating activity having an 18-minute half life, and the other, the activity of interest, having a 20-minute half life. Two observations were assumed: one starting at the end of irradiation and one starting 31.5 minutes later. The first observation had a time interval of one minute; the second observation, two minutes. The detection limit for the 20-minute activity at the end of the irradiation was calculated for three different situations as shown in the following table.

Table 12. Detection Limits

	18 minute contaminant initial activity	20 minute initial activity detection limit
interference-free	Absent	9.8 cpm
interference	0 cpm	740 cpm
interference	600 cpm	1080 cpm

A striking difference is seen between the interference-free case and that case where the 18-minute activity must be determined from the data, even though its contribution is zero. The difference is pronounced in the example, because the resolution

is difficult under the conditions of the hypothetical experiment. When such cases of "difficult" resolution arise, the plan of the experiment may be suitably modified - for example, by eliminating the 18-minute component or by determining it with another type of detector. One point in presenting such an extreme example is to indicate the significant effect of the possibility of interference, per se, even though the contribution of the interfering nuclide may be negligible.

By way of summary, the iterative approach is being applied to problems in activation analysis in order to (1) deduce detection limits for given procedures both in the presence and absence of specific kinds of interference, and (2) to assist in the design of the radiochemical and data-taking procedures in order to arrive at acceptable limits of detection.

(L. A. Currie)

E. Radiochemical Separations

"Radiochemical Separation of Copper by Amalgam Exchange"

1. Introduction

The radiochemical separation technique by amalgam exchange has been successfully developed for and applied to such elements as Cd, In, Zn, Bi, Pb, Tl, Sr, and Hg [24 - 32]. Symbolically, the process may be expressed as follows:

$$M^{o}(Hg) + M^{+n*}_{H_2O} \rightleftharpoons M^{o*}(Hg) + M^{+n}_{H_2O}$$

where $M^{o}(Hg)$ represents the metallic liquid amalgam and $M^{+n*}_{H_2O}$ is the radioactive metallic ion dissolved in the aqueous phase. These soluble amalgam systems have demonstrated high exchange yields with accompanying good decontamination when agitated with aqueous solutions of their respective radioactive metal ion in the presence of many interfering elements. It is desirable to expand this technique to other metals which possess little solubility in mercury.

Copper, an element only sparingly soluble in mercury [33], is often determined by activation analysis. Its high sensitivity

however, is sometimes difficult to obtain because of interfering gamma-ray activity in the 0.5 MeV energy region. A convenient method of successfully decontaminating ^{64}Cu from many elements would be desirable. Existing methods such as precipitation, ion-exchange, chromatography, or solvent extraction sometimes are not too efficient, specific enough, or must be coupled for best results [34]. Development of an amalgam exchange technique for this problem would be useful.

A liquid copper-mercury phase may be formed through electrolytic deposition of copper into mercury. The resulting mercury phase is composed primarily of a finely divided suspension of copper in an extremely dilute solution of copper amalgam. Preliminary experiments revealed that appreciable isotopic exchange readily occurred between the deposited copper in the mercury phase and radioactive cupric ions in the dilute acid solution. This was encouraging since previous investigators observed a slow, unfavorable exchange between fine copper dust and an aqueous solution [35].

In view of these results the system was investigated to determine first whether the general requirements for a radiochemical separation technique could be met. These include high overall yield, good decontamination, favorable reproducibility and convenient time of separation. This necessitated development of an optimized system derived from a careful study of all the parameters involved.

In order to understand the underlying exchange process, a kinetic study was undertaken. Parameters such as temperature, concentration, and agitation conditions were varied to help elucidate the mechanisms involved.

Finally, the evolved technique was tested for applicability on standard reference materials by activation analysis.

2. Experimental

a. Optimization Experiments

(1) Preparation and Use of Amalgam. It was found

that the best isotopic exchange yields were obtained by amalgams prepared and used within a reasonable period of time. For the preparation of a 1% copper amalgam, the electrolysis was performed at 5 to 10 volts with currents from 0.5 to 3 amperes using little stirring. When excessive agitation was employed (even under nitrogen atmosphere) the exchange yields were significantly lower. Upon completion of electrodeposition the amalgams were stored under distilled water and stirred before each use. Amalgams stored for more than a day rendered less quantitative results.

(2) Type of agitation. Various methods of intimate mixing of the amalgam phase with the aqueous solution were attempted and evaluated for percent exchange and reproducibility.

Moderate shaking at room temperature was found to give only 10% to 20% exchange in 5 minutes. A very high rate of agitation with a high speed shaker produced somewhat nonreproducible (± 20%) yields of 20% to 30% in 2 minutes with the added undesirable properties of amalgam decomposition.

An ultrasonic approach was tried by immersing the container of amalgam and solution in an ultrasonic bath (80 watt total power). This approach gave higher (50% to 90%) yields with a reproducibility of ± 4% in 5 to 30 minutes agitation in an approximately 50 °C water bath. Another procedure involved the use of an ultrasonic probe which was immersed into the aqueous phase at elevated temperatures (50 to 90 °C) and the system agitated severely at concentrated high power (75 watts). Agitation times of 5 to 10 minutes gave yields of 80% to 95% with moderate (± 2 - 3%) reproducibility; however, experimental conditions such as probe position, volume, and immersion levels were too critical for routine use.

Quantitative (>99%) and highly reproducible (<1%) yields were obtained in 10 to 12 minutes through moderate stirring ($\sim 5 \times 10^2$ r/min) of the system with nitrogen bubbling at ≥95 °C. This last approach, which is easy to manipulate and reproduce, was adopted for further study.

(3) Copper Concentration in Amalgam and Solution Phase. The % isotopic exchange was observed as a function of the copper concentration in the amalgam phase. A comparative study performed using the ultrasonic probe mixing technique at 90 °C showed 74%, 93%, and 93% exchange for 4 ml of 0.1%, 1%, and 2% amalgam using 5 minutes contact with a 20 ml aqueous solution containing 0.4 mg Cu^{++}. A similar study done with a 10-minute agitation at 95 °C showed 93% and 99.6% exchange for 0.1% and 1% amalgams interacting with 0.3 mg Cu^{++} in 20 ml aqueous solution.

Under comparable 10-minute stirring conditions with 1% amalgam at ≥95 °C the total cupric ion amount was varied and exchange yields of 99.6%, 99.6% and 94.9% were obtained for 0.32, 0.96, and 8.0 mg Cu^{++}, respectively.

These results indicate that conditions of ≥1% amalgam and ≤1 mg Cu^{++} should yield an optimized quantitative initial exchange.

(4) Temperature and Time of Stirring. Employing a volume of 20 ml 1 M H_2SO_4 containing 0.3 mg Cu^{++}, and mixing with 1% amalgam, the per cent exchange of 74%, 94% and 99.4% were obtained for 2, 5, and 10 minutes, respectively, of stirring at ~95 °C. The effect of temperature was evaluated thoroughly in a kinetic study and the data are summarized in that section.

(5) Post-exchange stripping of Copper from Copper-Amalgam. Since the radioactive amalgams, after having exchanged with radioactive ^{64}Cu solutions, gave nonreproducible and unpredictable counting results, a convenient stripping procedure was needed. A successful chemical procedure was developed which involved quantitative dissolution of the copper from the amalgam by a concentrated HNO_3-HCl mixture.

b. Optimized Procedure. A 1% amalgam is prepared by electroplating 5 g dissolved $CuSO_4$ from ~75 ml 0.2 M H_2SO_4 into 16 ml triple distilled mercury with an applied voltage greater than 6 volts and only very moderate stirring (100-200 r/min).

The resulting amalgam is stored in distilled water. In a 125 ml round bottom flask, four ml of the amalgam is agitated for 11 minutes by a fast rotation (~500 r/min) stirring rod with 20 ml 1 M H_2SO_4 solution containing less than 1 mg cupric ion. The procedure is performed while bubbling nitrogen through the aqueous phase and maintaining the whole apparatus at 95 to 100 °C in a water bath. The aqueous phase is removed, the amalgam washed with water, and then 30 ml of a 9 to 1 mixture of concentrated HCl and HNO_3 is added. This system is stirred for about 5 minutes after a dark green color appears in the aqueous layer. This copper stripping solution is removed, 10 ml more of the HCl-HNO_3 solution added and the system stirred again for 10 minutes. The second stripping solution is removed and the amalgam washed with 5 to 10 ml of 50% HCl solution. The two copper stripping solutions and the HCl wash solution are combined and diluted to a known volume. Suitable aliquots are taken for counting the 0.511-MeV peak of ^{64}Cu. The overall procedure requires about 40 to 50 minutes.

The optimized procedure described above was evaluated for overall yield and precision by performing replicate runs using 0.4 mg Cu^{++} ion. The decontamination ability was evaluated by subjecting the optimized procedure to various radioactive elements (2 mg inactive carrier each) and measuring the amount of carrier through the entire procedure. The effect of the presence of varying amounts of HCl, HNO_3, and $HClO_4$ upon the per cent yield was also evaluated. Similarly the effect of presence of macro amounts (~1 g) of some salts was evaluated for the system.

c. Procedure for Standard Reference Materials. Standard reference materials magnesium-base alloy 171 and nickel-chromium cast iron 82b were analyzed. Samples weighing from 0.2 to 0.4 g and copper standards were irradiated for one hour in a thermal neutron flux of ~8 x 10^{11} $n \cdot cm^{-2} s^{-1}$ with copper foil flux monitors. The copper metal standards were dissolved

in dilute HNO_3, taken almost to dryness in order to destroy excess acid, and then redissolved and diluted to a known volume with 1 M H_2SO_4.

After a 12-hour decay period the magnesium-base alloy was dissolved in ~20 ml 1 M H_2SO_4 and then treated according to the optimized amalgam exchange procedure. An aliquot of the standard was treated identically.

Similarly, after about 12 hours decay the nickel-chromium cast iron samples were dissolved in 20 to 25 ml 1 M H_2SO_4 with 0.8 mg inactive Cu^{++} carrier added. This was done to prevent any possible adsorption on the undissolved carbon residue. The samples were digested for ~1 hour, ~ 40 mg Zn° added and dissolved, and then the filtered solution treated according to the optimized amalgam procedure agitating for 15 minutes. The copper standard (0.808 mg) was exchanged in the presence of 0.2 g of dissolved inactive cast iron in order to approximate the sample conditions.

In all cases the radioactive copper stripped solutions were diluted to 50.0 ml, and 10.0 ml aliquots were taken for counting on a 3 in x 3 in NaI scintillation detector with a 400-channel analyzer, integrating the 0.511-MeV peak.

d. Mechanism and Kinetic Studies. In order to evaluate the influence of temperature upon reaction rate, temperatures of 1, 22, 49, 67 and 99 °C were employed and the percent isotopic exchange observed as a function of time. Volumes of 45.0 ml 1 M H_2SO_4 containing 2.0 mg Cu^{++} were agitated with 4 ml 1% amalgam bubbling nitrogen through the system. Moderate speed glass rod stirring (~ 5 x 10^2 r/min) was used. One or two ml aliquots were removed at various time intervals for measurement.

In order to evaluate the effect of change in concentration of cupric ion in the aqueous phase the concentration was increased fourfold and the percent exchange observed versus time at 67 °C.

In order to evaluate the change in concentration of copper in the amalgam phase the concentration was decreased tenfold and the percent exchange observed versus time at 67 °C.

In order to evaluate the influence of stirring rate, the rate was approximately doubled using the conditions of 1% amalgam and 2.0 mg Cu^{++} at both 49 and 99 °C.

3. Results

a. Evaluation of Technique for a Radiochemical Procedure. The technique appears to approach quantitative yields with good precision. These results and the values for decontamination from various metallic ions are shown in table 13.

Table 13. Separation of copper and contaminants by amalgam exchange

Tracer[a]	Reduction potential[b] volts	Separated[c] %
^{22}Na	Na^{+}/Na^{o}, - 2.71	0.0001
^{140}La	La^{+3}/La^{o}, - 2.52	0.001
^{54}Mn	Mn^{+2}/Mn^{o}, - 1.18	0.0001
^{54}Mn(C.F.)		0.001
^{65}Zn	Zn^{+2}/Zn^{o}, - 0.76	0.0001
^{59}Fe	Fe^{+2}/Fe^{o}, - 0.44	0.0001
^{60}Co	Co^{+2}/Co^{o}, - 0.28	0.001
^{113}Sn	Sn^{+2}/Sn^{o}, - 0.14	0.05
^{122}Sb	Sb^{+3}/Sb^{o}, + 0.15	1.9
^{64}Cu	Cu^{+2}/Cu^{o}, + 0.34	98.5 ± 0.9
^{110m}Ag	Ag^{+}/Ag^{o}, + 0.80	31

[a] Inactive amount of carrier in each case was 2 mg except for copper which was 0.4 mg. C.F. ≡ carrier free.

[b] Data taken from Latimer [36].

[c] Cu value is average of 5 runs. Error is standard deviation. Others represent two determinations.

Decontamination of most elements above copper in the electromotive series appears excellent, whereas those elements near copper or lower are poor.

The technique is fairly insensitive to H_2SO_4, HCl, and $HClO_4$ while HNO_3 is detrimental to good results. These data are graphically illustrated in figure 18. Concentrations of >1 M for HCl and $HClO_4$, >3 M for H_2SO_4, and >0.1 M HNO_3 should not be present if >98% yields are desired.

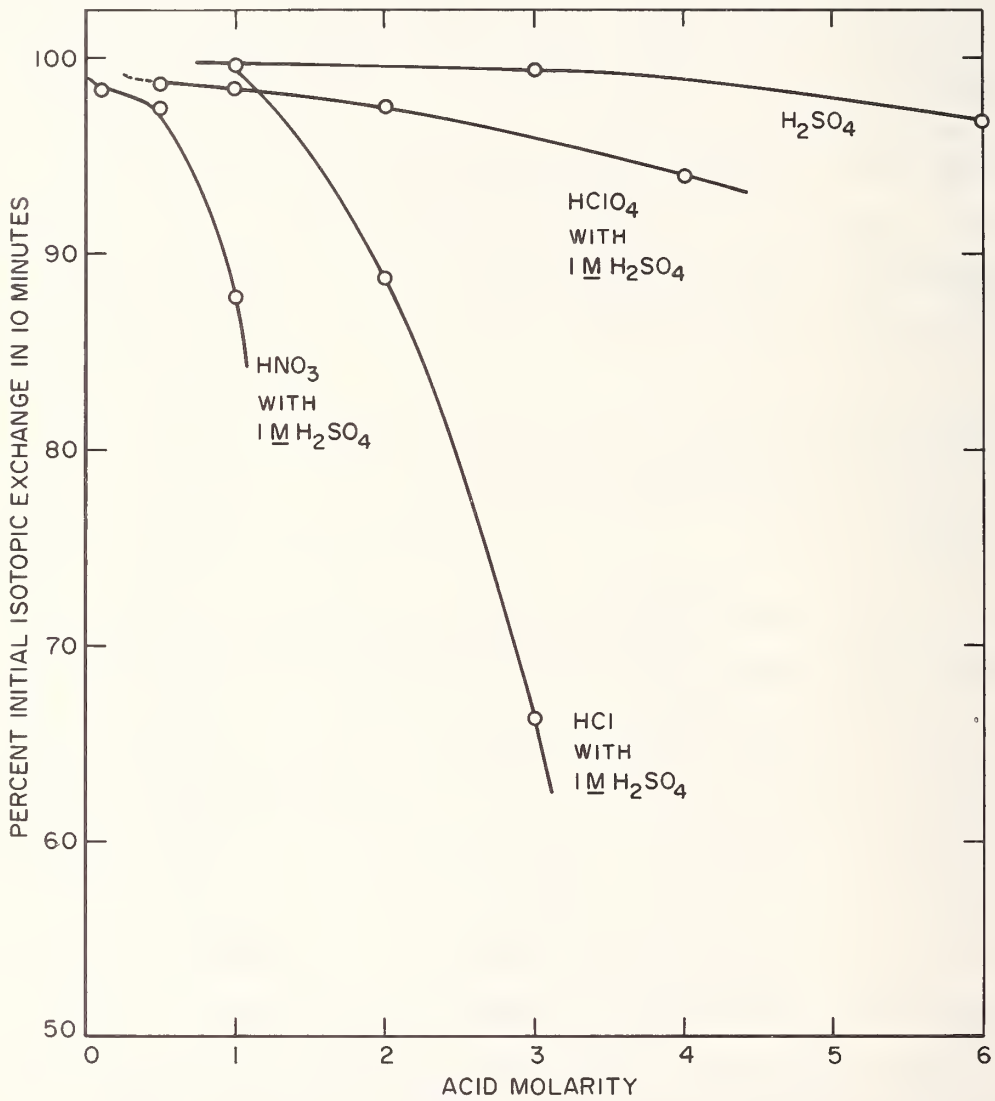

Figure 18. Effect of mineral acids upon isotopic exchange of cupric ion with 1% copper amalgam

Table 14. Activation analysis results.

Material	NBS cert. value for Cu,%	Sample size, g	Found,%	Ave %	Std dev %
Cast Iron 82b [a]	0.038	0.1915	0.0362	0.0369	2.2
		0.2487	0.0375		
Mg Base alloy 171 [b]	0.011	0.3722	0.0113	0.0108	6.4
		0.4148	0.0102		

[a] Fe = 92.7%, Mn = 0.75, Si = 2.1, Ni = 1.2, Cr = 0.33, C = 2.8, traces of V and Ti.

[b] Mg ≥95%, Al = 2.98, Zn = 1.05, Mn = 0.45, traces of Si, Pb, Fe, and Ni.

One gram quantities of Mn^{++}, Co^{++}, and Sn^{++} salts added to the system do not affect the initial isotopic exchange yield of > 99%. One gram of $AgNO_3$, however, caused extensive oxidation of the amalgam incapacitating the exchange. As expected, those salts having the metallic ion high in the electromotive series do not interfere, paralleling decontamination behavior.

b. Activation Analysis of Standard Reference Materials. The results from activation analysis of SRM nickel-chromium 82b and SRM magnesium-base alloy 171 are shown in table 14. Some of the error is due to the many steps involved in the overall activation process itself.

c. Kinetic Studies. A summary of the kinetic data is shown in table 15. Results obtained from comparable experimental conditions performed at five different temperatures yield data which fit two first order reactions. As the temperature increases both reaction rates increase markedly, such that at 99 °C only the slower step is experimentally observed. The reaction rates are plotted in figure 19 versus reciprocal absolute temperature and reveal general Arrhenius behavior over the temperature range. The energies of activation for the two steps are 5.1 ± 0.9 and 6.5 ± 0.8 k cal_{th}/mole for 1 and 2, respectively.

Table 15. Summary of kinetic data

Temp. °C	Total copper in aq. phase, mg	Amalgam used, %	Stirring rate r/min	1st step [a] $T_{1/2}$, min	1st step [a] K_1 g-atom/s	2nd step [a] $T_{1/2}$ min	2nd step [a] K_2 g-atom/s
1±1	2.0	1	$5x10^2$	15 ±2	$2.4x10^{-8}$	86 ±11	$4.1x10^{-9}$
22±1	2.0	1	$5x10^2$	8 ±1	$4.5x10^{-8}$	28 ±2	$1.3x10^{-8}$
49±1	2.0	1	$5x10^2$	4.9±0.6	$7.3x10^{-8}$	17 ±3	$2.1x10^{-8}$
67±1	2.0	1	$5x10^2$	1.9±0.4	$1.9x10^{-7}$	12 ±1	$3.0x10^{-8}$
99±1	2.0	1	$5x10^2$	[b]		3.1±0.1	$1.1x10^{-7}$
67±1	8.0	1	$5x10^2$	2.5±0.4		12 ±1	
67±1	2.0	0.1	$5x10^2$	1.8±0.4		[c]	
49±1	2.0	1	$1x10^3$	4.9±0.2		[d]	
99±1	2.0	1	$1x10^3$	[b]		3.0±0.1	

[a] Energy of activation; $\Delta E_1^* = 5.1 \pm 0.9$ k cal_{th}/mole, $\Delta E^*_2 = 6.5 \pm 0.8$ k cal_{th}/mole

[b] Not experimentally observed. Arrhenius plot estimation is <0.8 min.

[c] Decomposition of amalgam prohibits characterization of second step.

[d] Second step not observed.

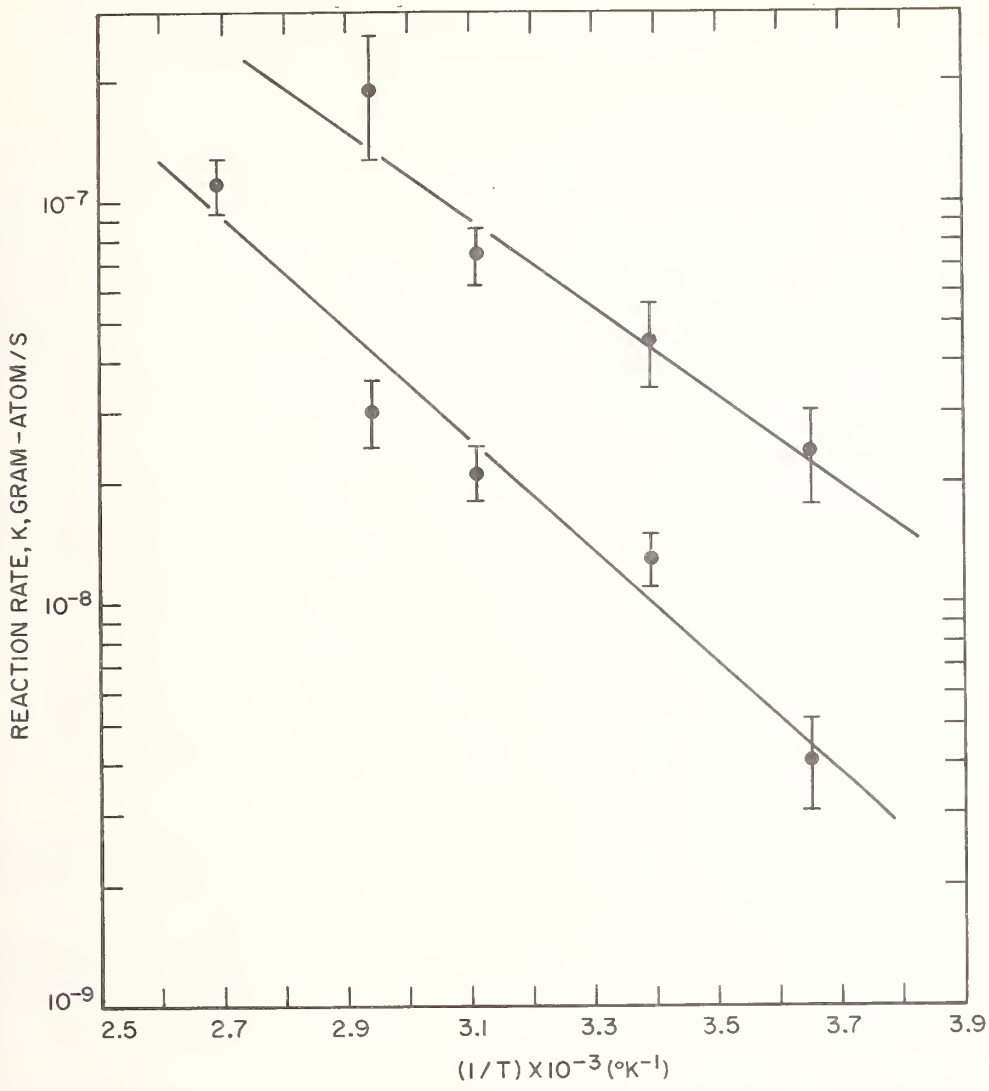

Figure 19. Plot of reaction rate versus reciprocal absolute temperature

The fourfold increase in cupric ion concentration does not result in much significant difference in half-life for the observed isotopic exchange. Similarly the tenfold decrease in percent amalgam yielded no significant difference in the observed half-life for the faster step; however, the system was too sensitive to oxidation, making the slower step nondiscernible.

The increased stirring rate at a lower temperature (49 °C) resulted in a single initial step with no evidence of the second

slower step. At 99 °C however, comparable results with the slower stirring rate were obtained.

4. Discussion of Results

The data indicate that the procedure satisfies general requirements for a radiochemical separation technique. Combined yield, decontamination, precision, and time requirements are favorable for general applicability. The technique is insensitive to many chemical interferences. Experimental conditions such as amalgam preparation, temperature, stirring, timing, and removal of copper from the amalgam are easily reproduced.

The technique has been successfully applied to some practical samples. The results demonstrate good overall accuracy and precision. The procedure has a certain amount of flexibility so that it may be adapted to many chemical situations. Certainly the analysis of low (<10 ppm) copper containing materials would benefit most since excellent decontamination is possible for many materials.

The kinetic data support the possibility that two dependent steps are occurring simultaneously and contributing to the overall isotopic exchange process. The first might be visualized as the faster initial surface exchange process followed by a second slower process of general diffusion to and from the surface, replenishing the surface with fresh copper. The rate of agitation definitely plays a major role in diminishing the slower step. A third opposing oxidizing step may interfere severely with the overall process if low-percent or improperly prepared (or handled) amalgams are used.

5. Conclusion

It has been clearly demonstrated that a finely suspended copper-copper amalgam system can be adapted to a successful amalgam exchange technique for the radiochemical separation of copper from a variety of materials.

(R. R. Ruch)

F. Consultation and Liaison Activities

1. Mr. Gilbert W. Smith has been responsible for all of the liaison activities indicated in Section 1-A of this report.
2. The following are the consultation and liaison activities of Dr. Lloyd A. Currie:
   a. Member of a task group preparing a report on the measurement of low-level radioactivity for International Commission on Radiological Units and Measurements.
   b. Discussed the merits of various types of low-level systems for β-detection with Dr. Hayes, of the Department of Agriculture (Agriculture Research Center).
   c. Discussed availability of isotope separators, particularly some of French design, and also the radiochemical aspects of planning for an underground, low-level laboratory with Mr. J. Callow of the National Physical Laboratory of the United Kingdom.
   d. Consultation on various patent applications which were related to radioactivity with Mr. H. Dixon, Patent Attorney of the Atomic Energy Commission.

G. Publications

1. Becker, D. A., and Smith, G. W., "Determination of Trace Amounts of Tellurium in Standard Reference Materials by Neutron-Activation Analysis," Proceedings of the 1965 International Conference: Modern Trends in Activation Analysis, Texas A & M Univ., College Station, Texas.
2. DeVoe, J. R., and Smith, G. W., "Activation-Analysis Program and Facilities at the National Bureau of Standards," Proceedings of the 1965 International Conference: Modern Trends in Activation Analysis, Texas A & M Univ., College Station, Texas.

3. INSTRUMENTATION

The efforts of the Instrumentation Group during the past year have been directed toward the improved handling of data gathered by automatic equipment. The completion of the interface project first described in a previous report [37] has been completed along with the design and construction of a fast rise preamplifier and the setting up of a solid state detector program. A high memory capacity pulse height analyzer, a TMC* 4096 channel system, was set up to be used with both the solid state detectors as well as scintillation detectors. The analyzer is capable of two parameter storage in binary subgroups up to a 64 x 64 channel array or a full 4096 channels for high resolution singles spectra. The input-output system for the 4096 channel analyzer incorporates a high speed line printer and computer-compatible magnetic tape unit.

A. Interface Units - Final Report

1. Interface Translator Units

Six of these units have been built which provide readin and readout capability for each of the multichannel analyzers in use by the Radiochemical and Activation Analysis Sections.

The interface units are completely described in a paper presented at the 1965 Activation Analysis Conference, College Station, Texas [38] and are discussed here briefly through excerpts from the paper with the final schematics including all subsequent changes and improvements.

The system is comprised of three parts: phase I (figure 20) is the interface translator unit providing the readout function, phase II (figure 21) is the readin section allowing data previously read out on punch tape to be reintroduced into an analyzer's memory, and phase III (figure 22) is the precursor data section which provides time of year, identification, and other externally gathered data to be formated ahead of the analyzer's

* For disclaimer of equipment and materials see last paragraph of preface.

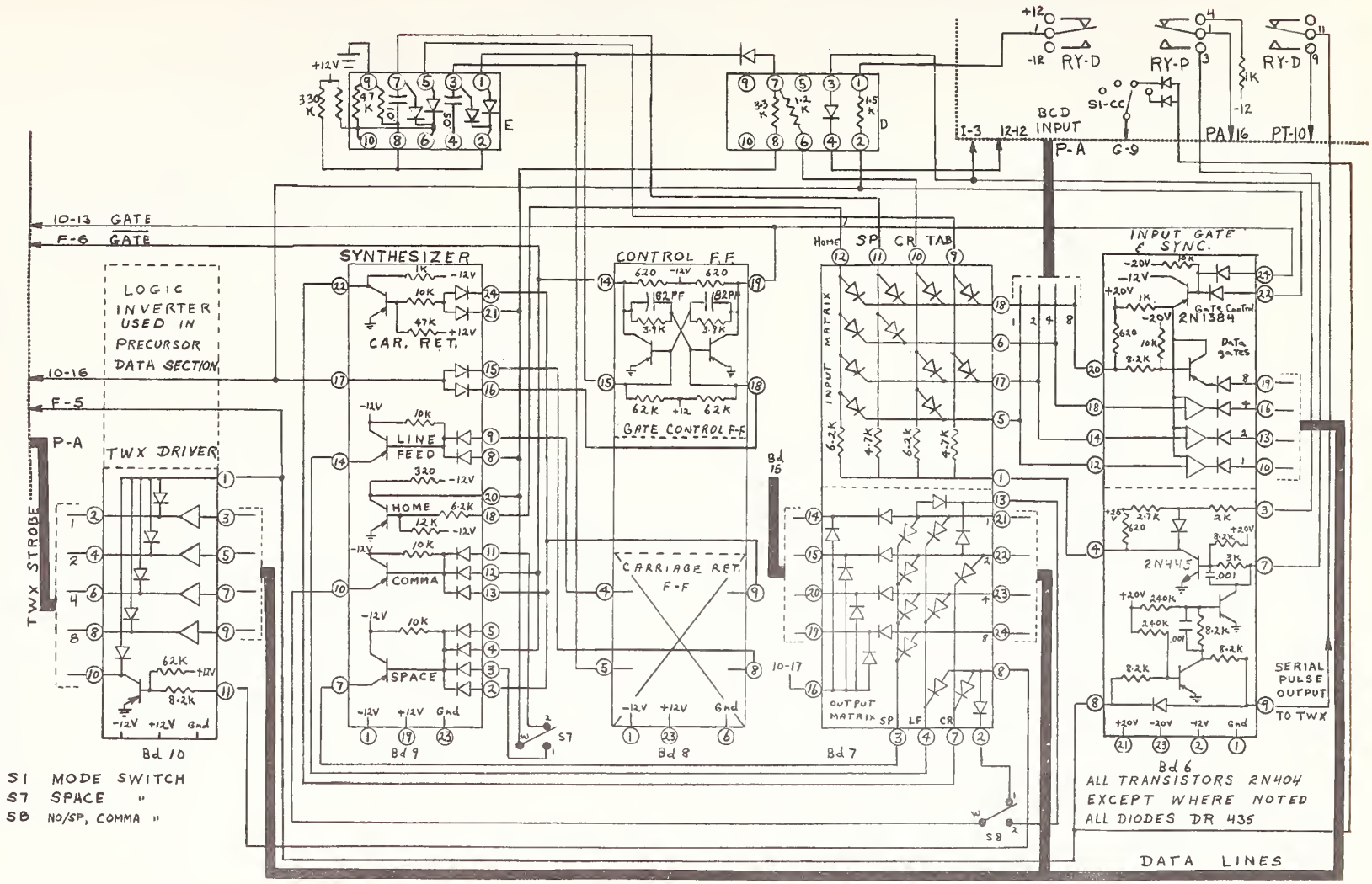

S1 MODE SWITCH
S7 SPACE "
S8 NO/SP, COMMA "

Figure 20. Interface translator (phase I)

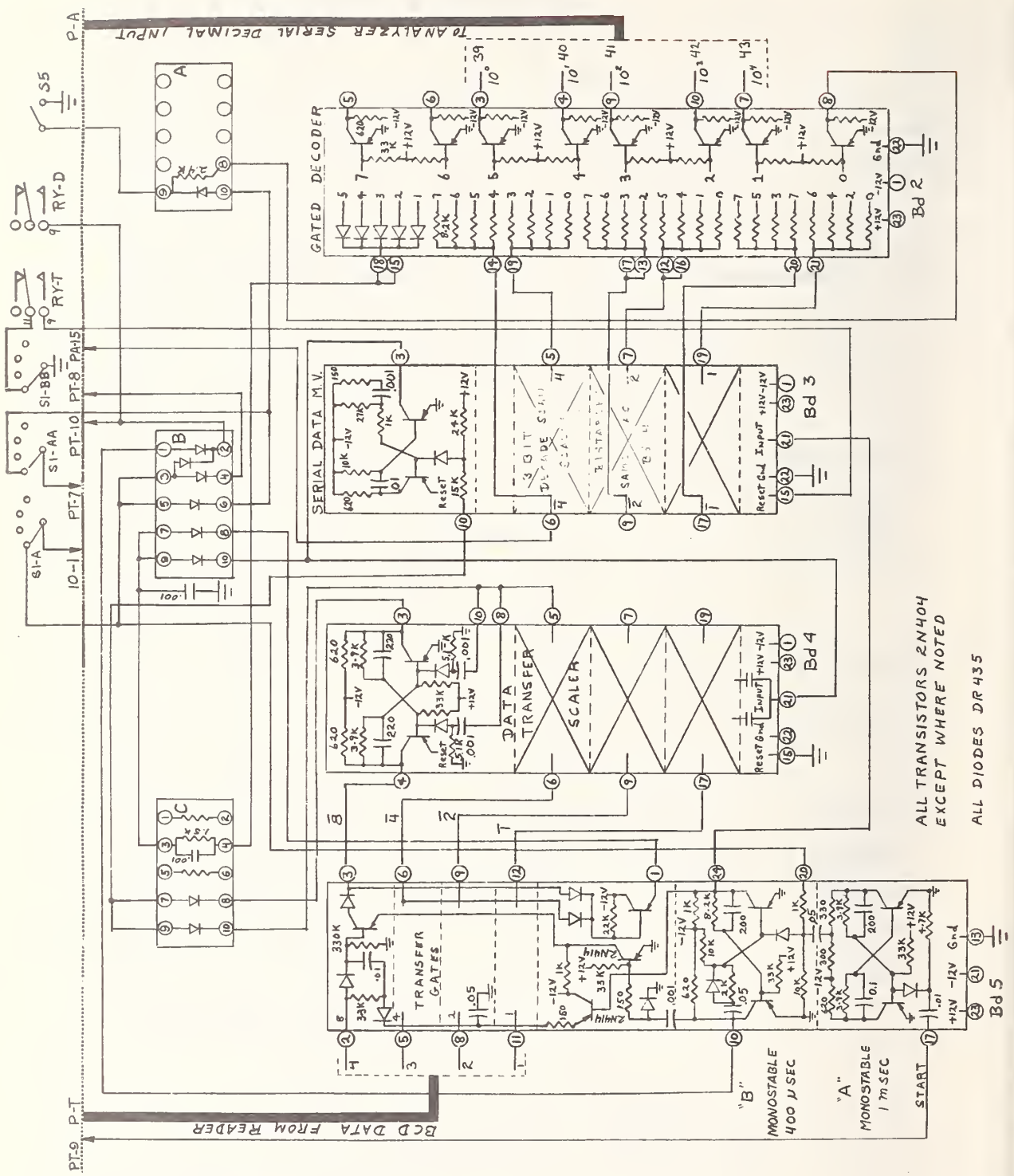

Figure 21. Punch tape readin (phase II)

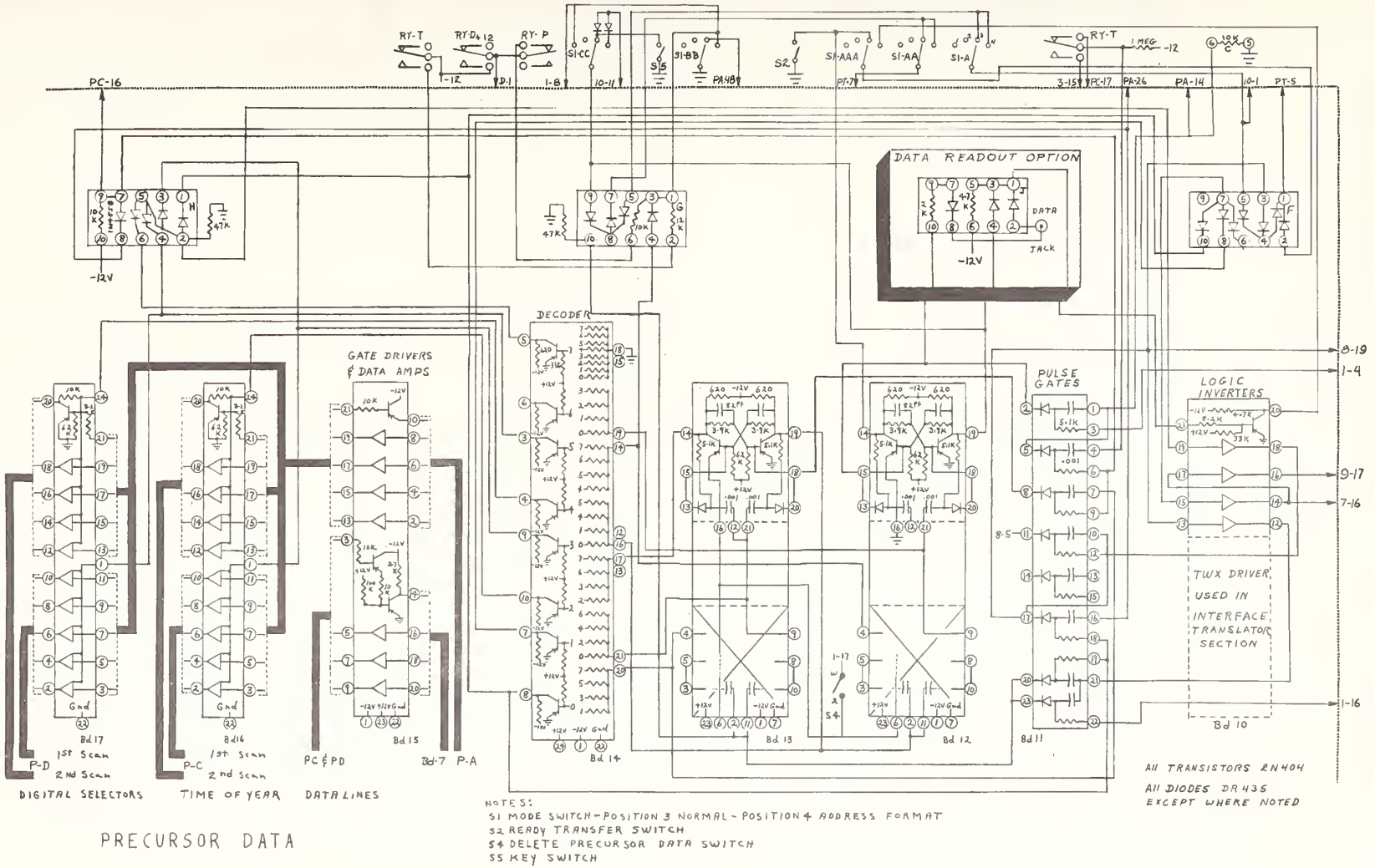

PRECURSOR DATA

Figure 22. Precursor data (phase III)

normal read out. System control is also provided by the circuit (figure 23). The interface units were built of modular circuit boards designed by the Data Automation Group of the National Bureau of Standards. [39]

2. "Basic" Format Units

Three of the interface units have been modified for special application for use with a multistation input computer which is programmed to accept data in the "BASIC" format. The format requires that each line of data be preceded by a line number and then the word "DATA." The serial converter board of the analyzer was reprogrammed such that only the first two digits of the address were scanned, then followed by four preprogrammed digits representing the BCD form of the word "DATA." Two additional leads were brought out from the serial converter board to provide the logic levels necessary for the interface to complete the code structure.

3. Adaptors for Interface Units

In order to use the interface units when an analyzer was coupled to a high speed magnetic tape system, it was necessary to introduce a switch-over box between the units. The modes of operation permitted are: teletype, readin and readout, magnetic tape record and playback and magnetic tape playback with teletype readout. This last function enables an operator to automatically print hard copy or punch tape of a series of spectra automatically accumulated on magnetic tape. Another switchover box similar in design was built to be used with the RIDL 34-26 "Nanolyzer"* thin film memory analyzer which eliminates the necessity for modification of the standard interface design.

4. The RIDL Model 34-27 Analyzer*

The RIDL Model 34-27 Analyzer can be used with the unmodified interface unit but requires some program changes and modification to the serial connector board in the analyzer.

* For disclaimer of equipment and materials see last paragraph of preface.

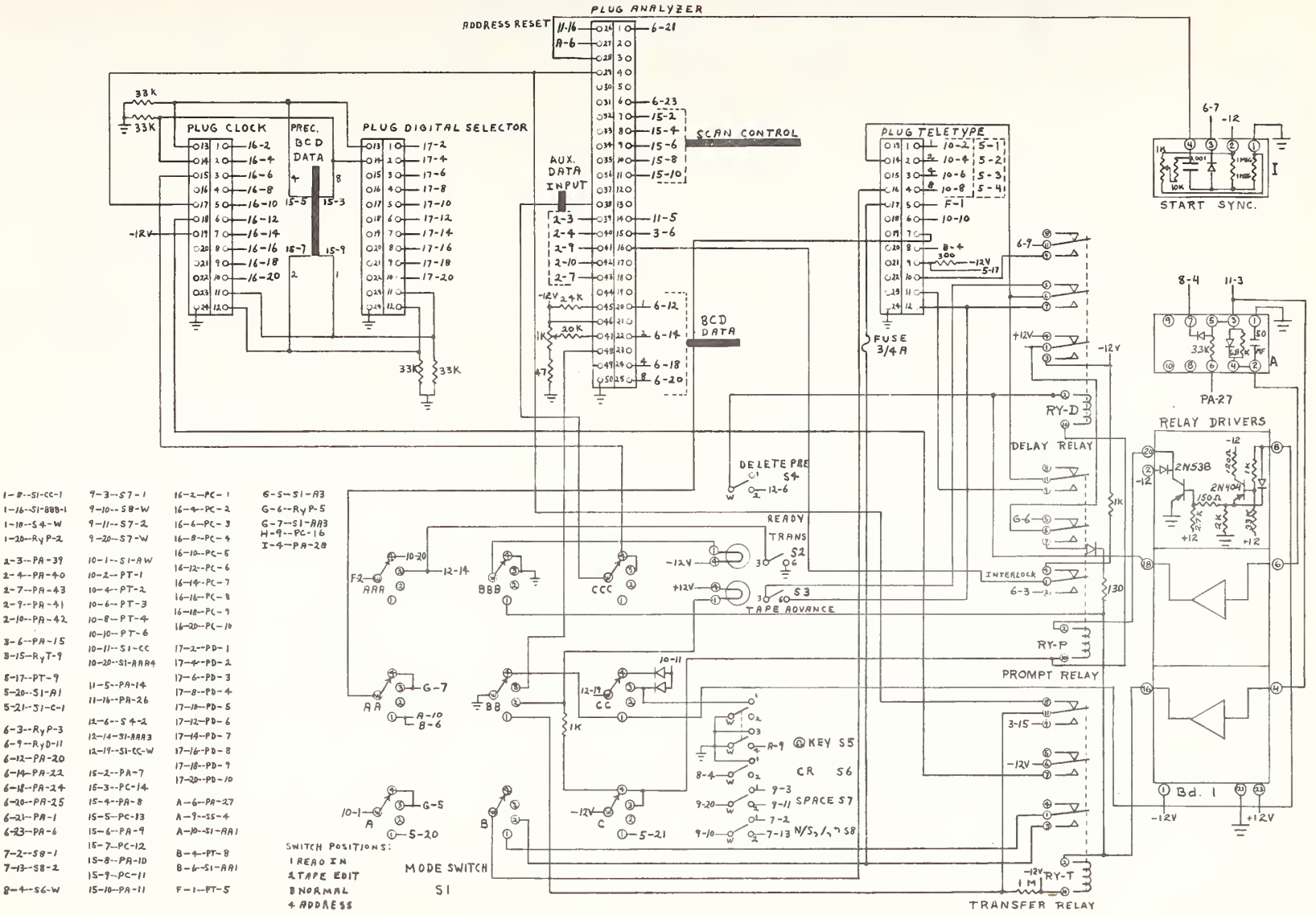

Figure 23. System control circuit

5. Reliability

The reliability of the interface units has on the whole been satisfactory. During the past year, however, several deficiencies have been noted and design changes made (See figures 20, 21, 22) notably, revision of the "interlock circuit" in phase I, the "bit transfer gates and monostables" in phase II, and the "precursor start up" phase III.

(R. W. Shideler)

B. Time of Year (TOY) System

1. Time of Year Clock

To provide time of year information to the interface-analyzer data readout system, a long term clock had to be obtained. Of the clocks known to be available commercially which are capable of electronic readout with sufficient resolution most had drawbacks. Decimal days were judged to be an inconvenient time form and electronic scalers had a tendency to fail to change state in the digits that remained unchanged for long periods. Also all of the clocks available were very expensive. A new design was made in order to overcome these deficiencies.

The design centers around an electromechanical digit counter having individual contacts for electrical readout and capable of very fast reset. Eight of these counters provide 999 days, 23 hours, and 59.9 minutes. A synchronous motor with a cam-operated switch provides impulses at six seconds (0.1 min) intervals driving the least significant digit (figure 24). Each digit provides a carry after the nine and relay logic performs the resets at 60 minutes and 24 hours. Provision is made to set the clock to any permitted state and a warning light and circuit shut off the clock in the event of a power failure. Provisions were made in the clock to allow time manipulations as described below. An anticipated addition will increase the readout resolution to 0.01 minutes.

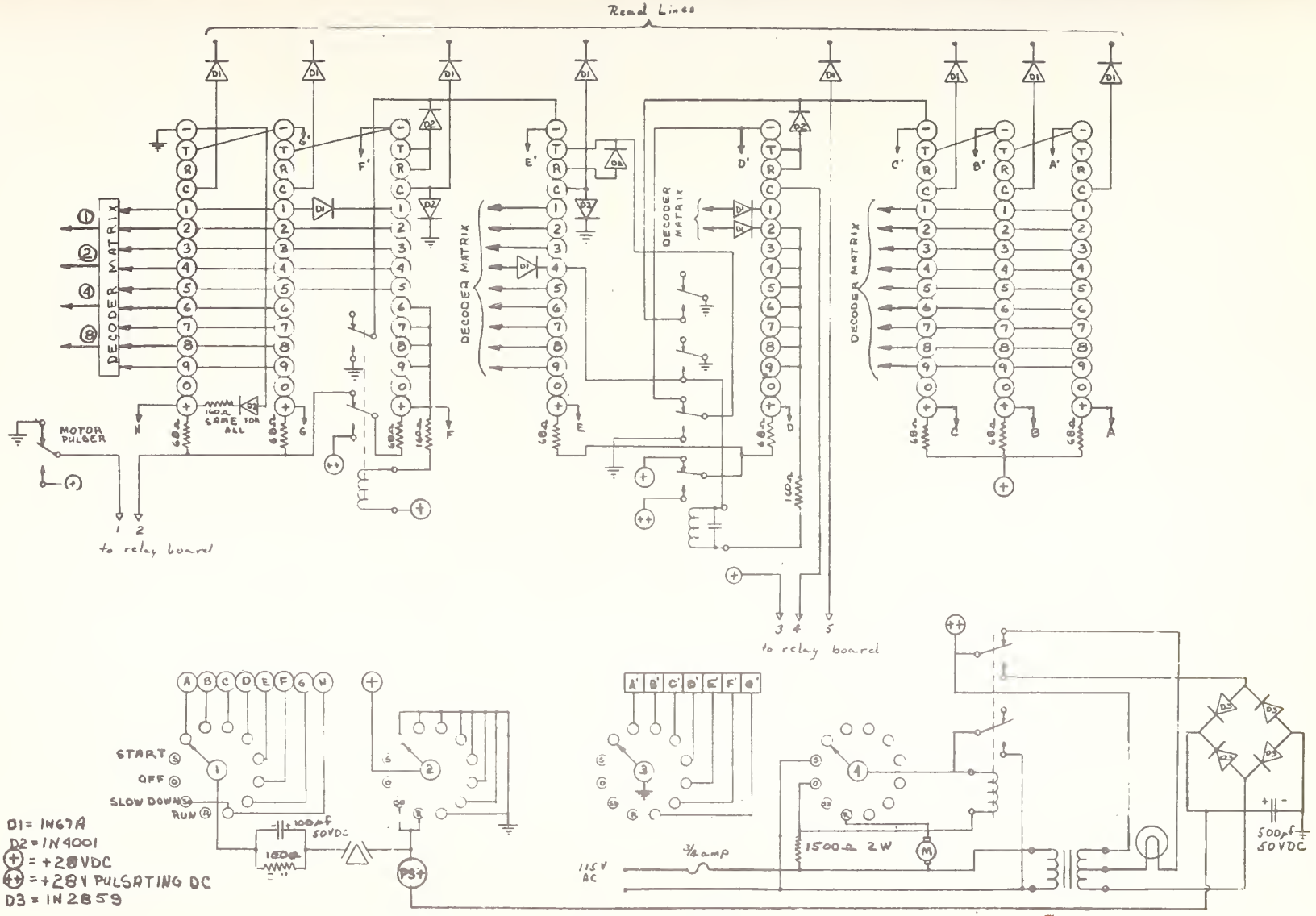

Figure 24, Time of year clock

2. Time of Year (TOY) Clock Controller

Complete timing information for a given spectrum is only obtained if one knows the start time, the stop time, and the live time of the analyzer taken during the run. It is therefore necessary to synchronize either the clock with the analyzer or vice versa. A control circuit (figure 25) was designed which sets the clock ahead 0.1 minute when the analyzer is manually set to store and prints this time only while holding the analyzer from storing. When the time pulse corresponding to the clock reading occurs, the analyzer is started synchronously while the clock resumes normal timing. At the end of the store cycle the analyzer automatically starts the readout cycle. The clock is stopped and held until the time has been read out and then restarted catching up by one time pulse if necessary. The logic for these operations is performed by a system of relays and contained in the clock chassis.

(R. W. Shideler)

C. Time Mode Control Unit

In multichannel scaling using the RIDL Model 34-12* series analyzer it is necessary to provide an external timing source to advance the address scaler. A convenient means for generating this signal is available in the analyzer by making use of the built in clock if the desired channel advance rates are not too high. A simple circuit (figure 26) has been designed for use with units not having built in** or auxiliary timers available. An additional mode of operation is included which allows the experimenter to start each time interval on an individual or channel-by-channel basis.

(R. W. Shideler)

---

* For disclaimer of equipment and materials see last paragraph of preface.

** Available as standard option by manufacturer.

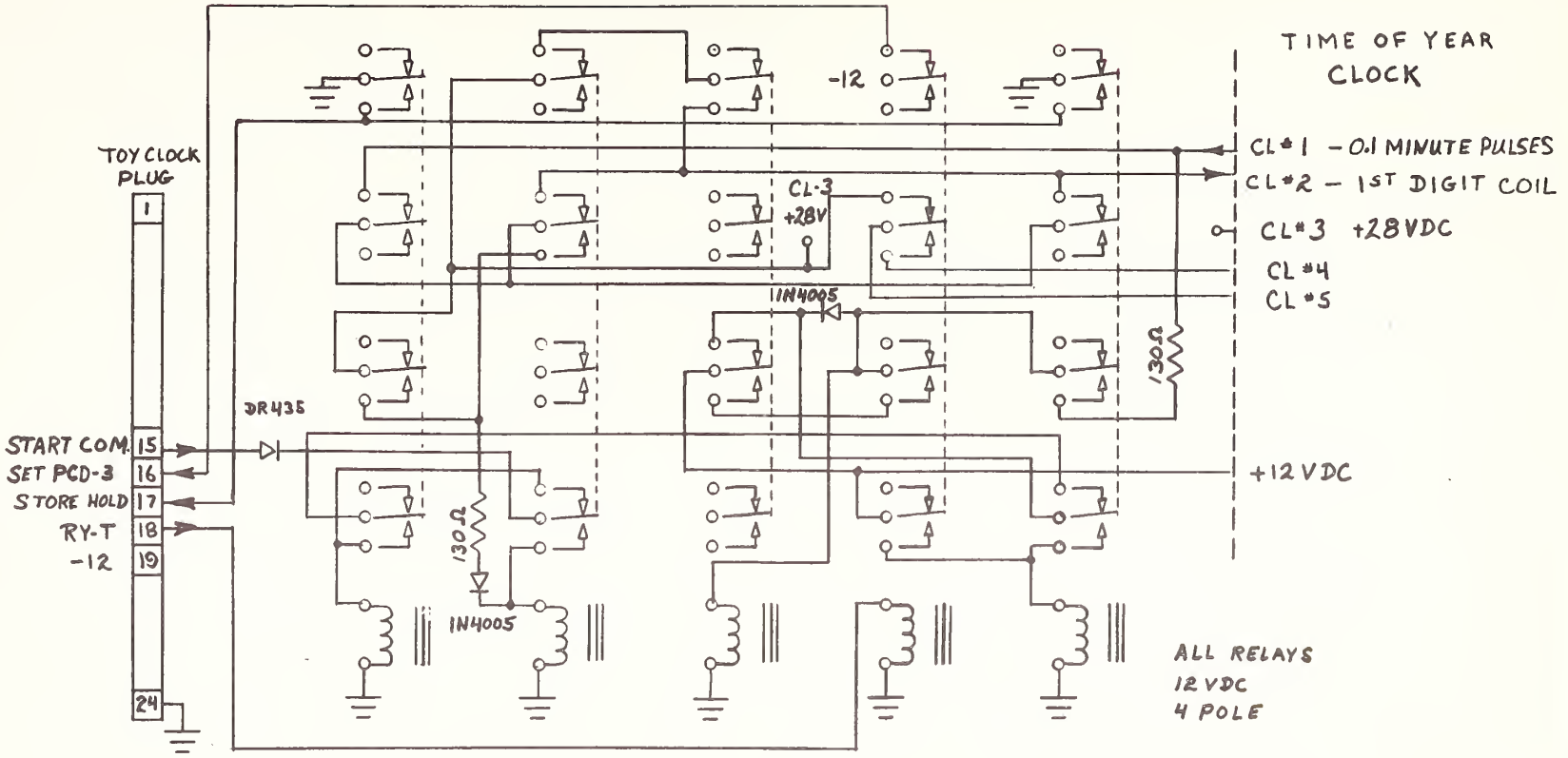

Figure 25. Time of year clock controller

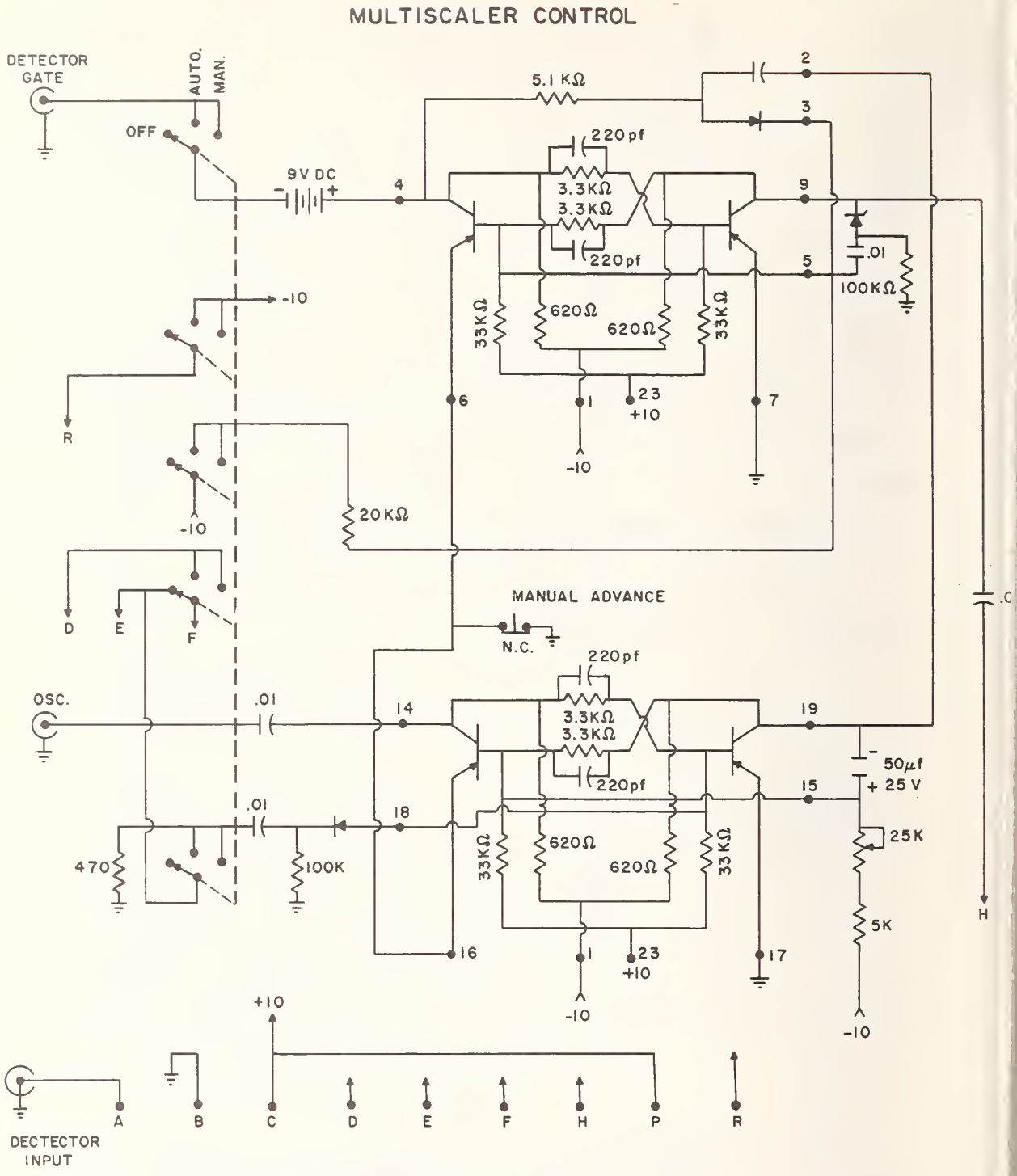

Figure 26. Time mode control unit

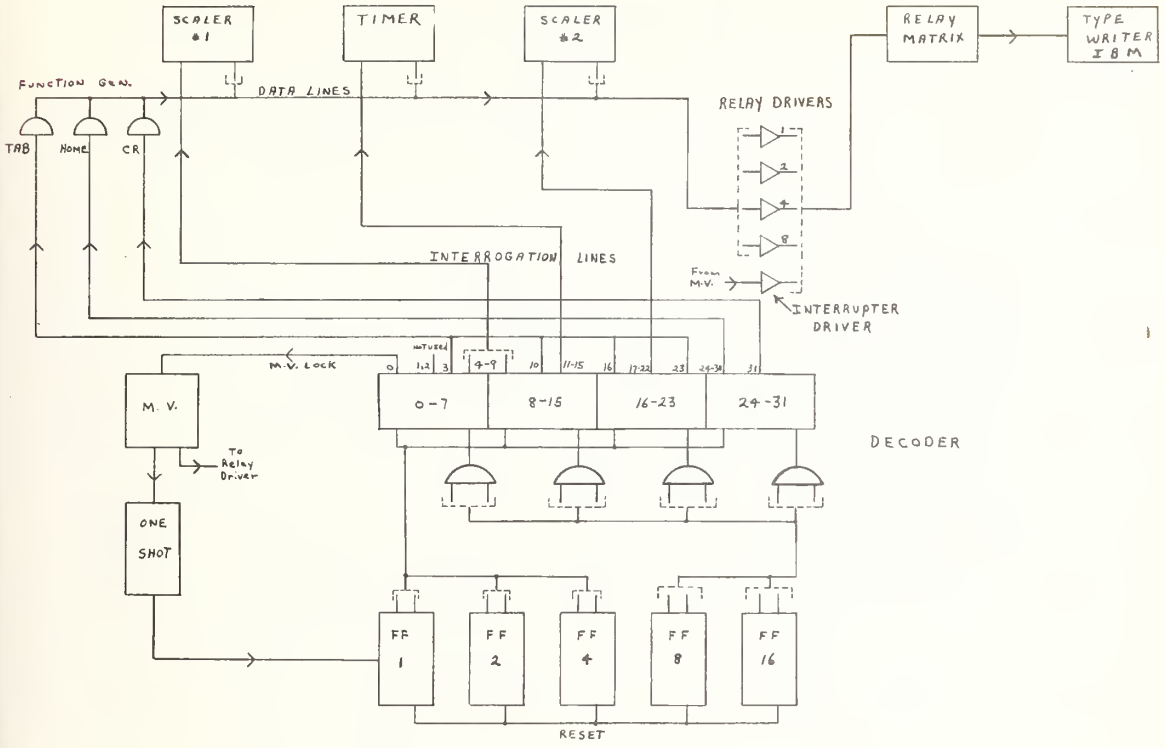

Figure 27. Data logging system (block diagram)

D. Data Logging System

A system comprising three scalers and a timer was assembled using an electric typewriter and relay driver formerly used as an analyzer readout. An interface unit (figure 27) was designed using modular circuit boards [39] although some modifications were required. The circuit provides 31 readout locations and resets automatically after printing.

(F. C. Ruegg and P. N. Thomas)

E. Fast Rise Preamplifier

For achieving meaningful results in very fast ≈20 ns coincidence work, a preamplifier must have rise times at least as fast as the time resolution of the coincidence experiment. A preamp was designed utilizing the properties of the relatively unpopular and unexplored current mode input (figure 28). The input stage (TI) base is grounded while the signal is introduced on the emitter which is directly coupled to the current signal source as well as to a stabilizing feedback bias. The

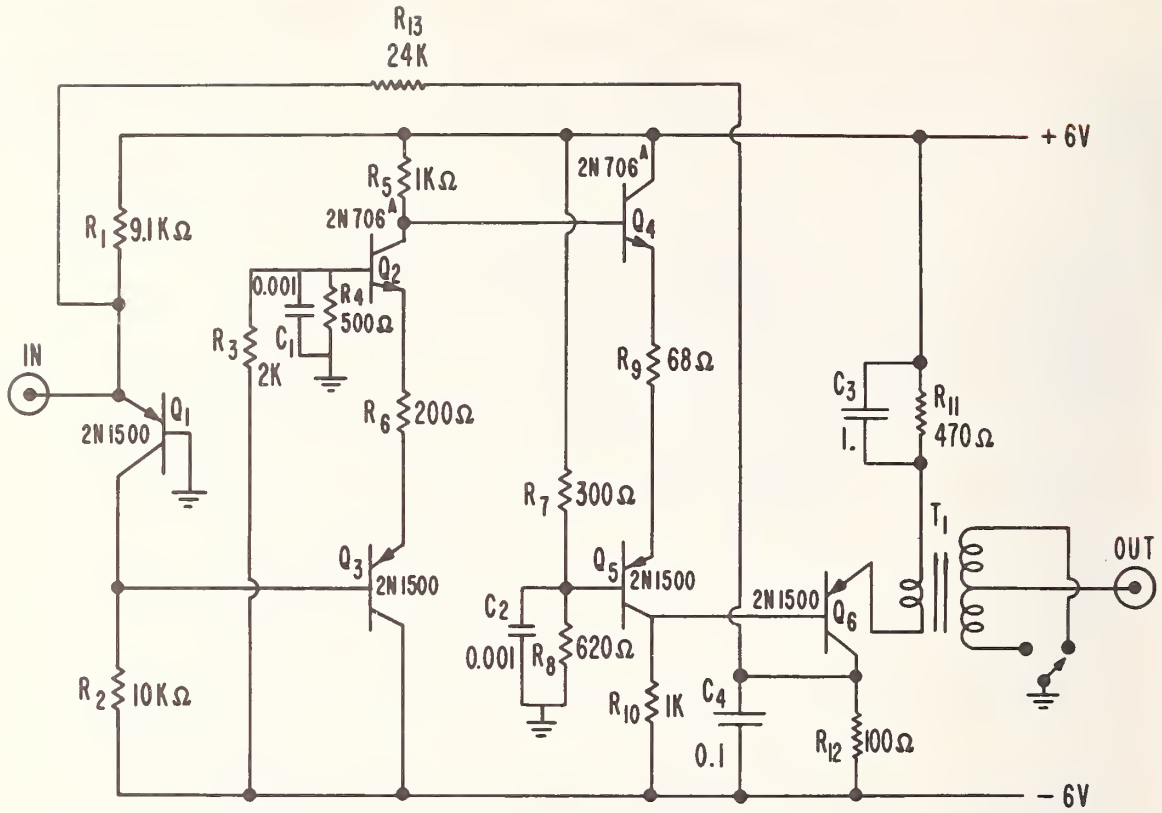

Figure 28. Fast rise preamplifier for current signals

input impedance in this mode is less than 50Ω. The transistor is operated at very low collector current to achieve low noise operation. This stage is followed by a double "Darlington" circuit made up of two complementary pairs of transistors (T_2 through T_5) in a direct coupled self-compensating circuit. The output is an emitter follower transformer coupled to match a 50Ω cable impedance. Exclusive of the transformer the D.C. current gain is on the order of 100 while with 20 ns pulses a current sensitivity of 200 μA/volt into a 50Ω load is realized. The preamplifier was designed for fast rise characteristics only and its gain and therefore linearity are dependent on input wave shape. Further work will be done to remove restrictions arising from wave shape dependency and broaden its utilization.

(R. W. Shideler and J. J. Spijkerman)

F. Solid-State Detector Systems

In the last few years gamma-ray spectrometry has been provided a new and most powerful tool in the cooled solid-state detector. In line with this fact a system has been set up to make these potentialities available to the activation analysis group as well as for other research. Although the germanium, lithium-drifted detectors are far superior in performance at high energies to silicon lithium drifted detectors, the silicon detectors are far more rugged and can be used at room temperature as particle detectors. These facts have caused us to divide our attention making use of a 300 mm^2 x 5 mm silicon lithium-drifted detector for low and medium energy (20 to 200 keV) work with a 100 mm^2 x 3 mm deep germanium lithium-drifted detector for higher energies. A second silicon lithium-drifted detector 60 mm^2 x 2 mm deep is being set up with a 10-mil beryllium window for very low energy X-ray work.

G. Observations on Calibration of a Pulse Height Analyzer Using a Sodium Iodide Detector

In a laboratory doing activation analysis where sodium iodide detectors are used to provide gamma-ray spectra of many various radioactive species, instrument calibration can present a problem. This is especially true if the experimenter wants only a quick look at a sample during or before further preparation. In this instance, unless the peaks obtained are close to the calibration points or are quickly recognized, an energy determination and isotope recognition becomes an arduous task or an idle speculation. This is due largely to nonlinearities (as much as 10 to 15%) inherently present in the sodium iodide detection mechanism shown by Engelkemeir [40]. Ordinarily, initial calibration for nonspecific or routine pulse height analysis is done in one of two ways. Either the photopeak of ^{137}Cs is used to establish 0.662 MeV on the energy scale with a zero intercept end point or the ^{137}Cs photopeak is used in conjunction with its associated Ba K X-ray to establish a lower

point at 32 keV. These calibration methods along with an improved technique are depicted graphically, figure 29, and include the position of several familiar photopeaks showing the Engelkemeir nonlinearities. The abscissa is the energy of the detected gamma ray with the ordinate being $\frac{\text{Pulse height units}}{\text{Energy}}$ and normalized to the ^{137}Cs photopeak. A one-point calibration normalized to the ^{137}Cs photopeak and zero intercept (figure 29a) shows large errors over the entire range. A two-point calibration normalized to both peaks of a ^{137}Cs source (figure 29b) is an improvement but has significant errors throughout most of the spectral range peaking between 60 and 85 keV at about 10%. The third graph (figure 29c) was normalized using the 60 keV photopeak of ^{241}Am as a convenient lower calibration point with a general improvement in rudimentary energy determinations over the most frequently used energy range with an error of no more than +6% at 85 keV and -4% at 3 MeV. Below 32 keV where there is an error of -15% the error becomes quite serious but this region is rarely used in routine work and never without careful calibration.

The above considerations clearly indicate the desirability of a two-source calibration using ^{137}Cs and ^{241}Am. Another technique, equally suitable, is to use ^{137}Cs and the BaK X-ray, but to consider the BaK X-ray not as 32 keV but instead 15% lower or approximately 27 keV. This approach produces equivalent results to that of using two separate sources.

H. Pneumatic Transport System Rabbit Sensor

In performing activation analysis and other precision irradiations it is often necessary to determine exactly the arrival and departure time of a rabbit or sample carrier to a high flux location. The high fluxes present in such a location make the problem difficult inasmuch as no known electrical device can survive in such a hostile environment for a time long enough to be practical. It is customary in such situations to measure the time as the rabbit goes past some point

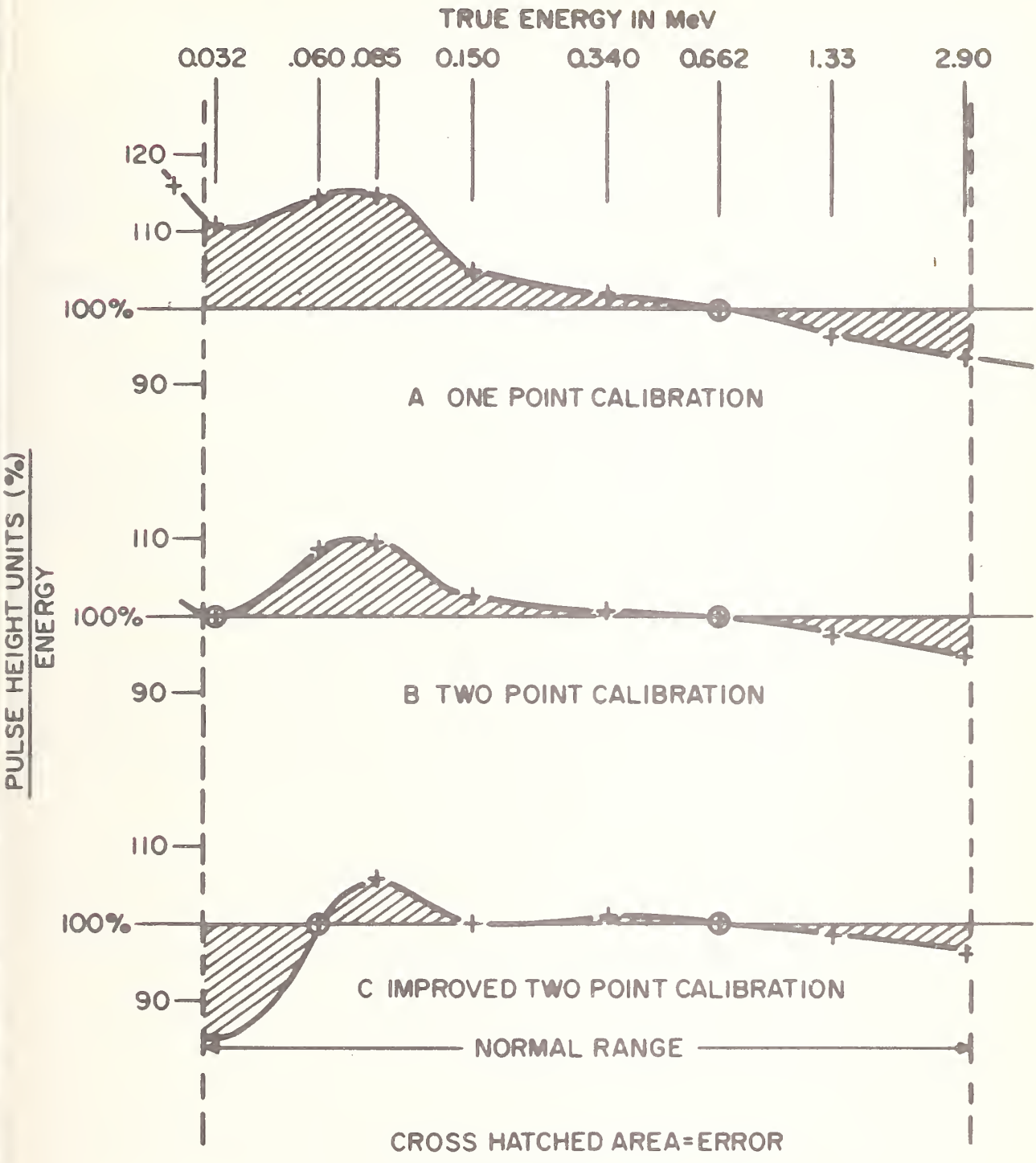

Figure 29. Calibration methods used with sodium iodide detectors

remote from the irradiation area and knowing the rate of travel extrapolate to determine the true time.

A new approach has been suggested and preliminary tests have been made on a system to alleviate this problem. The system is to make use of a principle known as pneumatic gaging. The end bumper for the rabbit is shaped to conform to the shape of the rabbit and contains a small orifice axially located which connects to a small bore tube that returns to an environmentally safe location. At this point, a fast response pressure transducer or switch and a source of high pressure gas (CO_2) is connected through a constant flow regulator which completes the system (figure 30).

In operation the system pressure at the pressure sensor is established as a dynamic equilibrium between the pressure drop across the constant flow regulator and the relatively small pressure drop due to the small bore tubing and the orifice. When the rabbit comes near to, or in contact with the orifice, the flow rate at the orifice drops dramatically causing the pressure at the sensor to rise sharply providing contact information. This sensing system is being incorporated in the pneumatic tube irradiation locations at the NBS reactor.

I. Consultation

In the past year, occasional consultation has been performed for persons or groups outside the section. Most notable was work done for Dr. Kurt Heinrich of the Spectrochemical Analysis Section in connection with adaptation of a 1600-channel analyzer to more appropriately serve his specialized requirements for the electron microprobe.

(R. W. Shideler)

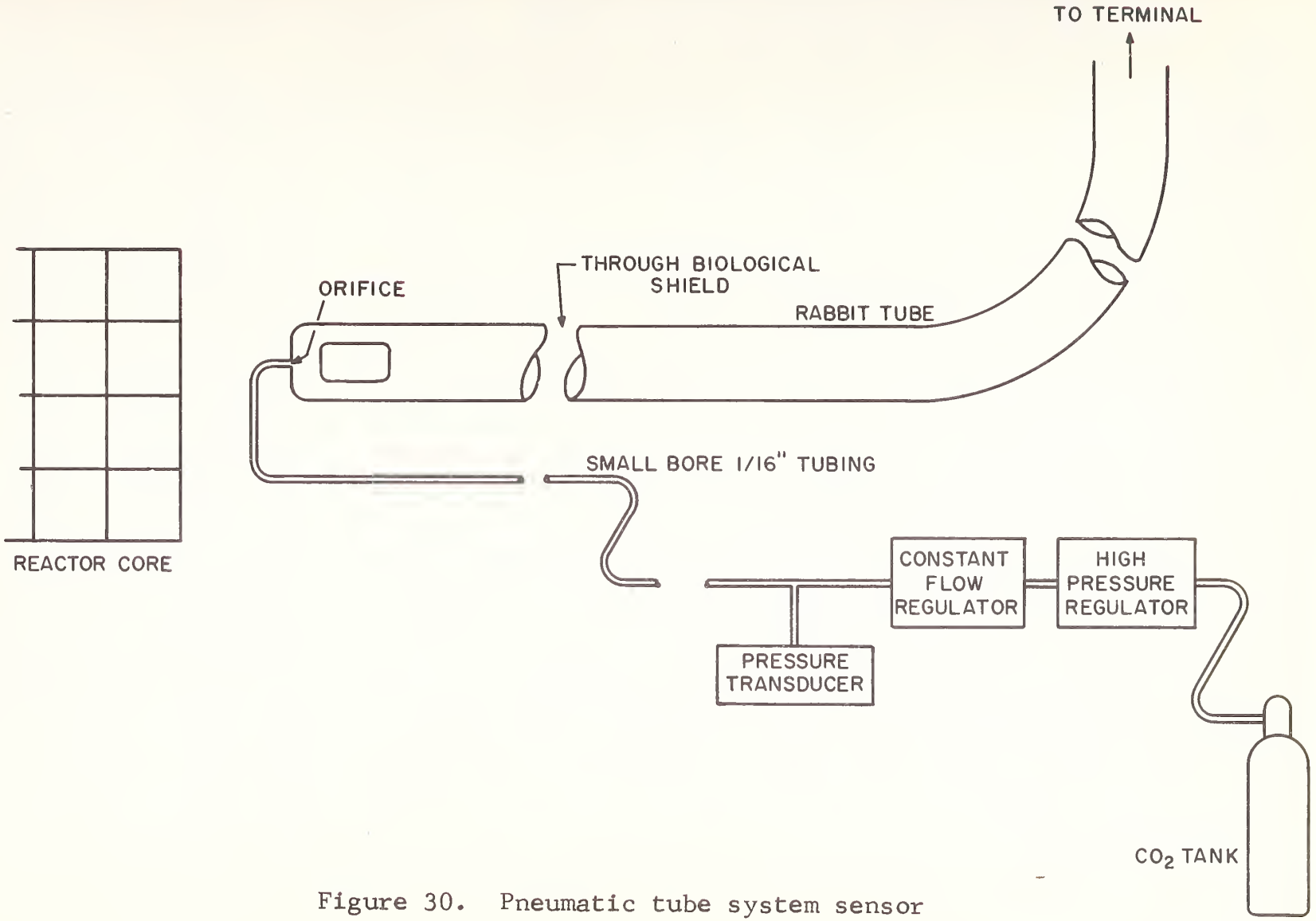

Figure 30. Pneumatic tube system sensor

Mössbauer Spectroscopy

A. Introduction

The continued increase in Mössbauer Spectroscopy research in the United States and abroad, and the applications in physics, chemistry, metallurgy and biology has encouraged the NBS group to continue their effort in instrumentation and standardization. The first Standard Reference Material for Mössbauer spectroscopy, SRM 725, (sodium nitroprusside) has been certified [41] and is available from the Office of Standard Reference Materials. Figure 31 shows the certificate accompanying each of these standards. The NBS Mössbauer spectrometer has been further improved by the addition of a multiplex unit to obtain true spectra simultaneously for comparison or for direct calibration against the standard. Further efforts were made in the interpretation of the chemical shift, by recalibration of the Walker, Wertheim and Jaccarino [42] diagram with the standard and correlation with molecular orbital calculation results.

The research in Mössbauer sources has been continued through a careful analysis of the Pd-Sn system [43]. The Pd_3Sn intermetallic compound exhibited better characteristics for a ^{119m}Sn source and a high specific activity source can be obtained.

In the last fiscal year 85 persons visited the Mössbauer laboratory, and approximately 14 hours a week were devoted to consultation with 60% U. S. Government agencies and 40% outside.

(J. J. Spijkerman)

B. Facilities

The relocation of the Radiochemical Analysis Section from the Washington laboratories to the new Gaithersburg site has made possible a considerable expansion of the Mössbauer spectroscopy program. The available space has been divided into a source preparation laboratory, absorber preparation and hot atom research laboratory and a measurement laboratory. The proximity to the NBS reactor, linear accelerator and the Activation Analysis Section neutron generator considerably extends the potential of the Mössbauer spectroscopy group in the area of new Mössbauer isotopes and sources.

U. S. Department of Commerce
John T. Connor, Secretary
National Bureau of Standards
A. V. Astin, Director

Certificate of Calibration

Standard Reference Material 725
for
Mössbauer Differential Chemical Shift for Iron-57
Disodium Pentacyanonitrosoferrate Dihydrate
(Sodium Nitroprusside)

This Standard Reference Material was prepared from a single crystal of the compound disodium pentacyanonitrosoferrate dihydrate ($Na_2Fe(CN)_5NO.2H_2O$). The purity of this compound, also known as sodium nitroprusside, meets the specifications of the American Chemical Society for reagent-grade materials as verified by quantitative analysis of the main constituents, but should not be considered as entirely free from impurities such as heavy metals. It is in the form of a platelet of dimensions 1x1x0.0775 ±0.003 cm that has been cut from a large single crystal. The 1x1 cm surface is parallel to the 100 crystal plane within ±2 degrees of arc. The opposite 1x1 cm surfaces are parallel to within 0.001 cm with a surface finish of 20 microns. The natural iron concentration is 25.0 ±4 percent mg/cm².

The chemical shift of this Standard is compared to that of the National Bureau of Standards Primary Standard, consisting of the average chemical shift of ten platelets which is given the value of zero chemical shift. The National Bureau of Standards dual-spectra Mössbauer spectrometer [1, 2] was used. This Standard has an average value for the chemical shift of 0.0000 ±0.0002 cm/s at 25.0°C. This uncertainty is expressed as the standard deviation of a single determination derived from single measurements on 50 platelets. The resonant spectra have considerable line-broadening due to the thickness of the absorber. The experimental line width (full width at half maximum) is 0.0305 ±0.0004 cm/s. The line width corrected for thickness broadening is 0.0202 cm/s. The Mössbauer effect is 17 percent.

To allow the user to calibrate the velocity scale of a Mössbauer spectrometer, the electric quadrupole splitting of the Standard Reference Material was measured. The velocity scale of the dual-spectra comparison spectrometer was calibrated by measurement of the electric quadrupole splitting of the Primary Standards using an optical interferometric technique. The average value of the electric quadrupole splitting for this Standard is 0.1726 ±0.0002 cm/s at 25.0°C where the uncertainty is expressed as the standard deviation of a single determination derived from single measurements on 10 platelets.

The details of the instrumentation and of preparation and measurement of the sodium nitroprusside crystals are given in NBS Miscellaneous Publication 260-13 entitled "Mössbauer Spectroscopy Standard for Chemical Shift of Iron Compounds."

The single crystal platelets of sodium nitroprusside were prepared by the Isomet Corporation of Palisades Park, New Jersey. The calibrations of the crystals were made within the National Bureau of Standards Institute for Materials Research, by J. J. Spijkerman, F. C. Ruegg, D. K. Snediker, and W. L. O'Neal of the Radiochemical Analysis Section, James R. DeVoe, Chief.

REFERENCES:

[1] Radiochemical Analysis: Activation Analysis, Instrumentation Radiation Techniques, and Radioisotope Techniques, July 1963 to June 1964, James R. DeVoe, Editor, NBS Tech. Note 248, pp 25-37 (1964). Available from Superintendent of Documents, Government Printing Office, Washington, D. C. 20402, 50 cents a copy.

[2] Radiochemical Analysis: Activation Analysis, Instrumentation, Radiation Techniques, and Radioisotopes Techniques, July 1964 to June 1965., James R. DeVoe, Editor, NBS Tech. Note 276, pp 74-110 (1966). Available from Superintendent of Documents, Government Printing Office, Washington, D. C. 20402, $1.00 a copy.

WASHINGTON, D. C.
April 6, 1966

W. Wayne Meinke, Chief
Office of Standard Reference Materials

(over)

Figure 31. Certificate of calibration for Mössbauer Standard, dated April 6, 1966

Directions for Use

The Standard Reference Material in the form of a single crystal platelet is sandwiched between two pieces of a 4 mil polyethylene film. Due to the advisability of keeping it free from moisture it is recommended that the platelet not be removed from this container. A suitable mounting consists of two concentric aluminum rings approximately 1.25 inches in diameter. The crystal, encased in the plastic envelope, is placed between the rings and the assembly is fastened together with small screws, thereby clamping the envelope firmly between the rings. Both rings have an inside diameter of 0.75 inch to expose the crystal and to prevent crushing of its edges. This was the procedure used in taking all of the data at NBS on this Standard Reference Material.

Place the Standard Reference Material as the absorber at 25.0° C in the Mössbauer spectrometer and take sufficient transmitted counts of the 14.4 kev gamma-ray from an iron-57 source to obtain counting statistics to the required degree of uncertainty. Determine the peak position of the electric quadrupole splitting. The use of digital computation techniques are recommended. Divide the distance between the peaks by two and assign this as the value for chemical shift indicated above. Replace the Standard crystal with the compound whose chemical shift is to be measured as the absorber in the spectrometer. Measure the peak position parameters as a difference between that of the unknown compound and the mid-point between the peaks of the Standard.

The equipping of the source preparation laboratory is still in progress. When completed this laboratory will contain a 10 kW induction furnace and a 10 kW electron beam evaporator which may be used in conjunction with a high vacuum evaporating unit. This apparatus is described in detail elsewhere [1, p 7]. The equipment in the source preparation laboratory, all of which may be used with radioactive materials, makes possible a wide range of functions in the preparation and purification of sources, the study of thin film and surface phenomena and the preparation of ultra-thin calibration absorbers.

The absorber preparation and hot atom research laboratory is a conventional radiochemical laboratory containing two radiochemical fume hoods and a glass vacuum line. A portion of this laboratory is shown in figure 32. These facilities allow the preparation of various compounds as may be required

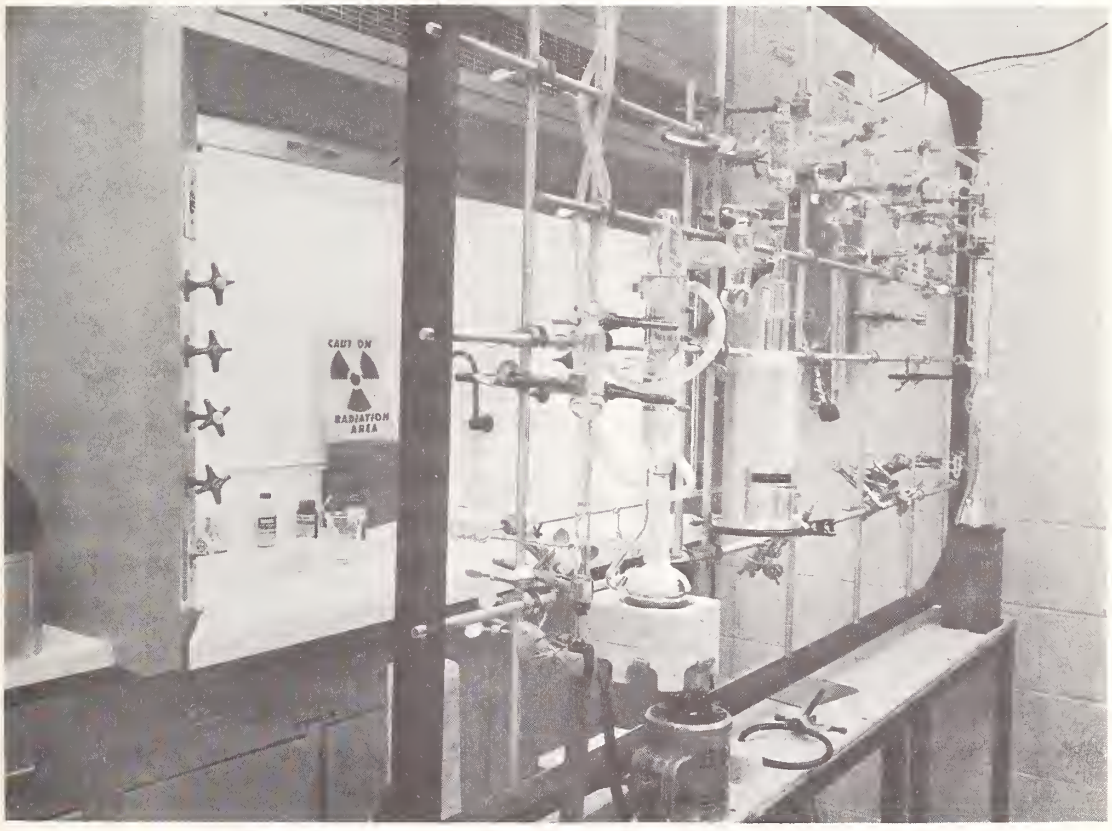

Figure 32. Radiochemical fume hoods and glass vacuum line

by the Mössbauer spectroscopist for use as absorbers or sources. In addition the laboratory will be used in conjunction with the expanding hot atom research program of the Radiochemical Analysis Section.

The measurement laboratory is equipped with two constant acceleration Mössbauer spectrometers [1, p 89][44] each capable of multiplex operation as described elsewhere in this report and a high precision constant velocity spectrometer [1, p 84]. The electronics associated with the two constant acceleration spectrometers have been integrated into a single console shown in figure 33. Supplementary to the new multiplex units, the

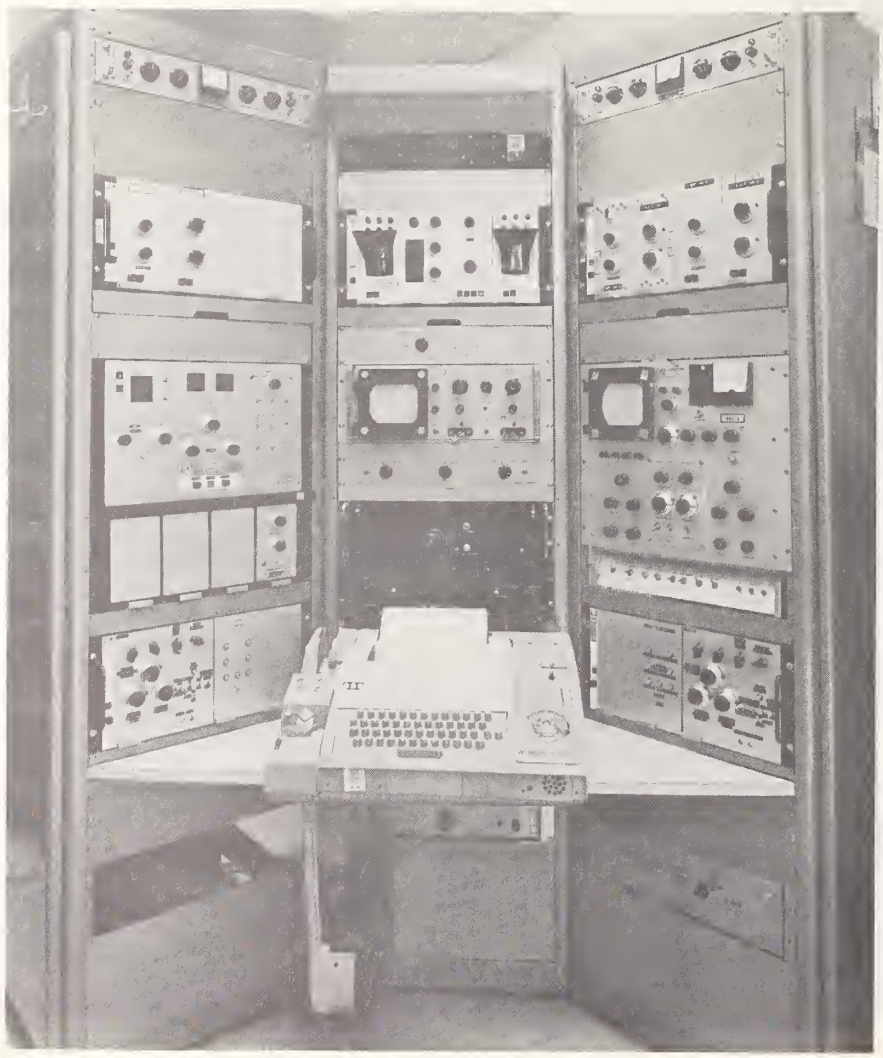

Figure 33. Control console for constant acceleration spectrometer

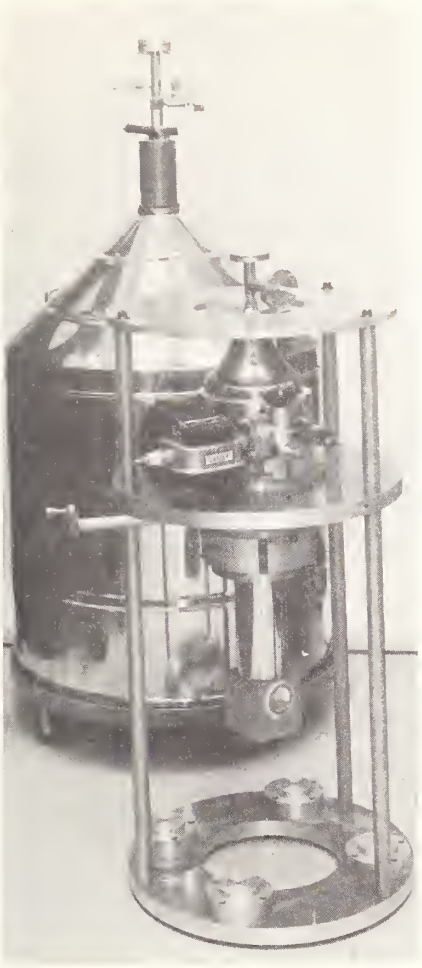

Figure 34. Helium cryostat

electronics have been expanded by the addition of a binary overflow scaler which determines the number of times a spectrum has overflowed the memory of the analyzer. The low temperature research capabilities have been expanded by the addition of a 50 liter helium Dewar to the 5 liter research cryostat (figure 34).

In addition, a teletypewriter computer station to two area computers is available. All spectra are recorded on paper tape and sent to the larger of the two computers via the teletypewriter for analysis using the program described elsewhere in this report. The smaller computer is extensively utilized for associated computations.

(D. K. Snediker)

C. Computer Program for Curve Fitting of Mössbauer Spectra

1. Introduction

A computer program based on an iterative least square fit has been written to process Mössbauer spectra. The program was designed to be used on a CDC 3600 computer, but can be easily modified to be used on a comparable computer with a Fortran IV compiler and double precision arithmetic. A curve plotting routine is also added to provide visual as well as numerical output of the analyzed spectra.

2. Iterative Least Squares Fit to an Arbitrary Number of Lorentzian shapes Superimposed on a Parabola

We assume the Mössbauer spectrum can be fitted to

$$y = \sum_{j=1}^{n} \left\{ \frac{A_j}{1+B'_j(x-C'_j)^2} \right\} + F + Gx + Hx^2 \qquad (1)$$

where x is the energy scale and n is the number of Lorentzian shapes with peaks at C'_j, heights A'_j, and half-widths at half-maximum $1/B'_j$. We now assume [5]

$$C'_j = C_j + \gamma_j \text{ where } C_j \gg \gamma_j \qquad (2)$$

and $$B'_j = B_j + \beta_j \text{ where } B_j \gg \beta_j. \qquad (3)$$

Keeping only first order terms in γ_j and β'_j,

$$y \cong \sum_j \left\{ \frac{A_j}{1 + B_j(x-C_j)^2 + \beta_j(x-C_j)^2 - 2\gamma_j B_j(x-C_j)} \right\} + F + Gx + Hx^2 \qquad (4)$$

Expanding equation 4 in a Taylor series about $\beta = \gamma = 0$ to first order, we have

$$y \cong \sum_j \left\{ \frac{A_j}{1+B_j(x-C_j)^2} + \frac{D_j(x-C_j)}{[1+B_j(x-C_j)^2]^2} + \frac{E_j(x-C_j)^2}{[1+B_j(x-C_j)^2]^2} \right\} + F + Gx + Hx^2 \qquad (5)$$

where $D_j = 2A_j\gamma_j B_j$ and $E_j = -A_j\beta_j$. (6,7)

Defining $P_{ij} = x_i - C_j$ and $q_{ij} = 1 + B_j(x-C_j)^2$, (8,9)

we now require that

$$S = \sum_i w_i \left\{ y_i - \sum_j \left[\frac{A_j}{q_{ij}} - \frac{D_j P_{ij}}{q_{ij}^2} - \frac{E_j P_{ij}^2}{q_{ij}^2} \right] - F - Gx_i - Hx_i^2 \right\}^2 \quad (10)$$

be a minimum, in order to obtain a least squares fit. In equation 10 the subscript i refers to the experimental data points or channel numbers and the w_i are arbitrary statistical weights which may be attached to the data if so desired. (In the current computer program, all data are equally weighted, that is, $w_i = 1$).

The constraints $\frac{\partial s}{\partial A_j} = \frac{\partial s}{\partial D_j} = \frac{\partial s}{\partial E_j} = \frac{\partial s}{\partial F} = \frac{\partial s}{\partial G} = \frac{\partial s}{\partial H} = 0$

yield $3n + 3$ (11)

linear equations in the $3n + 3$ unknown fit parameters A_j, D_j, E_j, F, G, and H. From $\partial s/\partial A_1 = 0$, we have n equations of the form

$$\sum_j \left[A_j \sum_i \frac{w_i}{q_{ij} a_{i1}} + D_j \sum_i \frac{w_i P_{ij}}{q_{ij}^2 q_{i1}} + E_j \sum_i \frac{w_i P_{ij}^2}{q_{ij}^2 q_{i1}} \right]$$

$$+ F \sum_i \frac{w_i}{q_{i1}} + G \sum_i \frac{w_i x_i}{q_{i1}} + H \sum_i \frac{w_i x_i^2}{q_{i1}} = \sum_i \frac{w_i y_i}{q_{i1}} \quad (12)$$

The n equations obtained from $\frac{\partial s}{\partial D} = 0$ are of the same form as equation 12, except that each term in the sums over i must be multiplied by P_{i1}/q_{i1}. The n equations from $\partial s/\partial E_\ell = 0$ may be obtained from those for a $\partial s/\partial D_\ell = 0$ by multiplying in g, each term in the sums over i by P_{i1}. From $\partial s/\partial F = 0$ we have an equation which may be obtained from equation 12 by

deleting q_{i1}. The equation from $\partial s/\partial G = 0$ can be derived from that for $\partial s/\partial F = 0$ by multiplying each term in the sums over i by x_i. The equation from $\partial s/\partial H = 0$ can then be obtained from that for $\partial s/\partial G = \partial 0$ by again multiplying each term in the sums over i by x_i.

The above 3n + 3 linear equations may then be solved for A_j, D_j, E_j, F, G, and H. (Computation time may be saved by noting that the coefficients of the unknown fit parameters in a least squares fit form a symmetric matrix). From A_j, D_j, and E_j, β_j and γ_j may be obtained from equations 6 and 7 above. Inserting these values into equations 2 and 3, one may replace C_j and B_j in the above 3n + 3 equations by C'_j and B'_j and again solve for the fit parameters. This iteration may be continued until desired accuracy is obtained, according to various convergence criteria. (In the current computer program, percentage difference convergence criteria are applied to A_j, B_j, and C_j).

Our linearization of equation 1 in the fit parameters B'_j and C'_j to a first order approximation thus leads to an iterative least squares fit which will converge to a least squares fit of the data for equation 1 itself, provided the initial estimates of the Lorentzian peak locations and widths are sufficiently close to the most probable locations and widths, assuming equation 1 is capable of giving a sufficiently good fit to the data. In practice, convergence is insensitive enough to the initial estimates, so that the desired accuracy is obtained in only a few iterations, according to our convergence criteria. We know of no simple transformation of equation 1 into one exactly linear in all of the parameters.

3. Error Calculations

For the error calculation it is sufficient to obtain the variance of the fitting parameters. Since the amplitude varies linearly, the variance can be obtained from

$$\mathrm{VAR}\ (A_j) = \frac{S \cdot A_j^{-1}}{A_j^2} \qquad (13)$$

where

$$S^2 = \frac{\sum^{R} dev^2}{k-N}$$

with N the number of coefficients to be fitted, and k the number of data points (channels).

In the least squares fitting technique by iterations, the peak parameters are not calculated, only their corrections. The error in the corrections will therefore equal the error in the final parameter value. Since the correction computed for the halfwidth is D_j, (equation 6), the variance of the halfwidth is

$$VAR(H_j) = \frac{A_{Hj}^2}{A_j^2} \frac{S \cdot A_j}{A_j^2} + \frac{S \cdot A_{Hj}}{A_{Hj}^2} + \frac{S \cdot A_{jHj}}{A_j \cdot A_{Hj}} \qquad (14)$$

Similarly for the peak position

$$VAR(P_j) = \frac{A_{Pj}^2}{2H_j A_j} \frac{S \cdot A_j}{A_j^2} + \frac{S \cdot A_{Pj}}{A_{Pj}^2} + \frac{S \cdot A_{jPj}}{A_j \cdot A_{Pj}} \qquad (15)$$

The standard deviation is now defined by the square root of the variance.

4. Computer program

The computer calculations are made using equations 10, 13, and 15. A flow diagram is shown in figure 35, and the loading of the instructions, identification and data in figure 36. The complete program is listed in Appendix II. The program is written for a Control Data Corporation 3600 computer in Fortran 5.1, with a plot package for the Calcomp plotter. The fitted spectra of a single crystal of $Na_2Fe(CN)_5NO \cdot 2H_2O$ and that of a commercially obtained enriched iron foil are shown in figures 37 and 38.

Conclusion

The program has been of great value in Mössbauer spectroscopy, particularly in resolving complex spectra. For doublet type spectra, computer running time is approximately 10 seconds per spectrum while for 9 line spectra about 1 minute is required.

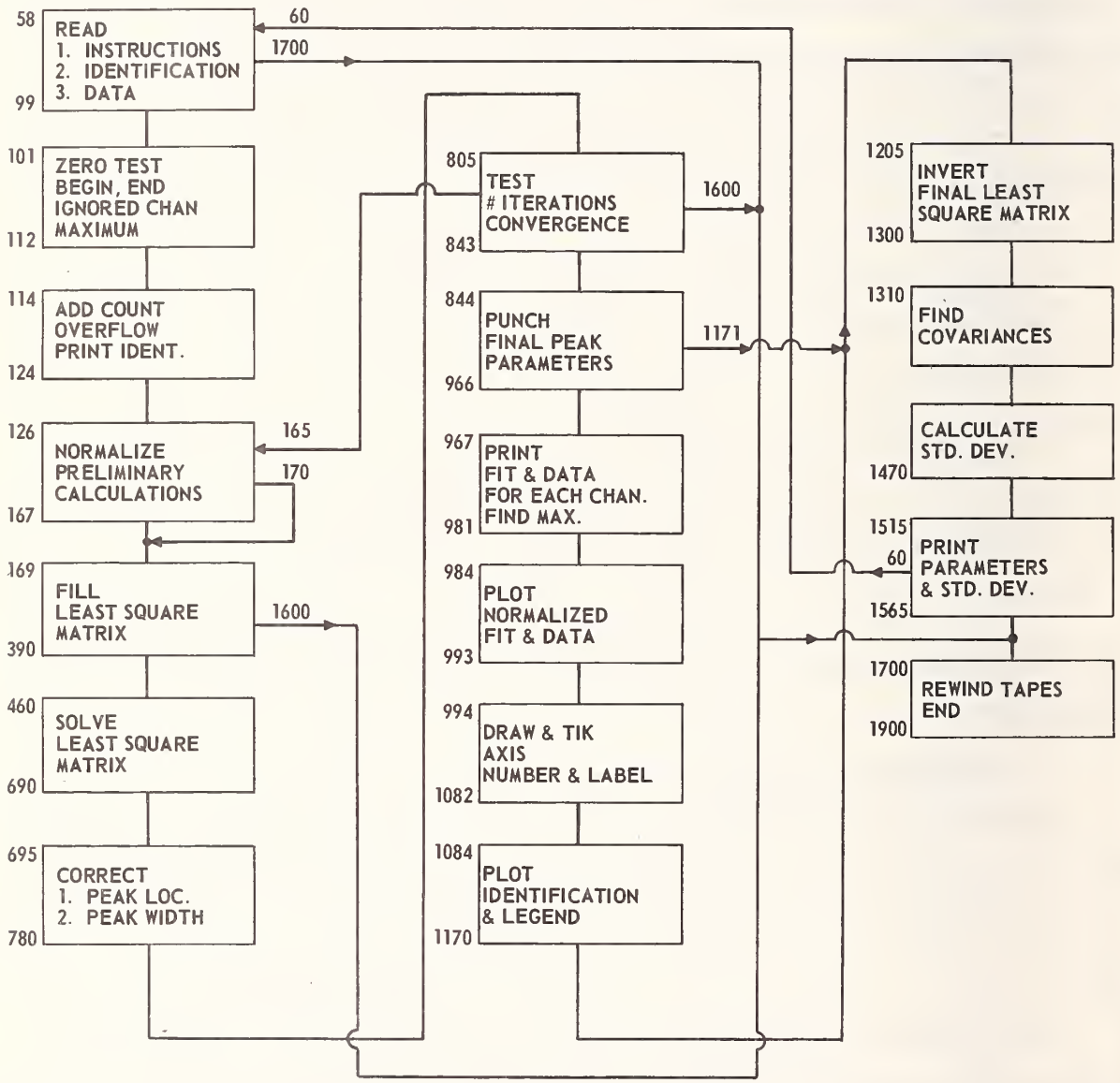

Figure 35. Flow diagram of computer program for curve fitting of Mössbauer spectra

The cost per spectrum including plotting averages about $8.00 per spectrum. Manual processing would cost approximately the same (4 man-hours) but the precision would be a factor of 10 lower, and an error analyses would not be possible. Two peaks separated by more than one half linewidth can be resolved.

The present program assumes Lorentzian line shapes, which is not valid for spectra with broad lines such as encountered in high spin Fe^{3+} compounds. Other mathematical models are being considered to more closely approximate the line shapes predicted by Mössbauer theories, including thickness broadening and relaxation phenomena.

(E. Rhodes, W. O'Neal, and J. J. Spijkerman)

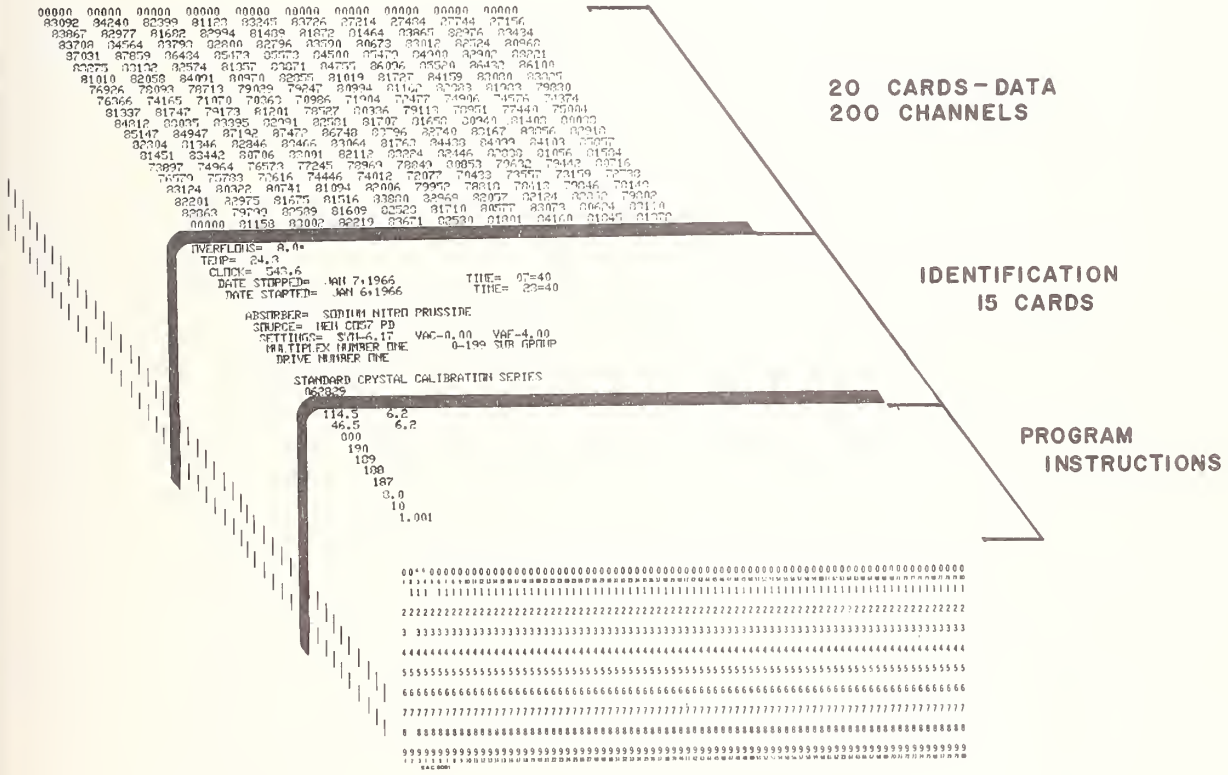

Figure 36. Loading instructions for computer program

Figure 36. Loading instructions for computer program

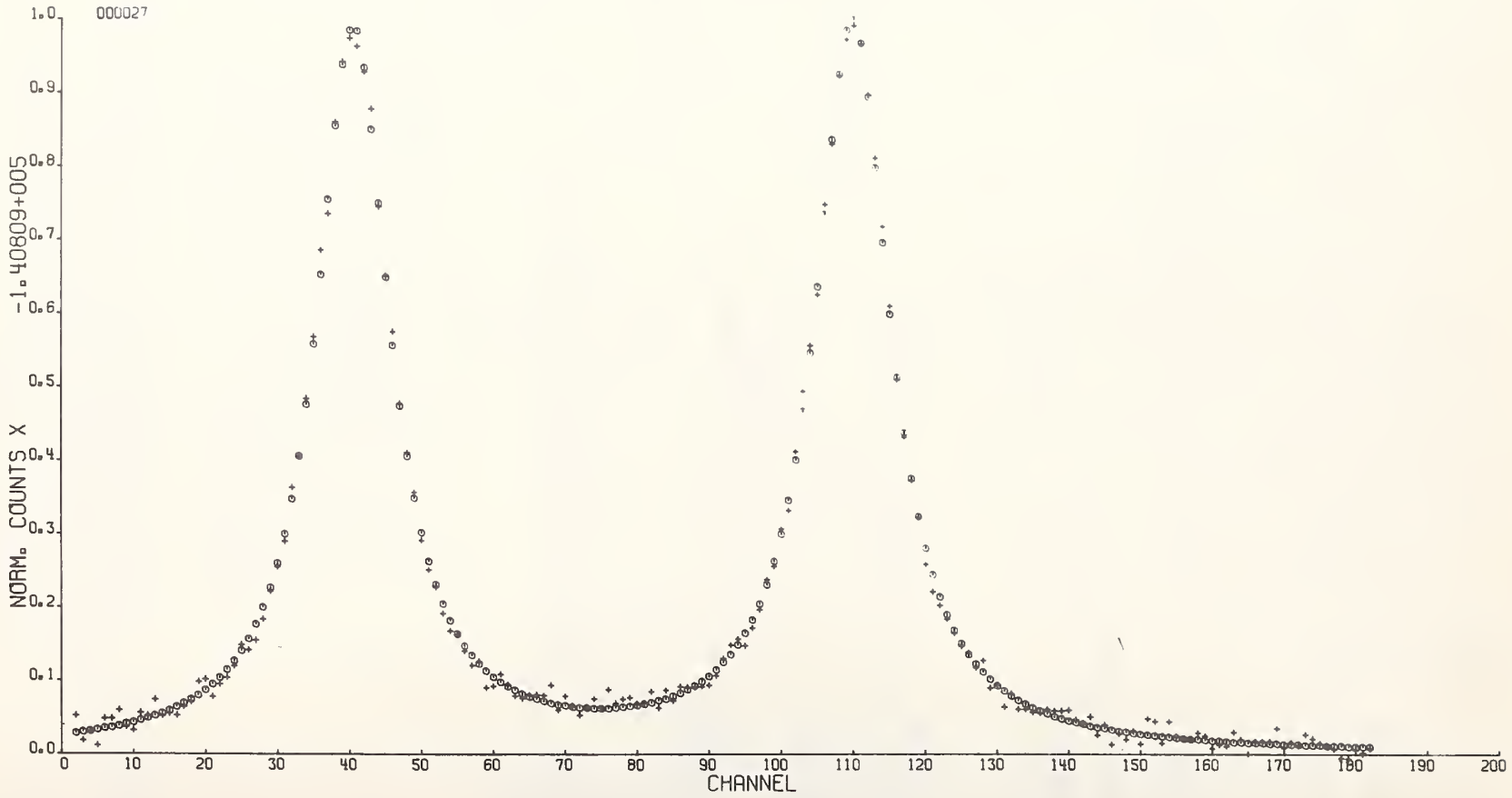

Figure 37. Curve of fitted spectrum of standard crystal

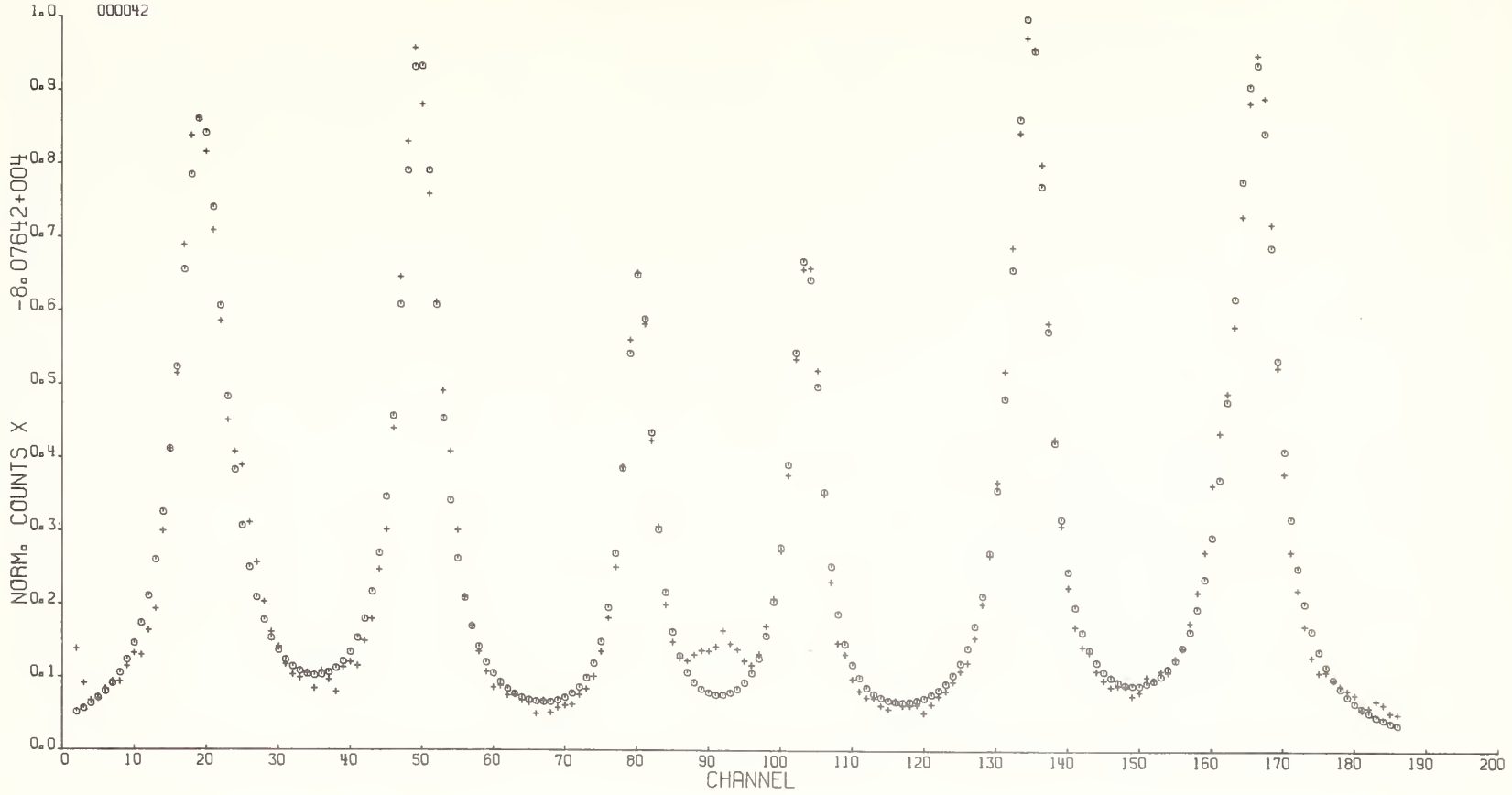

Figure 38. Curve of fitted spectrum of commercial iron foil (see Appendix II)

D. Instrumentation

1. Cell for Producing Powdered Mössbauer Absorbers of Reproducible Thickness

The analytical applications of Mössbauer spectroscopy require a means of producing a powdered absorber of known reproducible thickness. The beryllium-window powder cell described here provides the analytical chemist with an easily-used means of producing powdered absorbers of known thickness without resorting to a pellet press.

Figure 39 shows a cross-sectional view of the powder cell assembly. In general the cell consists of a thick aluminum disk (c) to which a fixed 10 mil beryllium bottom window (b) is fixed with a clamping ring (d). The removable 10 mil beryllium top window (b) is retained by a shim ring (a). The thickness of the center portion of this shim ring determines the cell thickness when a powder is placed in the volume between the windows. Table 16 shows the relationship between the shim thickness in inches (dimension x in figure 39) and the corresponding cell thickness in mm. These dimensions are valid only if 10 mil windows are used. The cell is designed such that it

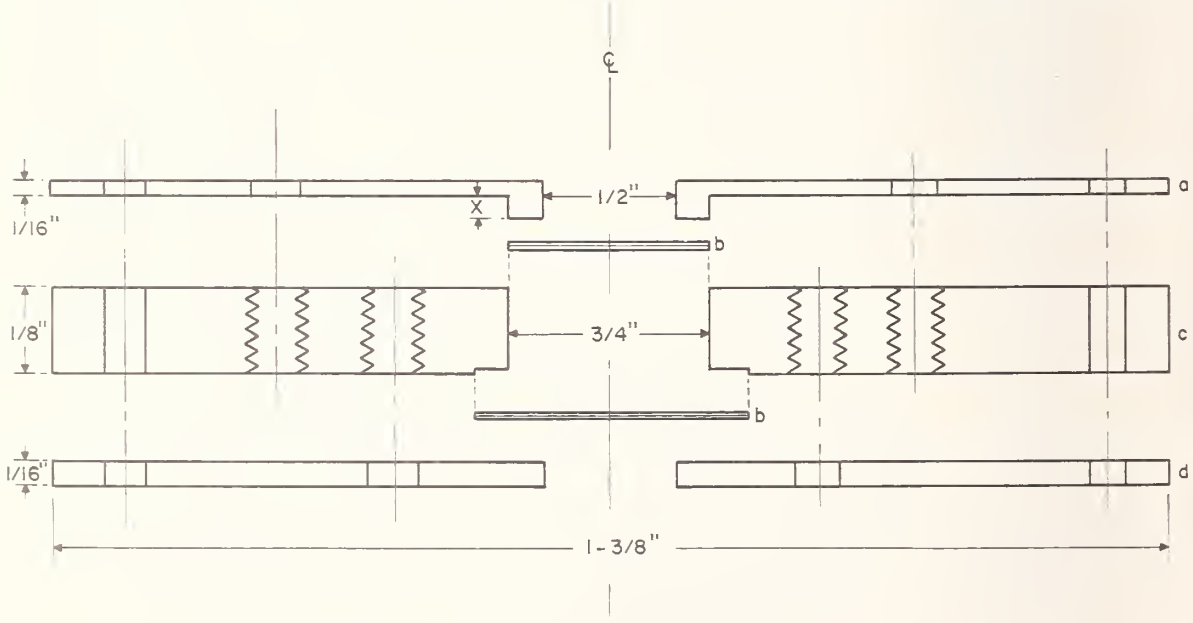

Figure 39. Cross sectional view of powder cell assembly

Table 16. Relationship between shim thickness and cell thickness

x (in)	0.0938	0.0544	0.0150
$t_{(mm)}$	1	2	3

may be loaded without removing the bottom window and clamping ring. With these pieces in place the assembly is a convenient container into which is weighed the absorber powder.

Figure 40 shows a spectrum of SnO_2 in the powder cell with a 1 mm cell thickness. The spectrum is identical in every respect to the SnO_2 spectra obtained using other commonly used absorber mounting methods. Although figure 40 represents a spectrum obtained using a moving source geometry, the aluminum cell is sufficiently light to allow a moving absorber geometry. The latter geometry is mandatory in the case of iron-bearing absorbers because of the interference resulting from trace iron impurities in the beryllium windows.

2. Fast Response Controlled Atmosphere Furnace

The synthesis of the various tin-119-palladium Mössbauer sources now in use [43, 45] requires a furnace with characteristics not found in common muffle-type furnaces. These characteristics are: extremely fast temperature response and controlled-atmosphere capabilities. In the synthesis of a tin-palladium alloy, it is necessary to melt β-tin ($\begin{matrix}\text{m.p.} = 232\ ^\circ\text{C} \\ \text{b.p.} = 2270\ ^\circ\text{C}\end{matrix}$) together with palladium foil (m.p. = 1552 °C). In order to minimize the evaporation of tin during the melting process the temperature of the crucible must be raised to ~ 1600 °C as rapidly as possible. Furthermore, the heating should be carried out in an inert atmosphere such as Ar or N_2 in order to minimize the oxidation of tin during the melting process. In general, furnaces meeting these specifications such as induction furnaces or self-contained vacuum systems are prohibitively expensive for occasional source making.

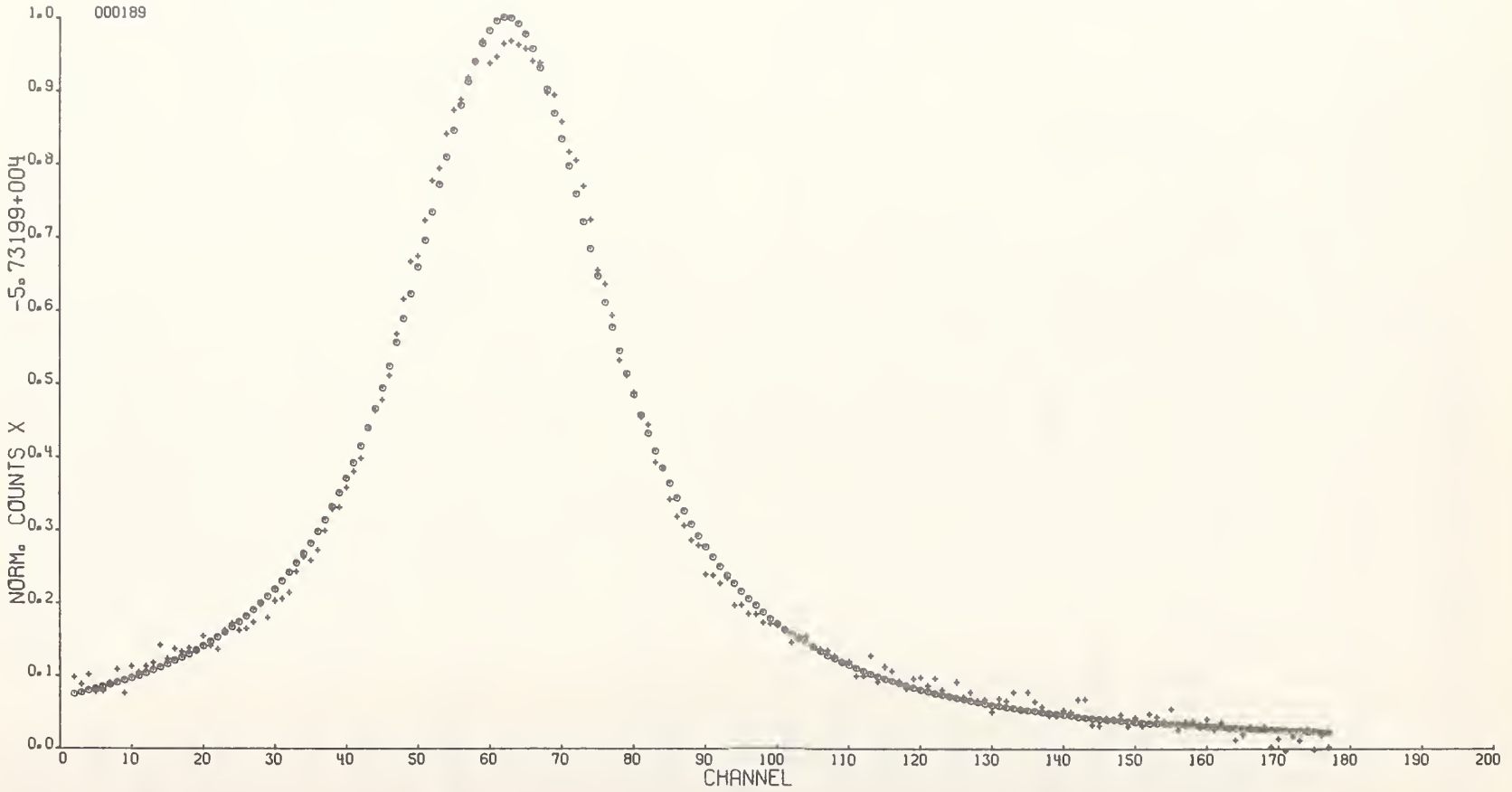

Figure 40. Curve of fitted spectrum of SnO_2

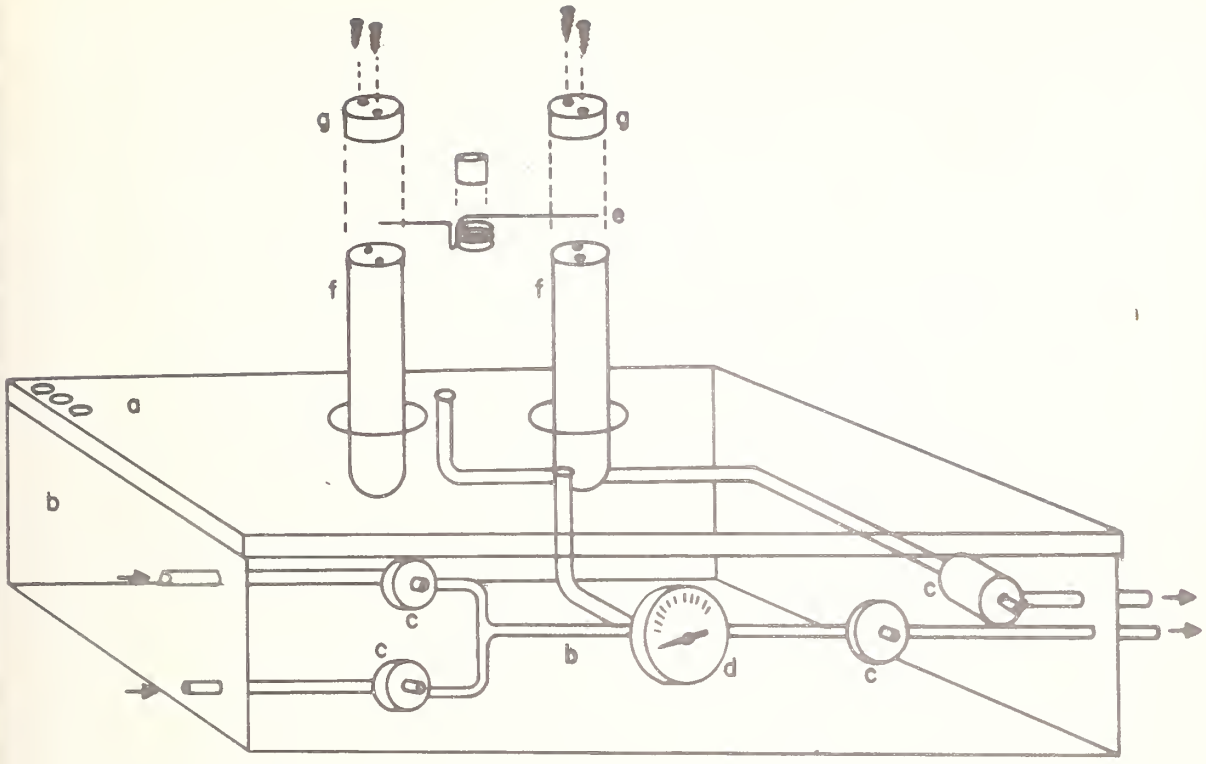

Figure 41. Phantom view of furnace

An inexpensive furnace has been designed and constructed at the National Bureau of Standards which has the requisite characteristics for ^{119m}Sn-Pd source synthesis. In principle, the furnace is similar to self-contained vacuum systems in that the crucible is surrounded by a tungsten basket that is connected to two feed-throughs. The crucible-basket assembly is contained in a bell jar and is heated by passing current from a high current power supply through the basket. Figure 41 shows a phantom view of the furnace. All dimensions are approximate.

The base-plate (a) of the furnace is made from 1/2" thick stainless steel. The surface is ground flat such that the Viton gasket will seat properly. Stainless steel is used for the plate because of its corrosion resistance and its relatively low heat transfer properties. The base-plate is supported by 1/4" thick aluminum side plates (b). These plates are in a box configuration in order to provide a stable platform for the heavy base plate.

The vacuum and gas flow system is constructed from 1/4" O.D. copper tubing and torque-free swaged tube fittings. The valves (c) are forged-body needle valves. The vacuum branch of the system is designed to allow the evacuation of the bell jar using a conventional positive-displacement pump. In addition to allowing operation as a vacuum furnace, the vacuum capability speeds the purging of the furnace for inert gas operation. The gas-flow branch is designed to allow the connection of two different gas cylinders to the system. Mixing can be done in this branch if desired. After passing through the bell jar the gases are conducted through a flow meter before being exhausted to the atmosphere in a radiochemical hood. A gauge (d) reading both vacuum and pressure is fitted to the manifold at a location common to both the vacuum and gas-flow branches.

The electrical connections to the tungsten basket (e) are made through a pair of 1/2" O.D. copper high current feedthroughs (f). The feed-throughs are attached to the bottom of the base plate with high vacuum flanges. Half-inch diameter copper caps (g) are used to clamp the tungsten basket to the tops of the feed-throughs. Current is provided by a 5 kVA power supply. The specific voltage and current requirements depend upon the type and size of tungsten heating element chosen.

For reasons of economy an inverted 15 cm vacuum desiccator bottom is used as a bell jar. A vacuum seal between the desiccator and the base plate is effected using a Viton gasket. This arrangement has proven quite satisfactory in nearly all respects. However, due to the relatively modest depth of the desiccator, the desiccator bottom is quite close to the tungsten coil and has a tendency to overheat. This characteristic limits the full power operation of the furnace to less than five minutes.

This inexpensive resistance furnace has all of the requisite performance characteristics for the synthesis of tin-palladium Mössbauer sources. Heating rates up to 1000 °C/min

have been observed. A maximum temperature of 1700 °C, determined at the crucible bottom with an optical pyrometer, has been measured. The furnace has great flexibility with regard to controlled atmosphere and vacuum operation.

The author wishes to acknowledge Dr. J. L. Thompson for contributing many of the basic concepts in the design of this furnace.

(D. K. Snediker)

3. Multiplex for Dual Spectra

a. Introduction. In order to improve the accuracy of data taken with the NBS Drift-Free Mössbauer Spectrometer [44], it is desirable to accumulate two spectra simultaneously with the velocities provided by one electromechanical drive. The data can be stored in the two memory halves of a multichannel analyzer. In this way, it is possible to take spectra of a standard and a sample at the same time with both having exactly the same velocity dependence. From the data taken with the standard, a velocity calibration of the spectrometer can be obtained, and this calibration can be used to express the results with high accuracy.

b. Analyzer. The analyzer that is being used is an RIDL 34-27*. The analyzer is operated in the time mode and the analog voltage of its address scaler is used as the input signal to the drive amplifier. A pulse is supplied to the analyzer time base input in the time mode to initiate a memory cycle and channel advance. This pulse begins the analyzer's memory cycle program which is as follows:

(1) Add-1 (Time 1.5μs) This part of the program adds one count to the analyzer's add-subtract scaler if the temporary store bistable was set when the analyzer was in the previous memory cycle.

---

* For disclaimer of equipment and materials see last paragraph of preface.

(2) Write (Time 2.5 μs) In this part of the program, the data stored in the add-subtract scaler is transferred into the proper channel location of the magnetic memory.

(3) End of Program (Time 1.5 μs) This part of the program acts as a delay in the time mode. At the end of its delay it produces a channel advance pulse (C.A.P.) which causes the address scaler to advance one channel.

(4) Delay (Time 3 μs) Delays program cycle 3 μs while address is advanced.

(5) Read (Time 2.5 μs) This is the last step in the memory cycle and it transfers the data for the new channel from the memory into the add-subtract scaler.

c. Multiplex Logic. In order to lower the data accumulation time, the multiplex (figure 42) was designed so that the memory of the analyzer would be used on a demand basis by the two detector systems. This is done because the memory cycle time of the analyzer is 12.5 μs. If the memory was not used on a demand basis each pulse from either detector would require a memory cycle and the dead time of the system would be increased.

In order to use the memory of the analyzer on a demand basis the multiplex must specify when the analyzer is to change subgroups. When data is being accumulated in one subgroup (e.g. for detector A) and a count comes in for the other subgroup (detector B) the analyzer receives a pulse (Store Pulse) which causes a memory cycle with a change of subgroup instead of a channel advance. The store pulse is derived from the change of state of bistable "A" which is triggered when a count which should be stored in the other subgroup arrives from one of the detector systems. The store pulse is introduced at the time base input and the analyzer starts its program cycle.

To save the pulse that caused the memory cycle and store it in the add-subtract scaler, it is necessary to delay the pulse until the analyzer is in its memory cycle and then set the temporary store bistable. When the analyzer goes through its next memory cycle, the count will be added to the data for that channel and stored in the memory.

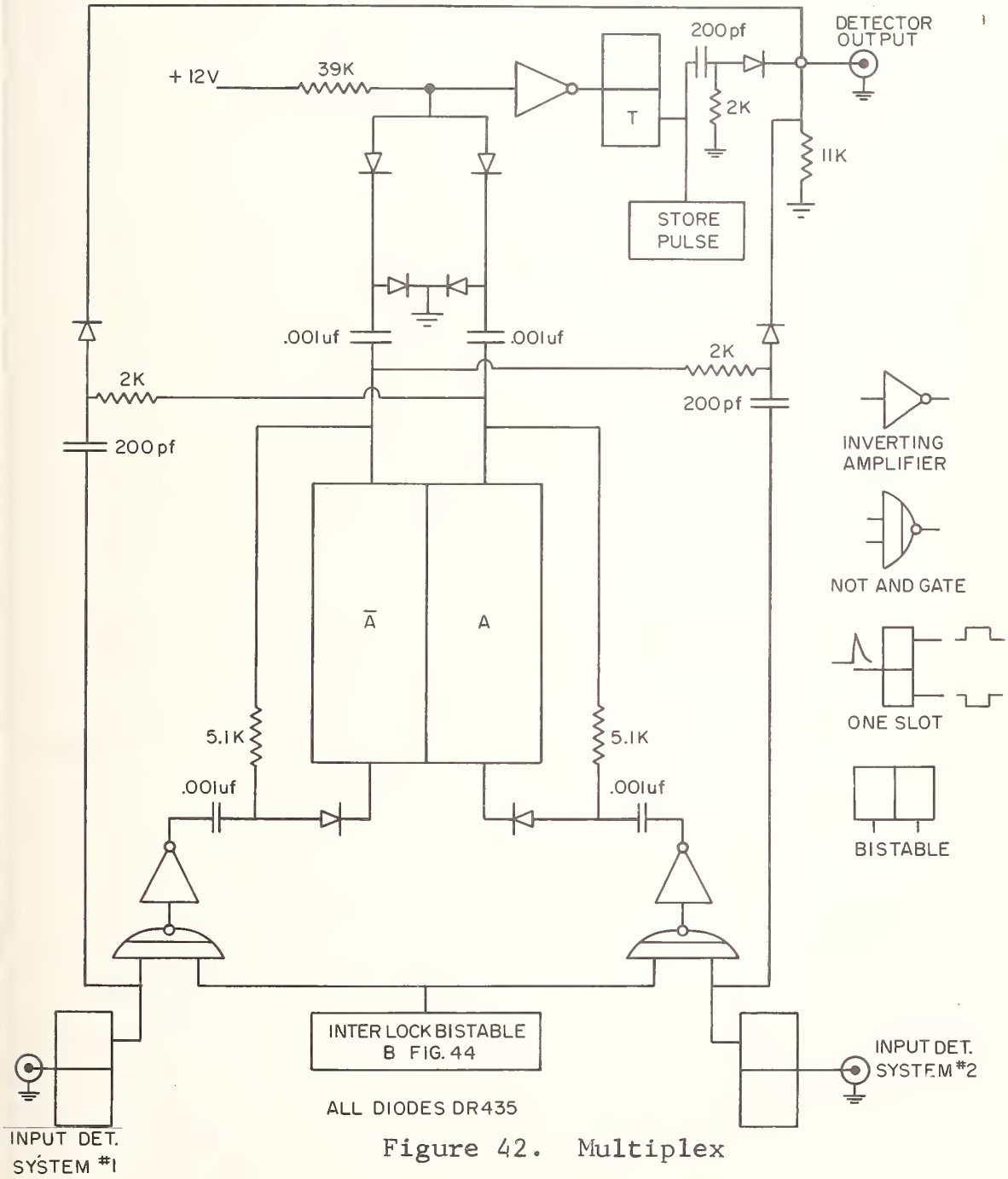

Figure 42. Multiplex

d. Logic to Interface Multiplex to Analyzer. In order to operate the analyzer in the multiplex mode, it is necessary to modify the program of the memory cycle slightly. There are, in fact, two program cycles necessary. When there is a pulse from the time mode oscillator, the analyzer program cycle should not be changed. When the analyzer receives a pulse from the multiplex telling it to change subgroups (store pulse), it must initiate a memory cycle which does not have a channel advance pulse after the End of Program. At this time the 200 bistable in the address scaler should change its state to correspond to the correct subgroup and the program should finish as in a normal cycle. The manner in which the second program is accomplished is to break the analyzer's memory cycle at the output of the End of Program one-shot. This output is taken to the interface and is tested by the C.A.P. gating circuit to see if a time mode oscillator pulse had occurred before it. If a time mode oscillator pulse had occurred, then the C.A.P. gate gives an output and the channel is advanced. If a C.A.P. had not occurred, the C.A.P. gate does not give an output, and the program cycle is completed with a change of subgroup and without a channel advance.

e. C.A.P. Gating Circuit. The analyzer can be made to go through a memory cycle by two events: (1) a store pulse, and (2) a time mode oscillator pulse. Because the analyzer could be in a memory cycle when the time mode oscillator pulse arrives, it is necessary to insure that the analyzer will have a channel advance. The channel advance pulse gating circuit (figure 43) contains the necessary logic to accomplish this. The time mode oscillator pulse triggers one-shots "P" and "Q" and bistable "C". One-shot "P" is set in order to inhibit the output of gate "V" which insures that bistable "C" can be set even in the presence of a C.A.P. If the analyzer is in a memory cycle, "C" can be set before or after the C.A.P. If C is set before the C.A.P., then the analyzer will have a channel advance and C will be reset. If "C" is set after the C.A.P., then the

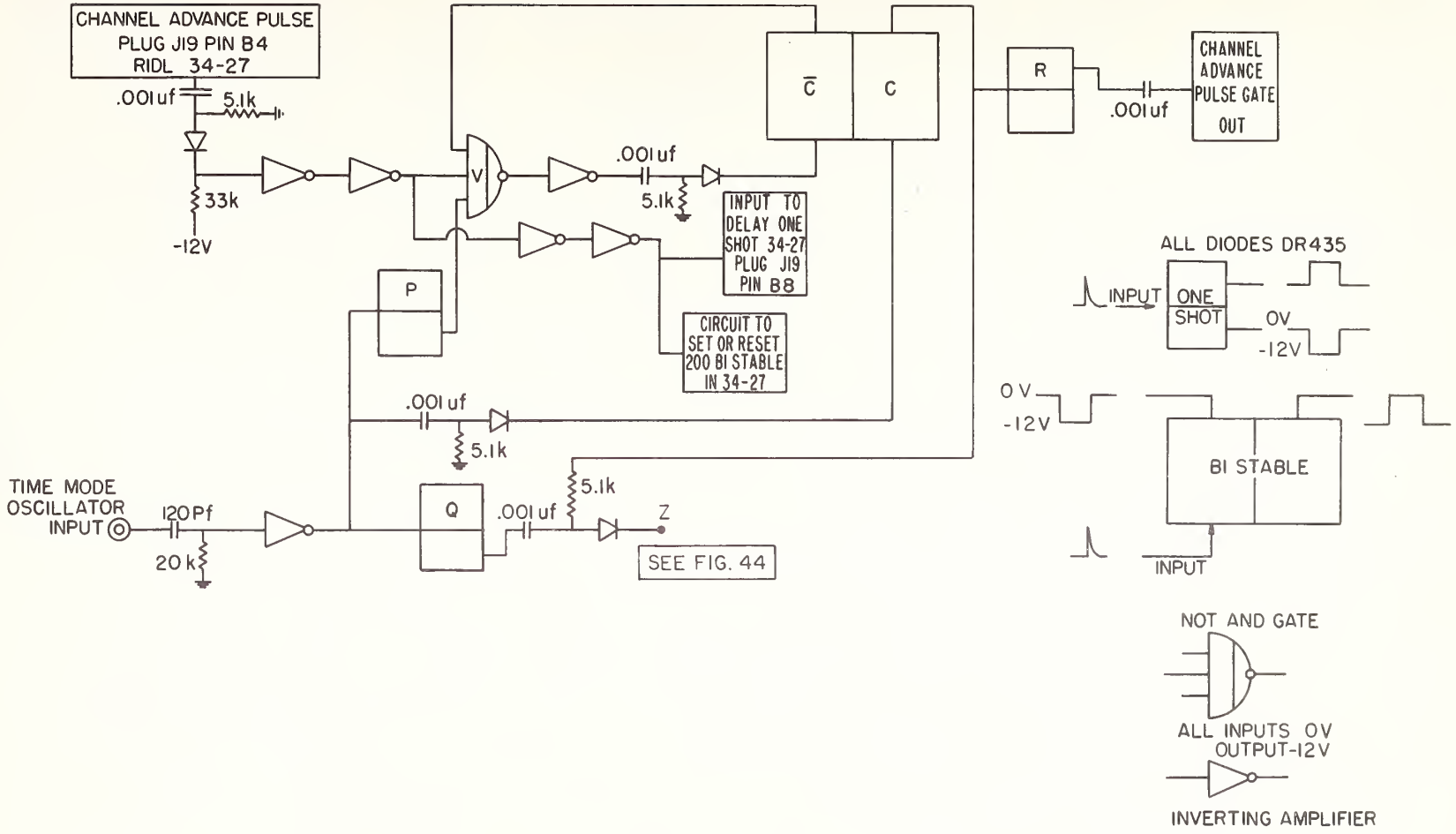

Figure 43. Channel advance pulse gating circuit

analyzer will continue to the end of its program cycle, and a new cycle is initiated when one-shot "Q" returns to its stable state. When the C.A.P. from this memory cycle arrives "C" is set. Therefore, the analyzer advances one channel and "C" is reset. If the analyzer was not in a memory cycle when the time mode oscillator pulse arrives then after a minimum of 8 μs delay the memory cycle with a channel advance is initiated.

f. Interlock Circuit. The memory cycle program of the analyzer would be disrupted if it received pulses on its time base input while it was in a memory cycle. To insure that the memory cycle is not disrupted, it is necessary to have an interlock circuit (figure 44) which inhibits all pulses to the time base input while the analyzer is in a memory cycle. The circuit works in the following manner. When there is a pulse at the time base input of the analyzer, bistable B is set into the state which inhibits and gate X until the end of time program pulse which resets B.

Bistable "B" is also used to inhibit and gates Y and Z so that the state of bistable A does not change during the analyzer memory cycle. If "Y" and "Z" were not inhibited and if the count rate on one side was much lower than on the other side, the fast side would accumulate almost all of the time to the complete exclusion of the slower side.

g. Conclusion. The Multiplex for Dual Beam Mössbauer Spectroscopy was designed using Transistorized Building Blocks for Data Instrumentation [46] with very few minor modifications.

The system when used with the NBS Mössbauer spectrometer has given good dual spectra. By the use of a sodium nitroprusside standard absorber [41], the errors in the reproducibility of the velocity have been reduced to 10^{-4} cm/s/month.

The author would like to acknowledge the assistance and helpful discussions with R. W. Shideler and J. J. Spijkerman.

(F. C. Ruegg)

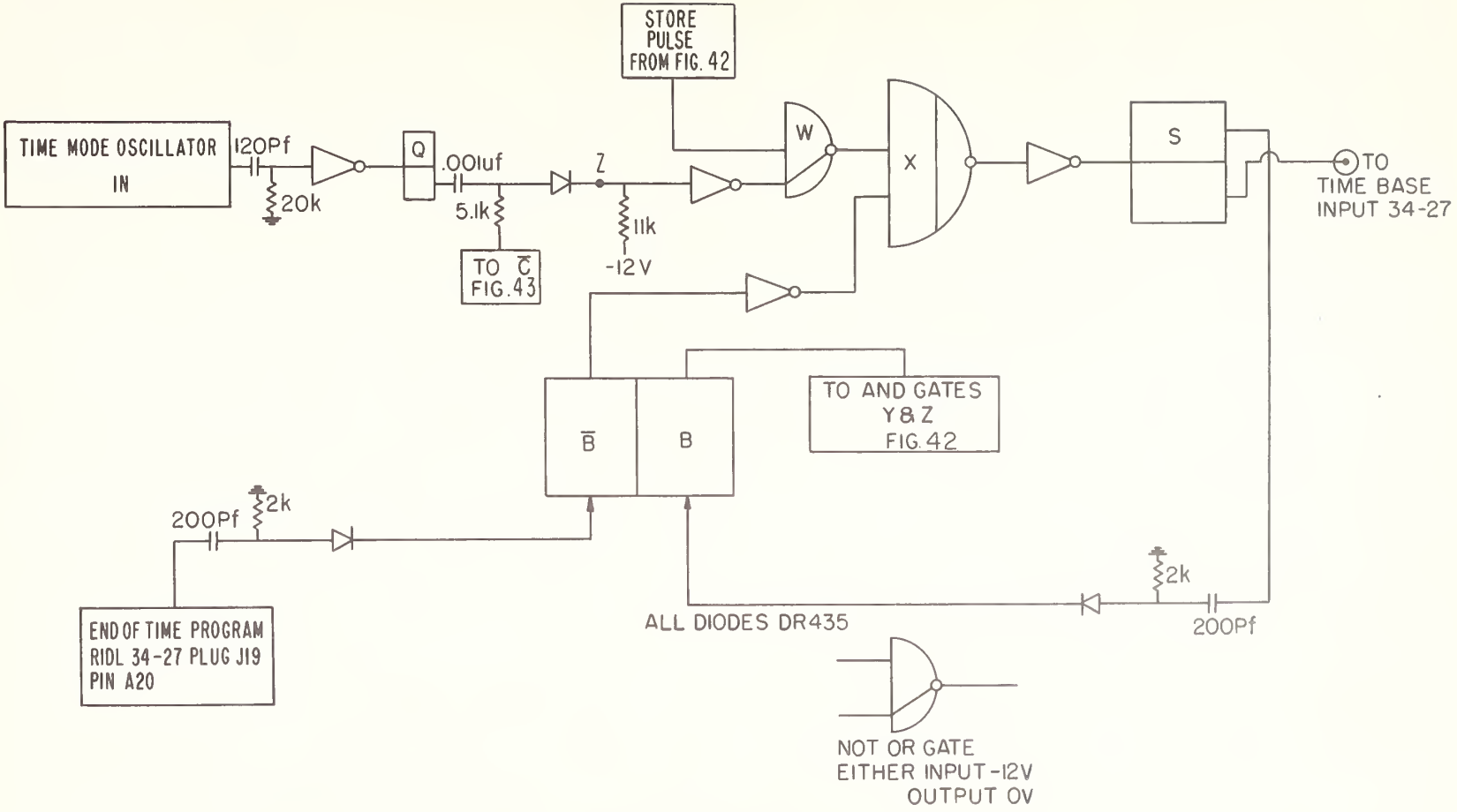

Figure 44. Interlock circuit

4. Gas Flow Proportional Counter for ^{57}Fe Mössbauer Spectroscopy

a. Introduction. The prerequisites for a detector for ^{57}Fe Mössbauer spectroscopy are that the detector be able to resolve the 14.4 keV gamma ray and 6.3 keV x-ray, and be as insensitive as possible to the 122 keV and 136 keV gamma ray of the nuclear energy spectrum of ^{57}Co. Because of the low energy of the 14.4 keV gamma ray of Mössbauer interest, a proportional counter is an ideal detector to use.

b. Gas Flow Proportional Counter for ^{57}Fe Mössbauer Spectroscopy. At NBS, a Reuter-Stokes model RSG-30A* proportional counter with a 90% xenon, 10% methane gas fill was used in our Mössbauer experiments. After using this detector for about a year, it was decided to use a gas flow system (figure 45) using 90% argon and 10% methane gas which has several advantages over the sealed counter. The life of the detector when >5 mCi sources are used is increased by many orders of magnitude. The signal-to-noise ratio is improved because the argon-methane gas is not as sensitive to the higher energy radiations. The gas has a higher gain at 2000 volts.

c. The Proportional Gas Filling. The argon-methane proportional gas gives a much improved signal-to-noise ratio for the 14.4 keV gamma ray because it is virtually insensitive to the higher energy radiations. The signal-to-noise ratio for the gas flow counter using the same geometry and detection system is approximately 3 times better than the signal-to-noise ratio for the sealed Xe-CH_4 detector. The geometry is: (1) the detector's Be window is covered by a 1/16-in lead backed with 1/6-in Al filter which has a .5-in diameter hole centered over the Be window, (2) the Be window is 7 cm from a 5 mCi ^{57}Co source. Using this geometry, removal of the lead shield causes the 14.4 keV gamma peak to be obliterated by the Compton scattering continuum in the case of the xenon-methane detector,

* For disclaimer of equipment and materials see last paragraph of preface.

while argon-methane flow detector continues to give a good spectrum with a signal-to-noise ratio (figure 46) better than the xenon-methane detector with lead shielding. The gas flow counter when moved still closer to the source continues to give a clean spectrum with a high signal-to-noise ratio.

d. Relative Efficiency of Two Gases. The relative efficiency of the two counters is shown in figure 47. The efficiency of the gas flow detector is 20% of the efficiency of the Xe-Ch_4 counter at 14.4 keV. The poorer efficiency is

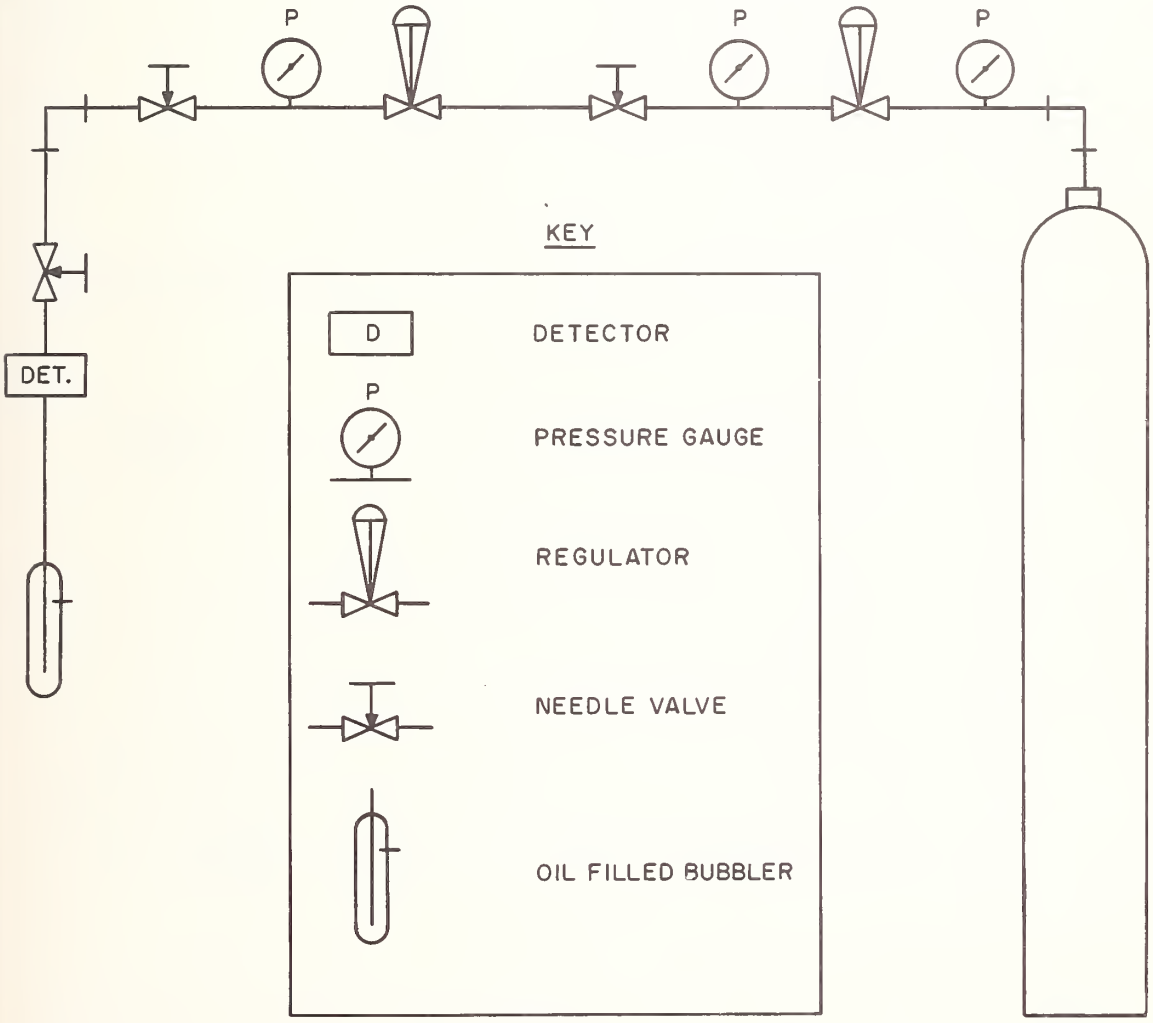

Figure 45. Schematic of gas flow system

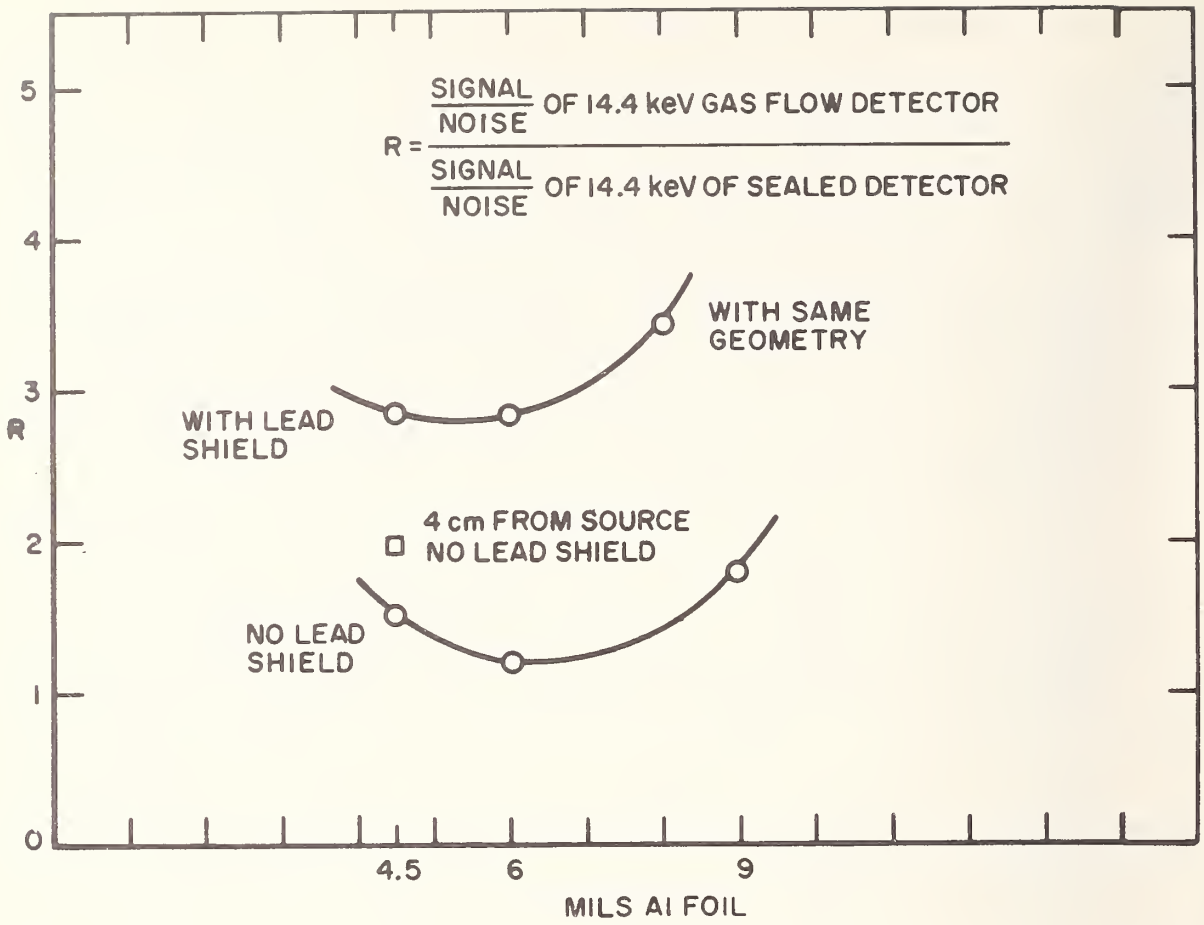

Figure 46. Plot of the signal-to-noise ratio of the gas flow detector compared to the sealed detector for the 14.4 MeV gamma ray

caused by the fact that argon is less dense than xenon and hence it does not absorb as many 14.4 keV gamma rays. The poorer efficiency can be compensated for by improving the geometry of the argon-methane detector. Therefore it is possible with a 5 mCi ^{57}Co source to handle more 14.4 keV gamma rays with a higher signal-to-noise ratio with improved resolution using the argon-methane detector than using the xenon-methane detector.

e. Filter. Because of the large number of 6.3 keV X-rays from the source, and because the two proportional gases have a larger efficiency for the X-rays than for the gamma rays,

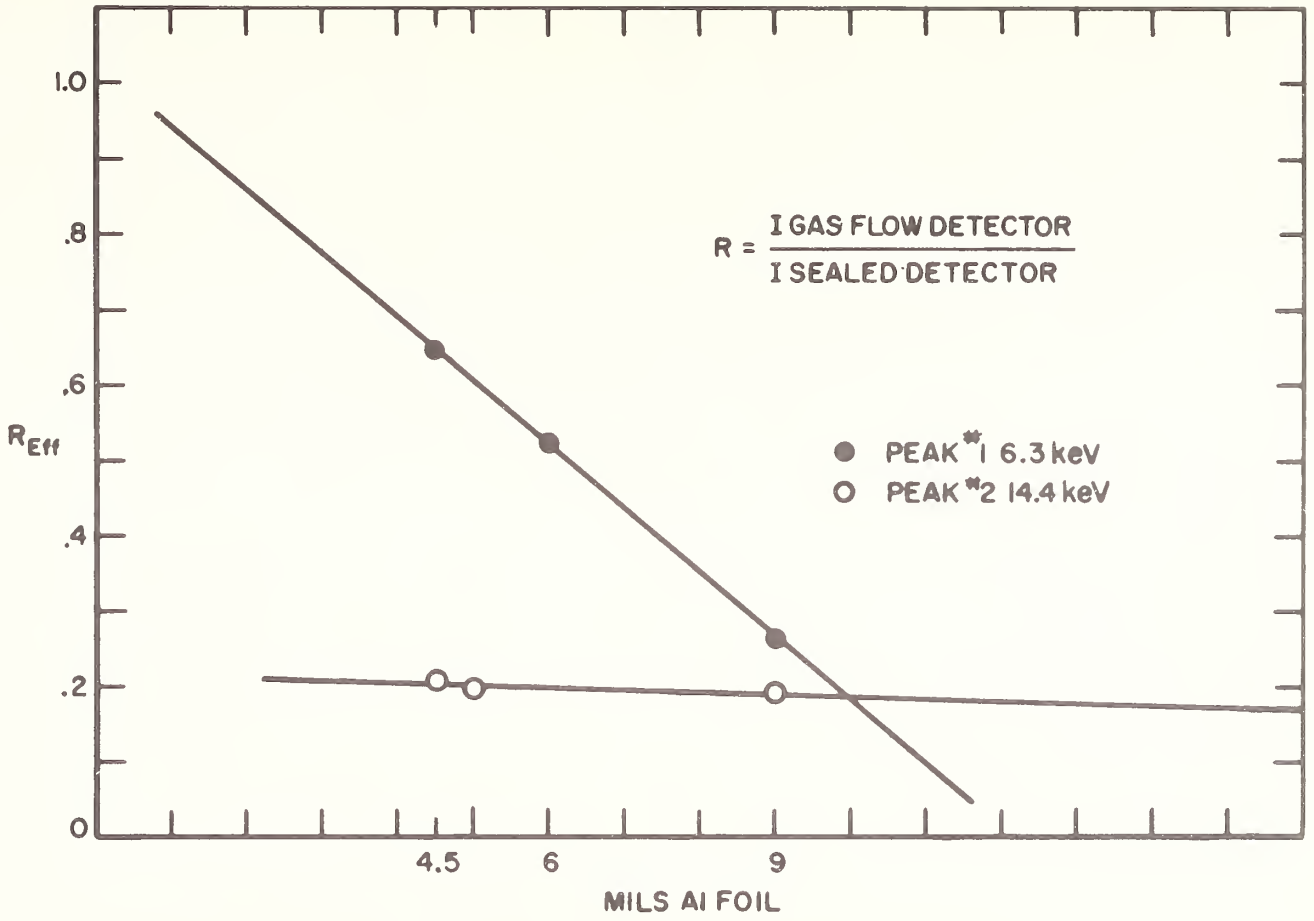

Figure 47. Plot of the relative efficiency of the two detectors

it is advisable to use a filter like aluminum to decrease the detector dead time resulting from the X rays. Figure 48 is a graph of the relative intensities of the 14.4 keV gamma ray and 6.3 keV X ray vs. the thickness of the aluminum filter.

f. The Gas Flow Detector. The gas flow detectors that are being used are modified tubes which no longer worked because the xenon-methane gas had been sufficiently degraded by the high gamma flux. The modifications necessary to convert them to flow counters are to drill two holes in the cylindrical counter at each end diametrically opposed to the Be window, and epoxy two bakelite inserts into the holes to provide an input and vent for the argon-methane gas. It is also possible to buy the flow detectors commercially.

g. The Detection System. The detection system is: the proportional counter, model 31-24A RIDL preamplifier for gas detector, model 30-23 RIDL double delay line amplifier and a model 34-12 RIDL multichannel analyzer.* A picture of a spectrum accumulated for .5 minutes of live time is shown in figure 49.

(F. C. Ruegg)

E. Search for Sn Standard

The theoretical interpretation of the Mössbauer chemical shift in tin has long been hindered by the lack of a standard to which the chemical shift can be related. At present, α- and β-tin, Mg_2Sn and SnO_2 are all used as differential chemical shift standards by various laboratories. Such a variety of standards renders the task of comparing chemical shift data from various laboratories virtually impossible. Furthermore, it is at present impossible to calibrate a tin spectrum with respect to velocity without changing the source to iron-57 and using a Sodium Nitroprusside Standard Reference Crystal as the absorber. Such a procedure is not only inconvenient, but also

* For disclaimer of equipment and materials see last paragraph of preface.

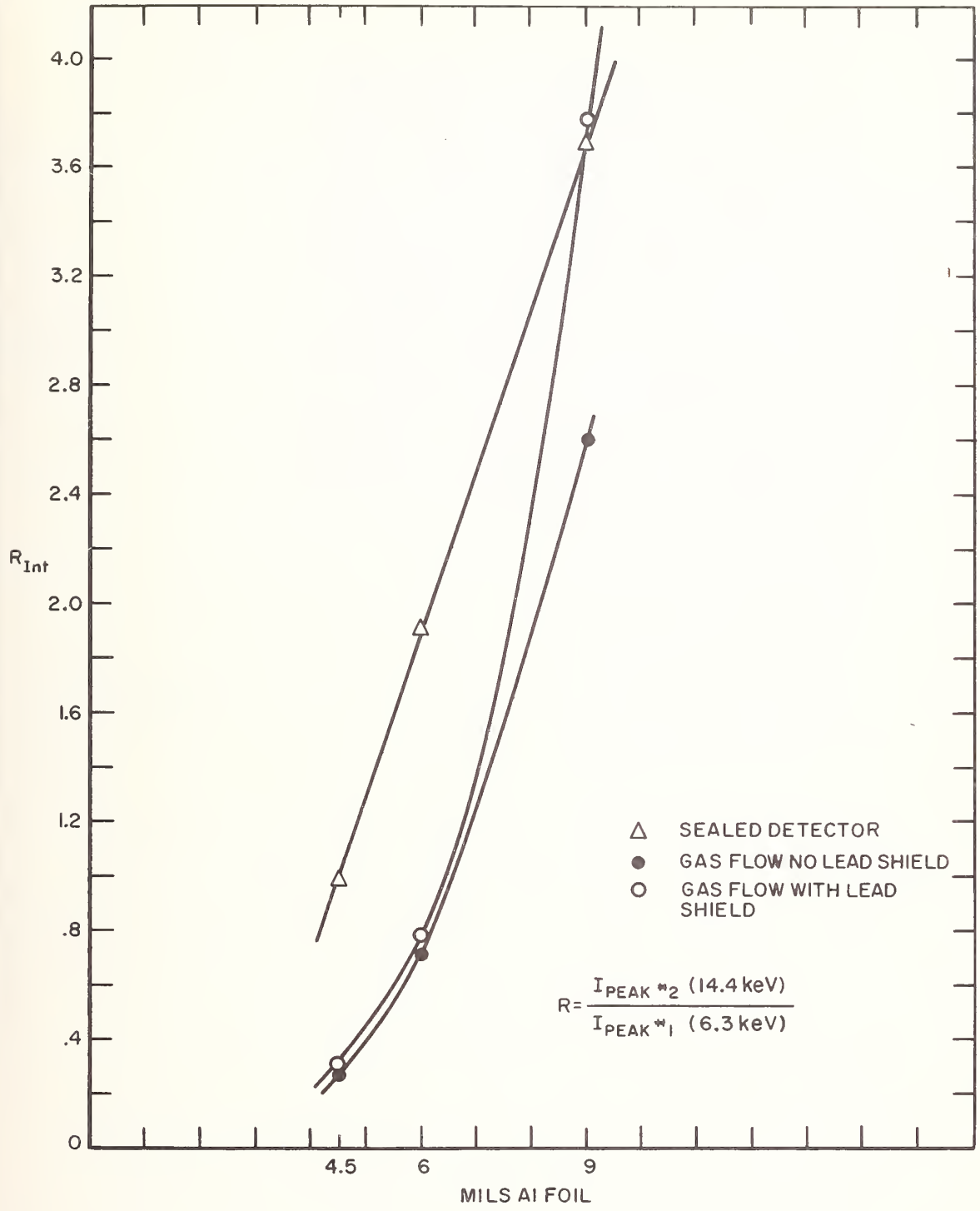

Figure 48. Graph of relative intensity of the ratio 14.4 keV gamma ray to the 6.3 keV x-ray versus thickness of the aluminum filter

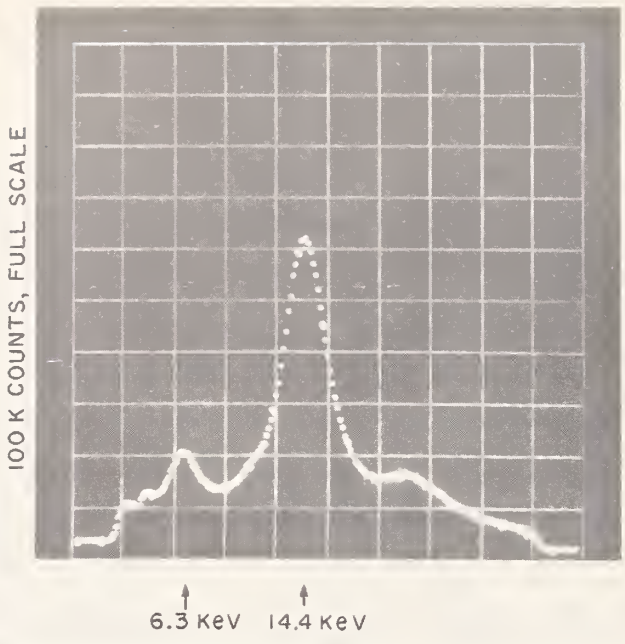

Figure 49. Pulse height spectrum of low energy region of ^{57}Co through 9 mil of Al foil. Source 1.5 cm from Be window. Spectrum accumulated for .5 min live time at 99% dead time.

resets the spectrometer unnecessarily. In addition, a tin "standard" such as β-tin must be employed for differential chemical shift, since sodium nitroprusside cannot be used for this purpose in a tin system. It is desirable that a suitable standard for differential chemical shift and velocity be developed for tin Mossbauer spectroscopy.

The Mössbauer spectrum of such a standard must have certain important characteristics:

1. The spectrum should be a doublet at all temperatures. This characteristic is important because defining a differential chemical shift relative to the midpoint of the doublet gives an internally consistent point of reference. Furthermore, the doublet provides a means of velocity calibration. Since the tin lines

are wide, relative to the ^{57}Fe lines, the splitting of the doublet should be greater than the 1.6 cm/s splitting of sodium nitroprusside by a factor of 2 to 2.5.

2. The standard should give a reasonably high percent effect in order to expedite the standardization process.

In addition, the standard should have the following chemical characteristics:

1. Chemical stability with respect to air and moisture.
2. No long-term phase transitions, alterations in crystal structure, or autocatalytic decomposition reactions should take place.
3. Reasonably low toxicity.
4. Capable of a high degree of purification with respect to tin-containing impurities.

The tin compounds for which spectra have been obtained by the various laboratories engaged in tin-119 Mössbauer spectroscopy have shown quadrupole splittings too low for use as a standard (i.e., up to 1.6 mm/s). The quadrupole splitting is related in part to the asymmetry of the ligands bonded to the tin atom. Since tin does not form coordination compounds, one is limited to inorganic salts, organo-tin compounds or alloys and intermetallics. Compounds of the former types possessing the necessary asymmetry are usually unstable and/or liquid. Alloys and intermetallics present the difficulty of phase effects, and to some extent difficulties in accurate synthesis.

The development of this standard is being approached in three ways. Tin compounds are being screened according to chemical and physical characteristics. Spectra are being obtained for all compounds meeting the previously discussed criteria. The possibility of using admixtures of compounds and/or alloys having singlet spectra with adequate splitting

is being investigated; and finally, the advice of persons active in tin-119 Mossbauer spectroscopy is being solicited with regard to suggested standards.

(D. K. Snediker)

F. Consultations

Dr. George Johns, Wright Field, Air Force Institute of Technology

Dr. Edward Allard, ERDL, Fort Belvoir

Dr. Serge Vinogradov, Yale University Medical School

Mr. Alfred Jakniunas, Biomedical Electronics Consultants, Inc.

Mr. Alan Michels, Radiation Instrument Development Laboratories

Dr. Rolf Herber, Rutgers University

Dr. Hobson, University of Richmond, Virginia Institute of Scientific Research

Mr. William Grote, Frazier Institute

Prof. P. C. Lall, Howard University

Mr. Robert Weiss, Nuclear Science and Engineering Corp.

G. Publications

1. DeVoe, J. R., and Spijkerman, J. J., "Mössbauer Spectrometry," Anal. Chem. 38, 382R-393R (1966).

   A review of the applications of Mössbauer spectrometry to chemical analysis, and a bibliography of publications on these applications in 1965 are presented. The principle of the spectrometer as well as a discussion of errors associated with its use are described. Current theoretical interpretations of some aspects of the Mössbauer spectrum are discussed. Chemical structure analysis is the most prevalent application to date, and other applications, such as metallurgy and quantitative analysis, appear to be promising.

2. DeVoe, J. R., and Spijkerman, J. J., "Mössbauer Applications in Aerospace," Proceedings of Symposium on Radioisotope Applications in Aerospace, Dayton, Ohio, February 1966, to be published.

   The principle of the Mössbauer effect will be discussed. A few possible applications of the technique with respect to physics and engineering in aerospace will be outlined. Of greater interest are the possible applications of the technique for determining chemical structure and solid state properties of materials. Solid phase transitions of materials subjected to severe conditions similar to that existing in space can be measured by Mössbauer effect.

   The National Bureau of Standards' Mössbauer spectrometer will be discussed and some data taken on a number of materials (such as tecktites, steels, glasses, and metal alloys) will be presented.

3. Ruegg, F. C., Spijkerman, J. J., and DeVoe, J. R., "A Mössbauer Spectrometer for the Structural Analysis of Materials," Proceedings of the International Atomic Energy Agency Symposium on Radioisotopic Instruments in Industry and Geophysics, Warsaw, Poland, Oct. 1965, to be published.

   A Mössbauer Spectrometer has been designed to provide high precision Mössbauer spectra. The instrument uses two electromechanical transducers, one driver and one sensor, in a feedback loop which incorporates an operational amplifier and a power amplifier. The transducer system is coupled to the scaler input of a multichannel analyzer. A high degree of synchronization between the channel number (which represents units of velocity) and the actual velocity produced by the

transducer is obtained by using the analogue voltage of the channel number as the input to the electro-mechanical system. By advancing sequentially the channel number as a linear function of time, a motion of constant acceleration is produced. Gamma rays from the radiation detector proportional counter of NaI(Tl) are then energy selected by a single channel pulse height analyzer and these pulses are presented to the multiscaler input. The spectrometer can be used to accept high counting rates by using a units scaler with a ten megahertz response.

The spectrometer can be used with a variety of auxiliary equipment such as to measure spectra at low temperature or high pressure.

4. Snediker, D. K., "The Mössbauer Effect of Sn^{119} in Palladium-Rich Palladium-Tin Solid Solutions," Mössbauer Effect Methodology, Vol. 2, Plenum Press, New York, in press.

A study of the palladium-rich end of the palladium-tin alloy system has been conducted using the Mössbauer effect of Sn^{119m}. Alloy absorbers of composition from 1 to 16 atom % tin and the intermetallic Pd_3Sn were studied.

The Mössbauer parameters, e. g. fractional effect, half-width and chemical shift, are reported for the various compositions. The Mössbauer spectrum of the alloy absorber has been determined to be a doublet consisting of spectra with chemical shifts corresponding to Pd_3Sn and the Sn-Pd solid solution.

A new source with a composition corresponding to Pd_3Sn was synthesized. Using this source with a β-tin absorber a spectrum was obtained with a half-width of 0.08 cm/s and an effect of 24%.

5. Spijkerman, J. J., Landgrebe, A. R., and Ruegg, F. C., "Mössbauer Effect in Ethylenediaminetetraacetatoiron III Compound," Presented at American Chem. Soc. Meeting September 1965.

The Mössbauer effect was used to investigate ethylene-diaminetetraacetato complexes of iron (III). The EDTA complex of iron, M(FeEDTA), was investigated for compounds where M was H, Li, Na, NH_4, K, and Cs. The spectra of the powered compounds were obtained at 21 and -130 °C. Two distinct chemical shifts were obtained indicating the iron complexes are in two chemical environments. The chemical shifts were positive

with respect to the NBS Mössbauer standard reference, sodium nitroprusside. The iron is definitely in the plus III valance state. Tentatively, we believe the iron to be in the octahedral configuration in the solid acid while the anion of the acid is in the pentagonal bipyramidal structure.

6. Spijkerman, J. J., Landgrebe, A. R., Ruegg, F. C., DeVoe, J. R., "The Use of Mössbauer Effect to Study the Adsorption of Iron on Cationic Ion Exchange Resins," Presented at Am. Chem. Soc. Meeting, September 1965.

The purpose of this study is to describe a capability of Mössbauer Spectroscopy to provide significant information regarding the structure of a wide variety of chemical systems. The chemical process and bonding of iron to cationic ion exchangers was investigated.

The ion exchange resins investigated were: Duolite C-10, Dowex 50, CG-50, and Bio-rex 63. Spectra were taken at 25 and -130 °C. The isomer shift in all cases was shown to be characteristic of iron (III) ion. Spectra were obtained for Dowex 50 of various cross-linkage and moisture content. The spectrum for the iron in Dowex 50 at room temperature, shows two closely-spaced peaks which indicate a small quadrupole interaction. Comparison of the Dowex 50 spectrum at the two temperatures with other data suggests that the iron is present as

$$\left[(H_2O)_4\ Fe\begin{matrix}\diagup OH \diagdown \\ \diagdown OH \diagup\end{matrix}Fe\ (H_2O)_4\right]^{+4}$$

Other corroborating evidence for the above structure is the absence of magnetic interaction to -130 °C.

7. Spijkerman, J. J., Ruegg, F. C., DeVoe, J. R., "Standardization of the Differential Chemical Shift for Fe^{57}," Mössbauer Effect Methodology, Plenum Press (1965) pp 115-120.

To provide Mössbauer data for Fe^{57} on a uniform basis, to eliminate recalculation of data from various laboratories, and to provide tables of Mössbauer spectra, the National Bureau of Standards has included disodium pentacyanonitrosylferrate dihydrate, $Na_2[Fe(CN)_5NO]\cdot 2H_2O$, in the Standard Reference Materials Program. Single crystals of sodium nitroprusside will be available by April 5, 1965, for this standardization. The crystals are supplied by a commercial manufacturer, and calibrated by NBS on a Mössbauer spectrometer, using an optical fringe counting technique.

The Mössbauer spectrum of a single crystal absorber, cut along the bc plane, is a well resolved, symmetric doublet. The center of this doublet is defined as zero reference point for the differential chemical shift, with the containing absorber at 25.0 °C. The absorber crystals supplied will be 1 cm x 1 cm with 25.0 mg/cm^2 of natural iron.

8. Spijkerman, J. J., Ruegg, F. C., May, L., "The Use of Mössbauer Spectroscopy in Iron Coordination Chemistry," Mössbauer Effect Methodology, Vol. 2, Plenum Press, New York, in press.

The application of Mössbauer spectroscopy to the study of iron coordination chemistry is discussed. The chemical shifts of iron compounds are adjusted to the new standard, sodium nitroprusside, and this differential chemical shift is correlated with the 4s electron contribution to the bonding in the compounds. A new interpretation of the chemical shift - 4s electron contribution diagram is proposed including the latest results of Molecular Orbital calculations. The quadrupole splitting is related to the total spin and structure of the compound. The asymmetry of the doublet intensities can be used to obtain additional information about the structure of the compound and the spin-spin relaxation time. The relationships between the Mössbauer parameters and the data from other spectroscopic measurements are discussed.

5. RADIOISOTOPE TECHNIQUES

A. Facilities

New laboratories have been recently equipped by the radioisotope techniques group at Gaithersburg. The new facilities consist of a nuclear instrumentation room, a darkroom, and two radiochemical laboratories. The present laboratories used for this work will be replaced in the future with laboratories designed to handle higher levels of radioactivity.

The nuclear instrumentation room contains automatic proportional, gamma and liquid scintillation counting systems and a radiochromatographic scanner for counting thin layer and paper chromatograms (see figure 50). This room constitutes a pool of radiation counting equipment of which the liquid scintillation counter belongs to the Organic Chemistry Section.

Figure 51 shows half of a double radiochemical laboratory module with an apparatus used for controlled potential coulometric analysis. Against the back wall is a glove box which contains the cells in a nitrogen atmosphere. Figure 52 shows the other half of this laboratory which is suitable for work on substoichiometric radioisotopic dilution analysis.

A standard double module which has been modified for the application of radiometric and chromatographic procedures is shown in figures 53 and 54. A hood which is suitable for radiochromatographic separations, an area for large developing tanks, and thin layer chromatographic tanks can be seen in figure 53. A paper chromatographic developing system mounted on an aluminum flexaframe, a polyethylene hood used for spraying chemical reagents, and a hood where the radiometric precipitation can be performed are shown in figure 54.

(A. R. Landgrebe)

Figure 50. Nuclear instrumentation room containing automatic proportional and gamma counting systems

Figure 51. Radiochemical laboratory module for substoichiometric radioisotopic dilution (SRDA)

B. The Application of Radioactive Isotopes to the Quantitative Analysis of Trace Amounts of Inorganic Substances on Paper and Thin Layer Chromatograms

1. Introduction

The basic techniques involve the following steps: (1) Evaporate a solution of the unknown mixture on a sheet of filter paper or a thin layer plate forming a spot near one end. The sample size may vary from 0.001 milliliter up to several milliliters. (2) Allow a suitable solvent to pass lengthwise through the paper starting near the spot. If the solvent is chosen correctly, the various components will be moved at different rates by the solvent. Ideally, each component will form

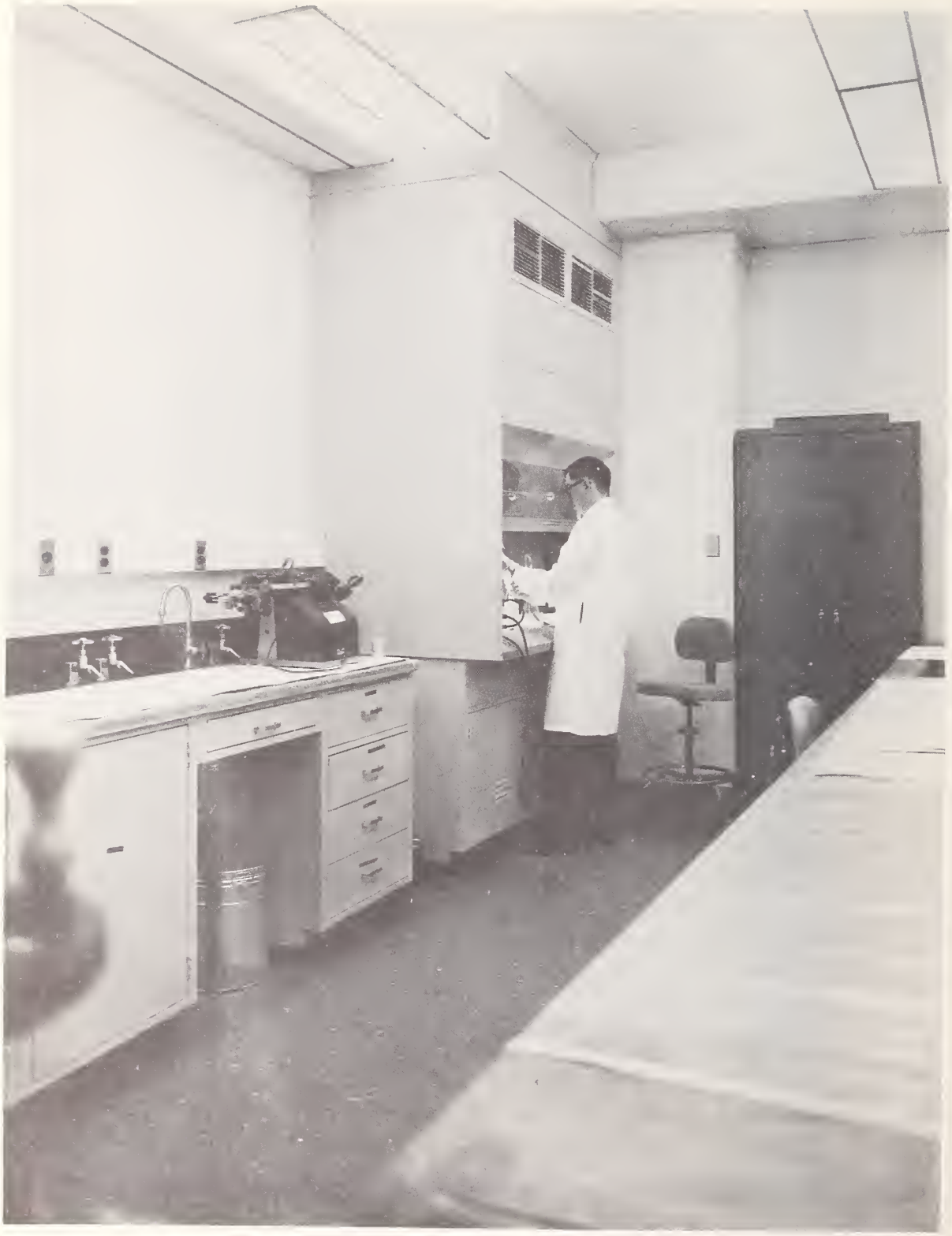

Figure 52. Other half of SRDA laboratory

a spot at a different place on the chromatogram. (3) After the solvent has moved to the other end of the sheet it is allowed to evaporate. (4) After separation of the ions, qualitative detection can be accomplished through the use of chemical reagents or radioisotopes. The chemical method of detection is based on the substance reacting to give colored or fluorescent spots. Some of the methods of detection using radioisotopes are autoradiography, automatic scanners with a proportional detector for beta emitters and NaI (Tl) well counters for gamma emitters. After having established the R_f factors, the last step (5) in the analysis is the quantitative determination of

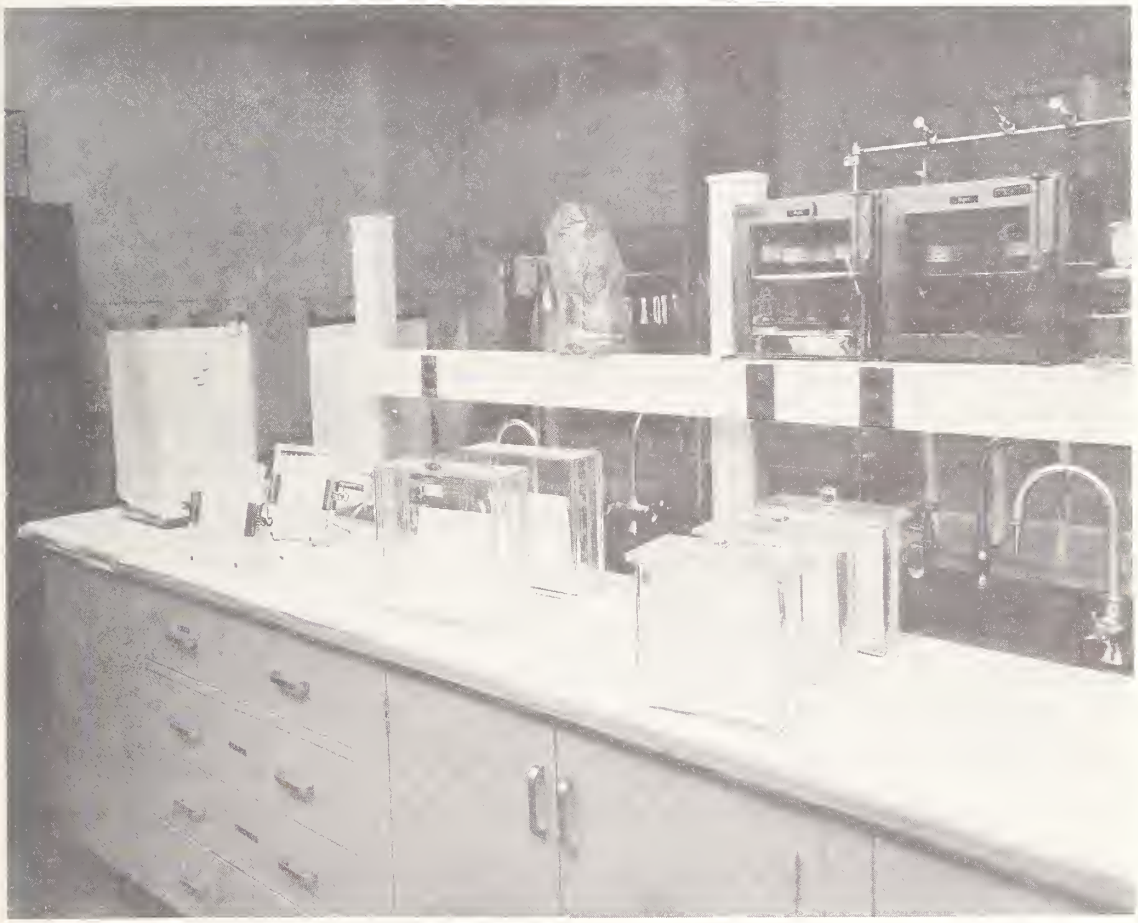

Figure 53. Radiometric laboratory

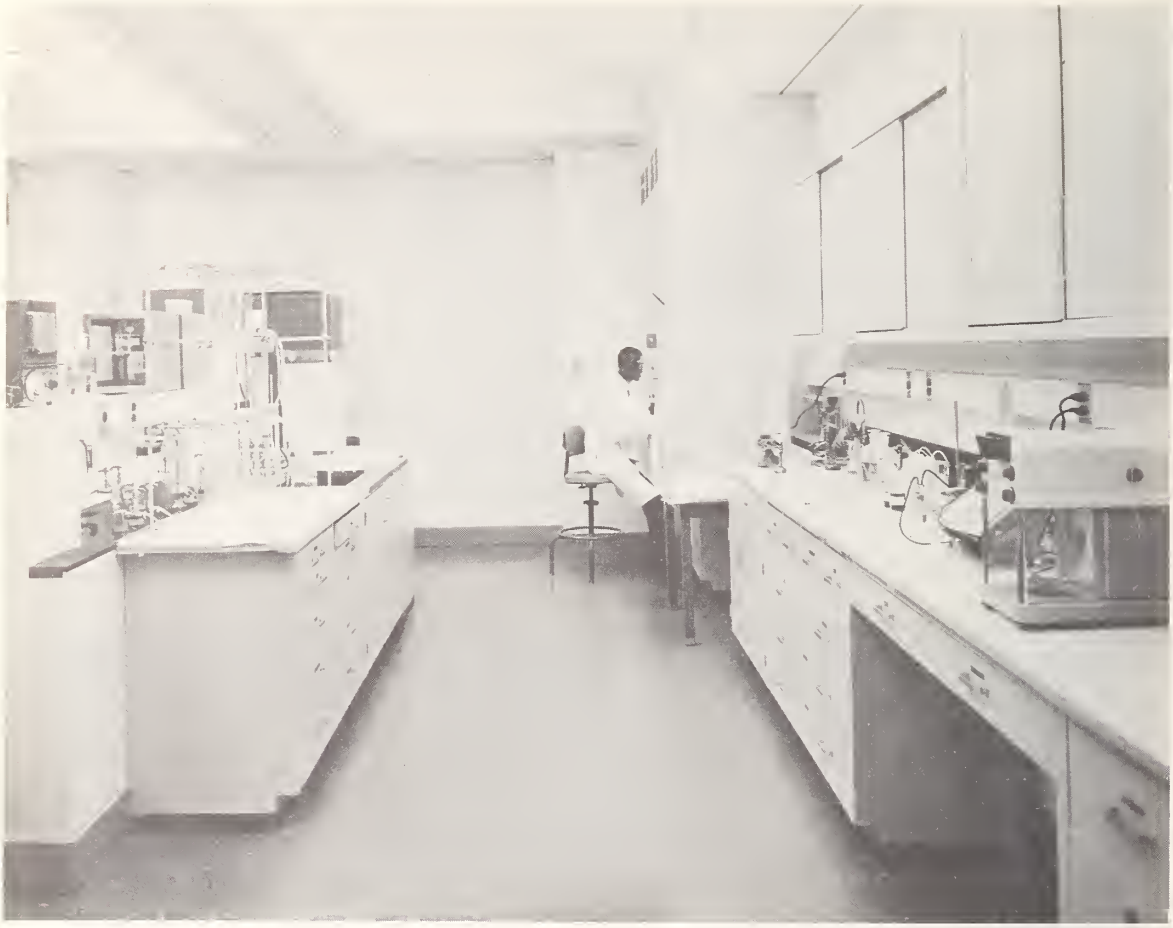

Figure 54. Radiometric laboratory

the elements of interest on the chromatograms. Analysis by means of radioisotopes can be performed by activation analysis, isotopic dilution analysis, radiometric precipitation (R.P.) or exchange of a radioactive reagent with a substance of interest. Examples of the quantitative determination of trace constituents by radiometric precipitation (R.P.) or exchange of a radioactive reagent will be treated in this paper. The latter will be called radiometric exchange analysis (R.E.)

The literature on inorganic separations on paper and thin layer chromatography is quite extensive but the studies are incomplete with a few notable exceptions [47,48]. In this study

we wished to separate the elements completely in order to test the radiometric precipitation methods which were developed; therefore, the separations which were developed are rather selective.

Van Erkelens [49] mentions the possibility of performing quantitative analysis of traces of metals separated by paper chromatography. He precipitated the elements in the chromatograph with radioactive hydrogen sulfide, but gave no data whereby the sensitivity or precision of the method could be estimated. In another paper [50], Van Erkelens described an analysis for lead, using phosphate labeled with ^{32}P, after separation from a number of interfering elements. This method was extended by Welford [51] and showed high sensitivity, but again no data were presented on the precision of the methods. The analysis of iron, copper and manganese has been accomplished by precipitation with ^{32}P labeled phosphate in our laboratory.

Radiometric precipitation can be described by the equation:

$$A + X^* = A\,X^*_s$$

The procedure is very similar to other types of precipitation. The radioactive precipitating agent (X*) is added to A, the cation, to be determined. Then the precipitate AX^*_s is separated from excess X*. In principle, either the excess of X* or AX^*_s should be counted, but in practice it is found that AX^*_s should be counted. It is to be noted that no measurement of mass in the actual radiometric procedure is required. The sensitivity of this method depends on the K_{sp}, the concentration and specific activity of X*, the precipitating agents.

A method of analysis has been developed on the basis of the exchange of ^{59}Fe with insoluble ferrocyanides, for example:

$$3M_2[Fe(CN)_6] + 4\ Fe^{*+3} = Fe^*_4\,[Fe(CN)_6]_3 + 6M^{++}$$

There are a great many elements that form insoluble ferrocyanides. The theoretical limit of detection of the following insoluble ferrocyanides is 1.9 μg for manganese, 0.009 μg for

cobalt, 0.008 μg for nickel, 0.003 μg for copper, 0.005 μg for zinc, 0.001 μg for gallium, 0.04 μg for silver ($Ag_3[Fe(CN)_6]$), 0.025 μg for cadmium, 0.000004 μg for indium, 0.04 μg for lead and 0.028 μg for the uranyl ion. The figures obtained for the limit of detection are based on solubility product considerations for the conditions used in this report.

The radiometric exchange analysis (R.E.) can be generalized by the following equation:

$$AX_{(s)} + B^* = B^* X_{(s)} + A$$

The signs are omitted for simplicity. The procedure involved the addition of the radioactive cation to the precipitate and required the isolation of $B^*X_{(s)}$ from excess B*. If the amount of activity isolated is proportional to the amount of $AX_{(s)}$ then a method of analysis is available. This procedure also requires no measurement of mass in the radiometric method and the activity measured could be B* at equilibrium or $B^*X_{(s)}$. The sensitivity depends on the $K_{sp's}$ of $AX_{(s)}$ and $B^*X_{(s)}$. The sensitivity is also dependent on the specific activity of the reagent B* and upon its concentration.

The usefulness of the radiometric method of analysis for iron, cobalt, copper and manganese will be demonstrated in this work by its application to NBS Standard Reference Material No. 671, nickel oxide, which contained traces of these metals.

2. Experimental

a. Reagents and Purification.

Purification of Paper: The chromatographic paper, Whatman No. 1, was purified by washing with 3N hydrochloric acid. The acid was allowed to migrate down the paper. The paper was washed downflow with water (3 times) and air dried.

Solvent Preparation:

1. Methyl ethyl ketone - HCl: 8 parts concentrated hydrochloric acid was added to 92 parts methyl ethyl ketone.
2. n-Butanol - HCl - ethyl acetate: 25 parts

hydrochloric acid was added to 30 parts n-Butanol and 45 parts ethyl acetate. Prior to use, the solvent was thoroughly mixed.

3. n-Butanol - HBr: 50 ml of concentrated hydrobromic was mixed with 50 ml of n-Butanol.
4. NH_4OH-NH_4Cl: pH = 10. 142 ml of concentrated ammonia solution was added to 250 ml of water containing 17.5 g of ammonium chloride.
5. Carbon tetrachloride - benzene: 50 parts of carbon tetrachloride was added to 50 parts of benzene.
6. Sym-collidine - 0.4 M HNO_3 (100 ml) of 2, 4, 6 trimethylpyridine is shaken with 0.4 N-nitric acid (100 ml); the heat generated by the mixing causes the temperature to rise. When the mixture cools to 25 °C the layers are separated. The organic layer is saved for use and the aqueous layer discarded.

Spray Reagents

1. Diphenylcarbazide - a 1% solution of diphenylcarbazide in 95% ethanol was prepared.
2. Dithizone - CCl_4 - a 0.05% solution of dithizone in carbon tetrachloride was prepared.
3. Quinalizarin - a 0.005% solution of quinalizarin in 95% ethanol was prepared.
4. Sodium hydroxide - a 1N solution of sodium hydroxide was prepared.
5. Ammonia - a glass chromatographic tank was saturated with ammonia vapor by placing four 100-ml beakers containing concentrated ammonia in the bottom of the tank.
6. Dithizone - $(CH_3)_2CO$ - a 0.05% of dithizone in acetone was prepared.
7. Alizarin - a 0.05% solution of alizarin in 95% ethanol was prepared.

8. Dimethylglyoxime - a 5% solution of dimethylglyoxime in 95% ethanol was prepared.
9. Tetrahydroxyquinone - a 5% solution of the disodium salt of tetrahydroxyquinone in 95% ethanol was prepared.
10. Morin (3, 5, 7, 2', 4' pentahydroxyflavone) - a 0.01% solution of morin in 95% ethanol was prepared.

Radioisotopes

1. ^{32}P - labeled phosphates. A solution of radioactive trisodium phosphate was prepared so that the phosphate concentration was 0.12M and contained 10^5 cpm of ^{32}P per ml.
2. ^{60}Co obtained from ORNL with a specific activity of 5.4×10^4 mCi/g was used. 10^6 cpm of ^{60}Co per ml was used in all experiments.
3. ^{59}Fe obtained from Nuclear Science and Engineering Corporation with a specific activity of 3×10^4 mCi/g was used. 10^6 - 10^5 mCi cpm of ^{59}Fe per ml was used in all experiments.

Metal Test Solution: The stock solutions had a concentration of 10 mg per ml and were diluted to the desired concentration for qualitative and quantitative analysis.

NiO Standard Reference Materials: 10.000 g of nickel oxide was dissolved in 9M hydrochloric acid. The final concentration of nickel oxide was 0.1000 g per ml.

12 h Steel Sample: 5.000 g of 12 h steel was dissolved in 6M hydrochloric acid containing a few ml of nitric acid. The final concentration of the steel sample was 0.0500 g/ml.

Cu-Be Alloy: The Cu-Be alloy was dissolved in 6M nitric acid. The final concentration was 0.1000 g per ml.

Potassium Ferrocyanide Solution: The potassium ferrocyanide was dissolved in 100 ml of distilled water and after stirring for a few hours the excess salt was filtered.

NaOH-H_2O_2 Solution: 90 ml of 0.1N sodium hydroxide was added to 10 ml of 30% hydrogen peroxide.

Metal Dithizonates: A 0.1% solution of Co, Ni, Cu, Zn, and Fe were extracted with an equal volume of 0.1% dithizone. The separated chloroform was washed with 0.02N nitric acid to remove the excess of dithizone.

b. Separation Procedures. Methods of separation were developed using synthetic solutions of the ions of interest as well as solutions of the samples. The procedure used to separate the ions in the nickel oxide, Cu-Be alloy, 12 h steel and metal dithizonates consisted of spotting several 0.01 ml aliquots of the original samples on the Whatman No. 1 chromatographic paper or on the thin layer plates. With the papers, descending chromatography was used and with the thin layer plates, ascending chromatography was used. The papers or TLC plates were removed from the chromatographic tanks, air dried, and placed in a tank saturated with ammonia vapor in order to neutralize the acid used in the separation. The papers were removed from the tank and air dried again.

The separation of the steel was performed by two-dimensional chromatographic methods. The initial separation was accomplished with methyl ethyl ketone-HCl and then the molybdenum plus iron, located at the solvent front, was separated with ethanol-HCl solvent in a second dimension. The paper was cut below the solvent front prior to the second separation. Using sym-collidine and 0.4 HNO_3 as a solvent an improved separation of the chromium and nickel could be obtained in the steel samples. The separation with the 12 h steel was accomplished by first separating the samples with methyl ethyl ketone-HCl, neutralizing the hydrochloric acid with ammonia vapor, air

drying, and separating down flow with the sym-collidine solvent in the same direction as the original solvent.

c. Qualitative Detection. The procedures for the use of spray reagents can be found in text books on paper or TLC chromatography [52,53]. The ions were detected with the appropriate spray reagents listed in table 17.

The R_f factors of gamma emitters have been determined using the NaI (Tl) well counter. An automatic scanner with a 2π proportional detecting system for beta emitters on thin layer plates or 4π proportional detecting system for beta emitters on paper chromatograms has been used. When quantitative determination of the radioactivity present in a chromatogram is desired, an automatic sample changer with a well type NaI (Tl) scintillator (gamma emitters) or proportional counter (beta emitters) was used for counting segments of the paper or thin layer which provide sufficient resolution of the chromatographic peaks.

d. Quantitative Analysis. The following procedures are used for the radiometric precipitation with ^{32}P labeled phosphate: The phosphates of iron, copper, and manganese were precipitated with radioactive trisodium phosphate in 50 ml beakers. The papers were removed, washed with water and air dried. The labeled precipitates were assayed with low background proportional beta counting systems.

The following procedure was used for the radioactivity exchange method of analysis for manganese: The manganous ion was oxidized with alkaline hydrogen peroxide, washed with water, and air dried. The papers containing the manganese dioxide were equilibrated with a solution containing a ^{60}Co in an ammonium hydroxide-ammonium chloride buffer, pH 10.00. Standards were prepared in the same way. The ^{60}Co was assayed using a scintillation NaI (Tl) well counter. As the amount of manganese dioxide on the paper is increased, more of the ^{60}Co is removed from solution.

Table 17. Colorimetric Reagents

Colorimetric Reagents/ Elements	Cu^{++}	Co^{++}	Fe^{+3}	Sn^{+2}	Cr^{+3}	Ag^{+1}	Pb^{+2}	Zn^{+2}	Be^{+2}	Al^{+3}	Mo^{+6}
Alazarin	Reddish	yellow	yellow	yellow	yellow	black	yellow	yellow	w/NH_3 brown	yellow	--[a]
Dithizone	--	pink	yellow	dp.pink	pink	orange	blue	pink	green		
Dithizone & NH_3	blue	purple	brown	blue	blue	pink	pink	pink			
Tetrahydroxy-quinone	yellow	--	blue	--	blue	red	purple	--	--	--	
" & NH_3	blue	gray	gray	white	yellow	brown	gray	white	--	--	
Cupferon in $CHCl_3$	--	yellow	--	--	--	brown	--	--	--	--	
Dimethyl-glyoxime	--	--	--	--	--	brown	--	--	--	--	
Morin	--	--	--	yellow	--	brown	--	--	--	green (fluor.)	--
Diphenyl carbazide	green purple	light tan	brown	violet	--	black	--	--	--	purple	--
Quinalizarin	--	--	--	--	--	brown	--	--	tan		
Ammonia Sulfide	gray brown	black	black-greenish	brown	--	black	brown	black	--	--	

[a] No reaction

The following procedure was used for the radioactivity exchange method of analysis of nickel, copper, cobalt, manganese, cadmium, zinc, and mercury. The ions were precipitated by reacting them with a saturated solution of potassium ferrocyanide. The papers were then washed with water, 0.1 N hydrochloric acid and water again. The papers were equilibrated with ^{59}Fe solution, washed with water, dried and counted using a scintillation NaI (Tl) well counter.

In all cases, the method of washing was standardized to give the lowest possible blank. Three to five milliliters are placed in the beakers along with the papers containing the ferrocyanide precipitant. After swirling for one minute the water was decanted and this procedure was repeated two more times.

The quantitative analysis of the nickel oxide sample was accomplished by the following procedure. After having established the R_f factors and, therefore, the relative position of the separated elements on three of the chromatograms, the corresponding areas on additional chromatograms were cut out and analyzed quantitatively. Iron, copper and manganese were determined by radiometric precipitation with labeled phosphate. The manganese was also determined by the radioactivity exchange method of analysis described above. Cobalt was determined by the radiometric exchange method with the ferrocyanide procedure.

3. Calculations

Blanks were subtracted from all data for each element and standard curves were prepared by plotting cpm isolated on the paper versus μg added. The experimental points were fitted to a straight line by least squares analysis.

4. Results and Discussions

Separations were developed for trace constituents in Cu-Be alloys containing Sn, Fe, Cu, Zn, Co, Ag, V, Be, Al, and Pb; for the metal dithizonates of Fe, Zn, Ni, Cu, Co; traces of Cu, Mo, V, Ni, Cr and Mn in Standard Reference Material 12 h steel and for nickel oxide containing traces of Fe, Cu, Co, Mn, Ti,

Cr, Al, and Mg. The R_f factors are listed in figure 55. The separation of the Cu-Be alloy with n-Butanol-HBr required fifteen hours and with the methyl ethyl ketone-HCl four hours. The separation of the nickel oxide sample with methyl ethyl ketone-HCl required three hours. The separation of the metal dithizonates with chloroform-benzene solvent system requires less than an hour. Due to their color, no qualitative detection is necessary with the dithizonates. The 12 h steel sample was separated on paper and TLC plates. The time required for paper chromatographic separation is eight hours and for the thin layer chromatographic separations, five hours. With the nickel oxide sample a separation of Mn, Co, Cu and Fe was obtained and all the trace constituents in the 12 h steel have been isolated using the three solvent systems as already explained. Only a partial separation was obtained with the Cu-Be alloy and the metal dithizonates.

From the limited amount of systematic work which has been done, few definite conclusions can be drawn. It seems best to have the matrix at the origin if possible, since the separations are sharper and the blank in the subsequent analysis is lower.

The lack of a thorough understanding of the processes involved in the separation of ions on paper or thin layer plates has led to an empirical approach to the choice of suitable solvent mixtures. The complexity of the processes involved in paper and thin layer separation can be seen in the variables concerned, all of which are interrelated. The main factors concerned in the separation of cations are as follows: the nature of the inorganic compound functioning in the process, the type of solvent, the water content of the solvent and humidity of the surrounding space, the acidity of the mobile phase and of the original solution of the salt, the interference of one cation with the movement of the other, the presence of certain anions, the time of running of the chromatogram, the temperature, and the condition and properties of the cellulose or silica gel support.

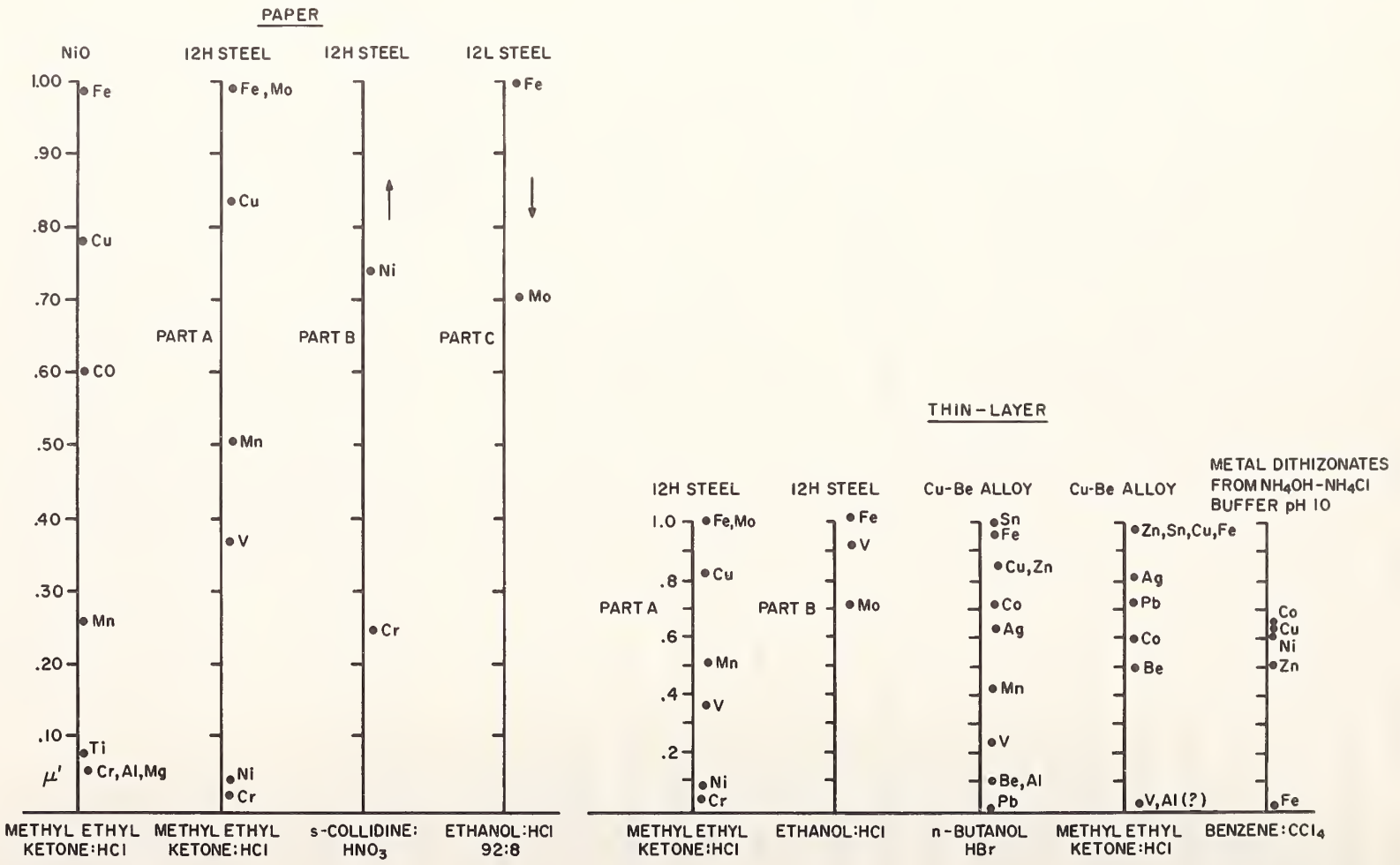

Figure 55. Separation of cations by paper and thin layer chromatography

In table 17 are listed a number of colorometric spray reagents and the color of the ion detected. The dash indicates no detection when the amount present was 1 μg. The tetrahydroxyquinone reagent is recommended for the detection of Cu and Fe, ammonium sulfide reagent for Ag and Co, the diphenylcarbazide for Sn, dithizone for Zn and Pb, and alizarin for the detection of Be and Al. The use of these chemical methods for qualitative detection is rapid and allows one to screen methods of separation but they are not very selective or highly sensitive with the exception of some fluorescent methods.

The use of radioisotopes has several advantages over the chemical methods of detection, such as the higher specificity and sensitivity of radioisotopes. These advantages are sometimes offset by difficulties in detection of the radioactive substance. Some of the difficulties are the blank problem and and the ability to distinguish between two radionuclides which were only partially separated. The use of the radioisotopes for qualitative detection has the added advantage of making quantitative yield corrections possible. The yield correction is important when the ions of interest are entrapped in the matrix and only part of the substance is recovered.

The radiometric phosphate procedure has been used to analyze iron, copper and manganese, the sensitivity of the method being 0.1 μg for iron and copper. The procedure is not recommended for manganese due to the poor precision obtained. The limit of detection seems to be limited by the blank. This procedure should be very sensitive for Th^{+4} and UO_2^{++}.

The exchange reaction of ^{59}Fe with insoluble ferrocyanides has been used to determine Ni and Cu with a sensitivity of 0.1 μg, Co with a sensitivity of 0.01 μg, Mn to 1.0 μg, Cd to 0.04 μg. Preliminary data indicate that Zn, Pb, Ga, In and uranyl ions can also be determined by this method.

Titanium, zirconium, hafnium, bismuth and thorium form insoluble ferrocyanides, but not enough information is available

to make a prediction as to the limit of detection. The alkaline earths (except beryllium), yttrium, lanthanum, actinium, and the cerium earths can be precipitated from aqueous solutions to which ethanol has been added. It may be possible to analyze for these elements using a mixed solvent system. Almost all the metal ferrocyanides are insoluble in the higher alcohols with the exception of the hydroferrocyanic acid. Niobium, tantalum, chromium, molybdenum and tungsten form insoluble ferrocyanides, but the rate of formation is slow, and complex anionic species of these ions which are likely to be present make the use of the radioactivity exchange analysis method rather difficult.

The stoichiometry is not known for many of the insoluble ferrocyanides. The stoichiometry may vary with pH and other conditions, for example the following cobalt species have been isolated with ferrocyanide $[Co(NH_3)_6]^{+3}$, $[Co(NH_3)_5H_2O]^{+3}$, $[Co(NH_3)_5Cl]^{+2}$, $[Co(NH_3)_5NO_2]^{+2}$, $[Co(NH_3)_5NO_3]^{+2}$.

A number of the elements form double salts, for example:

$$5[UO_2]_2\ [Fe(CN)_6] \cdot 3\ K_4Fe(CN)_6.$$

Table 18 lists the results obtained for the analysis of the nickel oxide sample. The amounts analyzed were 3.9 μg of iron, 2.0 μg of copper, 3.1 μg of cobalt, and 1.3 μg of manganese. The data show quite satisfactory precision and accuracy for all except the labeled manganese phosphate precipitate.

The precision of the analysis using radioactive tracers can be affected by a number of factors, some of which are: (1) the type of support media used and the impurities in this support, (2) the interaction of the cellulose or silica with the separated ions or the precipitating agent, (3) the solvent system used in the separation. The separation must be complete because in most cases the selectivity of the method is based on complete separation. The amount of material taken may also affect the precision. If interferences exist or the elements are not recovered completely, yield corrections and a method of standard addition must be applied along with the blank corrections.

Table 18. Nickel Oxide Standard Reference Material 671

Cation	Amount Present	Ave Amount Found	Rel Std Dev.[a]	No. Det.	Rel. Error	Method of Analysis
Fe^{+3}	0.39%	0.37%	7.1%	8	-5.7%	Ppt'd with Phosphate labeled with ^{32}P
Cu^{+2}	0.20%	0.19%	6.8%	8	-5.0%	Ppt'd with Phosphate labeled with ^{32}P
Mn^{+2}	0.13%	0.134%	39.5%	6	+3.0%	Ppt'd with Phosphate labeled with ^{32}P
Mn^{+2}	0.13%	0.138%	3.8%	8	+5.8%	Adsorption of ^{60}Co on Manganese Dioxide
Co^{++}	0.31%	0.316%	4.1%	8	-1.9%	Exchange of ^{59}Fe with $Co_2[Fe(CN)_6]$

[a]Of a single determination

The precision of the radiometric method compares favorably to most methods applied to paper or thin layer chromatography. The precision does not compare as favorably to other methods in general at the μg level but it must be remembered that this is a micro as well as a trace method.

The accuracy can be affected by the following factors: incomplete separation, entrapment of the element to be analyzed in the matrix, impurities in the paper, solvent, or from the environment. The experimental procedures used in preparation of the calibration curve and of the sample must be the same. The accuracy can be improved by using the proper correction factors when needed, such as yield and blank corrections. The accuracy does compare favorably to that of other methods.

The sensitivity of these radiometric methods is high. The sensitivity is limited by impurities in the system and from the environment. The blank is larger when the major matrix component is moved to the solvent front. The sensitivity is limited by the solubility product constant and/or the equilibrium constant of the exchange reaction. The specific activity and concentration of the radiometric reagent will also affect the sensitivity. Since these methods were developed for the determination of the separated components on a chromatogram, the sensitivity is limited by the amount of material taken for analysis, i.e., micro amounts. Other methods of separation which use larger amounts of sample could be used as well as preconcentration prior to chromatographic separation, thereby increasing the sensitivity of the method.

The main advantage of the paper chromatographic method is that it permits the analysis of a large number of elements in the same sample. The radiometric methods which are used to determine the separated elements have a greater sensitivity than most other methods of quantitative analysis which are applied to chromatographic separation on paper or thin layer plates.

(A. R. Landgrebe and T. E. Gills)

C. Differential Controlled-Potential Coulometry Utilizing Radioisotopic Tracers

1. Introduction

During the past year a differential method of analysis was developed. It consists of a controlled-potential coulometric procedure in which two identical electrolytic cells are connected in series. Under prescribed conditions the same amount of the element of interest is deposited in each cell. This permits the application of a technique called substoichiometric radioisotope dilution.

The procedure involves the addition of a known amount of the element to be analyzed to the control cell which is held at a constant-potential and an unknown amount to the sample cell. The addition of an equal, known amount of a radioisotope of that element to each cell then follows. Since the same amount of element is deposited in each cell, the difference in the amount (differential) may be determined by measuring the radioactivity left in each of the cells after a finite electrolysis time. The relationship derived from the radioisotopic dilution principle of radioactivity balance can be written in the form

$$\Delta M = M \frac{a_2 - a_1}{a_t - a_2} \qquad (1)$$

where ΔM is the differential, M is the known amount added to the control cell, a_1 and a_2 refer to counts per minute of a radioisotope of element M left in the control and sample cells, respectively, and a_t is an equal amount of radioactivity in counts per minute added initially to each cell. In order to obtain independent verification of the series controlled-potential method and to establish a means of comparison to the radioisotope technique, another approach was devised which consists of a current integration procedure.

For the current integration procedure to be applied each cell must contain identical reference electrodes. This is also desired in that preelectrolysis of the supporting electrolyte and sample solutions can be accomplished in each cell prior to

the start of the actual experiment. Since mercury was the cathode used in this study, preelectrolysis is necessary in order to remove traces of atmospheric oxygen which is reduced at the mercury electrode in two steps:

1. $2H^+ + O_2 + 2e^- = H_2O_2$ E = -.1 volt versus the Saturated Calomel Electrode (S.C.E.)
2. $2H^+ + H_2O_2 + 2e^- = 2\ H_2O$ E = -.9 volt vs S.C.E.

After the removal of oxygen, potential control is transferred to the control cell and maintained at a value where the only reaction that occurs at the mercury electrode is $M^{+n} + ne^- = M$ (Hg). The current arising from the reduction of M^{+n} will follow the equation $i_t = i_o e^{-kt}$ where i_o is the current just prior to the start of the electrolysis, i_t is the current at any time, and k is the cell constant. The cell constant, k, is unique for each particular cell geometry and is a function of the electrode area, volume of solution, rate of stirring, and the temperature. The current at any time is related to the concentration of metal ion in the bulk of the solution. Integration of this current-time data yields coulombs which are related through Faraday's law to the amount of metal ion electrolyzed. Precise and accurate integration of this electrolysis current is accomplished by developing a voltage across a standard resistor (see figure 56). This voltage is converted to a frequency by means of a voltage-to-frequency converter. The converter produces output pulses at a rate precisely proportional to the input voltage. These pulses are recorded on a scaler. The data thus obtained consists of the integral of the current-time curve.

Since the potential of the cathode of the control cell is maintained at a value such that only the desired electrochemical reaction occurs, attention may now be drawn to the sample cell cathode potential. Here it is also important to maintain the desired electrode reaction with the exclusion of all others. The potential of the cathode in the sample cell will determine

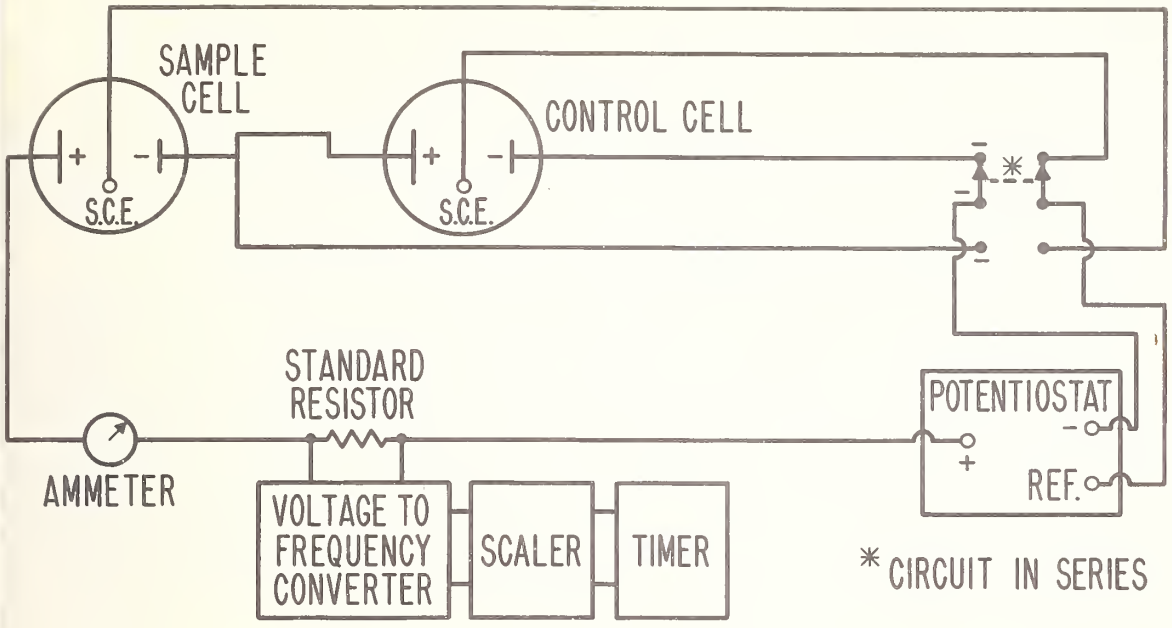

Figure 56. Schematic diagram for differential controlled-potential coulometry

the specificity of the electrode reactions. This potential is governed primarily by (1) the current density in the sample cell and is dependent on the control cell concentration, (2) the concentration present in the sample cell, and (3) the cell constant, k. To exclude undesired electrode reactions, the sample cell cathode potential must be equal to or more anodic than the control cell cathode potential. This can be accomplished by providing a concentration in the sample cell which is equal to or greater than that in the control cell. An actual study of the potential of the sample cell cathode was made and appears in the results section of this report.

2. Experimental

a. Apparatus. A diagram of the electrolysis cells employed is shown in figure 57. Both the control and sample cells are identical.

The anode consisted of a platinum wire bent in the shape of a helix and isolated from the solution by a "Thirsty"* vycor

* Corning Glass Co. For disclaimer of equipment and materials see last paragraph of preface.

glass tube about 9 mm x 5 1/2 in. The glass tube was of low electrical resistance. The reference electrodes used were identical saturated calomel electrodes of the commercial type with a porous pin liquid junction. The cathodes were mercury pools about 7 cm^2 in area. Stirring of the solution and pools was accomplished by means of a glass stirring rod fitted to a synchronous motor assembly and rotated at 1800 r/min. The cell cap was fabricated from lucite of one inch thickness. In addition to the holes drilled for the anode, reference electrode, stirrer, and nitrogen inlets, a hole drilled diagonally permitted the introduction of sample solutions into the cell without removal of the cap. This provision was convenient in that a positive nitrogen pressure could be maintained inside the cell while solutions were being introduced.

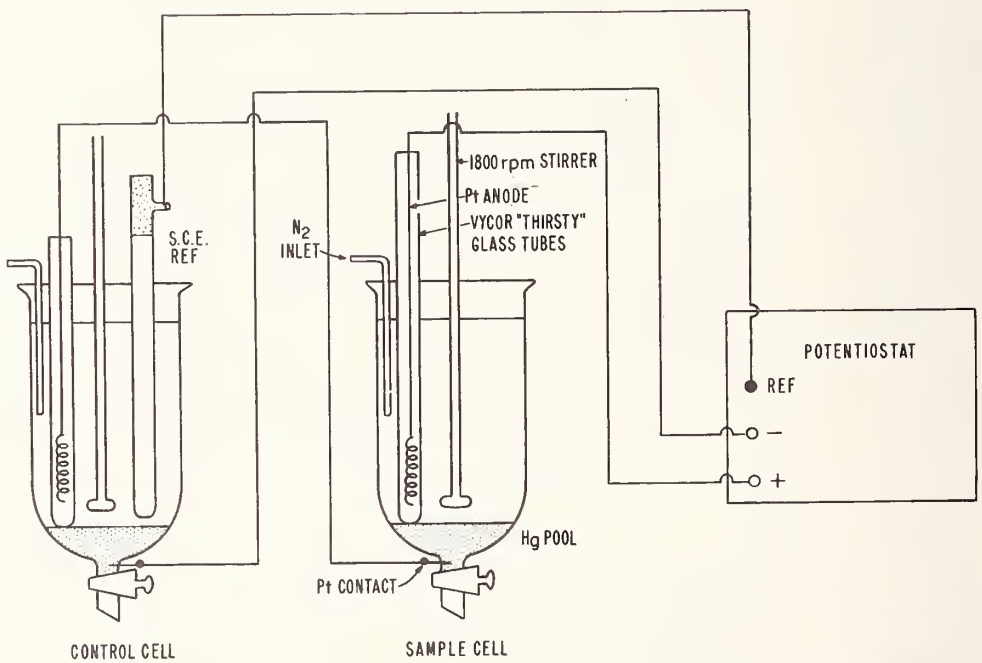

Figure 57. Diagram of apparatus

For studies at the microgram level, the entire cell assembly was enclosed in a dry box made of durable plastic and was filled with nitrogen prior to the start of the experiment. Withdrawal of the solutions from the cells was accomplished by inlets in each cell which were attached to a common vacuum pump.

b. Instrumentation. The potentiostat used in these experiments was built according to the design of Connally and Scott as described in their report [54]. The current integration equipment consisted of a voltage-to-frequency converter, scaler, timer, and constant-current calibration source. Counting equipment consisted of an automatic sample changer and scintillation counter with a well-type NaI (Tl) crystal. Potentials were measured with a millivolt potentiometer.

c. Reagents. Stock solutions of cadmium were prepared by dissolving high purity cadmium metal (99.99%) in a minimum amount of concentrated HCl and filled to volume with distilled water in volumetric flasks. The distilled water was purified by passing it through a mixed bed ion exchanger. The supporting electrolyte was prepared by dissolving analytical reagent grade potassium nitrate in distilled water. Further purification of this solution when required was accomplished by electrolysis at controlled-potential at -1.0 volt vs. S.C.E. A cadmium-109 stock solution was prepared by dilution of a 5 mCi cadmium-109 solution of high specific activity. Working solutions were prepared by dilution of the appropriate volumes of the cadmium metal and cadmium-109 stock solutions in volumetric flasks.

d. Procedure (Radioisotope Dilution). To each of the cells is added 3.00 ml of 0.1 F KNO_3 followed by 1.00 ml of cadmium solution containing ^{109}Cd. These solutions were previously deaerated by passing prepurified nitrogen first through a gas tower containing 0.1 F KNO_3 and then through these solutions. Each cell was preelectrolyzed at -0.40 volts vs. S.C.E. to remove traces of oxygen. Electrolysis was continued until the residual current in each cell was identical. With the

cells in series, the control cell potential was held at -0.75 volts vs. S.C.E. and the time of electrolysis was either five or ten minutes. Without interruption of the electrolysis, samples of solution were simultaneously withdrawn from each cell. Then 1.00 ml of each solution was accurately transferred to a counting tube, placed in the automatic well counter and counted, until 100,000 counts were accumulated.

e. Procedure (Current-integration). The same pre-electrolysis procedure is carried out as described above. With the cells in series and control cell potential at -0.75 volts vs. S.C.E., electrolysis is carried out to completion until the residual current is reached. The potential control is then immediately transferred to the sample cell where integration of the current is recorded until the same value of residual current as obtained in the control cell is reached. The time of electrolysis in each case is about 35 minutes. The residual current is then integrated for the same length of time and its contribution is subtracted from the entire integral. A similar technique as described above appears in an article by Rechnitz and Srinivasan [55].

3. Results and Discussion

Table 19 includes the data obtained by the radioisotope method and that obtained by the current integration procedure. Comparison of each technique at this concentration level leads to the conclusion that the precision (expressed as standard deviation of a single measurement) of the integration procedure is greater; however, the accuracy attained as shown in the above table is comparable. It can also be said from this study that for this concentration level, the accuracy of the amount analyzed in the sample cell becomes greater as the differential becomes smaller. The same conclusion was expressed in a similar study [55]. Also represented are results obtained at smaller concentrations.

In order to demonstrate the behavior of the sample cell

Table 19. Summary of the results of the determination of Cadmium (II) in 0.1 M KNO_3

Radioisotope method

Control cell(μg)	Sample cell(μg)	Found mean(μg)	% Rel. error	σ_s[a] (μg)	No.of deter
200.05	400.19	396.33	-0.96	3.44	5
248.93	400.19	401.80	+0.40	3.15	5
323.16	400.19	399.22	-0.24	2.56	5
381.18	400.19	400.81	+0.16	2.39	6
19.02	38.51	38.35	-0.42	.71	6
22.92	38.51	38.29	-0.57	.60	6
26.71	38.51	38.58	+0.18	.79	7
30.53	38.51	38.27	-0.62	.44	5
2.15	4.25	4.15	-2.35	.11	5
2.15	2.97	3.01	+1.35	.20	5
		Integration method			
200.05	400.19	397.06	-0.78	1.25	6
248.93	400.19	397.45	-0.68	1.49	5
323.16	400.19	401.11	+0.23	0.76	4
381.18	400.19	400.69	+0.12	0.70	6

[a] σ_s = Standard deviation of single measurement

cathode potential in the series arrangement, measurement of the potential versus the S.C.E. was made while electrolysis proceeded. In figure 58 is shown curves A, B, and C which represent the potential as a function of time and as a function of different ratios of sample to control cell concentrations. It can be seen that the potential assumes the most cathodic value immediately after electrolysis has begun and becomes more anodic as electrolysis proceeds and finally reaches a constant value. As the concentration in the sample cell approaches that in the control cell, the potential at the start of the electrolysis approaches that of the controlled-potential value. Thus, the trend observed indicates that the potential will become more cathodic than the controlled-potential value when the concentration in the sample cell falls below that in the control cell. As was indicated in the introduction, this should be prevented in order to exclude undesired electrode reactions and thus allow the application of the substoichiometric principle.

4. Conclusion

The substoichiometric radioisotopic dilution principle has been successfully applied to controlled-potential coulometry. Further research in this area will be directed toward analysis at the submicrogram concentration level. The factors affecting the sensitivity will be evaluated and attempts made to minimize them. Work in this direction is already in progress. The use of an inert N_2 dry box should provide a minimum of oxygen interference while purification of the supporting electrolyte by preelectrolysis at controlled potential should greatly reduce electroactive contaminants which affect the analysis. It is hoped that the high specific activity of many radioisotopes will provide high sensitivity with this method.

(P. A. Pella)

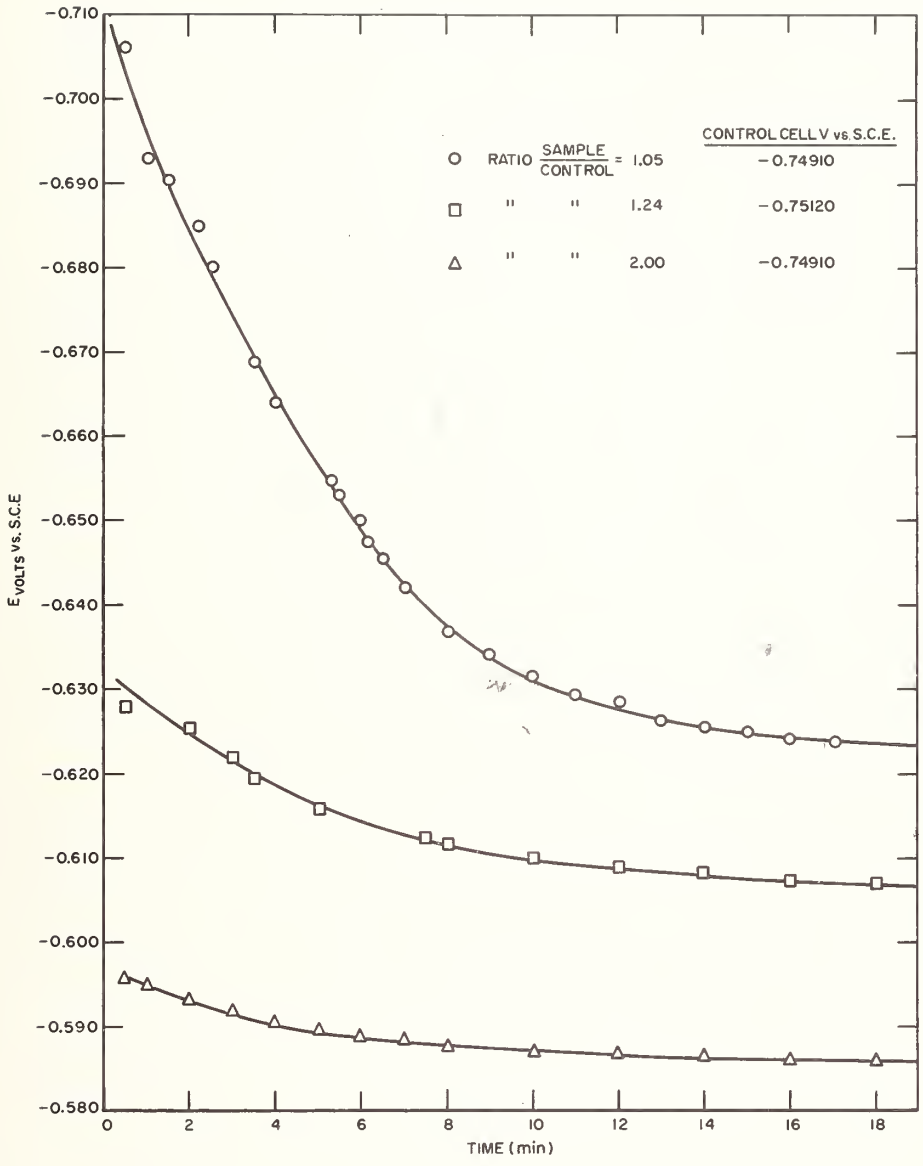

Figure 58. Potential of sample cell vs. time for various concentration ratios

D. Radioisotopic Dilution for Trace Chemical Analysis

1. Introduction

Two methods for trace elemental analysis have been developed. One which was originated by Ruzicka and Stary [56] is called substoichiometric radioisotopic dilution analysis, SRDA. The SRDA method differs from classical radioisotopic dilution [57] in that the same amount of material is isolated before and after dilution, eliminating the need to measure the specific activity. For some heterogeneous systems using a limiting amount of reagent, it is impossible to remove the same amount of element before and after dilution; however, if the variables are controlled a graphical relationship can be obtained between the amount of element present in the sample and the amount of diluted radioisotope that is separated. This method of analysis is called the concentration dependent method (CDM). These methods are related through the fundamental processes of chemical and isotopic exchange. By the application of the law of mass action to the chemical process, and the subsequent application of the radioactivity balance relation it will be shown that the relative radioactivity can be used in place of specific activity to measure the change in the initial concentration.

An inclusive theory has been developed and is partly described in this report. The theory of isotopic dilution analysis was reviewed by Alimarin [57] and the theory of SRDA was developed by Ruzicka [56]. The CDM has been developed by the present authors [58] and a theoretical treatment was developed by Kyrs [59]. A theoretical approach which differs from Ruzicka [56] and Kyrs [59] was developed. Also methods of standard additions have been developed for the CDM and SRDA [1].

H. Wieler [60] and J. Rykeer [61] have developed theoretical treatment of the accuracy and precision of classical isotopic dilution analysis. The theoretical and practical considerations in SRDA have been considered along with a procedure to minimize errors commonly arising in the application of the method. The CDM has associated with it the common advantages

and disadvantages of methods which rely on calibration curves. With respect to the sensitivity of the CDM and SRDA, the former has been found to be more sensitive [1, pp 112-148, 58, 59].

Ruzicka and Stary have reported an analysis for mercury and zinc using SRDA [62,63]. Their procedure was reinvestigated and some difficulties were found with the procedure for mercury. Cadmium was determined in this laboratory [64] using substoichiometric amounts of dithizone for both model solutions and for a zinc matrix where the cadmium was separated from interfering elements by controlled-potential electrolysis.

The concentration dependent method has been used to extend the sensitivity of the extraction procedures used to determine mercury and cobalt [58], by using a limiting amount of EDTA in an ion exchange separation. It has been found that the concentration dependent method could be applied to the adsorption of traces of material on chromatographic paper impregnated with manganese dioxide [1, pp 112-148].

The latter part of this report includes a summary of the theoretical treatment of SRDA and CDM. An example of applying the law of mass action to the radiochemical balance relationship for the solvent extraction of mercury with dithizone and an experimental procedure of verifying whether SRDA or CDM applies will be explained. The results obtained in the analysis of mercury and zinc along with a discussion of the precision, accuracy and sensitivity of these methods are also summarized.

2. Highlights of the Theoretical Treatment of SRDA and CDM

SRDA, CDM, as well as classical isotopic dilution analysis involve heterogeneous equilibria. It is necessary to transfer mass from one phase to another and the substance isolated must be in a pure form or isolated in a predictable manner. In order to understand the methods, (SRDA and CDM), it is necessary to apply the law of mass action to the heterogeneous equilibrium. The fundamental expression is

$$aB_I + bA = c\,C_{II} + dD \qquad (1)$$

where a, b, c, and d are the coefficients, B is the substance to be analyzed, A is the limiting reagent, C is the complex formed between A and B, and D is the ion replaced from B. The signs are omitted for simplicity. The subscripts I and II refer to phase I and II. A and D may be in one phase or the other, but B and C must be in different phases. The relationship

$$K = \frac{[C_{II}]^c\,[D]^d}{[A]^b\,[B_I]^a} \cdot \frac{\gamma_{c_{II}}^c\,\gamma_d^d}{\gamma_{BI}^a\,\gamma_A^b} = K_{AB}^m\,\Gamma_{AB} \qquad (2)$$

applies for the above equilibrium.

The γ's are the thermodynamic activities, K_{AB} is the thermodynamic constant, K_{AB}^m is the concentration quotient and Γ_{AB} is the activity quotient. Γ_{AB} may assume unpredictable values and in many cases is not known. If we can assume Γ_{AB} to be unity then K_{AB} is equal to K_{AB}^m. It is a simple matter using these assumptions to calculate m, the mass isolated of the element of interest before and after dilution.

This amount, m, can be related to the radioactivities isolated through the radioactivity mass balance relation. The radioactivity mass balance relation generally takes the form

$$(X + Y)\,\frac{a_2}{m_2} = \frac{a_1}{m_1}\,Y. \qquad (3)$$

where X is the unknown weight of the element, and Y is the known total elemental weight of the radioisotope. The specific activity of the radioisotope before dilution is $A_1 = \frac{a_1}{m_1}$, and $A_2 = \frac{a_2}{m_2}$ is the resultant specific activity after dilution, where a_1 and a_2 are the activities in counts per minute for a reproducible counting geometry which corresponds to weight m_1 and m_2 of the element before and after dilution, respectively.

SRDA requires that equal amounts are isolated before and after dilution through the use of a substoichiometric amount of reagent. This requires a high K_{AB}^m for the reaction. If

99.9% of the reagent is used up then $m_1 = m_2$ for all practical purposes. It is evident from equilibrium considerations that m_1 can never exactly equal m_2. If the equilibrium constant is low, 99.9% of the reagent is not consumed before and after dilution, and the amount isolated is not independent of the initial concentration. Using the proper amount of limiting reagent and appropriate experimental conditions, the assumption that equal amounts are isolated before and after dilution is valid for a number of systems. Then the following relation $(X + Y)\ a_2 = Ya_1$ (equation 4) can be used. The method only requires the measurement of the radioactivities (a_1 and a_2) and a knowledge of Y.

The CDM is based on the distribution of the elemental species between two phases as a function of the initial concentration. In the concentration dependent method the amount isolated is dependent on the initial concentration. This process must be combined with the process of specific activity change. For any given series of experiments a_1, Y, and m_1 are constants; $a_{2\cdots j}$, $X_{2\cdots j}$, $m_{2\cdots j}$, are variables; a_1, $a_{2\cdots j}$ are determinable experimentally, but m_2 and X cannot both be determined from the radioactive material balance relation. The total initial concentration C_t is equal to X plus Y. If one lets $\frac{a_1}{m_1} Y = K'$ it can be shown that $K' = a_t$, the total activity in the system. From the radioactivity material balance relation $a_2 C_t = a_t m_2$ (equation 6). It is possible to calculate m_2 for various values of C_t using the law of mass action and assuming values for the total radioactivity, (a_t, added to the system); it is a simple matter to calculate a_2, the radioactivity isolated. A plot of radioactivity isolated versus initial concentration can be obtained. The CDM is valid if the amount isolated before and after dilution is not constant but varies as a function of the initial concentration.

3. An Example of Applying the Law of Mass Action to the Radioactivity Mass Balance Relation

Ruzicka [56] assumed that 99.9% of the organic reagent is used in the reaction of interest. It is more useful not to make this assumption because it allows us to determine whether SRDA or CDM method applies. An example will be illustrated for the solvent extraction of mercury with substoichiometric amounts of dithizone. The solvent extraction of mercury with dithizone can be represented by the equation

$$Hg^{++}_{(aq)} + 2H_2Diz_o = Hg(HDiz)_2 + 2H^+_{(aq)} \qquad (7)$$

This equation does not take into consideration the side reactions of mercury or dithizone. For a more complete treatment of the equilibria see Sandell [65] and Ringbom [66].

Let $[H^+]$ = a constant for a given series of experiments

X = amount of mercury initially present in grams

m = amount of mercury dithizonate formed in grams

V_o = volume of the organic phase in milliliters

V = volume of aqueous phase in milliliters

C_{diz} = initial concentration of dithizone, in moles/liter

at.wt. = atomic weight of mercury

$$K = \frac{[Hg(HDiz)_2]_o[H^+]^2}{[Hg]\,[H_2Diz]_o^2} \qquad (8)$$

$$K = \frac{\left[\frac{\frac{m}{at.\ wt.}}{V_o}\,1000\right][H^+]^2}{\left[\frac{X-m}{V\ at.\ wt.}\,1000\right]\left[C_{Diz} - \frac{\frac{2m}{at.\ wt.}}{V_o}\,1000\right]^2} \qquad (9)$$

Since K, V_o, $[H^+]$, X, V and C_{Diz} are known, m can be readily solved for any series of experiments for the X_i value of X (where i denotes initial concentration). If m is relatively constant then SRDA is valid and if m varies, then from knowing m, a_t, and c_t the radioactivity one expects to isolate can be calculated

from equation 6. Using these relationships for the above example, SRDA was shown to apply.

This treatment is not completely valid since the amount of mercury present should be corrected for the formation of hydroxo complexes, $(HgOH)^{+}_{(aq)}$ and $Hg(OH)_{2(aq)}$ and for the solubility of mercury dithizonate at low concentrations in the aqueous phase. The solubility of dithizone in water has not been taken into account and a correction for this may be needed for low concentrations of dithizone. These corrections can be approximated [65 ,66].

4. An Experimental Procedure to Distinguish between SRDA and CDM

From the radioactive material balance relation (equation 3) it can be shown that when SRDA applies, $\frac{a_1}{a_2} = \frac{X}{Y} + 1$ (equation 10), a plot of the ratio of radioactivities versus the amount X should give a straight line with a slope of 1/Y and an intercept of 1. But if the SRDA principle does not apply, a curve which is still analytically useful can be obtained. When $m_1 \neq m_2$ then from the radioactivity material balance relation,

$$\left[\frac{a_1}{a_2}\right] m_2 = X\left[\frac{m_1}{Y}\right] + m_1 \qquad (11)$$

is obtained, where m_2 can be calculated from the law of mass action, and it is possible to obtain a straight line from the data. Let $\left[\frac{a_1}{a_2}\right] m_2 = Z$. A plot of Z versus X should give a slope of $\frac{m_1}{Y}$ and an intercept m_1.

5. Experimental

The procedure developed by Ruzicka was used to determine mercury [62] and zinc [63] with the following exceptions: the concentration of dithizone (see tables 20 and 21) and the specific activity of radioisotopes used was different. The specific activity of mercury-203 was 458 mCi/g and the specific activity of zinc-65 was 1784 mCi/g.

Table 20. Results obtained with zinc

Amount added μg/ml	Amount found μg/ml	Standard[a] deviation	% dev. from added value	Concen diz(M)	No. of deter
1.000	0.983	± 0.005	-1.7	$1x10^{-4}$	5
0.100	0.1030	± 0.0056	+3.00	$5x10^{-5}$	5
0.0010	0.0010	± 0.00008	+1.0	$2x10^{-6}$	5

[a] Of a single determination.

Table 21. Determination of Mercury

Amount added μg/ml	Amount found μg/ml	Rel std[a] dev %	% dev from added value	Concen diz(M)	No. of deter
1.00	1.02 ± 0.02	1.7	+ 2.00	$2x10^{-5}$	8
0.100	0.100 ± 0.002	2.0	< 1.00	$1x10^{-5}$	6
0.0100	0.0131 ± 0.0004	3.3	+31.0	$2x10^{-6}$	5
0.00100	0.00072 ± 0.0002	2.7	-28.0	$1x10^{-6}$	5

[a] Of a single determination.

6. Discussion

The graphical procedure was used to determine whether CDM or SRDA was applicable. The advantage of this approach is that it allows one to bracket the sample, and the curve can be used when the SRDA formula does not apply. Also the amount in the tracer need not be known and it is evident that the total elemental concentration of the tracer can be determined through the use of this approach. Also, when the amount in the tracer is small or well known one can apply a method of standard additions.

The way Ruzicka and Stary calculated the error associated with the analysis appears to be biased since they assumed no error is associated with the radioactivity isolated before dilution in the determination of mercury, and they paired the activities a_1, a_2 to obtain the most favorable results in the determination of zinc.

The data obtained in this laboratory for zinc have good precision and accuracy (see table 20). The data obtained for the determination of mercury is reported in table 21. The precision is acceptable by normal analytical standards, but the accuracy is poor at the 0.01 and 0.001 μg/ml levels. The accuracy can be corrected to within 4% of the added value by the use of a calibration curve which allows the sample to be bracketed.

The interrelationship between accuracy and precision varies in different ways for the different analytical methods. A detailed error analysis has been performed to conclusively demonstrate that for SRDA the accuracy and precision are inversely related, i.e., as one increases the other decreases. Ways of overcoming this paradox have been developed.

The precision and accuracy of the method can be affected by a number of factors. The most serious errors affecting the precision in solvent extraction are caused by the evaporation of the organic phase and oxidation of the dithizone. It is evident at the submicrogram level that contamination due to

reagents, apparatus and airborne contamination may affect the accuracy as well as the precision. The matrix may have a profound effect upon the accuracy of the method. If preconcentration is necessary, losses may occur and the blank is increased. It is possible through the use of tracers to correct for losses. The blank can be corrected for by a method of standard additions [1, pp 112-148]. Interferences from the matrix can also be corrected by a method of internal standards or by using masking agents [1, pp 112-148]. When $m_1 \neq m_2$ the graphical approach can be used to bracket the sample and the amount (Y) need not be known when calibration curves are used.

The blank and specific activity of the radioisotope are the two most important factors limiting sensitivity. The sensitivity of the method can be extended by the use of micro methods, methods of preconcentration, and a clean environment.

An attempt has been made to verify the concept of radioisotopic dilution techniques for tracer elemental analysis. Considerable effort has been expanded in demonstrating the precision, accuracy, and sensitivity of these methods, and a more detailed report of this work will be made in the near future.

(A. R. Landgrebe and L. T. McClendon)

E. Publications

Determination of Trace Amounts of Cadmium and Silver by Substoichiometric Radioisotopic Dilution Analysis. A. R. Landgrebe, J. R. DeVoe and L. T. McClendon, Trans. Am. Nucl. Soc., 8, 315-316, 1965.

F. Consultations

George Welford, Health and Safety Laboratory, Atomic Energy Commission, New York, New York

Emilio J. Trioanelb, Northeastern Radiological Health Lab. 109 Holton Street, Winchester, Massachusetts

6. LIST OF TALKS

1. A. R. Landgrebe, "Radiochromatographic Methods", American Chemical Society, Atlantic City, September 1965.

2. J. J. Spijkerman, A. R. Landgrebe, F. C. Ruegg and J. R. DeVoe, "The Use of Mössbauer Effect to Study the Adsorption of Iron on Cationic Exchange Resin", American Chemical Society, Atlantic City, September 1965.

3. J. J. Spijkerman, A. R. Landgrebe and F. C. Ruegg, Mössbauer Effect in Ethylenediaminetetraacetatoiron (III) Complexes", American Chemical Society, Atlantic City, September 1965.

4. A. R. Landgrebe, L. T. McClendon, and J. R. DeVoe, "A New Method of Analysis Using Radioisotopic Tracers - A Concentration Dependent Method", American Chemical Society, Atlantic City, September 1965.

5. P. A. Pella, A. R. Landgrebe, J. R. DeVoe and W. C. Purdy, "Differential Controlled-Potential Coulometry Utilizing Radioisotopes", American Chemical Society, Atlantic City, September 1965.

6. F. C. Ruegg, J. J. Spijkerman, and J. R. DeVoe, "A Mössbauer Spectrometer for the Structural Analysis of Materials", IAEA, Warsaw, October 1965.

7. J. R. DeVoe, "Applications of Mössbauer Spectrometry to Chemical Analysis", American Chemical Society, Central Ohio Valley Section, Marshall University, Huntington, West Virginia, November 1965.

8. J. R. DeVoe, "Applications of Mössbauer Spectrometry to Chemical Analysis", American Chemical Society, Louisville Section, Bellarmine College, Kentucky, November 1965.

9. J. R. DeVoe, "The Radiochemical Analysis Program at the National Bureau of Standards", American Chemical Society, Indiana-Kentucky Border Section, Evansville, November 1965.

10. A. R. Landgrebe, "Substoichiometric Radioisotopic Dilution Analysis of Silver and Cadmium", American Nuclear Society, Washington, D. C., November 1965.

11. A. R. Landgrebe, L. T. McClendon, and J. R. DeVoe, "A New Method of Analysis Using Radioisotopic Tracers - A Concentration Dependent Method", Eastern Analytical Symposium and Instrument Exhibit, New York, November 1965.

12. F. C. Ruegg, "Absolute Velocity Mössbauer Spectrometer", American Nuclear Society, Washington, D. C., November 1965.

13. J. J. Spijkerman and F. C. Ruegg, "Determination of Coordination Numbers for Iron Chemistry", New England Nuclear and Technical Measurement Corporation, joint sponsors, N. Y., January 1966.

14. D. K. Snediker, "The Mössbauer Effect of Sn^{119m} in Pd-rich Palladium-Tin Solid Solutions and the Intermetallic PdSn", New England Nuclear and Technical Measurement Corp., joint sponsors, N. Y., January 1966.

15. A. R. Landgrebe, "A Critical Evaluation of the Method of Substoichiometric Radioisotopic Dilution Analysis", Pittsburgh Conference on Analytical Chemistry and Applied Spectroscopy, Pittsburgh, February 1966.

16. J. R. DeVoe, "Activation Analysis on Nuclear Resonance Fluorescence Spectroscopy", Nuclear Science and Engineering Seminar, Catholic University, Washington, D. C., May 1966.

17. J. J. Spijkerman, "Standard for Chemical Shift of Iron Compounds in Mössbauer Spectroscopy", Society for Applied Spectroscopy, Chicago, June 1966.

18. L. May and J. J. Spijkerman, "A Study of Iron Coordination Chemistry by Mössbauer Spectroscopy", Society for Applied Spectroscopy, Chicago, June 1966.

19. L. A. Currie, "Systematic Errors in Recovery and Detection Efficiency as Related to Radiochemical Analysis", BioAssay and Analytical Chemistry Conference, Albuquerque, October 1965.

7. PERSONNEL

Radiochemical Analysis and Activation Analysis,
J. R. DeVoe, Section Chief

Activation Analysis

E. D. Anderson
D. A. Becker
B. S. Carpenter
W. D. Kinard
F. A. Lundgren
G. J. Lutz
S. S. Nargolwalla
W. P. Reed
G. L. Rhinehart - Terminated
R. R. Ruch
G. W. Smith
W. Jester - Summer student, 1965
M. R. Crambes - Guest Worker (6 months on NATO Fellowship and 1 year Contract) Atomic Energy Establishment of Grenoble, France

Instrumentation

W. N. Bettum
R. W. Shideler
P. N. Thomas

Nuclear Chemistry

L. A. Currie

Radiation Techniques

W. L. O'Neal
F. C. Ruegg
D. K. Snediker
J. J. Spijkerman
E. A. Rhodes - Summer student, 1965
M. G. Hollstein - 1 year contract - Karlsruhe Center of the German Atomic Energy Establishment

Radioisotope Tracer Techniques

T. E. Gills
A. R. Landgrebe
L. T. McClendon
P. A. Pella

8. ACKNOWLEDGMENTS

The Activation Analysis and Radiochemical Analysis Sections wish to thank Dr. J. Elliot, Dr. Keith Marlow, Mr. E. Nowstrop, Mr. E. Bebbs, Mr. L. Harris, and Mr. R. Vogt of the Naval Research Laboratory Reactor Facility for making the irradiation of samples possible. In addition, we wish to thank the NRL Metallurgy Division, which has assisted several times in the procurement of reliable, pure elemental standards for our work in neutron activation analysis. We also wish to acknowledge the assistance of the NBS Health Physics staff who have helped us with the safe handling of these samples.

We wish to express our thanks to Dr. C. O. Muehlhause and his staff for their cooperation in making arrangements for our use of the new facilities in the NBS Reactor Building. Further, the assistance of Dr. H. W. Koch, Dr. J. E. Leiss and staff of the Radiation Physics Division for arrangements to use the LINAC facilities is acknowledged. The assistance of Mr. Goetz, Acting Chief, as well as Mr. H. J. Rouse, Mr. T. B. McKneely, Jr., and Mr. M. F. Kelly of the Plant Division, NBS, is also acknowledged. We wish to thank Dr. J. Cameron and his staff for assistance in statistical analysis of experimental data.

These sections acknowledge Mrs. R. S. Maddock for her assistance in preparing this report.

Special appreciation is expressed to Mrs. M. Fenstermaker and Mrs. V. Durkay who typed the entire report and whose tireless efforts as section secretaries have made our entire operation more efficient and effective.

9. LIST OF REFERENCES

[1] DeVoe, J. R., editor, NBS Technical Note 276 (1965)

[2] Muehlhause, C. O., editor, NBS Report 8998 (1966)

[3] Sheely, W. F., NBS Report 9081 (1966)

[4] Anders, O. U. and Briden, D. W., Anal. Chem. 36, 287 (1964)

[5] Robinson, Berol L., "Precision Determination of Gamma Ray Energies with the Scintillation Spectrometer." G. D. O'Kelly, editor, Proceedings of a Symposium on Applications of Computers to Nuclear and Radiochemistry, Gatlinburg, Tenn., Oct. 1962, NAS-NS-3107, 67-73.

[6] Cumming, J. B., "CLSQ, The Brookhaven Decay Curve Analysis Program," G. D. O'Kelley, editor, Proceedings of a Symposium on Applications of Computers to Nuclear and Radiochemistry, Gatlinburg, Tenn., Oct. 1962, NAS-NS-3107, 25-33

[7] Brown, E., Hague, J. L., and Bright, H. A., J. Research, NBS 47, 380 (1951).

[8] "Experimental Statistics," Mary G. Natrella, editor, NBS Handbook 91 (1963)

[9] Table of Isotopes, Strominger, Hollander, and Seaborg, Rev. Mod. Phys., 30, No. 2(II) (1958).

[10] Hughes, D. J. and Schwartz, R. B., "Neutron Cross Sections," BNL-325 (1958) 2nd Ed.

[11] Ibid, Supplement No. 1, Jan. 1960.

[12] Macklin, R. L. and Pomerance, H. S., "Progress in Nuclear Energy-I", McGraw-Hill, New York (1956) p 180.

[13] Yule, H. P., Anal. Chem. 37, No. 1, 129-132 (1965).

[14] Bowen, H. J. M. and Gibbons, D.,"Radioactivation Analysis," Oxford University Press, Cambridge, U.K. (1963) p 98.

[15] Hoste, J., Pure and Applied Chemistry, 1, 99 (1960).

[16] Leliaert, G., Hoste, J., and Eeckhaut, J., Anal. Chim. Acta, 19, 100 (1958).

[17] Hoste, J., Bouten, F., and Adams, F., Nucleonics 19, 118 (1961).

[18] Berlandi, F. J., and Mark, H. B., Jr., Chem. Eng. News, p 84 (Sept. 1964).

[19] Mark, H. B., Jr., and Berlandi, F. J., Anal. Chem. 36, 2062 (1964).

[20] Mark, H. B., Jr., Berlandi, F. J., Vassos, B. H. and Neal, T. E., "Proceedings of the 1965 International Conference: Modern Trends in Activation Analysis," Texas A & M Univ., College Station, Texas.

[21] Vassos, B. H., Berlandi, F. J., Neal, T. E., and Mark, H. B., Jr., Anal. Chem. 37, 1653 (1965).

[22] General Electric Chart of the Nuclides, March 1965 ed.

[23] Heath, R. L., Phillips Petroleum Report, IDO-16408 (1957).

[24] DeVoe, J. R., Kim, C. K. and Meinke, W. W., Talanta 3, 298 (1960).

[25] DeVoe, J. R., Nass, H. W. and Meinke, W. W., Anal. Chem. 33, 1713 (1961).

[26] Silker, W. B., Anal. Chem. 33, 233 (1961).

[27] Ruch, R. R., DeVoe, J. R., and Meinke, W. W., Talanta 9, 33 (1962).

[28] Qureshi, I. H. and Meinke, W. W., Talanta 10, 737 (1963).

[29] Orbe, F. E., Qureshi, I. H., and Meinke, W. W., Anal. Chem. 35, 1436 (1963).

[30] Qureshi, I. H., and Meinke, W. W., Radiochimica Acta 2, 99 (1963).

[31] Kim, C. K., and Silverman, J., Anal. Chem. 37, 1616 (1965).

[32] Qureshi, I. H., personal communication.

[33] Jangg, G., Metall 16, 639 (1962).

[34] Dyer, F. F. and Leddicotte, G. W., "The Radiochemistry of Copper," NAS-NS 3027 (1961).

[35] Duncan, J. F. and Oakley, B. W., J. Chem. Soc. 1955, 1401 (1955).

[36] Latimer, W. M., "Oxidation Potentials," Prentice-Hall, Inc., Englewood Cliffs, N. J., (1961).

[37] DeVoe, J. R., editor, NBS Technical Note 248 (1964).

[38] Shideler, R. W., "Proceedings of the 1965 International Conference: Modern Trends in Activation Analysis," Texas A & M Univ., College Station, Texas.

[39] Hill, R. L. NBS Technical Note 168 (1963).

[40] Engelkemeir. D., Rev. Sci. Instr., 227 (No. 8) 589 (1956).

[41] Spijkerman, J. J., Ruegg, F. C., DeVoe, J. R., Snediker, D. K., O'Neal, W. L., NBS Technical Note 260-13, to be published.

[42] Walker, L. R., Wertheim, G. K. and Jaccarino, V., Phys. Rev. Letters, 6, 98 (1961).

[43] Snediker, D. K., "The Mössbauer Effect of Sn^{119} in Palladium-Rich Palladium-Tin Solid Solutions," Mössbauer Effect Methodology, Vol. 2, Plenum Press, New York, In press.

[44] Ruegg, F. C., Spijkerman, J. J., and DeVoe, J. R., Rev. Sci. Instr., 36, 356 (1965).

[45] Herber, R. W., and Spijkerman, J. J., J. Chem. Phys. 43, 4057 (1963).

[46] Hill, R. L., NBS Technical Note 168 (1963).

[47] Seiler, H., Helv. Chim. Acta 46, 2629-2635 (1963).

[48] Pollard, et al, Anal. Chim. Acta 14, 70 (1956); J. Chem. Soc., 466 (1951); J. Chem. Soc., 470 (1951); Nature 163, 292 (1949); J. Chromatog. 2, 282 (1959).

[49] Van Erkelens, P. C., Nature 172, 357-8 (1953).

[50] Van Erkelens, P. C., Anal. Chim. Acta 25, 570-578 (1961).

[51] Welford, G. A., Chiotes, E. L. and Morse, R. E., Anal. Chem. 36, 2350 (1964).

[52] Hais, I. M., and Macek, K., Paper Chromatography, Academic Press, N. Y. (1963).

[53] Stahl, E., editor, Thin Layer Chromatography: Ch. M., Thin Layer Chromatography of Inorganic Ions by A. Seiler; Ch. N., Spray Reagents for Thin Layer Chromatography by D. Waldi, Academic Press, Inc., N.Y. (1965).

[54] Connally, R. E. and Scott, F. A., "Hanford Controlled Potential Coulometer," AEC Report HW-65919 (1960).

[55] Rechnitz, G. A. and Srinivasan, K., Anal. Chem. 36, 2417 (1964).

[56] Ruzicka, J. and Stary, J., Talanta 8, 228-234 (1961).

[57] Alimarin, I. P. and Bilimavith, G. H., Int. J. Appl. Rad. Isotopes 7, 169 (1960).

[58] Landgrebe, A. R., McClendon, L. T., and DeVoe, J. R., Radiochemical Methods of Analysis, Vol. II, Inter. Atomic Energy Agency, Vienna, 321-333 (1965).

[59] Kyrs, M., Anal. Chim. Acta 33, 245-256 (1965).

[60] Weiler, H., Int. J. Appl. Rad. Isotopes 12, 49-52 (1961).

[61] Rykheer, J. and Bozalek, S., Application of Isotopes and Radiation, Vol. II, National Conf. on Nuclear Energy, Pretoria, Republic of South Africa, 72-82 (1963).

[62] Ruzicka, J. and Stary, J., Talanta 8, 535-38 (1961).

[63] Ibid. 8, 296-300 (1961).

[64] Landgrebe, A. R., DeVoe, J. R., McClendon, L. T., Trans. Am. Nuc. Soc. 8, 315-316 (1965).

[65] Kolthoff, I. M., Treatise on Analytical Chemistry, Pt. 1, I, Ch. 14, Complexation Reactions by Anders Ringbom, The Interscience Encyclopedia, Inc., N. Y.

[66] Sandell, E. B., Colorimetric Determination of Traces of Metals, Interscience Publishers, Inc., N. Y. (1959) pp 139-174.

APPENDIX I

NOTES ON THE USE OF THE G.E. TIME-SHARING COMPUTER FOR MULTICOMPONENT DECAY CURVE ANALYSIS

A. Introduction

Principles, method of use, interpretation, and illustrations of decay curve analysis will be presented below. The specific program referred to is "CLSQ-1". This program is a modification of "CLSQ" which was written by G. Lutz; "CLSQ", in turn, was prepared (in part) by translation of the original "CLSQ" (Fortran) of J. Cumming [A1] into BASIC. "CLSQ-1" takes observed numbers of counts, counting times, counting intervals, and half-lives, and it calculates initial counting rates with their standard deviations for data which may be treated by simultaneous equations or, if overdetermined, by least squares. In the case of least squares, the output also includes the RATIO of the observed deviation to the standard deviation for each point, and also the quantity, FIT, is calculated. The on-line feature allows convenient changes of model, elimination of negligible components, rejection of outliers, and evaluation of "true" observation variance.

B. Mathematics

1. Least-Squares Formulation

Observed counting-rates, Y_i, at observation (mid-) times, t_i, are related to the initial rates of the components, x_i, by the matrix equation:

$$A \mid x > = \mid y >$$

$$\text{or} \quad \sum_j A_{ij} x_j = y_i \qquad (1)$$

$$\text{where} \quad A_{ij} = e^{-\lambda j t_i}$$

Applying the criterion of minimum variance ("least-squares") one reduces equation (1) to a set of simultaneous equations:

$$B \mid x = \mid z > \qquad (2)$$

$$\text{where} \quad B_{kj} = \sum_i A_{ik} A_{ij} w_i = B_{jk}$$

$$z_k = \sum_i y_i A_{ik} w_i$$

w_i being the "weight" attached to the ith observation. Inversion of the B-matrix yields the solution for $|x>$,

$$|x> = B^{-1}B|x> = B^{-1}|z> \qquad (3)$$

$$\text{or} \quad x_j = \sum_k (B^{-1})_{jk} z_k$$

The variance for x_j is given by the product,

$$\sigma_j^2 = (B^{-1})_{jj} \cdot \frac{\sum_i w_i (y_i - y_i^{calc})^2}{\nu} \qquad (4)$$

where ν = (no. observations)- (no. unknowns) = no. degrees of freedom

2. Weights, w_i

Two cases may be considered,

(a) equal weights, $w_i = 1$

(b) unequal weights, $w_i = 1/\sigma_i^2$

If equal weights are assumed, the second factor on the right-hand side of equation (4)is just equal to s^2, the sample variance, and, therefore,

$$\sigma_j = [(B^{-1})_{jj}]^{1/2} \cdot s$$

If weights are derived from counting statistics, the second factor referred to above is equal to $(s/\sigma)^2$, and "in the long run" it has a mean value of unity. Thus, if observations are properly weighted according to their reciprocal variances, the standard errors are numerically equal to $[(B^{-1})_{jj}]^{1/2}$.

CLSQ-1, as written, expresses weights as in case (b), above, and includes variance contributions from sample counting, background standard deviation, and "external" (or additional) variance. One may set all weights equal to unity, if desired, by typing:

```
140 LET W(R) = 1
```

In this case, however, the standard errors of the results are given by Equation (4), and must be calculated from the product of the output data: "SIGMA" and "FIT", which are equal to $[(B^{-1})_{jj}]^{1/2}$ and s, respectively. "FIT" no longer has its previous meaning - that of indicating consistency between s and σ.

3. "FIT"

FIT is a measure of the consistency of the observed deviations with those expected from counting statistics. It is defined as $[\chi^2/\nu]^{1/2}$, where χ^2/ν serves as an estimate of $(s/\sigma)^2$, and in the long run, is expected to have the value, unity. Thus, $\nu \cdot (FIT)^2$ follows the χ^2 - distribution for ν - degrees of freedom. For large ν, $(FIT)^2 = \chi^2/\nu$, is approximately normal, with a mean of unity and a variance of $2/\nu$. "FIT" is calculated according to equation (5).

$$(FIT)^2 = \frac{1}{\nu} \sum_i \frac{(y_i - y_i^{calc})^2}{\sigma_i^2} \qquad (5)$$

4. "RATIO"

$$(RATIO)_i \equiv \frac{(y_i - y_i^{calc})}{\sigma_i} \qquad (6)$$

"RATIO" thus gives a measure of each deviation in terms of its corresponding standard deviation. This quantity (RATIO) should be approximately normal with a mean of zero and a variance of unity.

C. Use of CLSQ-1

1. Normal Use

a. Input Data. The READ statements are shown in the first part of the program (attached), and a sample of such input data is included in example 1a. Meanings of the symbols follow:

N = number of observations

P = number of components (unknowns)

B = background rate (cpm)

S9 = standard deviation of background (cpm)

F = "external" fractional standard deviation, i.e., remaining relative standard deviation, if that due to counting statistics were equal to zero. (Generally, F may be set equal to 0, or 0.01, if desired).

T(0),M(0) = initial ("zero") time - hours, minutes, respectively. [D(0) - days- assumed to be zero]

T(R),M(R) = time of the start of the $R^{\underline{th}}$ observation - hours, minutes - respectively.

U(R) = time interval for $R^{\underline{th}}$ observation (min)

Y(R) = number of counts accumulated during the $R^{\underline{th}}$ observation.

H(J) = half-life (min) for component, J.

b. Output

1) For simultaneous equations and least-squares analyses, the following information is "put-out", for each component:

component (index) number

half-life (min)

initial (zero-time) counting rate (cpm)

standard error of initial rate (cpm)

2) For least-squares analyses, only, the following additional data are typed:

T(R), mid-time for observation, R

Y(R), net rate (cpm) for observation, R

Y-CALC(R), net rate (cpm) for observation, R, based upon the calculated curve.

RATIO(R), ratio of observed deviation to standard deviation, as defined in equation (6).

FIT, $(\chi^2/\nu)^{1/2}$ - a measure of goodness-of-fit, as defined in equation (5).

2. Modifications

a. Dead-time Correction. Should it become necessary to correct for dead-time losses, one may include statements 113, 114, and 161, as shown with the first part of the program (attached). (T = dead-time in μs.)

b. D(R), T(R), M(R), U(R), Y(R). The above quantities have been given separate "READ" statements (No. 130 through No. 134) so that one or more may be given fixed values. For example, if all observations take place on the same day, one might type:

```
130 LET D(R) = 0
```

If all starting times are initially given in minutes, one would type:

```
130 LET D(R) = 0
131 LET T(R) = 0
```

(Cf. examples: 1, 2, and 3)

One could express time in any other units, if desired, setting D(R) and T(R) to 0, as above, and making sure that M(R), U(R), B, S9, M(0), and H(J) all have consistent units of time. (For example, all might be expressed in days or counts per day; counts per fortnight, etc.)

If the time intervals, U(R), or numbers of counts, Y(R), are fixed, such fixed values might be inserted:

```
133 LET U(R) = 10
```

or

```
134 LET Y(R) = 2500
```

If a simple counting program is followed - as with a multi-channel scaler, one might replace 132 with a statement such as,

```
132 LET M(R) = 65* (R-1)
```

c. "Internal" Background. As with the GEM-program,[A2] long-lived components and background may be treated together as a single component, especially if interest is primarily in a shorter-lived component. Greater accuracy may be achieved in this way, if a long-lived component might otherwise be ignored. If all components are properly included in the first

place, however, the precision is better if the observed background is subtracted in the normal fashion. (A component is "long-lived" in the above sense if its decay during the time period covered by the set of observations is small compared to the standard deviations of such observations. Thus, typically, a component having a half-life greater than about 100 times the total time interval of observation may be considered "long-lived.")

d. Trouble-Shooting. Perhaps the most significant aspect of the on-line approach is the possibility of rapid data or model changes following the output of previous calculations. Discussion of appropriate types of change will be dealt with below, but here it will be useful to summarize the "mechanics" of such changes.

First, as is probably obvious, one may readily alter or eliminate input data simply by retyping the appropriate input statement. Second, since the significance of changes are seen principally in "RATIO", "FIT", and the calculated initial rates and their standard errors, needless time and space are consumed in retyping the mid-times, "observed" net rates, and "calculated" net rates for each observation. Hence, instructions are given at the beginning of the program in REM's 2-5 to alter the program so as to eliminate the unnecessary steps during trouble-shooting.

D. Interpretation

1. Indicators of Trouble

a. Large negative results. If the result for a given component is negative by an amount significantly greater than its associated standard error there is something wrong with the input information. Since the results may be interpreted (generally) using the normal distribution, one may specify levels of confidence with which such negative results may occur. Using one-sided confidence intervals we reach the following conclusions:

Result	Probability of Occurring by Chance
$\leq -1\,\sigma$	15.87%
$\leq -2\,\sigma$	2.28%
$\leq -3\,\sigma$	0.13%

Thus, a result more negative than $-2\,\sigma$ suggests difficulty.

b. FIT. ("FIT")^2, which follows the χ^2/ν-distribution, and is an estimate of $(s/\sigma)^2$, would be expected to approach unity with increasing N. Acceptable limits for "FIT" vary with N, and a few such limits are given below.

	95% Confidence Interval*	
ν = N-P	Lower Limit	Upper Limit
1	0.031	2.24
5	0.407	1.60
10	0.569	1.43
20	0.692	1.30
100	0.860	1.14

Values smaller than the lower limit are only apt to arise from too large an "external" standard deviation, F, whereas values which are too large may arise from several sources, discussed subsequently; the great advantage is that one may quickly be alerted to trouble by examining "FIT".

c. RATIO. The individual "RATIO's" provide a means for spotting specific sources of trouble, rather than just being general indicators - like the two above. As with the indicator, FIT, however, RATIO is not available for simultaneous equations, but only for least-squares analyses.

Limits for the magnitude of "RATIO" may be deduced from the binomial and normal distributions. If one were to examine but one RATIO, upper and lower confidence limits could be deduced from the normal distribution, that is, the 95% confidence

* The limits stated are those for "FIT" or $(\chi^2/\nu)^{1/2}$; they correspond to the two-sided 95% confidence interval for $(FIT)^2$ or χ^2/ν.

interval would extend from -1.96 to +1.96. In examining a set of N-RATIO's, however, one must apply also the binomial distribution,

$$W(\geq 1) = 1 - W(0) = 1 - (1 - \alpha)^N$$

$$\text{or} \quad \alpha = 1 - [1 - W(\geq 1)]^{1/N} \tag{7}$$

where, $W(\geq 1)$ = probability that one or more RATIO will fall outside the prescribed limits, by chance.

α = corresponding level of significance for the normal distribution

(Thus, for N = 1, $\alpha = W(\geq 1)$.)

Intervals based upon equation (7) are given below, for the case, $W(\geq 1) = 0.05$. (Note: Application of the Chauvenet criterion would not be a correct procedure.)

N	Limits for RATIO
1	± 1.96
5	± 2.57
10	± 2.80
20	± 3.00
50	± 3.27

If an occasional value of RATIO lies outside the above limits, it might be considered an outlier, and treated accordingly. If a large portion of the RATIO's exceed the limits, then very likely something is wrong with the model or the assumed standard deviations (of the individual observations).

Another way in which RATIO's may be helpful is in indicating trends. That is, if a number of consecutive values are positive or negative, and especially if they proceed from positive to negative or vice versa, one may suspect that the "model" half-life is too long or too short, respectively. These effects are illustrated clearly in example 1b.

2. Sources of Trouble

a. Outliers. An outlier may most readily be detected by examination of the RATIO's. Although it may also affect the other "indicators", its effect on a specific ratio should be

most obvious, since one such ratio should show a deviation much greater than the others. If such is the case, one may eliminate the corresponding datum and reprocess the remaining data. It is unwise, however, to reject more than one or two points; if several of the RATIO's lie outside the limits given above, very likely another source of difficulty is at fault.

b. Additional (non-counting-statistics) Variance. If additional random errors are operating (e.g. positioning reproducibility, temperature fluctuations, etc.), but are not included in the weighting, the weights will be too great (σ_i's too small), and all three indicators may suggest trouble. This source of trouble may be likely if the RATIO's take on a range of values, whose magnitude is too large, but in which positive and negative values are more or less randomly interspersed. The solution to the difficulty is to insert a value for F, the extra relative standard deviation, such that FIT, on the average, is equal to unity. Such a value for F, however, should be reasonable in terms of expected or experienced performance, and other difficulties should not be indicated after this has been done. Perhaps a reasonable value for F, in most counting experiments, is about 0.01.

c. Incorrect Model. If components are missing from the model, or if incorrect half-lives have been used, all three indicators may be affected. This source of trouble is perhaps the most likely one, and it may be studied by examining the RATIO's for trends, as suggested above, and by testing the data using various reasonable models. In general, models including components which are really absent will give no trouble, except that standard errors will be larger because of the "more complicated" analysis.

d. General Comments

1) As stated earlier, the most convenient method for exploring the trouble sources discussed above, is to eliminate unnecessary parts of the program and output, as directed in REM's 2-5.

2) In the case of a poor FIT, a major component may be approximately estimated by the calculated result together with a standard error equal to:

$$[(B^{-1})_{ij} \cdot s^2]^{1/2} = \text{"SIGMA"} \cdot \text{"FIT"}$$

This is rigorously correct for equal weights, even though the weight be unknown, and is "expected" to give "safe" results even in the case of imperfect models or data. (This last suggestion comes from the paper by Nicholson et al. [A2].)

3) Elimination of "Undetectable" Components. If a component is undetectable in the sense that its standard error is comparable to or larger than the absolute value of its calculated (initial) rate, then one may consider eliminating such a component from the model. This will have the effect of "improving" (making smaller) standard errors of remaining components. Thus, if the hypothesis that certain ("undetectable") components are absent is reasonable, it is useful to eliminate them from the model. If it is not reasonable, they should remain, for the effect of their possible presence on the precision of the remaining results must be taken into consideration. As an extreme example, one might consider two components with nearly the same half-life. Analysis of the two-component model would result in answers having very large standard errors - which, however, would allow overlap with the "truth". Elimination of one of the components would give a considerably smaller standard error and perhaps a good "FIT", but the result could be quite wrong!

By way of summary, the least-squares analysis gives proper estimates of initial rates and their standard errors only for the correct model. Additional components make the standard errors too large, whereas missing components make them too small and may cause a poor FIT, etc., if the data are sufficiently sensitive. Even adjustments of half-lives, added variance, etc., to obtain the best FIT may be misleading, and are less desirable than independent (accurate) estimates of these

quantities. A poor FIT does indicate trouble, but a good FIT may mean either that the model and data are correct or that the data are insufficiently sensitive to indicate the difficulty.

E. Examples

1. $^{12}C(\gamma,n)^{11}C$

a. A simple, one-component, least-squares analysis of the decay of 20 min - ^{11}C. All of the "indicators" are consistent with the model and data being correct. This particular calculation has been checked with the Cumming (BNL) version of CLSQ.

b. Effect of wrong half life (increased by 10%). Note that the result is wrong; that the FIT and one of the RATIO's exceed the limits provided; especially note the trend in RATIO (+ → -).

2. $^{65}Cu(\gamma,n)^{64}Cu$; $^{63}Cu(\gamma,x_n)^{62}Cu$, ^{61}Cu, ^{60}Cu

Since counting times were available in minutes, it was convenient to set D(R) = 0, and T(R) = 0.

a. Comparison of simultaneous equations (N = P = 4) results with the least squares (Cumming-CLSQ) results (N = 22, P = 4). They are seen to be consistent; the least-squares (N = 22) results have somewhat smaller standard errors; both analyses indicate that ^{60}Cu is "undetectable" by this method (to be expected on the basis of the decay scheme and the method of detection).

b. Same data, ^{60}Cu eliminated from the model; all indicators satisfactory. Note the significant decrease in the standard error for ^{62}Cu.

3. $^{235}U(n,f)...$

A "trouble-shooting" example, unknown mixture of (I,Br,?) fission products, very good counting statistics (~ 0.1%). Again D(R) = 0, T(R) = 0. REM's 2-5 utilized.

a. A trial model - 4 components - additional standard deviation (F) set equal to zero - all indicators unacceptable.

b. Two components added - all indicators still unacceptable, but enormously improved.

c. For more rapid on-line "trouble-shooting", only the principal components (according to 3b) were retained, and an added relative standard deviation of 1.0% (F = 0.01) was included. Again, a large improvement has been effected, and there appear no negative components. But, FIT is still larger than its acceptable upper limit ($\sim$1.3), and RATIO's exceeding the appropriate limits ($\sim \pm 3.1$) appear. (These latter - only two points - might be outliers.)

List of references for Appendix I

[A1] Cumming, J. B., "Applications of Computers to Nuclear and Radiochemistry," G. D. O'Kelley, editor, NAS-NS 3107, 25 (1963).

[A2] Nicholson, W. L., Schlesser, J. E., Braver, F. P., Nucl. Inst. Meth. 25, 45 (1963).

APPENDIX I - PROGRAM LISTING

Example Ia

```
8
10 DATA 7,1                    10 N,F
11 DATA 20.5,0,0               11 B,59,F
12 DATA 16,29                  12 T(0),M(0)
13 DATA 20                     13 H(1)
14 DATA 0,16,56,1,943          14 (T(1),M(1),U(1),Y(1)
15 DATA 0,16,57.5,1,889        15          "
16 DATA 0,17,18,2,914          16          "
17 DATA 0,17,27,2,657          17          "
18 DATA 0,18,15,3,240          18          "
19 DATA 0,18,27,3,147          19          "
20 DATA 0,18,53,4,137          20 T(7),M(7),U(7),Y(7)

KEY
READY.

RUN
WAIT.


CLSQ-1     13:37    CFIR    07/22/66

DEADTIME [MICROSEC] =?0


T[R] (min)        Y[R] (cpm)        Y-CALC[R] (cpm)   SIGMA-Y[R](cpm)  RATIO[R]
 27.5              922.5             920.871           30.7083           5.30629 E-
 29                868.5             874.221           29.8161          -.191882
 50                436.5             422.221           15.1162           .944615
 59                308               309.084           12.816           -8.45709 E-
 107.5             59.5              57.5544           5.16398           .376762

 119.5             28.5              37.9717           4.04145          -2.34365
 146               13.75             15.1564           2.92618          -.480625


FIT= 1.06495

COMPONENT          HALF-LIFE (min)   CPM AT T[0]      SIGMA (cpm)
 1        (11C)    20                2388.44           41.2041


TIME:    4 SECS.
```

Example Ib

```
13 DATA 22
RUN
WAIT.

CLSG-1     13:40    CEIR    07/22/66

DEADTIME [MICROSEC] =?0

T[R]          Y[R]          Y-CALC[R]       SIGMA-Y[R]      RATIO[R]
 27.5          922.5          862.304          30.7083         1.96026
 29            868.5          822.499          29.8161         1.54281
 50            436.5          424.413          15.1162          .799602
 59            308            319.625          12.816          -.907031
 107.5         59.5           69.3435          5.16398         -1.90619

 119.5         28.5           47.5125          4.04145         -4.70437
 146           13.75          20.6159          2.92618         -2.34639

FIT= 2.54804

COMPONENT     HALF-LIFE       CPM AT T[0]     SIGMA
 1             22              2050.92          35.5517

TIME:    4 SECS.
```

Example 2a

```
130 LET D(R)=0
131 LET T(R)=0
10 DATA 4,4
11 DATA 20.5,0,0
12 DATA 0,0
13 DATA 770.4,199.8,24,9.9
14 DATA 34.5,1,1773
15 DATA 136,5,2150
16 DATA 360,20,5222
17 DATA 1219,40,3579
18 DATA
RUN


CLSG-1     14:06    CEIR    07/22/66

COMPONENT       HALF-LIFE        CPM AT T(0)                SIGMA
 1              64Cu 770.4       195.242 | 200.8          5.14424 | 2.4
 2              61Cu 199.8       363.228 | 344.1          19.7445 | 8.0
 3              60Cu 24          642.32  | 197.2          727.486 | 103.6
 4              62Cu 9.9         11685.6 | 13971.         2997.57 | 543.3
                                      ↑                          ↑
                                 Full Least Squares Results

TIME:    4 SECS.
```

Example 2b

```
10 DATA 4,3
13 DATA 770.4,199.8,9.9
RUN


CLSG-1     14:09    CEIR    07/22/66

T[R]            Y[R]            Y-CALC[R]       SIGMA-Y[R]      RATIO[R]
 35              1752.5          1752.59         42.107          -2.02254 E-
 138.5           409.5           403.702         9.27362          .625221
 370             240.6           242.669         3.61317         -.572518
 1239            68.975          68.606          1.49562          .246747


F1= .882931

COMPONENT       HALF-LIFE       CPM AT T[0]     SIGMA
 1               770.4           193.633         4.81052
 2               199.8           374.912         14.6535
 3               9.9             14294.8         502.071


TIME:    4 SECS.
```

Example 3a

```
10 DATA 30, 4
11 DATA .2083, 0, 0
12 DATA 0, 417
13 DATA 11606.6, 1260, 402, 137.4
14 DATA 417, 60, 2721672, 482, 60, 2243552, 547, 60, 1910661
15 DATA 612, 60, 1658734, 677, 60, 1448148, 744, 60, 1274099
16 DATA 807, 60, 1170784, 872, 60, 1058907, 937, 60, 964782
17 DATA 1002, 60, 877473, 1067, 60, 784558, 1132, 60, 740113
18 DATA 1197, 60, 681195, 1262, 60, 627028, 1458, 60, 500112
19 DATA 1523, 60, 470693, 1588, 60, 438193, 1653, 60, 409038
20 DATA 1854, 120, 636974, 1979, 120, 566404, 2104, 120, 511170
21 DATA 2229, 120, 457669, 2604, 120, 331485, 2729, 120, 301380
22 DATA 7220.8, 120, 20019
23 DATA 7345.8, 120, 17903, 7470.8, 120, 17746, 7595.8, 120, 16260
24 DATA 8345.8, 120, 11144, 8470.8, 120, 10441

130 LET D(R)=0
131 LET T(R)=0
720 PRINT "RATIO(R)"
788 PRINT (Y(R)-G)/Z,
RUN
WAIT.


CLSQ-1.    14:58    CEIR    07/22/66

RATIO[R]
 40.4412        -7.19511        -19.7176        -20.2547        -26.2354

-28.8263        -.488943         5.29539         11.8713         11.3912

-8.21908         16.1895         15.6724         12.8908         11.5351

 17.9331         15.5156         13.8419        -2.39846        -4.48345

 .915454        -2.51648        -18.5074        -19.4957        -4.78326

-9.64747        -.353976        -1.77907         7.95311         9.1763


FIT= 16.3558

COMPONENT       HALF-LIFE       CPM AT T[0]     SIGMA
 1               11606.6        -26.7601         .73906
 2               1260            8284.56         9.59787
 3               402             22506.6         31.3352
 4               137.4           17165.7         42.1761


TIME:  12 SECS.
```

Example 3b

```
10 DATA 30,6
13 DATA 11606.6,2118,1260,402,137.4,53
RUN


CLSQ-1     15:08    CEIR    07/22/66

RATIO[R]
--3.20662          4.06967          6.79639          4.98505         -7.83793

-18.4923           3.05919          3.37929          5.94939          2.69947

-18.7797           4.82017          3.95512          1.26521          1.92481

 9.35189           7.98302          7.41168         -5.82213         -4.87122

 3.41721           2.71889         -6.00095         -4.92987          4.33862

-2.20876           4.95923          1.57886         -2.28829         -3.59305


FIT= 7.56546

COMPONENT        HALF-LIFE        CPM AT T[0]      SIGMA
 1            131I  11606.6        104.936          6.20706
 2            82Br  2118          -1222.84          61.5783
 3            133I  1260           9645.92          85.6005
 4            135I  402            23255.5          69.37
 5            132I  137.4          12193.           106.386
 6            134I  53             6667.34          105.744


TIME:  18 SECS.
```

xample 3c

```
Ø DATA 3Ø,4
1 DATA .2Ø83,Ø,.Ø1
3 DATA 126Ø,4Ø2,137.4,53
UN


LSQ-1     15:13    CEIR    Ø7/22/66

ATIC[R]
1.20885          1.23219          1.83909          1.3925          -.229812

1.83617          -.402517         -.725736         -.683Ø59        -1.12125

3.5667           -.8Ø1Ø4          -.756434         -.9ØØ714        -7.84277 E-2

1.26625          1.375            1.59158          .633133          1.1328

2.58219          2.79748          1.8819           2.Ø4886         -1.84ØØ1

5.39347          -.414297         -1.89842         .765522          .999526

IT= 1.92825

OMPONENT         HALF-LIFE        CPM AT T[Ø]      SIGMA
1                 126Ø             7426.17          33.4417
2                 4Ø2              26577.5          219.441
3                 137.4            6381.34          833.754
4                 53               11670.3          1220.81

IME:  11 SECS.
```

PROGRAM LISTING

```
CLSQ-1     13:49    CEIR    07/22/66

1 REM MULTICOMPONENT DECAY CURVE ANALYSIS
2 REM - IF ONLY RATIO(R) DESIRED, TYPE:
3 REM - - - 720 PRINT "RATIO(R)" - -
4 REM - - - 788 PRINT (Y(R)-C)/Z, = =
5 REM - IF N>35, OMIT COMMA AT END OF 788 (4 REM)
6 REM - IF W(R) = 1, "FIT" = STD DEVN,
7 REM - AND "SIGMA(J)*"FIT" = STD ERROR(J)
100 DIM D(100),T(100),M(100),U(100),Y(100),W(100)
110 READ N,P
111 READ B,S9,F
112 READ T(0),M(0)
113 PRINT "DEADTIME (MICROSEC) =" ;
114 INPUT T
115 PRINT
116 LET T = (T/60)*1E-6
120 FOR J = 1 TO P
121 READ H(J)
122 LET L(J) = LOG(2)/H(J)
123 NEXT J
125 FOR R = 1 TO N
130 READ D(R)
131 READ T(R)
132 READ M(R)
133 READ U(R)
134 READ Y(R)
140 LET W(R) = (((Y(R)/U(R))↑2)*(F↑2+(1/Y(R))) + S9↑2)↑(-1)
145 LET T(R) = 1440*D(R) + 60*(T(R)-T(0))+M(R)-M(0)
150 LET T(R)=T(R)+.5*U(R)
160 LET Y(R) = (Y(R)/U(R))-B
161 LET Y(R)= Y(R)/(1-Y(R)*T)
168 NEXT R
210 FOR J = 1 TO P+1
220 FOR I = 1 TO P
230 LET B(I,J)=0
240NEXT I
250 NEXT J
260 FOR R = 1 TO N
270 FOR J = 1 TO P+1
```

```
280 FOR I = 1 TO J
290 IF J = P+1 THEN 320
300 LET A = W(R)*EXP(-((L(J)+L(I))*T(R)))
310 GO TO 330
320 LET A = W(R)*Y(R)*EXP(-L(I)*T(R))
330 LET B(I,J)=B(I,J)+A
340 LET B(J,I)=B(I,J)
350 NEXT I
360 NEXT J
370 NEXT R
390 FOR I = 1 TO P
400 FOR J = 1 TO P+1
420 NEXT J
430 NEXT I
440 FOR I = 1 TO P
445 LET F(I)=0
450 NEXT I
455 FOR X = 1 TO P
460 LET B1=0
465 FOR G = 1 TO P
470 IF F(G)<>0 THEN 490
475 IF(ABS(B1)-ABS(B(G,G)))>=0 THEN 490
480 LET B1=B(G,G)
485 LET L = G
490 NEXT G
495 LET F(L)=B1
500 LET B(L,L)=1
505 FOR K = 1 TO P
510 IF(K-L)=0 THEN 560
515 IF B(K,L)=0 THEN 560
520 LET R1=B(K,L)/B1
525 FOR D = 1 TO P
530 IF B(L,D)=0 THEN 555
535 IF (L-L)<>0 THEN 550
540 LET B(K,D)=-R1
545 GO TO 555
550 LET B(K,D)=B(K,D)-R1*B(L,D)
555 NEXT D
560 NEXT K
565 NEXT X
575 FOR K = 1 TO P
580 FOR D = 1 TO P
585 LET B(K,D)=B(K,D)/F(K)
```

```
600 NEXT D
610 NEXT K
620 FOR I = 1 TO P
630 LET C(I)=0
640 FOR J = 1 TO P
645 LET C(I)=C(I)+B(I,J)*B(J,P+1)
650 NEXT J
655 NEXT I
659 IF N=P THEN 670
660 GO TO 720
670 PRINT"COMPONENT","HALF-LIFE","CPM AT T(0)","SIGMA"
680 FOR J = 1 TO P
690 PRINT J,H(J),C(J),SQR(B(J,J))
700 NEXT J
710 GO TO 900
720 PRINT "T(R)", "Y(R)", "Y-CALC(R)", "SIGMA-Y(R)", "RATIO(R)"
725 LET S1=0
730 FOR R=1 TO N
740 LET G=0
750 FOR J = 1 TO P
760 LET G = G+C(J)*EXP(-(L(J)*T(R)))
770 NEXT J
780 LET Z = SQR(1/W(R))
781 LET S1 = S1 + W(R)*((Y(R)-G)↑2)
782 IF R = 6 THEN 790
783 IF R = 11 THEN 790
784 IF R = 16 THEN 790
785 IF R = 21 THEN 790
786 IF R = 26 THEN 790
787 IF R = 31 THEN 790
788 PRINT T(R),Y(R),G,Z,(Y(R)-G)/Z
789 GO TO 795
790 PRINT
791 GO TO 788
795 NEXT R
799 PRINT
800 PRINT
801 PRINT"FIT=";SQR(S1/(N-P))
805 PRINT
810 GO TO 670
900 END
```

APPENDIX II

FORTRAN PROGRAM FOR ANALYSIS OF MÖSSBAUER SPECTRA

This appendix lists the Fortran program for analysis of Mössbauer spectra. The input is divided into three parts: instructions (figure 36), identification and data.

The first card of the instructions consists of a plot (0), or no-plot (1) in punch position one. The next five punch positions are reserved for the fixed point convergence criterion. The second card contains the number of iterations in the first two punch positions. The third card contains the number of overflows in fixed point for a 100 K counts-per-channel analyzer. The following cards contain the number of ignored channels, one card for each channel. This set is terminated by a zero card. Following the zero card is a set of cards containing the estimated peak position and half-width for each peak in the spectrum. The instruction section is terminated by a blank card.

The identification section consists of 15 cards identifying the spectrum or blank cards. Following this group are 20 data cards for the 200 channel spectrum.

The readout associated with this program consists of a plot and a channel-by-channel analysis of the spectrum. The plot program is written for a Calcomp plotter and the spectrum is inverted (figures 37, 38).

Modifications to the program are presently in progress to allow the analysis of up to twenty peaks and to allow greater flexibility of format, particularly with regard to the plotting routine. Spectrum stripping capabilities are being incorporated, and in addition, the plot routine is being modified to conform with the format prescribed by the NBS Standard Reference Spectrum Program (e.g. inversion of the spectrum).

Fortran 3600 cards for this program can be obtained from W. L. O'Neal, Section 310.01.

We would like to acknowledge the assistance of Mr. A. L. Polinger, of the Engineering Metallurgy Section, 312.01, for making modifications to this computer program.

```
FTN5,10                                                    04/07/66

      PROGRAM PARLOR 4
C   10  ITERATIVE LEAST SQUARE FIT TO PARABOLA PLUS UP TO 10 LORENTZIANS 1547
C   17 ER=RATIO CONVERGENCE CRITERION                                  15 X
C   21 IT=MAXIMUM NUMBER OF ITERATIONS                                 15470
C   25 OV=COUNT OVERFLOW FACTOR                                        15470
C   29 J=IMBEDDED CHANNELS TO BE IGNORED (IMBEDDED ZEROS MUST BE IGNORED)15470
C   31 ALABL=1080 CHARACTER ALPHAMERIC FIELD FOR LABELING CASES        15470
C   32 FIRST 6 CHARACTERS OF ALABL LABEL PUNCHED OUTPUT COLUMNS 75-80  15470
C   35 P(I)=ESTIMATED LOCATION OF PEAK I                               15470
C   37 H(I)=ESTIMATED HALF-WIDTH AT HALF-MAXIMUM OF PEAK I             15470
C   39 Y(I)=COUNTS IN CHANNEL I (CHANNELS 1-200)                       15470
C   41 ZERO TEST DETERMINES BEGIN AND END CHANNELS FOR CALCULATION     15470
C   43 IF NO PREVIOUS END ZERO,CHANNEL 199 MUST BE ZEROED              15470
C   45 ZERO TEST DETERMINES END OF EACH DATA SET OF ARBITRARY LENGTH   15470
C   46 BASE-LINE FOR PUNCHED SPECTRUM=MAXIMUM COUNTS                   15470
C   47 TAPE 02 GENERATES XY PLOT FOR EACH CASE                         PLOT
      49 DIMENSION VARA(12),VARP(12),VARS(12),BASE(12),VARG(12),VARB(12)
      50 DIMENSION Y(200),A(33,34),B(34),P(11),P1(10),R(10),H(11),H1(10)  15470
      51 DIMENSION AA(33,34),BB(720),T(33,34),AINV(720)
      52 DIMENSION OA(10),IG(200),ALABL(9,15),S1(10),G1(10),E1(10),Y1(200) 15470
      53 DIMENSION XYPLOT(900),Y2(200)                                   PLOT
      54 DOUBLE PRECISION A,B,C,H,H1,P,P1                                15470
      55 DOUBLE PRECISION AA,BB,T,AINV
      56 CALL PLOTS(XYPLOT,900,2)                                        PLOT
      57 REWIND 02                                                       PLOT
C     58 READ DATA,DO ZERO TESTS,SET UP IGNORED CHANNELS                 15470
      60 READ(5,61)IPLOT,ER
      61 FORMAT(I1,F14.0)
      62 IF(EOF,5) 1700,67
      67 READ(5,68)IT
      68 FORMAT(I4)
      72 READ(5,73)OV
      73 FORMAT(F4.0)
      79 DO 80 I=1,200                                                   15470
      80 IG(I)=0                                                         15470
      81 DO 84 I=1,200                                                   15470
      82 READ(5,85)J                                                     15470
      83 IF(J.EQ.0)GO TO 86
      84 IG(J)=1                                                         15470
      85 FORMAT(I3)
      86 IGN=IGN+1
      90 DO 93 NL=1,12                                                   15470
      91 READ(5,94)P(NL),H(NL)                                           15470
      92 IF(H(NL).EQ.0.0)GO TO 95                                        15470
      93 CONTINUE                                                        15470
      94 FORMAT(2F7.0)                                                   15470
      95 NL=NL-1                                                         15470
      96 READ(5,97)((ALABL(I,J),I=1,9),J=1,15)                           15470
      97 FORMAT(9A8)                                                     15470
      98 READ(5,99)(Y(I),I=1,200)                                        15470
      99 FORMAT(10F7.0)                                                  15470
C   101 ZERO TEST FOR BEGIN,END,IGNORED CHANNELS/FIND COUNT MAXIMUM      15470
     102 DO 105 N1=1,200                                                 15470
     103 IF(IG(N1).NE.0)GO TO 105                                        15470
     104 IF(Y(N1).NE.0.0)GO TO 106                                       15470
     105 CONTINUE                                                        15470
```

```
      106 EM=0.0                                                        15470
      107 DO 111 N=N1,200                                               15470
      108 IF(IG(N).NE.0)GO TO 111                                       15470
      109 IF(Y(N).EQ.0.0)GO TO 112                                      15470
      110 IF(Y(N).GT.EM)EM=Y(N)                                         15470
      111 CONTINUE                                                      15470
      112 N=N-1                                                         15470
    C 114 CORRECT FOR COUNT OVERFLOW,PUNCH AND PRINT ALPHAMERIC DATA    15470
      115 DO 116 I=N1,N                                                 15470
      116 Y(I)=Y(I)+OV*1.0E5                                            15470
      117 EM=EM+1.0E5*OV                                                15470
      118 WRITE(6,119)                                                  15470
      119 FORMAT(1H1,20X)                                               15470
      120 WRITE(6,121)((ALABL(I,J),I=1,9),J=1,15)                       15470
      121 FORMAT(1X,9A8)                                                15470
      122 CONTINUE
      123 CONTINUE
      124 CONTINUE
    C 126 NORMALIZE COUNTS,DO PRELIMINARY CALCULATIONS                  15470
      127 DO 128 I=N1,N                                                 15470
      128 Y(I)=Y(I)/EM                                                  15470
      130 L1=3*NL+4                                                     15470
      140 L2=L1-1                                                       15470
      150 DO 157 I=1,NL                                                 15470
      155 W(I)=1.0/(W(I)+W(I))                                          15470
      157 DA(I)=0.0                                                     15470
      160 LIM=0                                                         15470
      161 LIMQ=0                                                        15470
      162 GO TO 170                                                     15470
      165 DO 167 I=1,NL                                                 15470
      167 DA(I)=A(3*I-2,L1)                                             15470
    C 169 FILL LEAST SQUARES MATRIX                                     15470
      170 DO 210 J=1,L1                                                 15470
      180 DO 210 I=1,   ← L2                                            15470
ERROR                                                                 15470
      200 A(I,J)=0.0                                                    15470
      210 CONTINUE                                                      15470
      230 DO 390 K=N1,N                                                 15470
      235 IF(IG(K).NE.0)GO TO 390                                       15470
      240 C=K                                                           15470
      250 DO 280 I =1,NL                                                15470
      255 J=3*I                                                         15470
      260 B(J-2)=1.0/(1.0+W(I)*(C-P(I))**2)                             15470
      270 B(J-1)=B(J-2)*B(J-2)*(C-P(I))                                 15470
      280 B(J)=B(J-1)*(C-P(I))                                          15470
      290 DO 300 I=1,3                                                  15470
      300 B(L2-3*I)=C**(I-1)                                            15470
      320 DO 390 J=1,L1                                                 15470
      330 DO 390 I =1,J                                                 15470
      340 IF(J.EQ.L1)GO TO 370                                          15470
      350 A(I,J)=A(I,J)+B(I)*B(J)                                       15470
      360 GO TO 390                                                     15470
      370 IF(I.EQ.L1)GO TO 390                                          15470
      380 A(I,J)=A(I,J)+B(I)*Y(K)                                       15470
      390 CONTINUE                                                      15470
    C 460 SOLVE LEAST SQUARES MATRIX                                    15470
```

```
      470 DO 490 J=1,L2                                                 15470
      480 DO 490 I=1,J                                                  15470
      482 AA(I,J)=A(I,J)
      484 AA(J,I)=A(I,J)
      490 A(J,I)=A(I,J)                                                 15470
      500 DO 690 I=1,L2                                                 15470
      510 DO 580 J=I,L2                                                 15470
      520 IF(A(I,J),EQ,0,0)GO TO 530                                    15470
      530 DO 560 K=1,L1                                                 15470
      540 B(K)=A(I,K)                                                   15470
      550 A(I,K)=A(J,K)                                                 15470
      560 A(J,K)=B(K)                                                   15470
      570 GO TO 600                                                     15470
      580 CONTINUE                                                      15470
      590 GO TO 690                                                     15470
      600 C=A(I,I)                                                      15470
      610 DO 620 K=1,L1                                                 15470
      620 A(I,K)=A(I,K)/C                                               15470
      630 DO 680 K=1,L2                                                 15470
      640 IF(K,EQ,I)GO TO 680                                           15470
      650 C=A(K,I)                                                      15470
      660 DO 670 J=1,L1                                                 15470
      670 A(K,J)=A(K,J)-C*A(I,J)                                        15470
      680 CONTINUE                                                      15470
      690 CONTINUE                                                      15470
    C 695 CORRECT PEAK LOCATION AND WIDTH,PRINT RESULTS                 15470
      698 WRITE(6,780)                                                  15470
      700 DO 709 IQ=1,NL                                                15470
      701 JQ= 3*IQ                                                      15470
      702 R(IQ)= A(JQ-2,L1)                                             15470
      703 H1(IQ)= -A(JQ,L1)/R(IQ)                                       15470
      704 IF((H(IQ)+H1(IQ)),GT,0,0)GO TO 709                            15470
      705 IF(LIMQ,GT,10)GO TO 711                                       15470
      706 LIMQ= LIMQ + 1                                                15470
      707 H(IQ)= 1,1*H(IQ)                                              15470
     7707 WRITE(6,770)I,P(I),S1(I),E1(I),G1(I)                          15470
      708 GO TO 165                                                     15470
      709 CONTINUE                                                      15470
      710 GO TO 715                                                     15470
      711 WRITE(6,712)IQ                                                15470
      712 FORMAT(//34H WRONG HALFWIDTH ESTIMATE FOR PEAK,I5)
      713 GO TO 1600
      715 DO 760 I=1,NL                                                 15470
      717 J=3*I                                                         15470
      719 R(I)=A(J-2,L1)                                                15470
      720 P1(I)=A(J-1,L1)/(2,0*H(I)*R(I))
      725 P(I)=P(I) + P1(I)                                             15470
      732 H1(I)=-A(J,L1)/R(I)                                           15470
      734 H(I)=H(I)+ 0,0*H1(I)
      736 S1(I)=1,0/SQRT(H(I))                                          15470
      740 E1(I)=R(I)*EM                                                 15470
      750 G1(I)=S1(I)*E1(I)*3,14159                                     15470
      760 WRITE(6,770)I,P(I),S1(I),E1(I),G1(I)                          15470
      770 FORMAT(1X,I2,4E20,8)                                          15470
     7800FORMAT(//10X,8HNEW PEAK,11X,14HNEW HALF-WIDTH,7X,10HNEW HEIGHT,10X15470
     7801,8HNEW AREA)                                                   15470
```

```
C 805 TEST NUMBER OF ITERATIONS AND CONVERGENCE                          15470
  810 LIM=LIM+1                                                         15470
  820 IF(LIM .GE. 17) GO TO 1600
  830 DO 843 I=1,NL                                                     15470
  835 IF(ABS(W1(I)/W(I))1,GT,ER)GO TO 165                               15470
  840 IF(ABS(P1(I)/P(I)),GT,ER)GO TO 165                                15470
  842 IF(ABS((R(I)+GA(I))/R(I));GT,ER)GO TO 165                         15470
  843 CONTINUE                                                          15470
C 844 PUNCH FINAL PEAK PARAMETERS                                       15470
  846 CONTINUE
  847 GONTINUE
  848 DO 849 I=1,200                                                    15470
  849 Y1(I)=0,0                                                         15470
  850 S=0,0                                                             15470
C 851 PRINT FIT AND DATA FOR EACH CHANNEL,FIND MAXIMUM OF LORENTZIAN FIT15470
 1851 PARA0=A(L2-2,L1)*EM                                               15470
 2851 PARA1=A(L2-1,L1)*EM                                               15470
 3851 PARA2=A(L2,L1)*EM                                                 15470
 4851 WRITE(6,5851)PARA0,PARA1,PARA2
 5851 FORMAT(//5X,10HPARABOLA= ,E15;8,4H + (,E15;8,7H)*C + (,E15,8,
 58511  5H)*C*C)
  852 WRITE(6,854)                                                      15470
 8540FORMAT(//7X,5HCHNL,,6X,11HLORENTZIANS,9X,8HPARABOLA,12X,13HCOUNTS 15470
 8541+ PAR,,7X,8HRESIDUAL)                                              15470
  856 YM=0,0                                                            15470
  861 DO 935 K=N1,N                                                     15470
  862 IF(IG(K),NE,0)GO TO 935                                           15470
  865 Y2(K)=0,0                                                         15470
  870 G=K                                                               15470
  875 DO 880 I=1,NL                                                     15470
  880 Y2(K)=Y2(K)+R(I)/(1,0+W(I)*(G-P(I))**2)                           15470
  890 PAR=A(L2-2,L1)+C*(A(L2-1,L1)+C*A(L2,L1))                          15470
  900 Y1(K)=Y(K)-PAR                                                    15470
  910 D=Y1(K)-Y2(K)                                                     15470
  920 S=S+D**2                                                          15470
  927 G=Y1(K)*EM                                                        15470
  928 PAR=PAR*EM                                                        15470
  929 E=Y2(K)*EM                                                        15470
  930 IF(YM,GT,Y2(K))YM=Y2(K)                                           15470
  931 WRITE(6,940)K,E,PAR,G,D
  935 GONTINUE                                                          15470
  937 YM=YM*,1                                                          15470
  940 FORMAT(1X,I10,4E20,8)                                             15470
  950 D=SQRT(S/(N-N1-IGN-L2))*EM
  960 WRITE(6,961)D,EM                                                  15470
  961 FORMAT(1H0,*AVERAGE MEAN SQUARE RESIDUAL =*E17,8,10X,26HMAXIMUM NU
     1MBER OF COUNTS =,E10,8//)
  966 IF(IPLOT.EQ,1)GO TO 1177
C 967 PLOT NORMALIZED FIT AND DATA                                      15470
  968 DO 981 K=N1,N                                                     PLOT
  969 IF(IG(K),NE,0)GO TO 981
  970 D=K/10,0                                                          PLOT
  971 G=Y2(K)/YM                                                        PLOT
  972 CALL SYMBOL(D,G,,08,1,0,0,-1)                                     PLOT
  973 E=Y1(K)/YM                                                        PLOT
  974 IF(E+,4)978,976,976                                               PLOT
```

955 D1 = D

```
      975 IF(E.GT.10.4)GO TO 980                                          PLOT
      976 CALL SYMBOL(D,E-,08,3.0,J,-1)                                   PLOT
      977 GO TO 981                                                       PLOT
      978 CALL SYMBOL(D,-,3,,08,6,180,0,-1)                               PLOT
      979 GO TO 981                                                       PLOT
      980 CALL SYMBOL(D,10,J,,08,6.0,0.-1)                                PLOT
      981 CONTINUE                                                        PLOT
C     984 DRAW AND TICK X AND Y AXES                                      15470
      985 CALL PLOT(0,0,0,0,3)                                            PLOT
      986 CALL PLOT(20,0,0,0,2)                                           PLOT
      987 DO 989 I=1,21                                                   PLOT
      988 D=21-I                                                          PLOT
      989 CALL SYMBOL(D,0,3,,12,13.0,0,-1)                                PLOT
      990 CALL PLOT(0,0,10,0,2)                                           PLOT
      991 DO 993 I=1,11                                                   PLOT
      992 D=11-I                                                          PLOT
      993 CALL SYMBOL(0,0,D,,12,13.90,0,-1)                               PLOT
C     994 NUMBER AND LABEL AXES                                           15470
      995 DO 1020 I=1,201,10                                              PLOT
     1000 J=I-1                                                           PLOT
     1010 D=J/10.0-,24                                                    PLOT
     1020 CALL NUMBER(D,-,24,,14,J.0,0,2HI3)                              PLOT
     1030 DO 1060 I=1,11                                                  PLOT
     1040 D=I-1                                                           PLOT
     1050 E=D/10.0                                                        PLOT
     1060 CALL NUMBER(-,43,D,,14,E.0,0,4HF3,1)                            PLOT
     1070 CALL SYMBOL(9,00,-,50,,24,7HCHANNEL,0,0,7)                      PLOT
     1080 CALL SYMBOL(-0.50,2,00,0,21.15HNORM; COUNTS X ,90,0,15)         15470
     1081 D=YM-EM-10.0                                                    15470
     1082 CALL NUMBER(-0,50,6,0,0,21.D,90,0,5HE12,5)                      15470
C    1084 PLOT ALPHAMERIC DATA AND LEGEND                                 15470
     1090 CALL SYMBOL(0,5,10.0,0,0,14,ALABL(1,1),0.0,8)                   15470
     1170 CALL PLOT(30.0,0,0,-3)                                          PLOT
C    1176 PUNCH COUNTS MINUS PARABOLA FOR EACH CHANNEL(IGNORED COUNTS=0)  15470
     1177 CONTINUE
     1178 CONTINUE
     1180 DO 1186 I=N1,N                                                  15470
     1182 IF(IG(I).NE.0)GO TO 1186                                        15470
     1184 Y1(I)=EM*(Y1(I)+1.0)                                            15470
     1186 CONTINUE                                                        15470
     1188 DO 1194 J=1,191,10                                              15470
     1190 K=J+9                                                           15470
     1192 L=K/10                                                          15470
     1194 CONTINUE
     1196 CONTINUE
     1200 WRITE(6,1205)
     1205 FORMAT(2H1 ,15H ERROR ANALYSIS)
     1207 D = D1
     1210 DO 1225 I=1,L2
     1215 DO 1225 J=1,L2
     1220 IJ=J+((I-1)*(2*L2-I))/2
     1225 BB(IJ)=AA(I,J)
     1230 IFSING=0
     1235 CALL TRIAN(BB,L2,I,T,1,IFSING)
     1240 IF(IFSING.EQ.0)GO TO 1250
     1245 GO TO 711
     1250 CALL TIMPY(T,L2,AINV,L2,0)
```

```
      1300 WRITE (6,1310)
      1310 FORMAT (2X,10H VARIANCES)
      1320 IPAR=(L2*(L2+1))/2
      1330 VRPR0=D*SQRT(AINV(IPAR+5))
      1340 VRPR1=D*SQRT(AINV(IPAR+2))
      1350 VRPR2=D*SQRT(AINV(IPAR+0))
      1360 WRITE (6,1362)PARA0,VRPR0
      1362 FORMAT(4X,5H A0= ,E15.8,4X,6H VAR= ,E15.8)
      1364 WRITE(6,1366)PARA1,VRPR1
      1366 FORMAT(4X,5H A1= ,E15.8,4X,6H VAR= ,E15.8)
      1368 WRITE(6,1370)PARA2,VRPR2
      1370 FORMAT(4X,5H A2= ,E15.8,4X,6H VAR= ,E15.8)
      1375 WRITE(7,1377)ALABL(1,1)
      1377 FORMAT(A8)
      1380 WRITE(7,1390)PARA0,VRPR0,PARA1,VRPR1,PARA2,VRPR2,ALABL(1,1)
      1390 FORMAT(6E12.5,A8)
      1392 WRITE(6,1394)
      1394 FORMAT(4X,5H PEAK,7X,9H POSITION,11X,15H HALFWIDTH-HMAX,7X,
           1  7H HEIGHT,12X,5H AREA,15X,9H BASELINE)
      1400 DO 1560 I=1,NL
      1410 IVA=(3*I-2)*((3*I-3)*(2*L2-3*I+2))/2
      1420 VARA(I)=D*SQRT(AINV(IVA))
      1430 IVP=(3*I-1)*((3*I-2)*(2*L2-3*I+1))/2
      1441 COVA=(AINV(IVA))/(E1(I)*E1(I))
      1442 COVP=(AINV(IVP))/(A(3*I-1,L1)*A(3*I-1,L1))
      1443 COVAP= (AINV(IVA+1))/(A(3*I-1,L1)*E1(I))
      1444 COV=SQRT(COVA*COVP*COVAP)
      1445 VARP(I)= D*(A(3*I-1,L1)/(2.0*H(I)*E1(I)       ))*COV
      1450 IVH= (3*I)+ ((3*I-1)*(2*L2-3*I))/2
      1461 COVA=(AINV(IVA))/(E1(I)*E1(I))
      1462 COVH=(AINV(IVH))/(A(3*I-1,L1)*A(3*I-1,L1))
      1463 COVAH=(AINV(IVA+2))/(A(3*I,L1)*E1(I))
      1465 VARH   =D*(A(3*I,L1)/E1(I)       )*SQRT(COVA*COVH*COVAH)
      1470 VARS(I)= S1(I)*(VARH/H(I))/2.0
     C     PRINTOUT OF VARIANCES
      1515 BASE(I)= PARA0+PARA1*P(I)+ PARA2*P(I)*P(I)
      1520 VARB(I)= (ABS(VARS(I)/S1(I))+ ABS(VARA(I)/E1(I)))*G1(I)
      1525 VARB(I)=VRPR0+ VRPR1 + VRPR2
      1530 WRITE(7,1535)I,P(I),S1(I),E1(I),G1(I),BASE(I),ALABL(1,1)
      1531 WRITE(7,1535)I,VARP(I),VARS(I),VARA(I),VARB(I),VARB(I),ALABL(1,1)
      1535 FORMAT(I2,5E14.6,A8)
      1550  WRITE(6,1555)I,P(I),S1(I),E1(I),G1(I),BASE(I)
      1555 FORMAT(4X,I3,5E20.8)
      1560 WRITE(6,1565)VARP(I),VARS(I),VARA(I),VARB(I),VARB(I)
      1565 FORMAT(4X,8HVARIANCE,5E20.8)
      1600 GO TO 60
      1700 REWIND 02
      1800 STOP
      1900 END
```

```
5.1A    PARLORM                                          04/07/66        ED

                                        IDENT     PARLORM
        PROGRAM LENGTH              31374
        ENTRY POINTS    PARLORM     26251
        EXTERNAL SYMBOLS
                        Q8QENTRY
                        THEND.
                        Q1Q10210
                        Q1Q10020
                        Q2Q07220
                        Q1Q04210
                        Q1Q05210
                        Q1Q02210
                        Q8QSTOPS
                        Q8QDICT.
                        PLOTS
                        SYMBOL
                        PLOT
                        NUMBER
                        TRIAN
                        TTMPY
                        SORTF
                        Q8QIFEOF
                        REW.
                        TSM.
                        STM.
                        QNSINGL.
                        QNDOUBL.
    01117 SYMBOLS
```

FTN5,10 04/07/66

```
      SUBROUTINE TTMPY(T,N,A,K,IFTL)
      DIMENSION T(100),A(100)
      DOUBLE PRECISION A,T
      NX2=N*2
      IJ=0
      IF (IFTL.NE.1) GO TO 30
      DO 20 I=1,K
      DO 20 J=I,K
      IJ=IJ+1
      A(IJ)=0.D0
      DO 10 L=1,I
      I1=I+((L-1)*(NX2-L))/2
      I2=I1+J-I
   10 A(IJ)=A(IJ)+T(I1)*T(I2)
   20 CONTINUE
      RETURN
   30 DO 50 I=1,K
      NO=K-I+1
      NPT=((NX2-I)*(I-1))/2
      JJ=1
      DO 50 J=I,K
      I1=I+JJ-1+NPT
      I2=I+JJ-1+((NX2-J)*(J-1))/2
      IJ=IJ+1
      A(IJ)=0.D0
      DO 40 L=1,NO
      A(IJ)=A(IJ)+T(I1)*T(I2)
      I1=I1+1
   40 I2=I2+1
      JJ=JJ+1
   50 NO=NO-1
      RETURN
      END
```

```
5.1A      TRMPY                                          04/07/66      ED

                                        IDENT     TRMPY
      PROGRAM LENGTH              00367
      ENTRY POINTS     TRMPY      03003
      EXTERNAL SYMBOLS
                     000DICT.
         00126 SYMBOLS
```

```
FTN5.10                                                    04/07/66
      SUBROUTINE TRIAN(A,N,T,TINV,K,KAY)
      DIMENSION A(1275),T(1275),TINV(1275)
      DOUBLE PRECISION  A,T,TINV,TEMPO,ONE,ZERO,DSQRT                00021
      NX2=2*N
      KAY=0                                                          00021
      ONE=1.D0                                                       00021
      ZERO=0.D0                                                      00021
      NA=(N*(N+1))/2                                                 00021
      DO 10 I=1,NA                                                   00021
   10 T(I)=A(I)                                                      00021
      IJ=0                                                           00021
      DO 90 J=1,N                                                    00021
      DO 80 I=J,N                                                    00021
      J1=J                                                           00021
      IJ=IJ+1                                                        00021
      TEMPO=T(IJ)                                                    00021
      IF (I.GT.J) GO TO 60                                           00021
   20 IF (J1.GT.1) GO TO 50                                          00021
      IF (TEMPO.LE.ZERO) GO TO 150                                   00021
      T(IJ)=DSQRT(TEMPO)                                             00021
      GO TO 80                                                       00021
   50 J1=J1-1                                                        00021
      I1=I+((J1-1)*(NX2-J1))/2                                       00021
      TEMPO=TEMPO-T(I1)*T(I1)                                        00021
      GO TO 20                                                       00021
   60 IF (J1.GT.1) GO TO 70                                          00021
      I1=IJ-I+J                                                      00021
      T(IJ)=TEMPO/T(I1)                                              00021
      CALL DVCHK(L)                                                  00021
      IF (L.EQ.1) GO TO 150                                          00021
      GO TO 80                                                       00021
   70 J1=J1-1                                                        00021
      I1=I+((J1-1)*(NX2-J1))/2                                       00021
      I2=I1-I+J                                                      00021
      TEMPO=TEMPO-T(I1)*T(I2)                                        00021
      GO TO 60                                                       00021
   80 CONTINUE                                                       00021
   90 CONTINUE                                                       00021
      IF (K.EQ.0) GO TO 170                                          00021
      DO 100 I=1,NA
  100 TINV(I)=T(I)                                                   00021
      IJ=0                                                           00021
      DO 140  J=1,N                                                  00021
      DO 130  I=J,N                                                  00021
      IJ=IJ+1                                                        00021
      J1=J                                                           00021
      TEMPO=ZERO                                                     00021
      IF (I.GT.J) GO TO 110                                          00021
      TINV(IJ)=ONE/T(IJ)                                             00021
      CALL DVCHK(L)                                                  00021
      IF (L.EQ.1) GO TO 150                                          00021
      GO TO 130                                                      00021
  110 I1=I+((J1-1)*(NX2-J1))/2                                       00021
      I2=J1+((J-1)*(NX2-J))/2                                        00021
      TEMPO=TEMPO-TINV(I1)*TINV(I2)                                  00021
      IF (I-J1.LE.1) GO TO 120                                       00021
                                                                     00021
```

```
      J1=J1+1                                                          00021
      GO TO 110                                                        00021
  120 I1=I+((I-1)*(NX2-I))/2                                           00021
      TINV(IJ)=TEMPO/T(I1)                                             00021
      CALL DVCHK(L)                                                    00021
      IF (L.EQ.1) GO TO 150                                            00021
  130 CONTINUE                                                         00021
  140 CONTINUE                                                         00021
      RETURN                                                           00021
  150 WRITE (6,160)
  160 FORMAT (16H SINGULAR MATRIX)                                     00021
      KAY=-1                                                           00021
  170 RETURN
      END                                                              00021
```

```
5.1A      TRIAN                                          04/07/66          ED

                                        IDENT     TRIAN
      PROGRAM LENGTH                  00614
      ENTRY POINTS     TRIAN          00010
      EXTERNAL SYMBOLS
                       THEND.
                       Q8QDICT
                       DVCHK
                       DSQRT
                       STH.
         00176 SYMBOLS
```

```
FTN5.10                                                    04/07/66

      SUBROUTINE TRMPY(T,N,R,NR,NC,W,TLEFT)
      DIMENSION  T(1275),R(2500),W(2500)                          00021
      INTEGER TLEFT
      DOUBLE PRECISION T,R,W                                      00021
      NX2=2*N                                                     00021
      IJ=1                                                        00021
      NB=NC*NR                                                    00021
      DO 10 I=1,NB                                                00021
   10 W(I)=0.D0                                                   00021
      IF (TLEFT.EQ.0) GO TO 40
      DO 30 J=1,NC                                                00021
      MRSUB=NR*(J-1)                                              00021
      DO 30 I=1,NR                                                00021
      DO 20 L=1,I
      MT=I+((L-1)*(NX2-L))/2                                      00021
      MR=MRSUB+L
   20 W(IJ)=W(IJ)+T(MT)*R(MR)                                     00021
   30 IJ=IJ+1                                                     00021
      RETURN                                                      00021
   40 DO 60 J=1,NC
      MTSUB=((J-1)*(NX2-J))/2                                     00021
      DO 60 I=1,NR                                                00021
      DO 50 L=J,NC
      MR=(L-1)*NR+I                                               00021
      MT=MTSUB+L                                                  00021
   50 W(IJ)=W(IJ)+T(MT)*R(MR)                                     00021
   60 IJ=IJ+1                                                     00021
      RETURN                                                      00021
      END                                                         00021
```

```
5.1A     TTMPY                                          04/07/66        ED

                                        IDENT     TTMPY
     PROGRAM LENGTH              00542
     ENTRY POINTS     TTMPY      00003
     EXTERNAL SYMBOLS
                   080DICT.
        00111 SYMBOLS
```


* U.S. GOVERNMENT PRINTING OFFICE: 1966—251-021/44

U.S. DEPARTMENT OF COMMERCE
WASHINGTON, D.C. 20230

OFFICIAL BUSINESS

POSTAGE AND FEES PAID
U.S. DEPARTMENT OF COMMERCE